



UNIVERSITY OF
KWAZULU-NATAL

INYUVESI
YAKWAZULU-NATALI

DISCIPLINE OF MECHANICAL
ENGINEERING

**Design and analysis of the tooling to manipulate and
install complete sectors in the ATLAS New Small Wheel
within narrowly defined stress parameters**

Shuvay Singh

Submitted in fulfilment of the academic requirements for the degree of Master of Science in
Mechanical Engineering, College of Agriculture, Engineering and Science,
University of KwaZulu-Natal Submitted:

The financial assistance of the National Research Foundation (NRF) towards this research is hereby
acknowledged. Opinions expressed and conclusions arrived at, are those of the author and are not
necessarily to be attributed to the NRF.

Supervisors: Dr Clinton Bemont, Dr Sahal Yacoob

December 2015

Declaration

I, Shuvay Singh, declare that

- (i) The research reported in this dissertation/thesis, except where otherwise indicated, is my original work.
- (ii) This dissertation/thesis has not been submitted for any degree or examination at any other university.
- (iii) This dissertation/thesis does not contain other persons' data, pictures, graphs or other information, unless specifically acknowledged as being sourced from other persons.
- (iv) This dissertation/thesis does not contain other persons' writing, unless specifically acknowledged as being sourced from other researchers. Where other written sources have been quoted, then:
 - a) their words have been re-written but the general information attributed to them has been referenced;
 - b) where their exact words have been used, their writing has been placed inside quotation marks, and referenced.
- (v) Where I have reproduced a publication of which I am an author, co-author or editor, I have indicated in detail which part of the publication was actually written by myself alone and have fully referenced such publications.
- (vi) This dissertation/thesis does not contain text, graphics or tables copied and pasted from the Internet, unless specifically acknowledged, and the source being detailed in the dissertation/thesis and in the References sections.

Signed _____ Date _____

Mr Shuvay Singh

As the candidate's supervisor I have approved this dissertation for submission.

Signed _____ Date _____

Dr Clinton Bemont

As the candidate's supervisor I have approved this dissertation for submission.

Signed _____ Date _____

Dr Sahal Yacoob

Acknowledgements

Thanks are first and foremost due to my supervisors, Dr Clinton Bemont and Dr Sahal Yacoob for their unstinting enthusiasm and encouragement, guidance, support and efforts towards making this venture possible.

I would like to thank my ATLAS supervisors Dr Giancarlo Spigo, Dr Patrick Ponsot and Dr Augusto Sciucati for their extensive assistance and advice. I would further like to express my gratitude to colleagues in the ATLAS Technical Coordination Design Office for providing a congenial and stimulating working atmosphere as well as offering much support and entertainment. Credit is also due to Peter Sinclair for invaluable technical assistance and companionship throughout my research.

I would especially like to acknowledge Fiona Leverone whom I shared many a useful discussion with during the final stages of this research and Matthew Woods for his priceless assistance.

Finally, I would like to thank my family and close friends for their support and motivation throughout.

Abstract

The ATLAS Experiment New Small Wheel will be installed at Point 1 of the LHC in Geneva in 2017. It has a vast array of detectors and triggers, yet due to its size and delicate nature, special attention needs to be given to the installation procedures and equipment. This dissertation entails the design of the NSW installation tooling as well as the procedure of optimising such a tooling with Finite Element Analysis. The NSW detector design team work simultaneously with the engineering and services team which results in constantly changing design specifications. A procedure has been explored to account for this frequent change to adapt the design in an efficient manner. The overall tooling is made up of the main tooling beam, the counter weight assembly, the rotating and locking head and the sector grabber frames. Focus is also given to the optimisation via Finite Element Analysis using ANSYS Mechanical. This covers the structural integrity of the entire tooling as well as weight minimisation. In addition a detailed study explores the effects of stress relief grooves on a stepped shaft.

Table of Contents

List of Figures	iv
List of Tables	vii
Nomenclature.....	viii
Chapter: 1 Introduction.....	1
Chapter: 2 Literature Survey.....	4
2.1 New Small Wheel	4
2.1.1 Large sector.....	5
2.1.2 Small sector.....	7
2.1.3 Foot spoke	7
2.1.4 Kinematic mounts for large and small sectors:	8
2.2 Installation Tooling.....	9
2.2.1 Types of installation toolings	9
2.2.2 Wisconsin Tooling	9
2.3 The Finite Element Analysis (FEA) procedure.....	10
2.3.1 Discretisation	11
2.3.2 Finite Elements	12
2.3.3 Governing equations for computational solid mechanics	13
2.4 Nonlinear FEA.....	15
2.4.1 Newton-Raphson Method	15
2.4.2 Radius of convergence.....	16
2.5 Basic overview of ANSYS Workbench and ANSYS Mechanical	17
2.5.1 Workbench layout.....	17
2.5.2 Design Modeller.....	18
2.5.3 Mechanical layout.....	19
2.5.4 ANSYS Solvers	19
2.6 Stress relief grooves	20
2.7 Mechanical design philosophy.....	21
2.7.1 Euro-code compliance.....	21

2.7.2	ATLAS Good Practice	22
Chapter: 3	Design approach.....	23
3.1	Functional requirements and system constraints.....	23
3.2	Review of existing design	24
3.2.1	Layout of Wisconsin Tooling	24
3.2.2	Principle of operation.....	25
3.2.3	Counter weight assembly	26
3.2.4	Overview of the rotation head and locking mechanism.....	26
3.2.5	Sector COG adjustment	27
3.2.6	Motorised actuation of tooling	28
3.3	Proposed design methodology	28
3.3.1	Conventional design methodology for a component.....	29
3.3.2	Design methodology for NSW Installation Tooling	30
Chapter: 4	Tooling concept generation.....	32
4.1	Principle of operation of the NSW Installation Tooling	32
4.2	Tooling balance.....	32
4.3	Large sector grabber.....	33
4.4	Counter weight carriage	40
4.5	Main tooling beam	42
4.6	Sector rotational orientation mechanism.....	43
4.7	Rotation-locking mechanism:	44
4.8	COG translation mechanism	47
4.9	Small sector grabber	48
4.10	Foot spoke grabber.....	51
4.11	Tooling storage stand.....	53
4.12	Counter weight adjustment motor.....	54
Chapter: 5	Final design and simulation of the NSW Tooling.....	55
5.1	Large sector grabber and spacer frame	55
5.2	Small sector grabber and grabber mounts.....	58

5.3	Foot spoke grabber.....	60
5.4	Main beam	61
5.4.1	Main beam balance and bending.....	61
5.4.2	Main beam weld.....	63
5.4.3	Main beam hoist thread.....	67
5.5	Trunnion shaft study	72
5.6	Hoisting and spatial consideration of final tooling	75
5.7	Final design specifications	77
Chapter: 6	Design evaluation and discussion	79
6.1	Comparison of NSW Installation Tooling to Wisconsin Tooling.....	79
6.2	Specialised FEA procedures	80
6.3	Manufacture of NSW Installation Tooling	80
6.4	Practical stress analysis.....	81
6.5	Refinement of flexible analysis programs.....	81
6.6	Final tooling certification.....	82
6.7	Trunnion shaft study findings	82
Chapter: 7	Conclusion	83
References.....		84
Appendix A.....		86
Appendix B		107
Appendix C		114
Appendix D.....		157
Appendix E		161

List of Figures

Figure 1-1. The ATLAS Experiment with Small Wheel visible (Bini, 2013).	1
Figure 1-2. Wisconsin Tooling with chamber grabber (Cattai, et al., 2014).	2
Figure 2-1. Present Small Wheel assembly and shielding (Ponsot & Spigo, 2015).	4
Figure 2-2. NSW assembly sequence (Ponsot, 2014).	5
Figure 2-3. Make up of NSW sectors (Ponsot & Spigo, 2015).	6
Figure 2-4. Front view of the NSW large sector (Ciapetti & Ponsot, 2015).	6
Figure 2-5. Front view of the NSW Small sector (Ciapetti & Ponsot, 2015).	7
Figure 2-6. Foot spoke of NSW (Ciapetti & Ponsot, 2015).	8
Figure 2-7. Kinematic joints used for sector and sTGC mounting and alignment (Cattai, et al., 2014).	8
Figure 2-8. Balanced hoist tooling (University of Wisconsin, 2001).	9
Figure 2-9. Forklift with Jib attachment (BAHRNS, 2010).	9
Figure 2-10. Wisconsin Tooling installing sector on CMS (Ponsot, 2014).	10
Figure 2-11. Basic schematic of the Black Box (Pitot, 2011).	11
Figure 2-12. Graph showing visual representation of discretisation (Pitot, 2011).	12
Figure 2-13. Approaching the point of mesh independence (Pitot, 2011).	13
Figure 2-14. Displacement vector $\{u\}$ of a node (Pitot, 2011).	14
Figure 2-15. Assemblage of elemental equations to achieve global equation (Pitot, 2011).	15
Figure 2-16. Global matrix with load and constraint (Pitot, 2011).	15
Figure 2-17. Newton-Raphson iteration of load increment (ANSYS Inc, 2013).	16
Figure 2-18. The radius of convergence around real solution (ANSYS Inc, 2013).	17
Figure 2-19. ANSYS R15.0 Workbench layout.	18
Figure 2-20. ANSYS R15.0 Design Modeller layout.	18
Figure 2-21. ANSYS R15.0 Mechanical layout.	19
Figure 2-22. Force flow lines through a shaft shoulder (Schwalb, 2014).	20
Figure 2-23. Force flow lines through shaft with radius at step (Schwalb, 2014).	21
Figure 2-24. Stress relief groove effect on force flow lines (Schwalb, 2014).	21
Figure 2-25. Section 5.1.1 of BS EN 13155:2003+A2 (The British Standard Institution, 2010).	22
Figure 3-1. Wisconsin Tooling Setup showing (a) the rotating head, (b) the main beam and (c) the counter weight assembly (University of Wisconsin, 2001).	24
Figure 3-2. Adjusting balance of Wisconsin Tooling (University of Wisconsin, 2001).	25
Figure 3-3. Assembled counter weight bank of Wisconsin Tooling (University of Wisconsin, 2001).	26
Figure 3-4. Cross section of Wisconsin Tooling trunnion assembly (University of Wisconsin, 2001).	27
Figure 3-5. COG adjustment mechanism on Wisconsin Tooling (University of Wisconsin, 2001).	27
Figure 3-6. Drive actuation unit for Wisconsin Tooling (University of Wisconsin, 2001).	28

Figure 3-7. Standard component design methodology.	29
Figure 3-8. NSW Installation Tooling design methodology.	31
Figure 4-1. First concept of NSW Installation Tooling.	32
Figure 4-2. Basic forces that make up weight balance of tooling.	33
Figure 4-3. Old sector grabber with side arm mounts (University of Wisconsin, 2001).	34
Figure 4-4. Concept for LS grabber using welded tubes.	35
Figure 4-5. Concept of detachable grabber arm.	36
Figure 4-6. LS with positions of sTGC kinematic mounts indicated (Pinnell, 2015).	37
Figure 4-7. LS spacer frame with reinforced mounts for grabber mounts (Schweiger, 2015).	38
Figure 4-8. Proposed grabber mount concept for sector installation and storage tooling (Singh, 2015).	39
Figure 4-9. LS grabber concept with finalised grabber mount positions.	40
Figure 4-10. Concept of a mobile counter weight carriage.	41
Figure 4-11. Counter weight carriage with add-on weight slices.	42
Figure 4-12. Main beam tooling concept with forward-biased hoist point.	43
Figure 4-13. Modified trunnion assembly concept.	44
Figure 4-14. Rotating and stationary wheel concept.	45
Figure 4-15. Concept of threaded pin frictional locking system.	46
Figure 4-16. Modified pin locking fail safe concept with 5° leeway.	46
Figure 4-17. Toggle clamp locking concept.	47
Figure 4-18. Concept for the COG adjustment translation system for the NSW Installation Tooling.	48
Figure 4-19. Small sector in NSW assembly (Pinnell, 2015).	49
Figure 4-20. SS grabber mount positions (Schweiger, 2015).	50
Figure 4-21. SS grabber concept.	51
Figure 4-22. Foot spoke with mounting plates for LS spokes (Ciapetti, et al., 2015).	52
Figure 4-23. Universal foot spoke grabber with two mount positions.	53
Figure 4-24. NSW Installation Tooling storage stand.	54
Figure 5-1. LS grabber simulation at 0° without spacer frame.	56
Figure 5-2. Deformation probe comparison of top and bottom grabber arm.	56
Figure 5-3. Von Mises stresses of LS grabber with spacer frame.	57
Figure 5-4. Von Mises stress result of worst stressed LS spacer frame panel.	58
Figure 5-5. SS grabber Von Mises stresses at 90°.	59
Figure 5-6. LS grabber mount and aluminium insert FEA Von Mises plot.	60
Figure 5-7. Forces applied to foot spoke grabber in simulation.	60
Figure 5-8. Von Mises stress experienced by foot spoke grabber.	61
Figure 5-9. Combining bodies with separate material properties.	64
Figure 5-10. Loads applied to main beam.	65

Figure 5-11. Main beam assembly Von Mises stress plot.	66
Figure 5-12. Weld penetration stresses of main beam.	67
Figure 5-13. Geometric modification details for bolt thread simulation.....	68
Figure 5-14. Connecting ‘Solution’ to ‘Setup’ for Sub-modelling.	69
Figure 5-15. Sliced portion of main beam with hoist bolt hole.	70
Figure 5-16. Imported Cut Boundary Constraint to adopt full model solution for sub-modelling.	70
Figure 5-17. Finer mesh required for accuracy of threaded hole.	71
Figure 5-18. Thread Von Mises stresses of front hoist point hole.	71
Figure 5-19. Trunnion shaft groove symbol diagram.	73
Figure 5-20. Stress experienced by trunnion shaft with stress relief groove.	75
Figure 5-21. Minimum SS grabber clearance (left) and LS grabber clearance (right) (Singh, 2015). .	76
Figure 5-22. Overhead crane clearance when installing Small sector (Singh, 2015).	76
Figure 5-23. Full NSW Installation Tooling with LS grabber.	77
Figure 6-1. Size comparison of Wisconsin Tooling (a) to NSW Installation Tooling (b) (Singh, 2015).	79

List of Tables

Table 5-1. Counter weight positions for tooling balance.	63
Table 5-2. Changes to Sizing Details for accurate Bolt Thread simulation in ANSYS.	68
Table 5-3. Peak Von Mises stresses for different relief groove permutations.	74
Table 5-4. Final NSW Installation Tooling design specifications.	78

Nomenclature

Abbreviations

3D – Three dimensional

AFNOR – Association Française de Normalisation

ATLAS – A Toroidal LHC ApparatuS

BS – British Standards

BSI – British Standards Institution

CAD – Computer Aided Design

CERN – European Union for Nuclear Research (previously “*Conseil Européen pour la Recherche Nucléaire*”)

CMS – Compact Muon Solenoid

COG – Centre of Gravity

CW – Counter weight

DC – Direct current

DM – Design Modeller

DSS – Direct Sparse Solver

FEA – Finite Element Analysis

FEM – Finite Element Method

LHC – Large Hadron Collider

LS – Large Sector

MM - MicroMega

NSW – New Small Wheel

PCG – Preconditioned Conjugate Gradient

SS – Small Sector

sTGC – small Thin Gap Chamber

UTS – Ultimate Tensile Strength

Chapter: 1 Introduction

The purpose of an installation tooling is to manipulate a particular component into a position and would require specific orientation. The New Small Wheel (NSW) of the ATLAS Experiment collider requires such a tooling in order to carry out its sector assembly. The ATLAS Experiment (ATLAS Collaboration, 2008) is a 7000 ton cylindrical particle collision detector that spans 44 m with a diameter of 22 m. It is one of 4 colliders on the Large Hadron Collider (LHC) 27 km loop (Bini, 2013). In order to detect particle dispersion upon collision, the detector is designed with a combination of cylindrical and end cap configurations. This allows a near complete three dimension capture volume in all directions from the central collision point. The cylindrical layers of detectors track the radial trajectories, while the end cap detectors track the more axially biased paths. The NSWs form part of the inner end cap muon detectors and are therefore disc like in shape as seen in Figure 1-1.

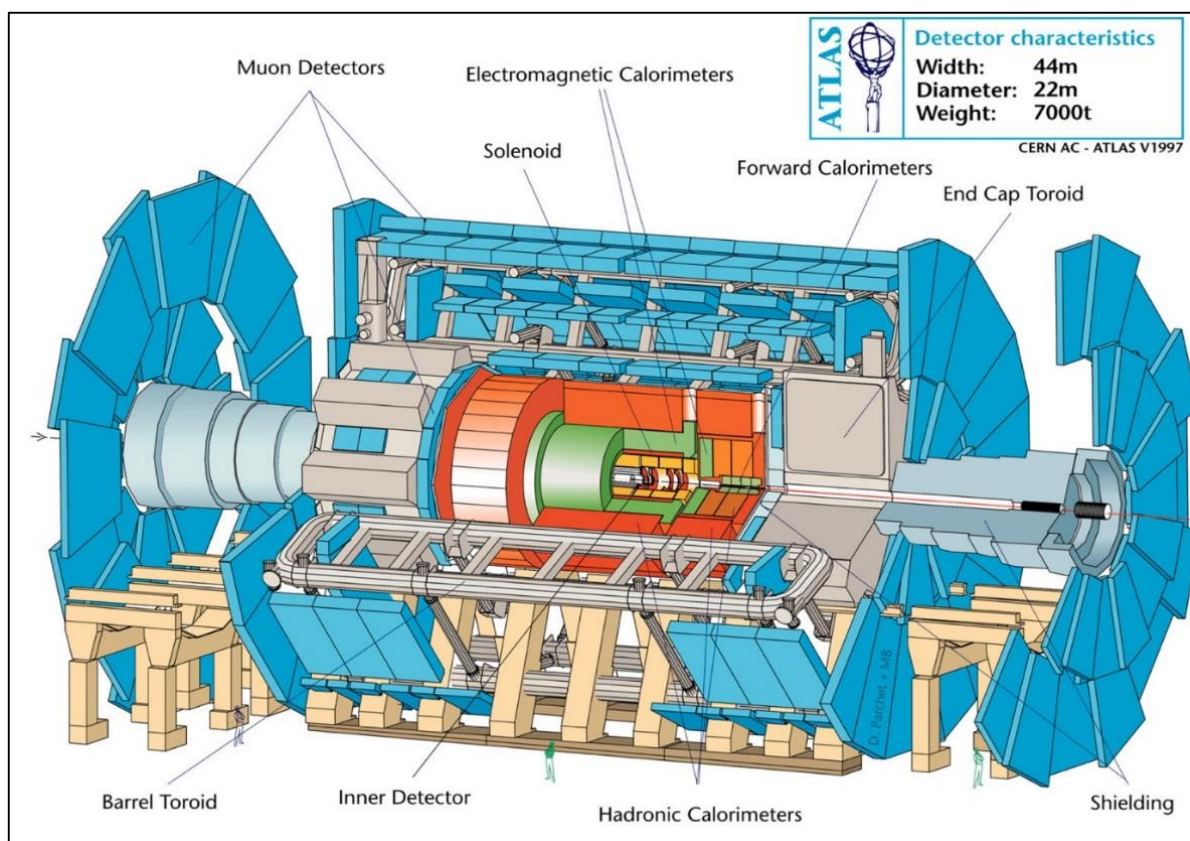


Figure 1-1. The ATLAS Experiment with Small Wheel visible (Bini, 2013).

Muons are sub-atomic particles sometimes created during proton-proton collisions. The muon requires a specific type of detector to record its path as it travels away from the collision point at the centre of the collider. The muons are detected in the end caps by means of small Thin Gap Chambers (sTGC) and MicroMegas (MM) (ATLAS Collaboration, 2013).

The NSW, positioned at the central most muon detector in Figure 1-1, comprises simplified sectors in a triangular shape to form the wheel. There are two offset layers of these sectors in order to capture areas in between the sectors of the first layer as shown in Figure 1-1. This ensures a complete area of detection along the wheel as one layer detects trajectories in the gaps left by the other layer. The layer closest to the centre is made up of small sectors (SS). These sectors, as the name mentions, are smaller in size than the sectors in the layer that surrounds it, the large sectors (LS). Both sectors share the same detector make up, but the shapes and sizes are different (Ponsot, 2014).

In order to assemble these sectors on the NSW structure, there is a need for a specialised installation tooling. An example of a sector installation tooling would be the Wisconsin Tooling previously used at CERN as seen in Figure 1-2.



Figure 1-2. Wisconsin Tooling with chamber grabber (Cattai, et al., 2014).

The exact design specifications of the NSW sectors change as the design of the sector physics are optimised. The engineering team that designs the mechanical structures, services and toolings therefore need to account for these changes until the physics-based design is finalised. A project on a large scale such as the NSW therefore poses a unique working environment for engineering design where requirements are altered frequently. Such projects are common among the various improvements and upgrades at CERN.

Since CERN is a large centre for nuclear research in Europe, there are various protocols with regards to engineering principles and standards that have to be adhered to. CERN also has a particular list of

supported software for design purposes to ensure literacy amongst all personnel. The primary software for mechanical simulations used at CERN is ANSYS R15.0 Workbench: Mechanical. This allows various simulations using Finite Element Analysis (FEA) to determine mechanical results from various loads such as pressure, force and thermal gradients.

For complex geometries and force profiles where calculations are not always linear it offers accuracy and efficiency far greater than that of conventional hand calculations. The majority of the simulation and optimisation procedures in this dissertation utilises finite element analysis via ANSYS.

This dissertation is made up of seven chapters that further portray the research conducted towards the design and analysis of a suitable sector installation tooling as per the requirements in chapter 3.1.

Chapter 2 is the literature survey which gives the necessary background information and history regarding the NSW sectors, previous tooling and fundamentals of FEA. It serves to familiarise the reader with the fundamental concepts upon which the dissertation is based.

Chapter 3, Design approach, describes the particular design approach that the author carried out by analysing the design functional and system requirements. This includes the design methodology and analysis of previously manufactured installation toolings.

Chapter 4, Tooling concept generation, shows the initial tooling conceptual designs and specifically describes the logical process and points of optimisation for the various design problems presented in the requirements for the new tooling.

Chapter 5 forms the final design and simulation section of the dissertation. This chapter contains the detailed procedures and results of the FEA carried out as well as the various programs written to optimise the design process itself.

Chapter 6 is a complete evaluation of the final design and discussion regarding the significant improvements made over the previous tooling as well as the unique FEA methods used for specialised simulations. Special mention is also made about the future manufacture of the tooling and practical testing that can be carried out.

Chapter 7 concludes the dissertation by highlighting the key points of the various designs, procedures and methods of optimisation developed through the work.

Chapter: 2 Literature Survey

To initiate the study a detailed literature survey was conducted. This allowed for the required background understanding and evaluation of work requirements, details of the design conditions and theory of the FEA solver.

2.1 New Small Wheel

The NSW is made up of 2 layers of sectors. The first layer is made up of 8 Large Sectors (LS) that are positioned in a circular pattern around a central hub. The second layer is made up of 8 Small Sectors (SS) that are also positioned in a circular pattern, but with a 22.5° rotation about the central axis with respect to the vertical. This acts to position the second layer of sectors directly in the gaps left by the first layer of sectors. Figure 2-1 shows the Small and Large sectors on the present Small Wheel assembly (Ponsot, 2014).

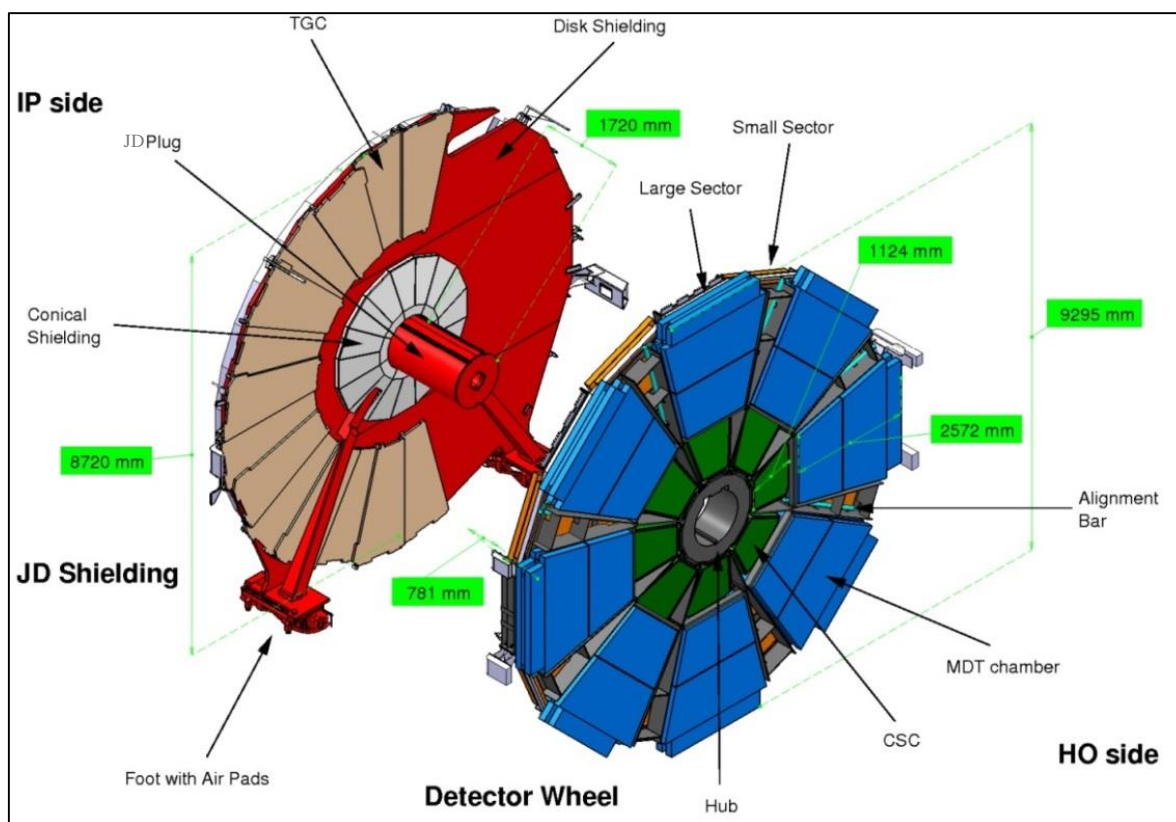


Figure 2-1. Present Small Wheel assembly and shielding (Ponsot & Spigo, 2015).

The small sectors are attached via kinematic mounts to SS spokes. These spokes connect to both the JD shielding and JD Plug. The large sectors connect to similar LS spokes. These spokes connect to the SS spokes in addition to the JD Plug. Since the Small and Large sectors act to exert a cantilevered load on the JD Plug, the SS spoke area of the wheel is supported by two modified Foot spokes. These spokes provide structural support to the JD Plug as well as a means for the Small sectors in that area to connect to. Figure 2-2 shows the intended assembly procedure whereby SS spokes and Foot spokes are first

attached (1) to JD followed by the Small sectors (2). The LS spokes are then installed (3). The last step involves installing the large sectors to the assembly (4).

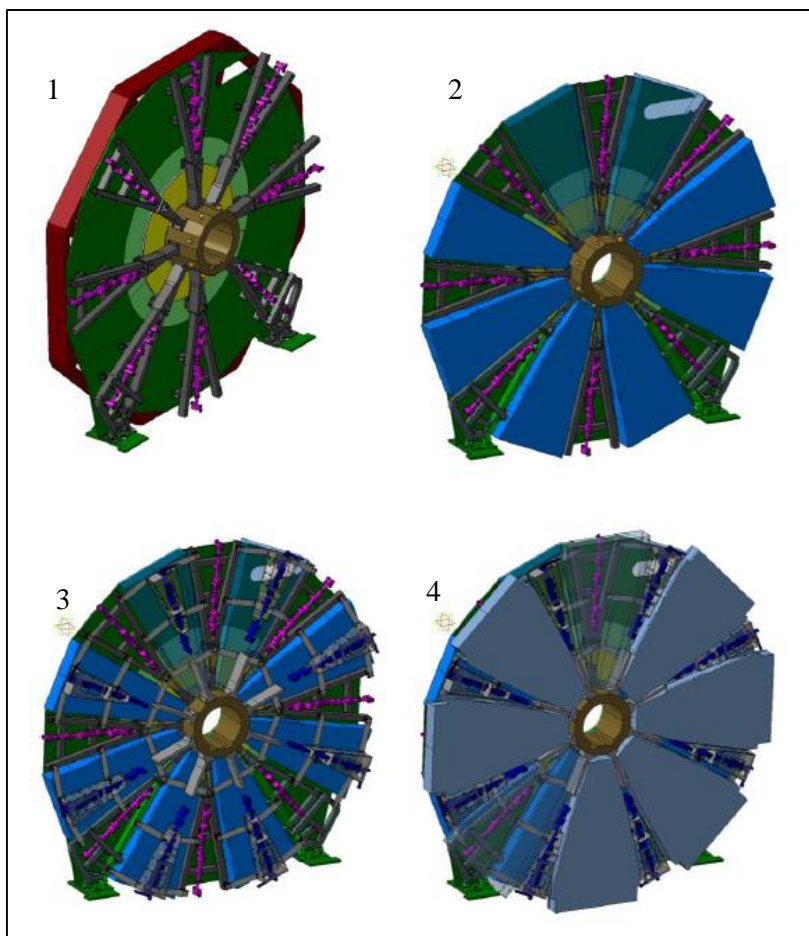


Figure 2-2. NSW assembly sequence (Ponsot, 2014).

2.1.1 Large sector

The LS comprises various layers of detectors. It has an aluminium spacer frame centre that behaves as the main structural member of the sector. MicroMega detectors are then bolted onto either side of the spacer frame. The sTGC detectors are then attached by means of four kinematic mounts to the spacer frame as seen in Figure 2-3 (also see Figure 2-7). These kinematic mounts allow for the sTGC layers to be aligned to one another (Ponsot, 2014).

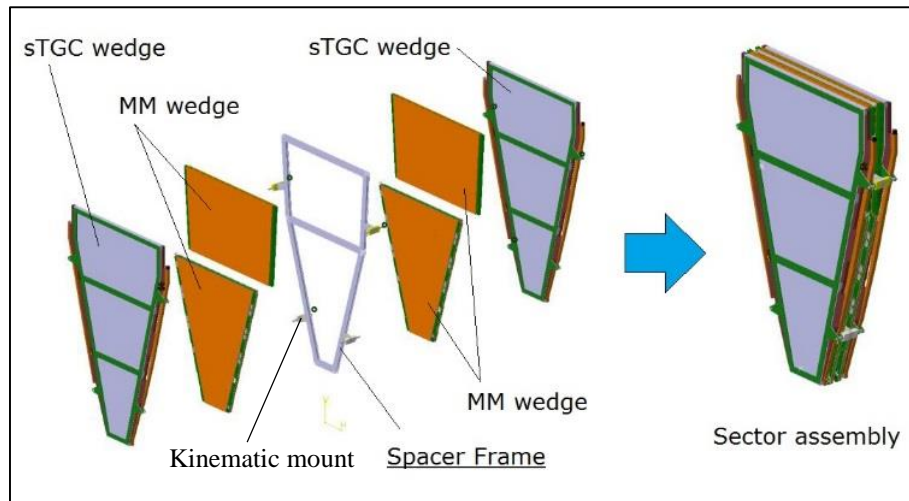


Figure 2-3. Make up of NSW sectors (Ponsot & Spigo, 2015).

The LS weighs 1450 kg and this weight is evenly distributed throughout its volume; constant density can be assumed. The LS has a height of 3725 mm and a maximum width of 2376 mm. A fully assembled LS is 404 mm thick from sTGC frame-to-sTGC frame. The shape of a LS is shown in Figure 2-4 (Ciapetti & Spigo, 2014).

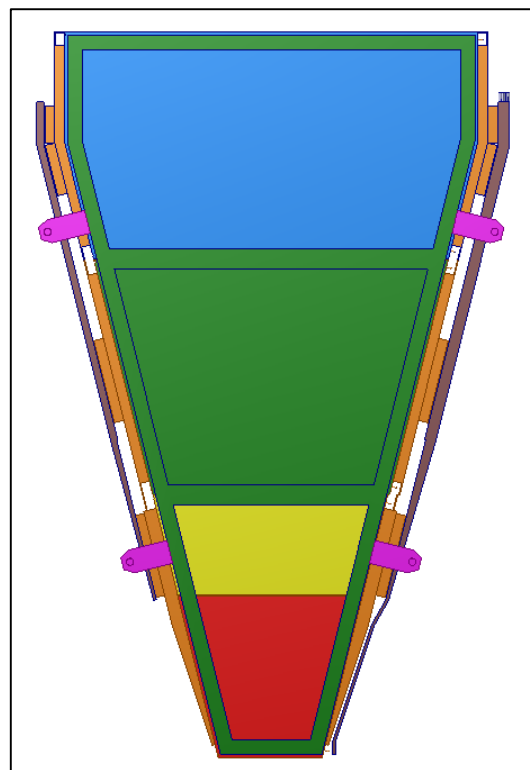


Figure 2-4. Front view of the NSW large sector (Ciapetti & Ponsot, 2015).

2.1.2 Small sector

The SS shares the same layer composition and therefore has the same thickness as the LS, however with different frontal dimensions. The SS is also 3725 mm high, yet its maximum width is only 1785 mm. The SS weighs 1100 kg as a result and is also assumed to have constant density throughout its volume. The SS has a simpler triangular shape as seen in Figure 2-5 (Ciapetti & Spigo, 2014).

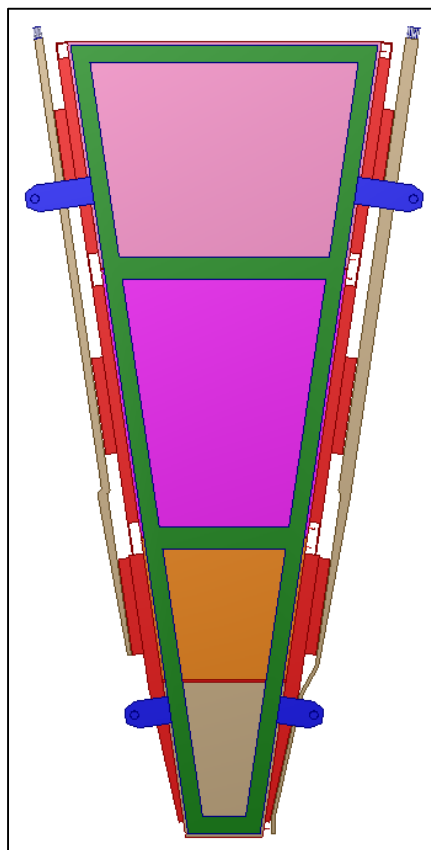


Figure 2-5. Front view of the NSW Small sector (Ciapetti & Ponsot, 2015).

2.1.3 Foot spoke

The Foot spoke is a modified small spoke that has a mount to the ground. The purpose of this is to support the cantilevered hub of the NSW as both the Large and Small sector layers attach to the hub. There are two Foot spokes per NSW. All standard Small spokes are made completely of aluminium, but since the Foot spokes need to support the additional weight, certain profiles are manufactured from 316L stainless steel. The reason for using this particular grade of stainless steel is its non-magnetic properties, so that it will not interfere with the magnet systems of the detector or alter particle paths. The Foot spoke weighs 1000 kg and is asymmetrical unlike the standard spoke. In addition to supporting the hub and providing an interface for the Small sectors to mount on, the Foot spoke also holds an alignment bar used to adjust sectors when the wheel is assembled. Each Foot spoke has the alignment bar mounted at different positions, therefore the COG of each spoke is not the same. Figure 2-6 shows the left Foot spoke viewed from the outside of the collider (Ciapetti, et al., 2015).

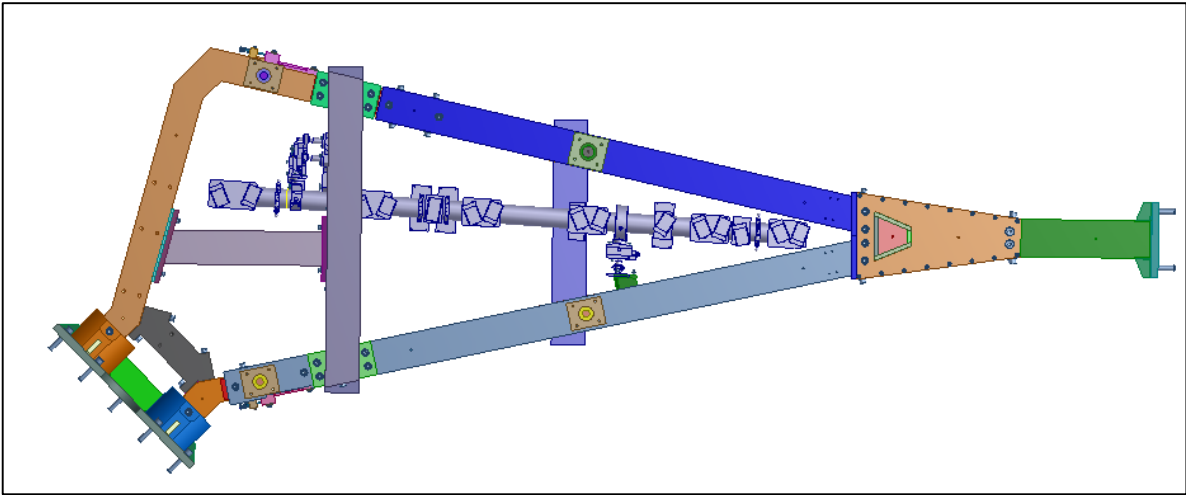


Figure 2-6. Foot spoke of NSW (Ciapetti & Ponsot, 2015).

2.1.4 Kinematic mounts for large and small sectors:

The large and small sectors connect to their respective spokes by means of kinematic mounts. The sTGC modules also connect to the sector spacer frame by means of kinematic mounts. There are 3 types of mounts for each sector; a spherical fixed joint, a guide and a fork. Depending on the sector's orientation, the kinematic joints will be placed at varying positions for the most appropriate weight distribution and adjustment access. The use of these kinematic mounts allow for the necessary translation of each sector with a fine enough resolution to make appropriate alignments. Figure 2-7 shows the three different types of kinematic joints used (Cattai, et al., 2014).

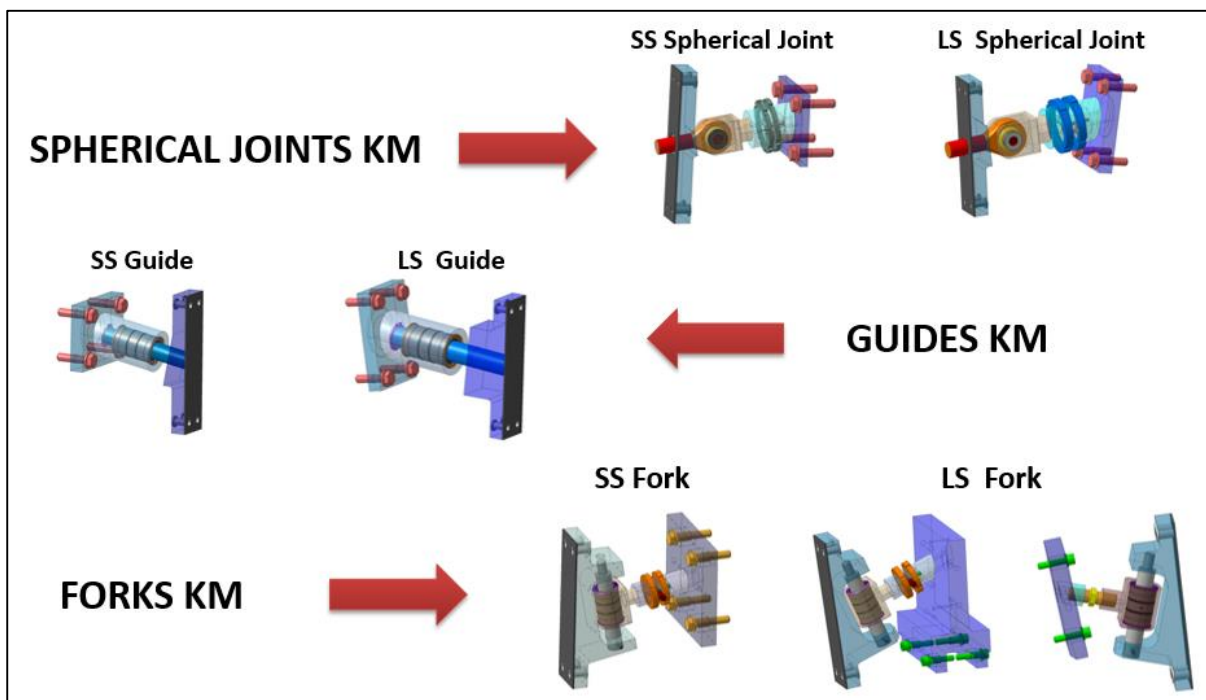


Figure 2-7. Kinematic joints used for sector and sTGC mounting and alignment (Cattai, et al., 2014).

2.2 Installation Tooling

2.2.1 Types of installation toolings

The assembly site for the NSW, Building 191 at the Meyrin site of CERN has a large 140 ton overhead crane and a smooth concrete floor. This leaves two possibilities for the nature of the installation tooling design. The tooling can either be hoisted or made to travel along the ground (Ponsot & Spigo, 2015).

A hoisted tooling would need a counter weight and a central beam about which the tooling can be balanced about the hoist point as shown in Figure 2-8 (University of Wisconsin, 2001).

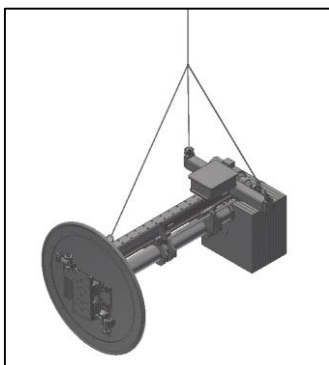


Figure 2-8. Balanced hoist tooling (University of Wisconsin, 2001).

A floor based tooling can take the form of a modified forklift with a jib interface. Here the actual forklift is used as the counter weight and can accommodate a large range of component masses. Figure 2-9 shows a conventional forklift with a bolt-on jib attachment (BAHRNS, 2010).



Figure 2-9. Forklift with Jib attachment (BAHRNS, 2010).

2.2.2 Wisconsin Tooling

The Wisconsin Tooling is the current installation tooling used for sectors, wedges and chambers for the ATLAS and CMS experiments. It was designed, manufactured and tested in 2001 by the University of Wisconsin in Madison Wisconsin USA, from which it gets its name. The Wisconsin Tooling is a hoist type tooling that utilises an overhead crane for operation. Its functional features include counter balance adjustment for various weights, sector rotation and sector centre-of-gravity translation adjustment. This

allows a wide range of components to be installed within its maximum weight range of 400 kg. Figure 2-10 shows the Wisconsin Tooling installing a gas chamber in the CMS assembly (University of Wisconsin, 2001).

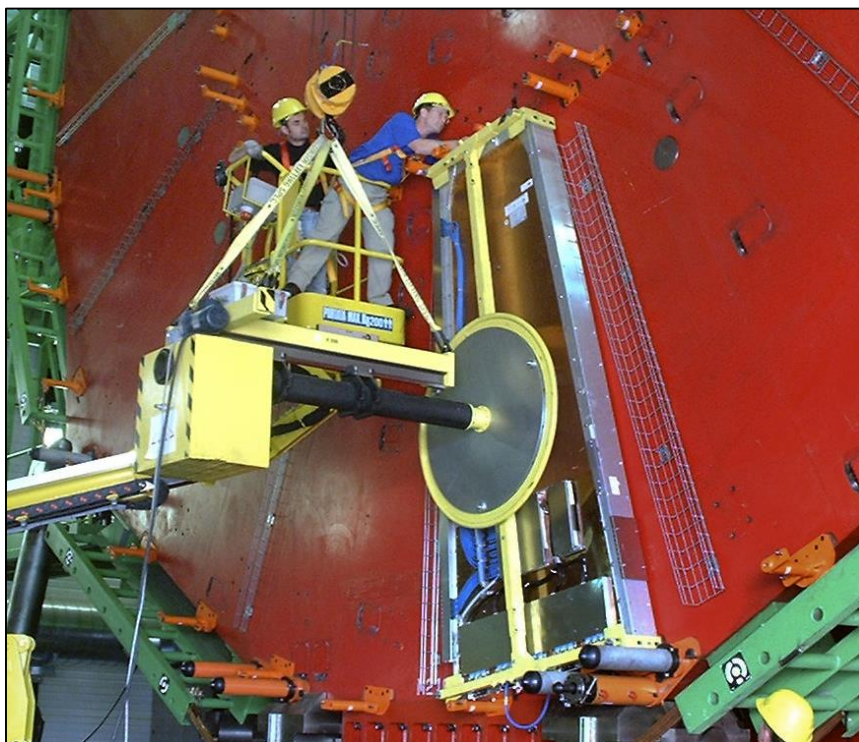


Figure 2-10. Wisconsin Tooling installing sector on CMS (Ponsot, 2014).

The Wisconsin Tooling has become a beneficial asset to CERN due its robustness and versatility. It set the benchmark for many other fixed weight toolings that were designed for specialised environments at CERN.

Technical details and review of the Wisconsin Tooling occurs in Chapter 3 of this dissertation.

2.3 The Finite Element Analysis (FEA) procedure

Finite Element Analysis, as described in the Engineering Computational Methods notes prepared by Jean Pitot in 2011, is a particular branch of computational analysis that specifically deals with simulating mechanical and thermal stresses that components experience when under a particular load. FEA has become increasingly important as it offers a way to accurately find solutions to problems that may not have linear analytical solutions and to a degree of accuracy that is often not feasible by experimental or analytical approaches (Pitot, 2011). In addition it offers greater flexibility and efficiency than experimental methods and has become accepted and often a legal requirement for engineering design.

The basic principle of computational analysis is commonly explained by the black box. The black box orders the various components of computational analysis. The first component is the mathematical models which are an assemblage of governing equations which define the physical parameters of the problem at hand. The next component is the numerical methods that solve these mathematical models by providing solutions. Lastly are the hardware and software components which offer the computing ability and protocol or instructions to carry out the calculations respectively. Figure 2-11 show a simple schematic of how these components are utilised to achieve the desired results (Pitot, 2011).

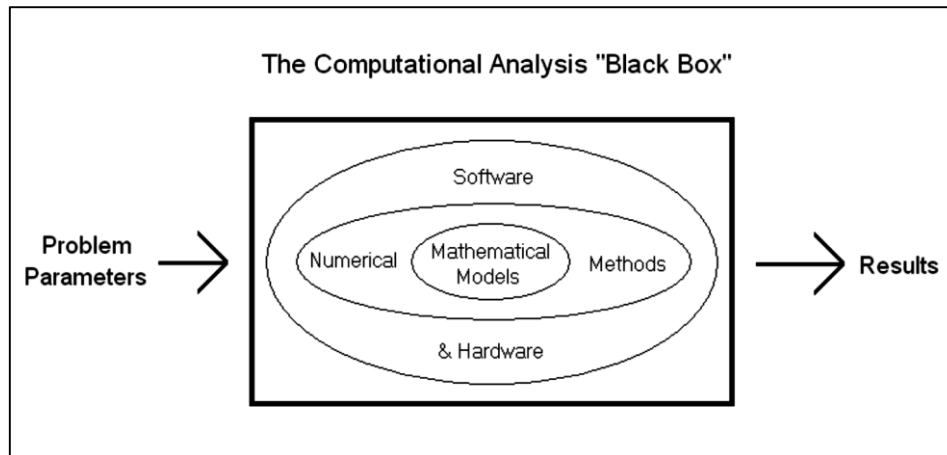


Figure 2-11. Basic schematic of the Black Box (Pitot, 2011).

The software utilised to conduct the FEA in this dissertation is ANSYS Workbench R15.0. ANSYS Mechanical provides a FEA package that makes use of the Finite Element Method.

2.3.1 Discretisation

Discretisation is the concept that represents a continuous function by a number of discrete points that can be achieved analytically. Discretisation only gives solutions at certain points in the domain and can therefore be used to approximate a continuous function. Figure 2-12 gives a graphical representation of discretisation. The function $f(x)$ is the continuous solution to an arbitrary stress calculation and $f'(x)$ is the discretised function. x_1 , x_i and x_n all show discrete points. x_i corresponds to y_i' at the discrete point and to y_i on the continuous function (Pitot, 2011).

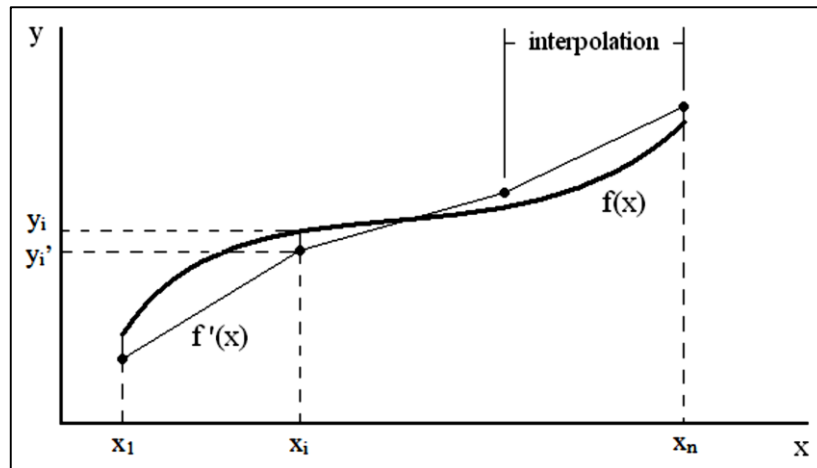


Figure 2-12. Graph showing visual representation of discretisation (Pitot, 2011).

Discretisation is the fundamental principle of how computational analysis can solve a complex problem in small and simple discrete steps.

2.3.2 Finite Elements

In order to run the mathematical models and equations on the component, the component geometry must first be divided into small and roughly homogenous elements (discrete points) as mentioned. This is done so that a component of complex geometry can be broken down into simple shapes therefore making the processing of calculations on each element simpler to complete and more accurate. A general rule is that the finer the mesh or element density, the greater degree of accuracy. This however is proportional to computational time. The finer the mesh, the greater the processing time due to the greater number of calculations that need to be done. There is a point where a critical mesh density is reached; any finer will not improve the result accuracy. This point is called the mesh independence point. It is the optimum way that a model should be run to ensure the greatest accuracy at the best available computational efficiency. Figure 2-13 shows a visual description of mesh independence (Pitot, 2011).

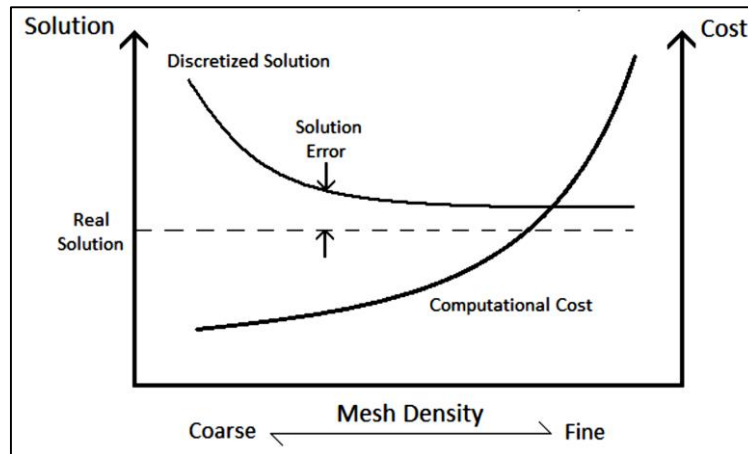


Figure 2-13. Approaching the point of mesh independence (Pitot, 2011).

2.3.3 Governing equations for computational solid mechanics

The governing equations allow the behaviour of a component in response to a load to be monitored. The three points of interest for FEA are usually displacement, stress and strain. To obtain these results there are three main governing equations that are used namely; the equilibrium equation, the compatibility equation and the constitutive equation (Pitot, 2011).

The equilibrium equation is expressed by:

$$\text{div}\{\sigma\} + \{F\} = \rho\{\ddot{u}\} \quad (1)$$

From the equation div is the divergence operator, $\{\sigma\}$ is the stress tensor for normal and shear stresses, $\{F\}$ is the force vector, ρ is the density of the material and $\{\ddot{u}\}$ is the second derivative of the displacement with respect to time, therefore the acceleration vector. The equilibrium equation is a form of Newton's second law. The equilibrium equation serves to balance the forces experienced by the body by summing the internal and body forces to obtain the inertial force.

The compatibility equation is expressed by:

$$\{\varepsilon\} = \frac{1}{2}(\text{grad}\{u\} + (\text{grad}\{u\})^T) \quad (2)$$

In this equation $\{\varepsilon\}$ is the strain tensor and grad is the gradient operator on the displacement vector $\{u\}$ which accounts for displacements in both the translational and rotational directions. The purpose of the compatibility equation is to determine strains experienced by the volume by means of the change of displacements.

The constitutive equation is expressed by:

$$\{\sigma\} = [C] \{\varepsilon\} \quad (3)$$

The term $[C]$ is the stiffness matrix that contains the relevant elastic and shear moduli. The stress tensor of the constitutive equation is common with the equilibrium equation and strain is common with the compatibility equation. The constitutive equation is also known as Hooke's Law. The purpose of this equation is to determine the stresses induced in the volume based on the strain tensor and the stiffness matrix. The term $[C]$ is Young's Modulus term and therefore this can only apply for the linear elastic region of materials.

These equations feed directly into the finite element method (FEM). A complex geometry volume is discretised into elements and governing equations are applied to each individual element. Each element has a node its corners. These nodes each have their own displacement vectors for the six degrees of freedom; three directions of translation and three directions of rotation. Figure 2-14 shows the node of a 2D element with the displacement vector (Pitot, 2011).

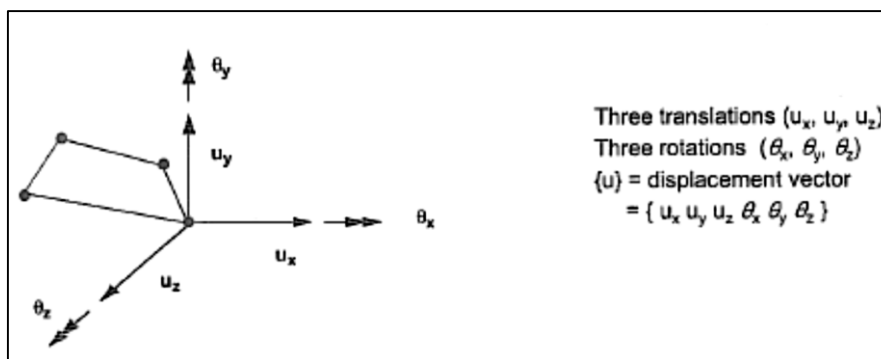


Figure 2-14. Displacement vector $\{u\}$ of a node (Pitot, 2011).

The interaction of an element with other nodes is given by an expression known as the Elemental equation:

$$[k]_e \{u\}_e = \{f\}_e \quad (4)$$

This is a form of the Equilibrium equation, specifically one describing a spring experiencing an external force. The term $[k]$ is the elemental stiffness matrix derived from the element geometry and material properties. $\{f\}_e$ is the elemental load vector and $\{u\}_e$ is the elemental displacement vector which shows the movement of the nodes in response to an applied load. The displacement vector is the unknown of the equation.

The elemental stiffness and load vectors are then assembled to form a global stiffness and load vector denoted by:

$$[K]\{u\} = \{F\} \quad (5)$$

Each individual element is therefore linked together by common nodes to achieve the global mesh as seen in Figure 2-15 (Pitot, 2011).

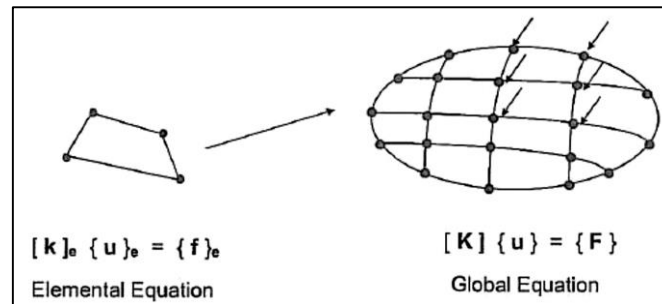


Figure 2-15. Assemblage of elemental equations to achieve global equation (Pitot, 2011).

The final step is applying the constraints or boundary conditions which acts to restrict a type of movement of certain nodes. This must allow the equations to be calculated without rigid body motion, an otherwise result of an under-constrained body. Figure 2-16 shows a body with a boundary condition and load applied denoted by arrows.

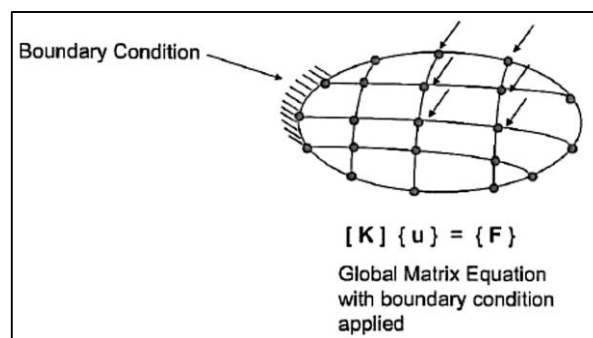


Figure 2-16. Global matrix with load and constraint (Pitot, 2011).

Once these actions are complete the global equation can be solved to determine the individual nodal displacements. Based on these displacements the relevant governing equations can be used to determine the element stresses and strains.

2.4 Nonlinear FEA

A simulation model is said to be nonlinear if the loading causes significant changes in stiffness. There are three main reasons that stiffness changes and causes nonlinearities: A body experiences large geometric deformation, the material is stressed beyond its linear elastic region and if loading causes bodies to come into contact with each other. In a nonlinear analysis where one or more of these cases are present, the response cannot be calculated directly with the linear equations. They can however be analysed by using iterative series of linear approximations with corrective terms (ANSYS Inc, 2013).

2.4.1 Newton-Raphson Method

The Newton-Raphson method is an iterative process used by ANSYS Mechanical to compute nonlinear analyses (ANSYS Inc, 2013). Each iterative step performed is known as an equilibrium iteration. Figure 2-17 shows a full Newton-Raphson iterative analysis for an increment of a load; it shows four iterations.

The relationship between the load F and displacement x , the dotted line, is not known beforehand. For the Newton-Raphson method, the total load F_a is applied in the first iteration. This results in a displacement of x_1 . Based on the displacements, the internal force F_1 can be calculated. If $F_a \neq F_1$ then the system is not in equilibrium and a new stiffness matrix is calculated based on the conditions and represented by the dotted line. The difference between F_a and F_1 is called the residual. The residual must be acceptably small enough before the solution is said to be converged. The process is repeated until an iteration will give a small enough residual at which point the system is in equilibrium and converges (ANSYS Inc, 2013).

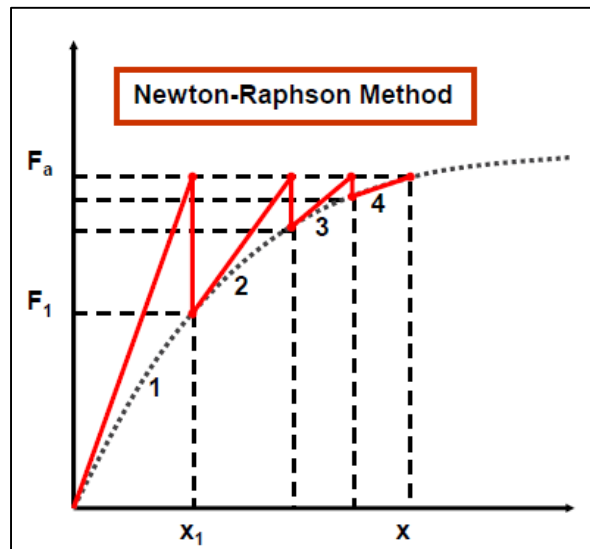


Figure 2-17. Newton-Raphson iteration of load increment (ANSYS Inc, 2013).

2.4.2 Radius of convergence

The Newton-Raphson method will not always converge. For a solution to converge, the starting configuration must lie within the radius of convergence. The radius of convergence is best understood visually as in Figure 2-18 . If the initial configuration is too far from the real solution, the calculated solution will diverge. If however the initial configuration starts within the radius of convergence, the calculated solution will approach the real solution after iterations that factor in the residuals (ANSYS Inc, 2013).

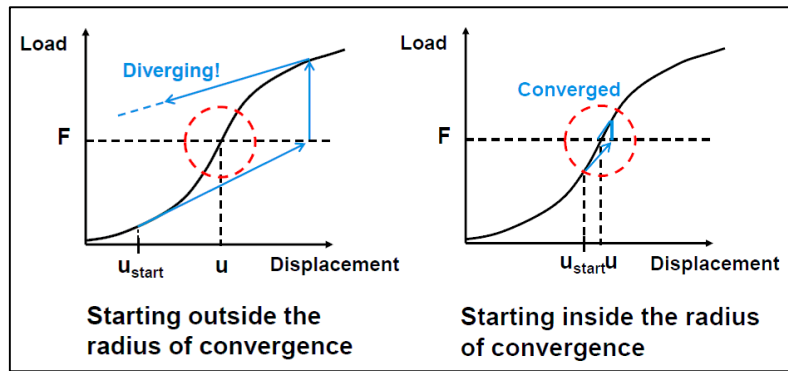


Figure 2-18. The radius of convergence around real solution (ANSYS Inc, 2013).

ANSYS Mechanical uses two tools to aid the initial configuration in falling within the radius of convergence. The first method is to apply the load in increments which effectively moves the target closer. Another method utilises convergence-enhancement tools which act to enlarge the radius of convergence, hence making the initial configuration more likely to lie inside it (ANSYS Inc, 2013).

2.5 Basic overview of ANSYS Workbench and ANSYS Mechanical

ANSYS 15 was utilised to conduct the FEA for the components in this dissertation. There are three main environments with the ANSYS package that are used for these simulations.

2.5.1 Workbench layout

The Workbench environment of ANSYS is the graphic interface where the particular type of simulation is configured. CAD models are imported at this point and materials properties can be assigned. This allows relevant strengths, densities and fatigue cycle properties from the ANSYS Material library to be selected. Most of the functions in this environment are geared towards user friendliness and therefore incorporates many drag-and-drop interfaces. Figure 2-19 shows an example of an ANSYS Workbench with a number of static simulations open. A significant feature of the Workbench is that it allows the user to link results, models and constraints from one simulation directly into another. This leads to streamlined analyses without having to repeat the time intensive setup of a common model or desired result. This is seen by the arrow that feeds from one simulation block into another (Sciuccati, 2015).

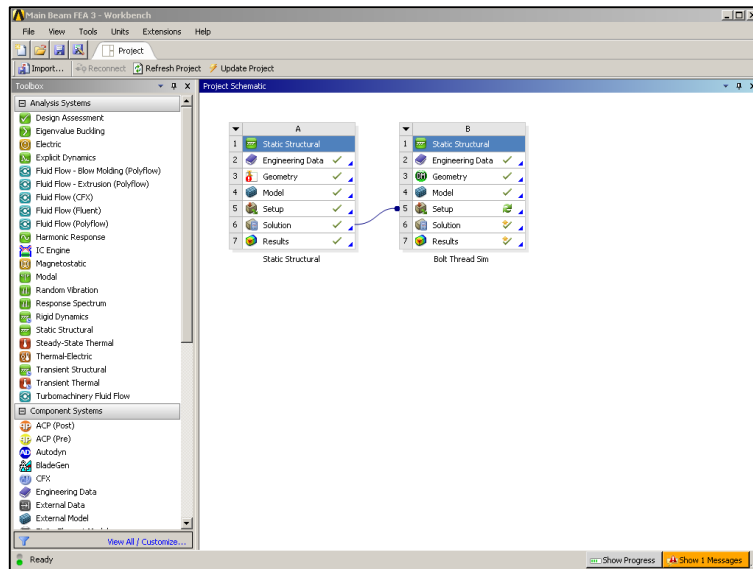


Figure 2-19. ANSYS R15.0 Workbench layout.

2.5.2 Design Modeller

ANSYS has a built in CAD modelling and editing environment called Design Modeller (DM). The DM environment can be used to develop the CAD models for simulation, however complex geometry can be quite challenging compared to other standalone CAD packages like Autodesk Inventor or Solidworks. The DM is usually used for tweaking imported models as certain simulations need preparation for specialised cases. The DM has specific editing tools that are not common on the stand alone packages for these cases and is therefore an important environment. A benefit of using the DM is that all references and coordinates appear precisely, once the Mechanical environment is entered, which is not always the case when an external model is imported. Figure 2-20 shows the basic DM layout.

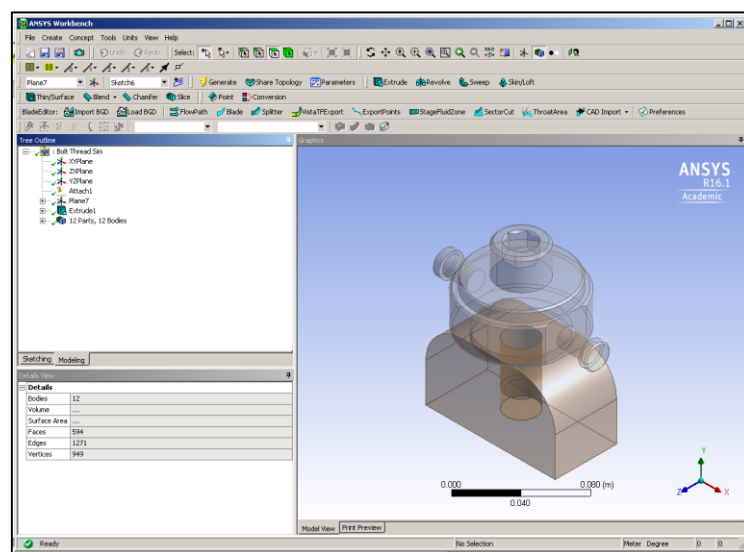


Figure 2-20. ANSYS R15.0 Design Modeller layout.

2.5.3 Mechanical layout

The ANSYS Mechanical environment is where the model is setup. Here individual material properties are applied to parts. Bodies are meshed and boundary conditions in the forms of fixtures or loads are applied sequentially. When model is ready to be simulated, an execution function sends the model data to the solver. During the solving process the convergence can be monitored and minor adjustment can be made on the run. Once the solving process is complete, the results are returned to the Mechanical environment. Here particular types of stresses, strains, displacements and other factors can be examined. The bottom window of the environment displays all messages of the model status and will return any errors or failures. Figure 2-21 shows the basic Mechanical layout with the project tree in the left pane.

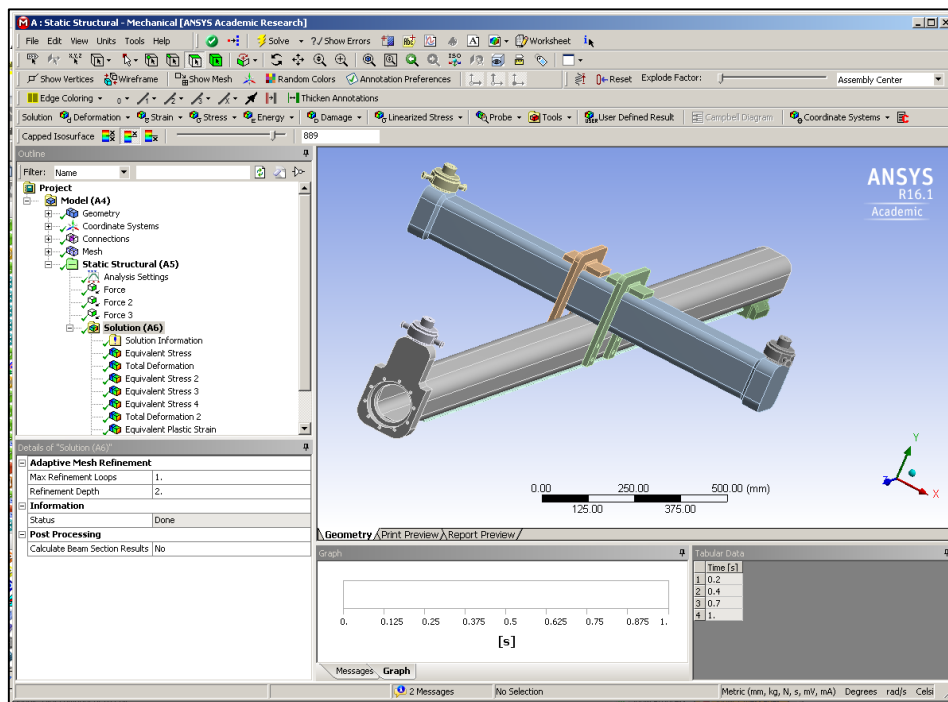


Figure 2-21. ANSYS R15.0 Mechanical layout.

2.5.4 ANSYS Solvers

The solver is responsible for extracting that material, elements, loads and boundary conditions from the model environments and carrying out the actual calculations. Here it will apply the relevant calculation either directly or iteratively, depending on whether the analysis is linear or nonlinear, and then feed the information back into the model environment to be displayed as results. ANSYS makes use of two types of solvers namely the Direct Sparse Solver (DSS) and the Preconditioned Conjugate Gradient Solver (PCG) also known as the Iterative solver. These form a reference as to which method is used to build each stiffness matrix for every Newton-Raphson iteration (ANSYS Inc, 2013).

The DSS is more robust and generally selected for complex nonlinear models and specifically for non-continuum type elements. This solver is therefore quite computationally expensive.

The PCG (Iterative) solver is far more efficient than the DSS with regards to run time and computational resources and is therefore normally used for models that do not exceed the linear elastic region.

ANSYS Mechanical has the ability to automatically select which solver would be most suitable, however manual selection of a solver guarantees accurate results when the degree of nonlinearity is known.

2.6 Stress relief grooves

Stress concentrations occur in various areas of component design. These are often in the form of holes, notches and shoulders. A stress concentration can arise from either a sharp point or edge of one part coming into contact with another or a sudden change in a component geometry. Figure 2-22 shows a shaft experiencing a bending load. The shoulder is a sudden change in geometry and therefore it is seen that the force lines bend from the smaller diameter section to the larger diameter section. The force lines bunch closer at the shoulder and therefore the stresses increase at this point (Peterson, 1953) (Spigo, 2015).

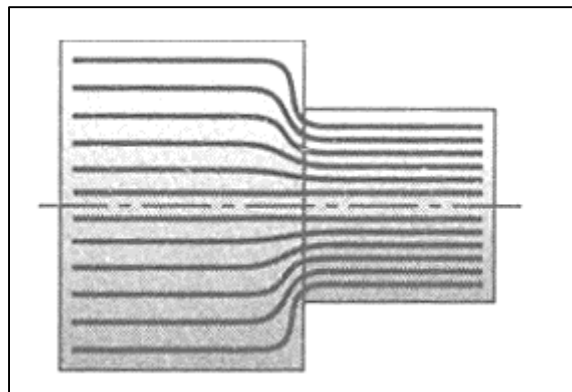


Figure 2-22. Force flow lines through a shaft shoulder (Schwalb, 2014).

A common method of alleviating such concentrations is the inclusion of a gradual radius at the point of sudden change. This gradual change allows the force lines to transition from one diameter to the other without a large degree of bunching (Spigo, 2015). Figure 2-23 shows how a radius on a shaft allows the flow lines to transition without as much bunching as Figure 2-22. The radius allows more material at the step point through which flow lines can travel (Peterson, 1953).

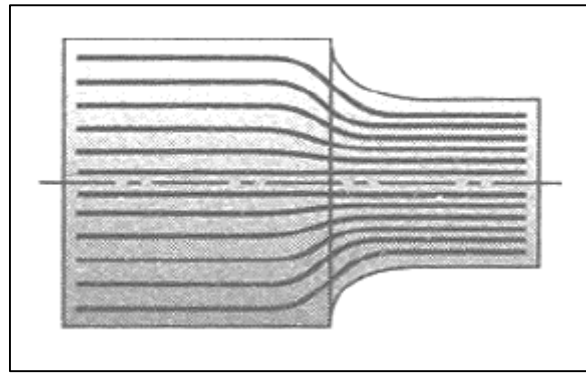


Figure 2-23. Force flow lines through shaft with radius at step (Schwalb, 2014).

In severe cases of loading a simple radius may not be sufficient in lowering the stresses to an acceptable level. For these cases another type of mechanism called stress relief grooves can be implemented. Stress relief grooves differ from the principle of reducing stress from introducing a radius. Instead of introducing more material to allow flow lines to travel through, material is removed in a particular fashion to curb flow lines away from a point of bunching. Figure 2-24 shows a comparison between a standard shaft shoulder and a grooved shaft. The force flow lines behave in a similar fashion to the shaft with a radius, except here material was removed. By choosing the optimum shape, size and position of the stress relief groove, the peak stresses can be significantly decreased (Schwalb, 2014).

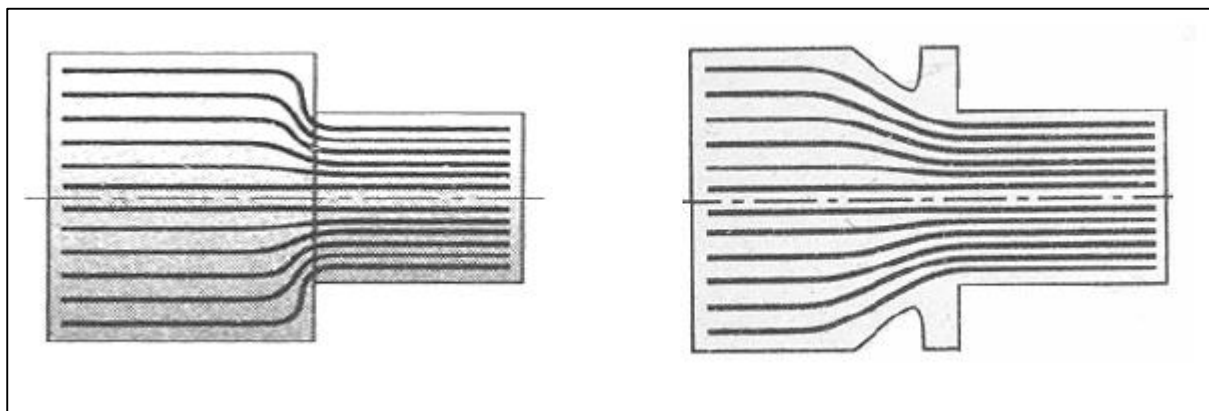


Figure 2-24. Stress relief groove effect on force flow lines (Schwalb, 2014).

2.7 Mechanical design philosophy

2.7.1 Euro-code compliance

All structures, machinery and design based components manufactured for use at CERN need to comply with the *European Committee of Standardization* rules (Ponsot & Spigo, 2015). These rules, called *Eurocode*, are harmonized standards for a broad range of engineering applications to ensure safety and longevity of manufactured components. The particular *Eurocodes* adhered to in this dissertation for the NSW Installation Tooling are standards EN1993.1.8.2005 - *Design of Joints*, EN1993.1.11.2006 - *Design of Structures with Tension Components* and EN1993.1.12.2007 – *General Rules for High*

Strength Steels. These standards all form part of *Eurocode 3* (European Committee for Standardization, 2005).

2.7.2 ATLAS Good Practice

CERN adheres to standards in addition to the Eurocode (Ponsot & Ciapetti, 2015). Specifically with cranes and lifting equipment, compliance with the relevant British Standards (BS) must be met, set by the *British Standards Institution (BSI)*. CERN have specially prepared documents by *Association Française de Normalisation (AFNOR)* with the exact BS that have been adopted for the organisation's good practice protocols. The particular standard adhered to in this dissertation for the compliance of the NSW Installation Tooling is BS EN 13155:2003+A2, amended August 2003, titled *Cranes – Safety – Non-fixed load lifting attachments*. The most significant aspect of this standard towards the design was adherence to section 5.1.1.1 for mechanical load bearing parts. This section states that all load bearing parts of the design must have a safety factor of at least 2 before permanent deformation. Figure 2-25 shows an extract of the particular standard stating the safety factor (The British Standard Institution, 2010).

<p>5.1.1 Mechanical load bearing parts</p> <p>5.1.1.1 The mechanical load bearing parts shall have a mechanical strength to fulfil the following requirements:</p> <ol style="list-style-type: none">1) the attachment shall be designed to withstand a static load of three times the working load limit without releasing the load even if permanent deformation occurs;2) the attachment shall be designed to withstand a static load of two times the working load limit without permanent deformation.
--

Figure 2-25. Section 5.1.1 of BS EN 13155:2003+A2 (The British Standard Institution, 2010).

Chapter: 3 Design approach

This chapter describes the structured method in which the design process was carried out for the NSW Installation Tooling. The first step was to understand the functional requirements and system constraints as per initial design brief from ATLAS Technical Coordination. The previous installation tooling was then analysed to learn its principle of operation, effectiveness and areas that could be improved. Lastly the overall design methodology was presented showing the step-by-step procedure of how decisions was carried out.

Since the design of the actual NSW sectors was finalised simultaneously with the design of mechanical toolings and structures, an ongoing change of design requirements must be anticipated.

3.1 Functional requirements and system constraints

The functional requirements for the NSW installation tooling is as follows as per design brief (Ponsot & Spigo, 2015):

- Attach to small and large sectors by means of a small and large grabber from storage tooling, without interference
- Attach to foot spoke by means of a dedicated foot spoke grabber from storage tooling
- Adjust the centre of gravity of the tooling to compensate for a crane lift of various weighted sectors, spokes or grabbers
- Adjust the orientation of each sector or spoke by allowing rotation at the grabber's centre
- Adjust the centre of gravity of the sectors and foot spoke to allow for free rotation by hand
- Rotate each sector or spoke to correspond to their individual installation orientations
- Transport the sector or spoke to its position on the NSW structure and JD disk
- Adjust the crane hook balance to remove the tooling after sector or spoke has been installed to avoid uncontrolled tooling behaviour
- Must be storable on a suitable support structure

The set of system constraints as per design brief (Ponsot & Spigo, 2015):

- The materials of manufacture must withstand the NSW assembly operation period without structural failure due to varying loads, thermal effects and humidity in the assembly and storage areas
- The envelope of the tooling should not violate relevant system envelopes, thus preventing interference with other parts of the NSW assembly or surrounding environment
- All sector and spoke grabber positions should be suitable for all steps of installation and logistic procedures

- Tooling must comply with the European norms of EN – 13155 which requires a CE certification manual

The design description requires a versatile installation like the Wisconsin Tooling, but for a suitable capacity for the NSW components. The approach would be to develop a concept that addresses this change as well as improve any limitations of the Wisconsin Tooling concept of operation.

3.2 Review of existing design

The Wisconsin Tooling has many traits and features that have made it successful at carrying out the tasks it was designed for. It was therefore essential to study its design to see what aspects of it could be incorporated, improved and replaced for the new installation tooling.

3.2.1 Layout of Wisconsin Tooling

The Wisconsin Tooling is made up of 4 main sections; the rotating head, the main stationary beam, the moving hoist beam and the counter weight assembly. Each section is connected to each other in unique ways for functional purposes as seen in Figure 3-1. The rotating head assembly is connected to the stationary beam by means of a trunnion assembly. This allows the rotating head, and by extension the grabber and sector/chamber, to be rotatable through 360° relative to the rest of the tooling. The counter weight assembly is directly bolted onto the main stationary beam by friction bolts and restricting collars. This ensures the counter weight slices will not slide or move in any way relative to the main beam. The hoist beam is connected to the main beam by linear guides. This allows them to slide relative to each other along their lengths. This movement is critical to the counter balance adjustment of the entire tooling.

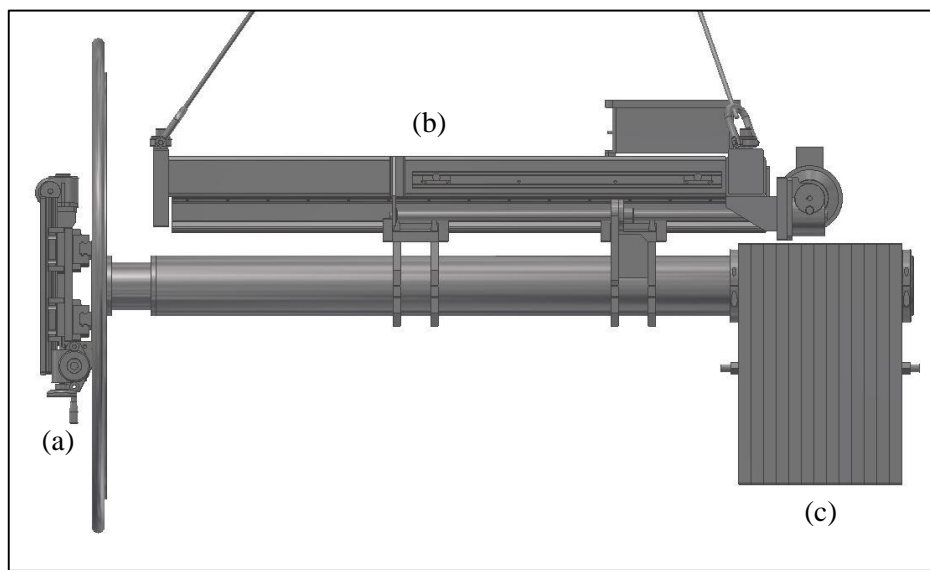


Figure 3-1. Wisconsin Tooling Setup showing (a) the rotating head, (b) the main beam and (c) the counter weight assembly (University of Wisconsin, 2001).

3.2.2 Principle of operation

The tooling is designed to install a sector or chamber with a maximum weight of 400 kg. It can manipulate a wide weight variety under this maximum due to its adjustable mechanism of altering the counter balance. This feature is also critical in the installation process of a single sector or chamber, not just to accommodate different components. The Wisconsin Tooling uses a unique approach to achieve this adjustment.

The basic principle of operation is as follows:

1. Tooling is lifted from storage stand
2. Overhead crane moves tooling to sector storage tooling
3. Tooling is fastened to sector
4. Overhead crane and tooling motor are simultaneously actuated to adjust COG for attached sector
5. Fasteners holding sector to sector storage tooling are removed
6. Overhead crane moves tooling away from sector storage tooling
7. Sector COG is adjusted by translation (if needed)
8. Sector is rotated to required orientation
9. Tooling is moved to position the sector in sector support frame work
10. Sector is fastened to frame work
11. Counter weight is adjusted by means of crane and tooling motor to make tooling balanced when sector is removed
12. Sector is loosened from tooling and overhead crane moves tooling away

Figure 3-2 shows the adjustment of the tooling by means of translation between the hoist and main beam along the linear guides. This is achieved by motor driving a ball screw causing the linear actuation.

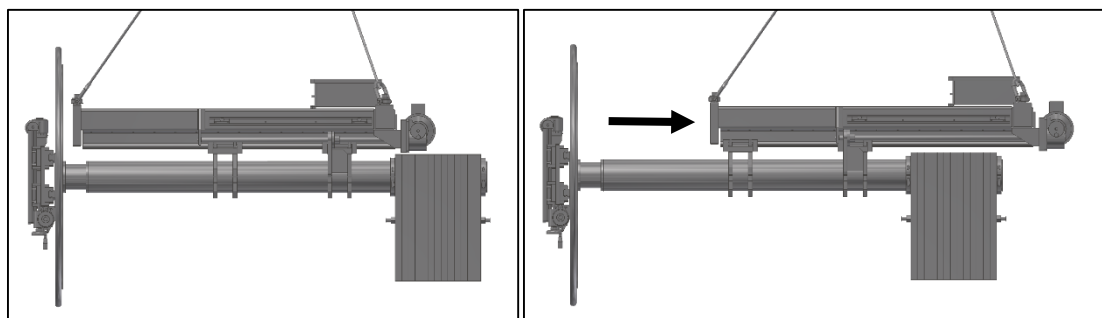


Figure 3-2. Adjusting balance of Wisconsin Tooling (University of Wisconsin, 2001).

This simplified procedure for installing a sector is fairly straight forward and sequential except for steps 4 and 11. Here it can be seen that both the overhead crane and tooling motor need to be simultaneously actuated. These steps require precise coordination between the speed of these two motors as failure to do so can result in severe damage to the critical sectors as well as the sector structure. The crane driver

has to communicate with the tooling controller technician via two way radio and attempt to achieve this high level of synchronisation. This step is therefore significantly time consuming and risky.

To address this issue the new design would have to eliminate the need for this precision based synchronisation.

3.2.3 Counter weight assembly

The Wisconsin Tooling uses a bank of counter weights to achieve balance of the tooling during its various loads. The bank is made up of individual weight slices that slide onto the main beam and are held in place by frictional bolts through the top as well as clamping rings on either side of the bank. Each weight slice is 610 mm x 610 mm x 31.75 mm and manufactured out of mild steel. The weight of each slice is therefore 88 kg, and 1144 kg for the entire bank of 13 slices. This method of fixture does allow for slices to be added or removed. Figure 3-3 shows the assembled counter weight bank on the main beam.

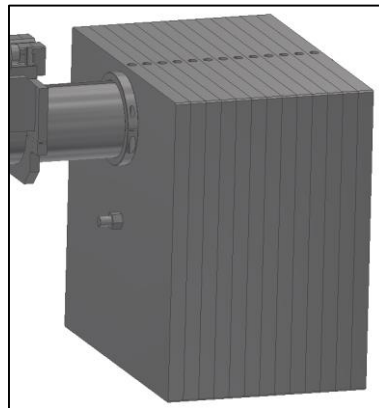


Figure 3-3. Assembled counter weight bank of Wisconsin Tooling (University of Wisconsin, 2001).

3.2.4 Overview of the rotation head and locking mechanism

The front portion of the tooling is important as it provides much of the tooling's functionality. The trunnion assembly allows the rotation, the linear guides allow COG adjustment for the sectors or chambers as well as an interface to the grabber and subsequently the sector/chamber. It also is the point where the locking mechanism is positioned. This holds the component at a particular rotational orientation for both safety and accuracy. The first aspect to inspect would be the trunnion assembly. Figure 3-4 shows the simple make up of this part. A central shaft is supported by two bearings and can be denoted as the rotating side. The bearings then sit in the trunnion coupling which is fixed onto the main beam, the stationary side. A large nut holds the shaft in place inside the machined trunnion coupling to prevent any axial movement.

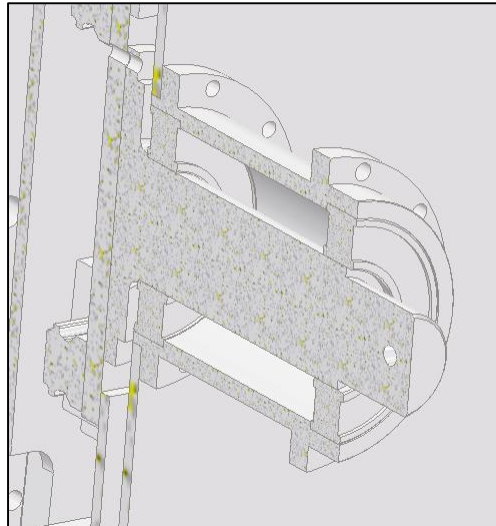


Figure 3-4. Cross section of Wisconsin Tooling trunnion assembly (University of Wisconsin, 2001).

This arrangement offers a compact, robust and mechanically simple method of fixing the rotating head to the main beam while allowing smooth rotation. The double bearing allows for bending stress to be distributed and the machined end of the trunnion collar sits inside the main beam tube to provide fixture.

3.2.5 Sector COG adjustment

Since not all sectors or chambers are made completely symmetrical in shape or weight distribution, the ability to adjust the COG relative to the tooling becomes vital in allowing easy rotation of the tooling by hand. The ability to adjust also helps deal with unforeseen changes or inaccuracies in the manufacture of grabbers or even the sector itself. The Wisconsin Tooling achieved this by utilising two set of linear guides that are hand actuated by worm gearboxes. The one set allows translation horizontally while the other offers translation vertically. The linear guides allow 40 mm of translation in either direction on each set of guides. Figure 3-5 shows the configuration in which they are mounted to the tooling rotation head.

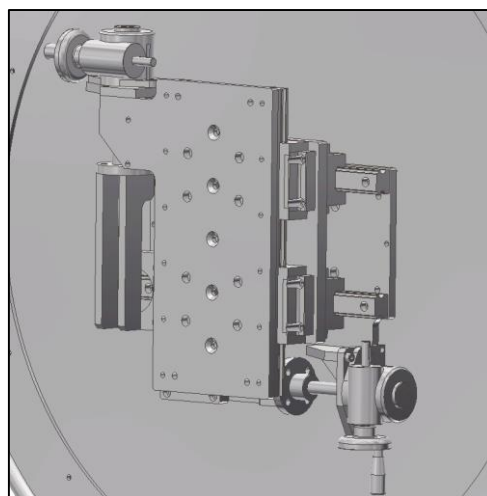


Figure 3-5. COG adjustment mechanism on Wisconsin Tooling (University of Wisconsin, 2001).

3.2.6 Motorised actuation of tooling

The Wisconsin tooling utilises a DC permanent magnet motor to actuate the hoist beam along the main beam for tooling adjustment. The large mass of the counter weight results in significant friction on the linear guides as well as direct force pushing or pulling when the tooling is not balanced. For this reason a great force is needed to actuate the tooling and in addition to this a great force is required to hold the two beams stationary even when tooling tilts. It is for this reason that the Wisconsin Tooling uses a worm gearbox. A worm gear is self-locking in nature, therefore it will hold the adjustment in place when not actuated by the motor. It also provides a high gearing ratio meaning that the motor can be small and still provide the correct torque needed by the screw. This ratio also aids in controlling the speed of actuation as fine adjustments need to be made to achieve a favourable degree of balance of the tooling. Figure 3-6 shows the toolings motor position as well as the connection to the worm gearbox and screw.

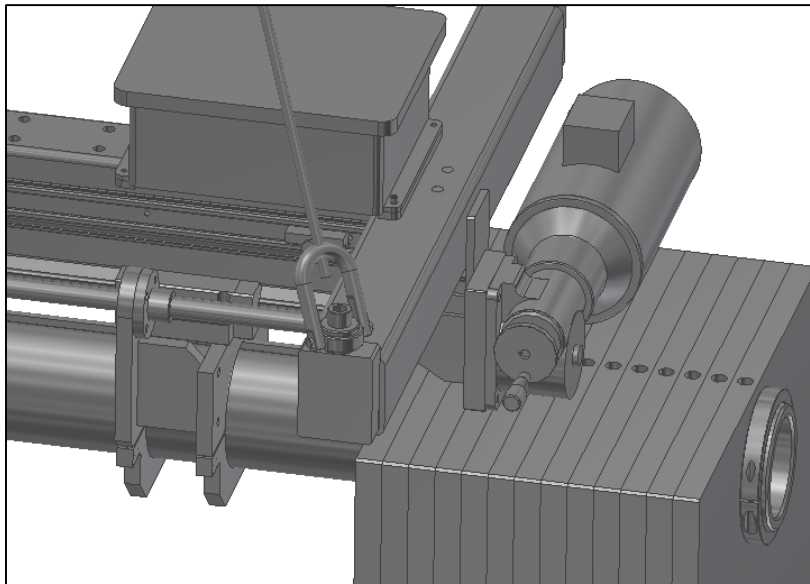


Figure 3-6. Drive actuation unit for Wisconsin Tooling (University of Wisconsin, 2001).

3.3 Proposed design methodology

The design procedure at CERN is unique from conventional design procedure, as component design is carried out simultaneously with system design directly dependant on the latest relevant system design. The designs for the sectors and spokes of the NSW were being modified while other engineering teams design services, integration and transportation toolings. This is particularly inconvenient from the installation tooling designer's perspective since the weight and spatial changes have a significant impact when setting up the delicate balance required of the tooling. It is for this reason that a non-conventional design methodology was developed.

3.3.1 Conventional design methodology for a component

Figure 3-7 shows the usual steps of the design process that would be carried for fixed functional requirements and parameters of the design brief.

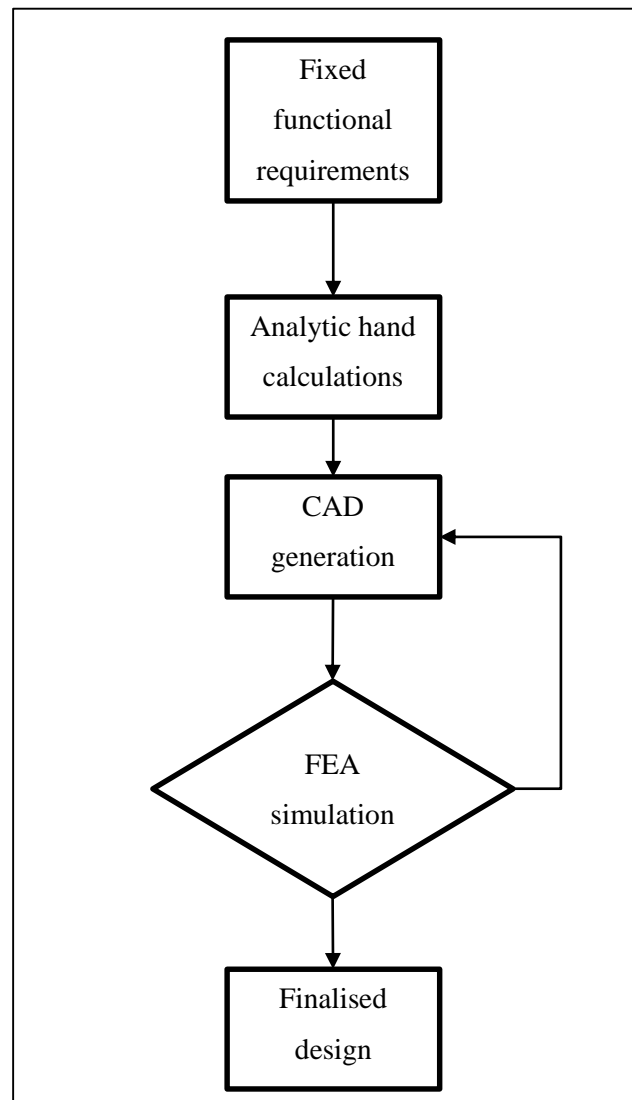


Figure 3-7. Standard component design methodology.

When the functional requirements for the design are fixed, analytical calculations can be done by hand in order to determine approximations for dimensions of the CAD design. These calculations will most likely only have to be done once therefore merely recording them is sufficient. The next step is the CAD generation of the component. Straight forward drawing procedure can be carried out in any fashion whether it be drawing from the base up or manually extruding and manipulating 3D features. Once this step is complete, the CAD geometry can be imported into the FEA package and simulation can go ahead. Based on the outcome of the simulation minor modifications may have to be made to the CAD model. Once the FEA provides satisfactory results the design can be deemed finalised.

3.3.2 Design methodology for NSW Installation Tooling

The design methodology for the NSW Installation Tooling development will need to change due to a new input in the form of system modifications or new functional requirements. Changes in functional requirements might include design modifications in the sector or spoke mass, a repositioning of services or inclusion of asymmetry in the weight distribution.

The number of times this such changes will occur, as well as the frequency and magnitude of the changes, remains unknown. For this reason the methodology of the design process must be modified. The first and most significant modification was to develop simple programs that are capable of performing the analytical equations necessary for the CAD generation. This program should have all critical information stored as input variables and should perform the relevant stress, balance and dimension equations to give the needed output for the 3D model. This way new design requirements, regardless of frequency and degree, can efficiently processed to determine the desired information without repeating the detailed and time intensive calculations manually.

The next alteration of design procedure would be the manner in which CAD models are generated. Since it is known initially that requirements could see ongoing changes, it is important to account for this when constructing the 3D models. A flexible CAD generation method should be used that allows major changes to be made to models by only changing dimensions of a few critical sketches. All extrusions and sketches should be referenced in a manner that preserves fixed dimensions based on the changes made but also automatically updates dependant positions and orientations to conform to the input.

Figure 3-8 shows the innovative design methodology to be utilised for the design procedures in this dissertation.

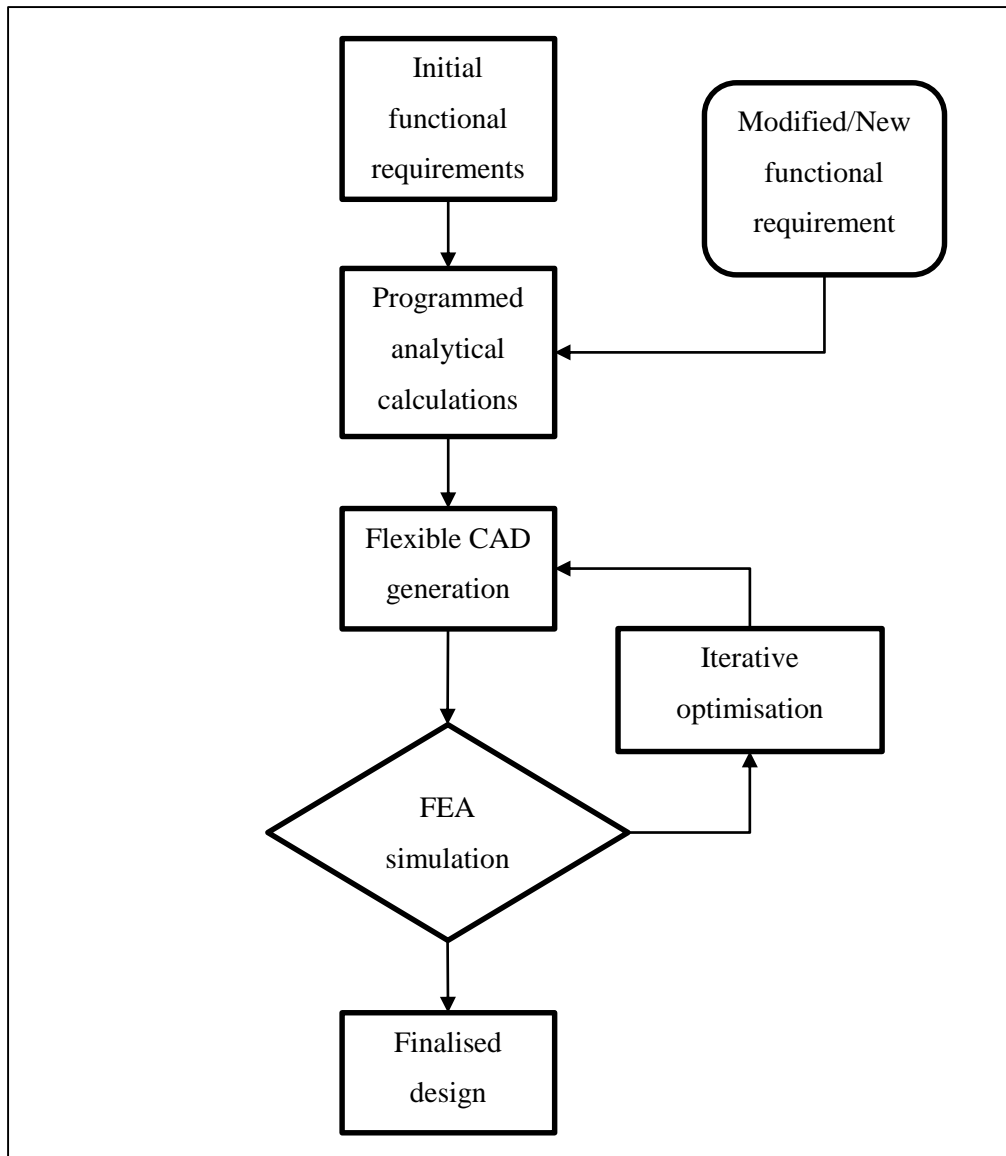


Figure 3-8. NSW Installation Tooling design methodology.

Chapter: 4 Tooling concept generation

The generation of the tooling conceptual designs are pivotal on the path to the final design. This chapter describes the early steps of the design, beginning with the critical insight into the tooling balance and principle of operation.

4.1 Principle of operation of the NSW Installation Tooling

The initial step in developing a concept for the new tooling was addressing the problem with the principle of operation of the Wisconsin Tooling. The need to synchronise the coarse crane movement with the fine tooling motor actuation was detrimental to efficient installation of sectors. It also increased the risk of damage and required additional man power and accurate coordination between operators. This was mainly due to the design including a fixed counter weight and a moving hoist. To address this problem the first conceptual drawing included a fixed hoist point with a moving counter weight as seen in Figure 4-1.

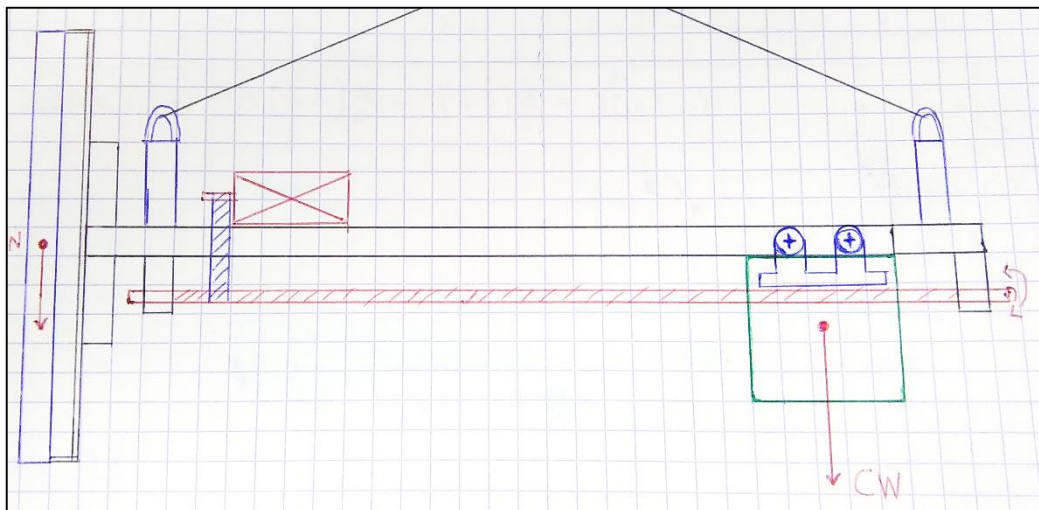


Figure 4-1. First concept of NSW Installation Tooling.

The moving counter weight would mean that when the tooling is used to install a sector or spoke and needs its balance adjusted, just the tooling motor would need to be actuated while the overhead crane can remain stationary. This system would not be dependent on any other for its operation. This would result in a quicker, safer and overall more efficient method of operation than the Wisconsin Tooling.

4.2 Tooling balance

The primary purpose of the tooling is to manipulate various components in a controlled fashion. The main aspect that controls this is the balance of the tooling. Since the tooling is supported by slings to a singular overhead crane, changing the weights at one end of the tooling affects the centre of gravity. For any load to be stable when using the tooling, the centre of gravity needs to be adjusted to ensure it remains precisely beneath the crane hoist point. Achieving tooling balance is done by accounting for

every object that exerts a moment on the tooling. By knowing the net moment about the hoist point, the position or magnitude of the moveable counter weight can be determined. A simplified diagram of the masses contributing moments is shown in Figure 4-2.

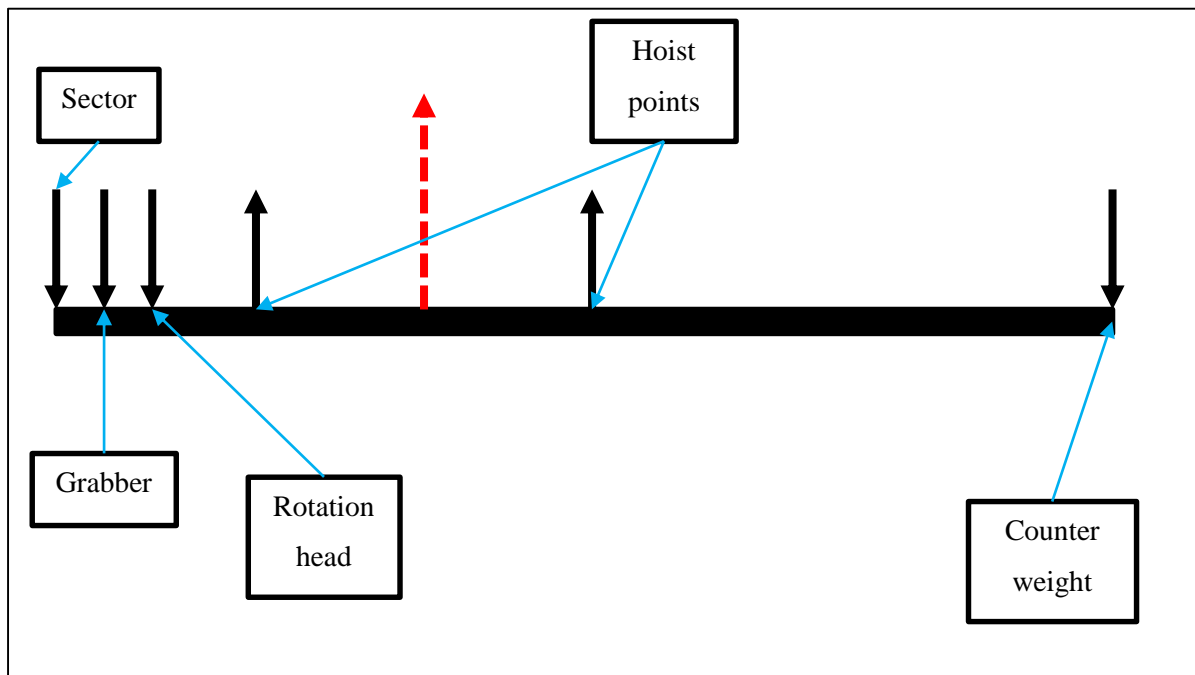


Figure 4-2. Basic forces that make up weight balance of tooling.

The first step in designing the tooling system was to determine approximate masses for the various components. Masses for the LS, SS and foot spoke were initially supplied at 1200 kg, 800 kg and 900 kg respectively. Since the tooling would have to account for the maximum weight and counter balance of the LS, it was decided to design for allowing the forces and counter balance capability for the LS. The SS and foot spoke functionality of the tooling would be valid as a result of them being lighter.

The next step was preparing a concept of a LS grabber to determine an estimate of the weight.

4.3 Large sector grabber

In order to develop a first estimate of the overall tooling dimensions, rough concepts of all the masses of components were made. The LS grabber was conceptualised first. It would be most desirable for the grabber to fall within the LS frontal shadow in order to avoid any possible interference with other parts of the NSW. It was assumed that the most suitable position to attach to the sector would be close to the existing kinematic mounts as these areas should be of sufficient structural integrity to support the entire load of the sector.

The next consideration was the method of fixing the grabber to the sector. Previously the grabber would include arms that reached around the sides of the sector or chamber and bolted onto it from a sideways direction as seen in Figure 4-3.

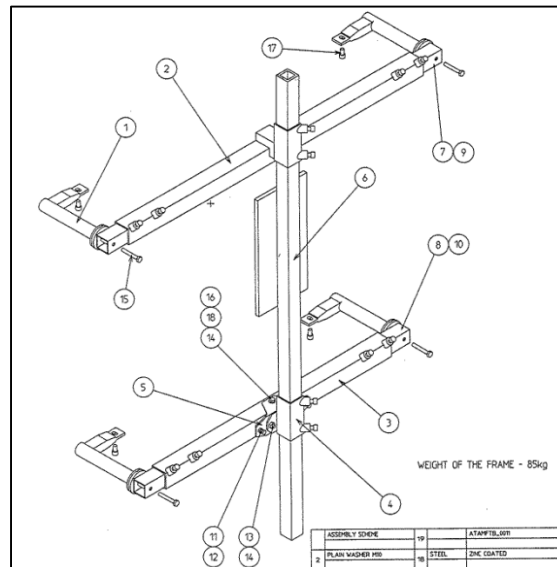


Figure 4-3. Old sector grabber with side arm mounts (University of Wisconsin, 2001).

In the case of the NSW however, the restricted space would not allow this approach. Instead a method that requires the least amount of space around the sector had to be investigated. Thus a method involving a threaded bar screwing into a mount attached to the sector, and therefore only extending the sector envelope by approximately the diameter of the threaded bar, was devised. The first concept was designed using 50 mm x 50 mm x 5 mm square tubing and was based on the shape of the LS as seen in Figure 4-4. This concept included two vertical uprights to provide fixture to the tooling and an additional two diagonal uprights to reach the mount points to the sector. The concept included welded tubes at each of the mounting points. This would allow a large bolt to sit through the tube and thread into the threaded mount on the sector. This way the bolt would clamp the grabber to the sector requiring only access on the tool end to tighten and loosen bolt. The corner points also had place for gusset plates to bolt onto, offering higher strength and rigidity at these points.



Figure 4-4. Concept for LS grabber using welded tubes.

There were some areas of concern with this initial concept. Firstly the decision to weld on the fixture tubes might cause slight welding deformation and imperfections. This would make aligning the grabber to the sector time consuming and possibly unachievable. The next concern was that the exact positions to attach the grabber on the spacer frame of the sector was not known yet, as it depended on feedback from the spacer frame design engineer. To address the first concern, a concept including removable grabber arms was developed. This involved welding the grabber clamping tube to a smaller section of square tubing that would bolt onto the main grabber frame. The holes on the frame where these arms bolt through could be marginally larger than the bolt diameter meaning that some minor adjustment would be possible when fixing the arms to the frame. Another positive on this concept is that the grabber arms can be attached easily at each mount point of the sector before the large grabber frame and installation tooling is brought near the sector. This would also result in the entire size of the grabber frame decreasing marginally as only the grabber arms would need to reach the mounting points. Figure 4-5 shows a concept of the grabber arm. It uses the same 50 mm x 50 mm x 5 mm tubing as the frame and has the thicker circular tubing welded to it.

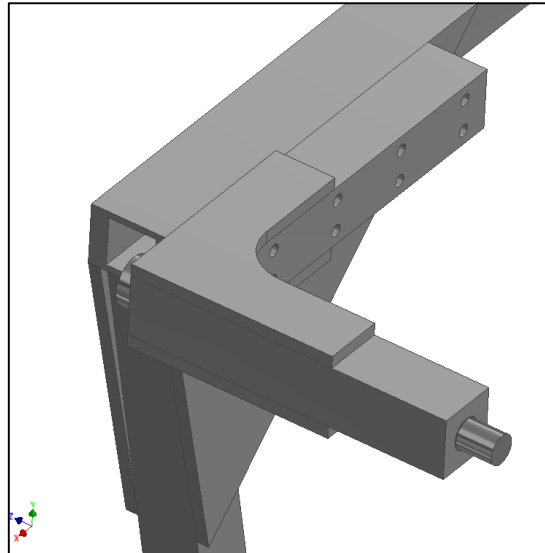


Figure 4-5. Concept of detachable grabber arm.

After conducting hand calculations for bending and deformation of the grabber frame, a decision was made to opt for 100 mm x 50 mm x 5 mm rectangular tubing for the uprights instead. Utilising this profile for the grabber arm mount section would also increase that frictional area for bolting onto the frame. The LS grabber frame was generated in a flexible fashion as to allow for quick dimensional changes without having to redo large portions of the CAD drawing. Symmetry was an important factor of reducing the 3D modelling that had to be done as the frame is symmetrical about the vertical axis. The drawing procedure was as follows: First sketches for the top and bottom profiles were drawn and constrained to each other by an adjustable dimension. These were then extruded from the middle plane outwards. Next all upright members on one side of the frame were sketched at the mid-point of the two existing profiles. These were then extruded until contact with other surfaces were reached. This meant that if at any point the distance between the top and bottom profiles needed to change, the lengths of the upright extrusions are automatically adjusted to always come into contact with the top and bottom profiles. These uprights were then mirrored about the symmetry plane. This also ensured that changes to one side of the uprights would automatically adjust the mirrored side.

At this point in improving the concept, new information regarding the positions of the sTGC kinematic mounts was obtained. Figure 4-6 shows the location of positions.

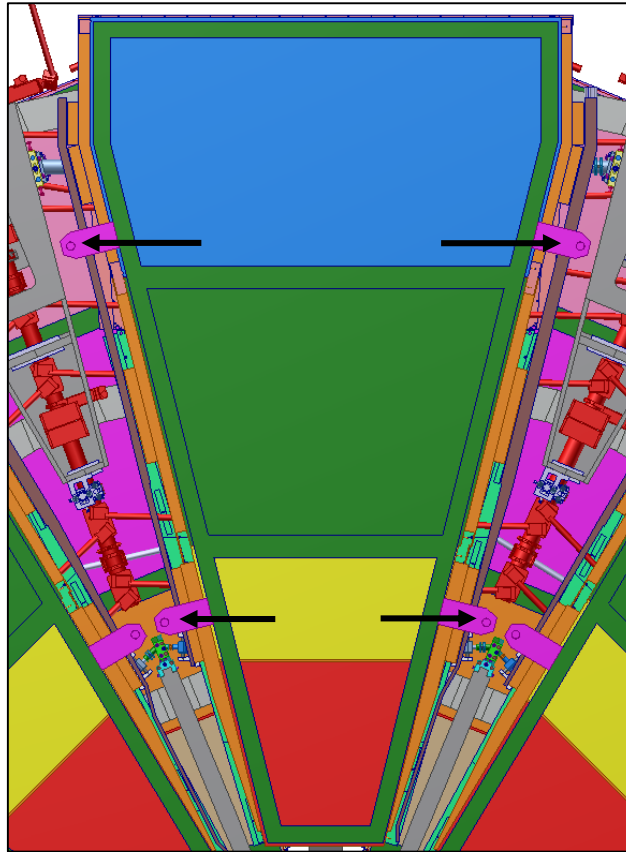


Figure 4-6. LS with positions of sTGC kinematic mounts indicated (Pinnell, 2015).

This information allowed space appropriate areas to be chosen for the grabber mounts. The idea was to keep the grabber mounts as close to the kinematic mounts as possible to avoid having to significantly increase spacer frame reinforcement, but also to make sure that all service, spokes and sTGC kinematic mounts were avoided. This information was discussed with the spacer frame design engineer and the spacer frame in Figure 4-7 was then conceptualised.

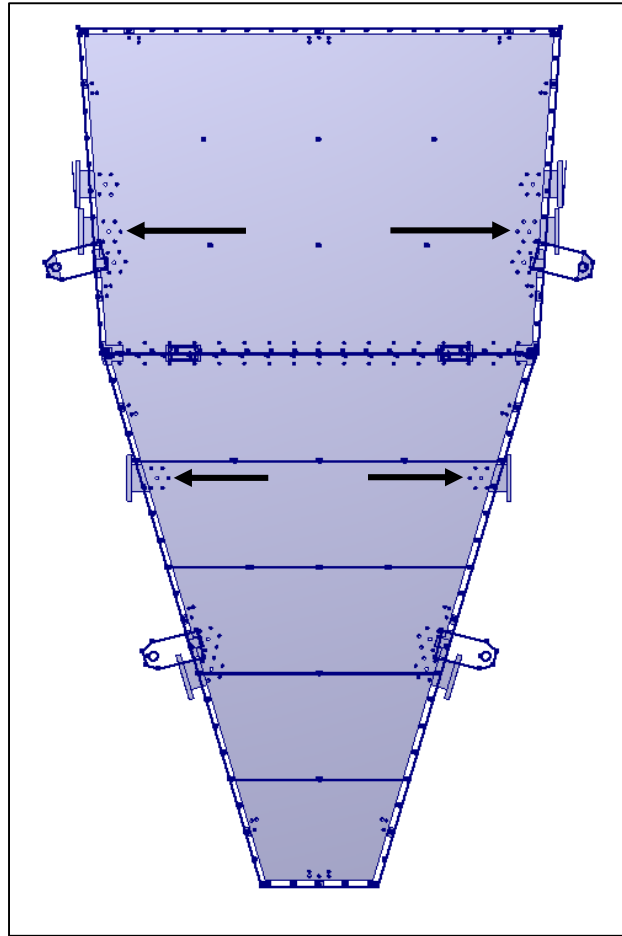


Figure 4-7. LS spacer frame with reinforced mounts for grabber mounts (Schweiger, 2015).

Once these positions were selected, removable grabber mounts had to be conceptualised in order for the grabber pins to thread in and hold the sector. An additional requirement for these mounts was the ability to hang the sectors on the storage tooling. This would require an additional threaded hole facing the side of the sector. Since the sectors are intended to be hung with one edge parallel to the ground during storage, the grabber mounts had to be designed to account for the deviation from vertical. Figure 4-8 shows the grabber mount concept with the angled face for hanging and how it provides the interface between sector and grabber. The large diameter of material around the hole ensures that the grabber pin clamps against this material when tightened. Since the grabber mounts would be removed once installation was complete, the material choice was not critical and therefore the most affordable 50 mm plate (T690) would be utilised, similar to other 50 mm components of the tooling. (Sinclair, 2015).

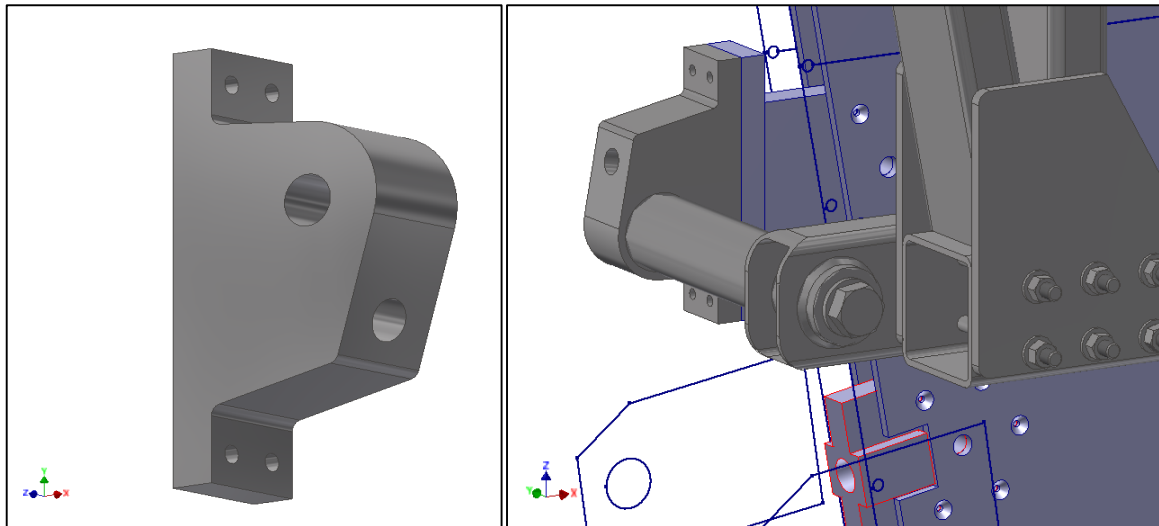


Figure 4-8. Proposed grabber mount concept for sector installation and storage tooling (Singh, 2015).

Based on these new mounting positions for the grabber mounts, the dimensions of the LS grabber required modification. The new concept for the LS grabber was a lot smaller than the first concepts due to the relatively close grabber mount positions on the spacer frame. Top and bottom steel profiles were changed to 100 mm x 100 mm x 5 mm to allow grabber arms to be wider and still accommodate the rectangular upright welds along the entire width. Another benefit of the size increase was the fact that the weights for the LS, SS and Foot spoke had increased to 1450 kg, 1100 kg and 1000 kg respectively. The number of uprights also had to be modified to accommodate the grabber mounting plate for fixture to the main tooling. The grabber mounting plate was positioned to lie perfectly at the COG of the sector as determined by the CAD software and analytical calculations assuming constant density of the sectors. Figure 4-9 shows the final concept with these modifications included.

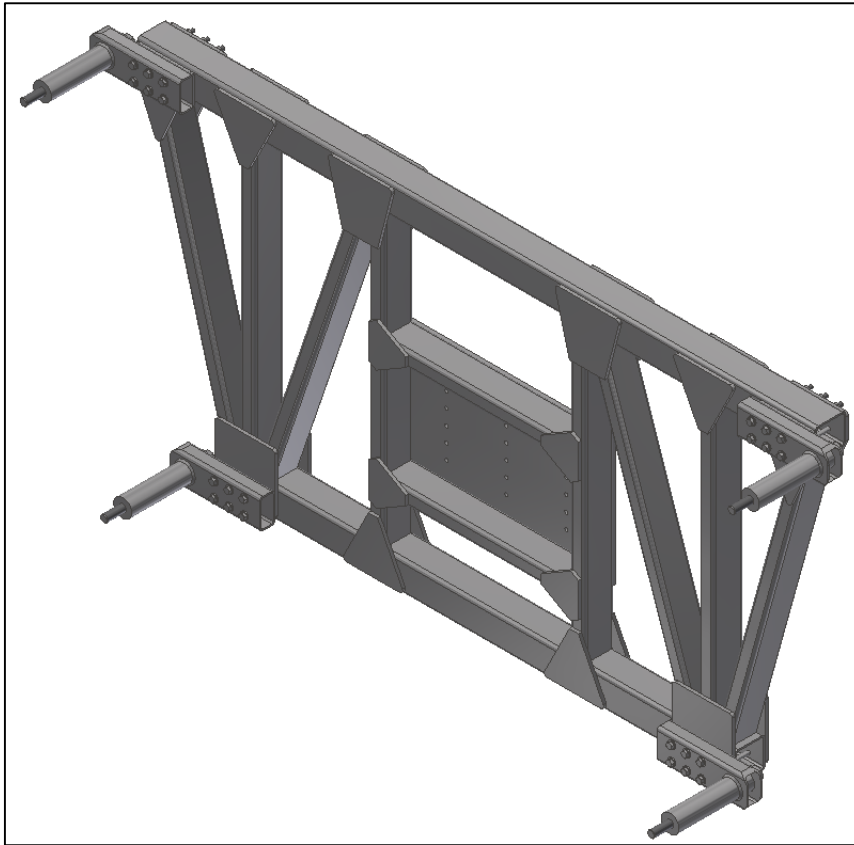


Figure 4-9. LS grabber concept with finalised grabber mount positions.

The CAD package used, Autodesk Inventor, utilises many features in material study, specifically material densities and volume. Based on this information, by selecting the desired material, an accurate weight estimation of the LS grabber could be generated by the software.

4.4 Counter weight carriage

A significant change in the principle of operation for the NSW Installation tooling is the mobile counter weight. From Chapter 3.2, the design review of the Wisconsin Tooling, it was determined that the idea of using counter weight slices was beneficial as weight could be adjusted. It was decided to use this type of counter weight bank and construct a counter weight carriage that could move along linear guides of the main beam. The concept developed included 50 mm thick mild steel slices on an 80 mm x 80 mm x 10 mm square tubing profile. Each slice has a locking bolt on top and in addition to this there are four brackets that sit on either end of the bank to aid locking. These brackets serve a dual purpose as they are also a mounting point for the linear guide blocks. This concept makes use of two linear guide blocks that will run on a common linear guide rail. Figure 4-10 shows the initial counter weight carriage setup.

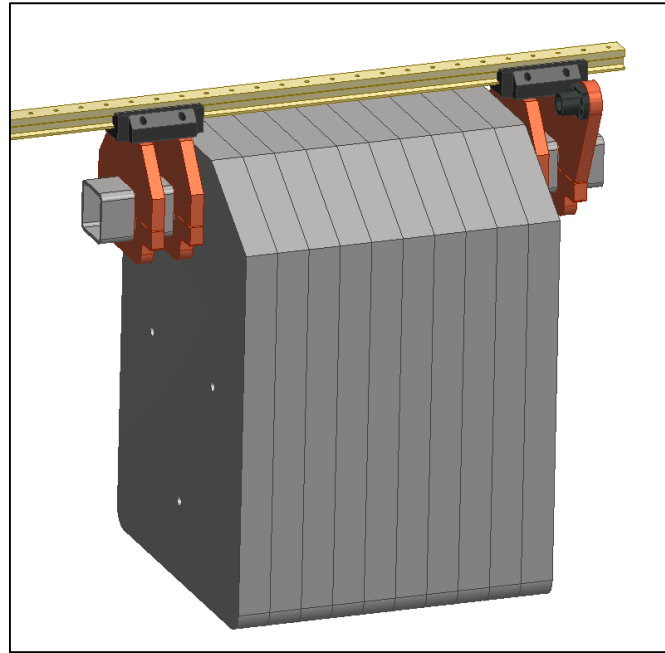


Figure 4-10. Concept of a mobile counter weight carriage.

The slices also have three holes that are used to bolt the entire bank together for added rigidity of the bank. The corners of each slice were also chamfered for both aesthetics and to avoid contact with any other components that may be present in that area. One of the counter weight brackets was modified to include a ball screw nut which would be used for actuation of the entire counter weight carriage along the tool.

Upon analysis of the first concept, an area of concern arose when having to increase the number of slices on the carriage. The effective load of the entire bank can be simplified to a point load at the COG of the bank. If the bank size is increased, this point remains at the centre, but since the bank is limited by the end of the tooling beam, the load is effectively applied further away from the end of the tool. To combat this problem it was decided to make use of add-on weight slice. These weights would not connect to the square profile, but instead only be held by the three bolts that run through the bank. In order to avoid contact with the brackets and beam, these weights were drawn up smaller than the main weights. The benefit of this is that the weight of the entire bank can be increased without moving the actual bank further away from the end of the tooling, therefore the effective point load remains in the same place. Figure 4-11 shows the final concept of the counter weight carriage with add-on slices attached.

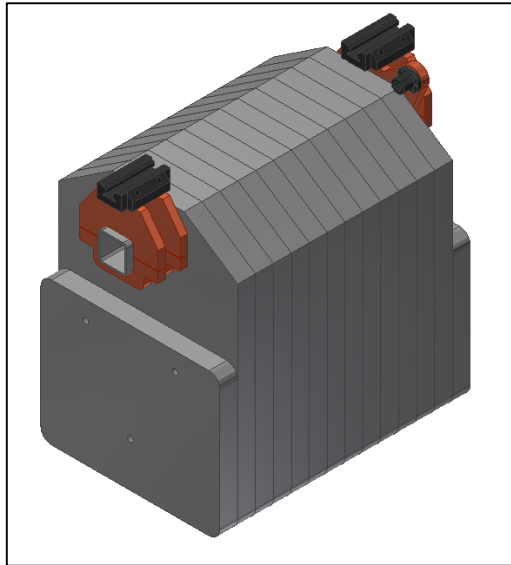


Figure 4-11. Counter weight carriage with add-on weight slices.

Since the counter weight bank would be in excess of the 1450 kg sector, it was essential to choose a linear guide that could support this load. Linear guides were sourced that used rollers instead of balls, similar to the guides used on the Wisconsin tooling. The roller type guide can support higher loads than balls with the same diameter. This meant that a smaller profile could be selected therefore aiding in the initial goal of keeping tooling mass to a minimum.

4.5 Main tooling beam

The principal step in developing the main tooling beam would be consideration for the tooling balance. Once an estimate of the LS grabber weight was obtained, the main tooling beam could be conceptualised. To obtain suitable dimension for the main beam, it was decided to develop a program to calculate the dimensions needed for tooling balance through the various stages of installation. The program is based on the simple balance of moments caused by all the loads on the main beam.

To set up the equation for the program, the first consideration was the general locations of all the loads, specifically the hoist point based on the review of the Wisconsin Tooling. The Wisconsin Tooling had its hoist point at the very front and end of the beam. This puts the effective hoist point directly midpoint of the two hoists. Since the effective pivot of the tooling was at the midpoint of the beam, the counter weight had to be greater than the sector weight by a factor of nearly 4. This was due to the fact that the counter weight moment arm was restricted by the rear end of the beam while the sector moment lies beyond the front end of the beam and therefore had a much greater moment arm length. To avoid having to make the new counter weight 4 times the weight of the sector, it was decided to move the effective hoist or pivot point to a quarter of the way along the beam from the front. This would act to give the counter weight a larger moment arm. Initial assumptions of length and counter weight size was made, and the program was coded.

The program was coded in Matlab with the masses of the sector, grabber, rotation head and counter weight as inputs with the intention of adding masses as the design became more detailed. The weight of half the main beam was utilised, as the length between the hoists does not result in a moment.

Next, assumptions were made about required profiles and initial tooling length. Although no dimensional restrictions exist in the design brief, it is still in the best interest under CERN good practice to keep designs as efficient as possible. Therefore an initial length of 3 m for the main beam was selected. This would make it only 1 m longer than the Wisconsin Tooling. A square profile was chosen instead of a circular tube for the main beam. This decision was made for ease of attaching the linear guides for the counter weight and other components such as the cross beam and motor. A 120 mm x 120 mm x 12 mm square tubing profile was first selected. An additional program was coded to calculate the bending stresses and deflections of the main beam. After using the estimates of weights from the LS grabber and inputting the values in the program, the concept for the tooling shown in Figure 4-12 was developed. The results from the program allowed a suitable counter weight bank to be decided upon that would allow for desired operation of the tooling balance within the 3 m length.

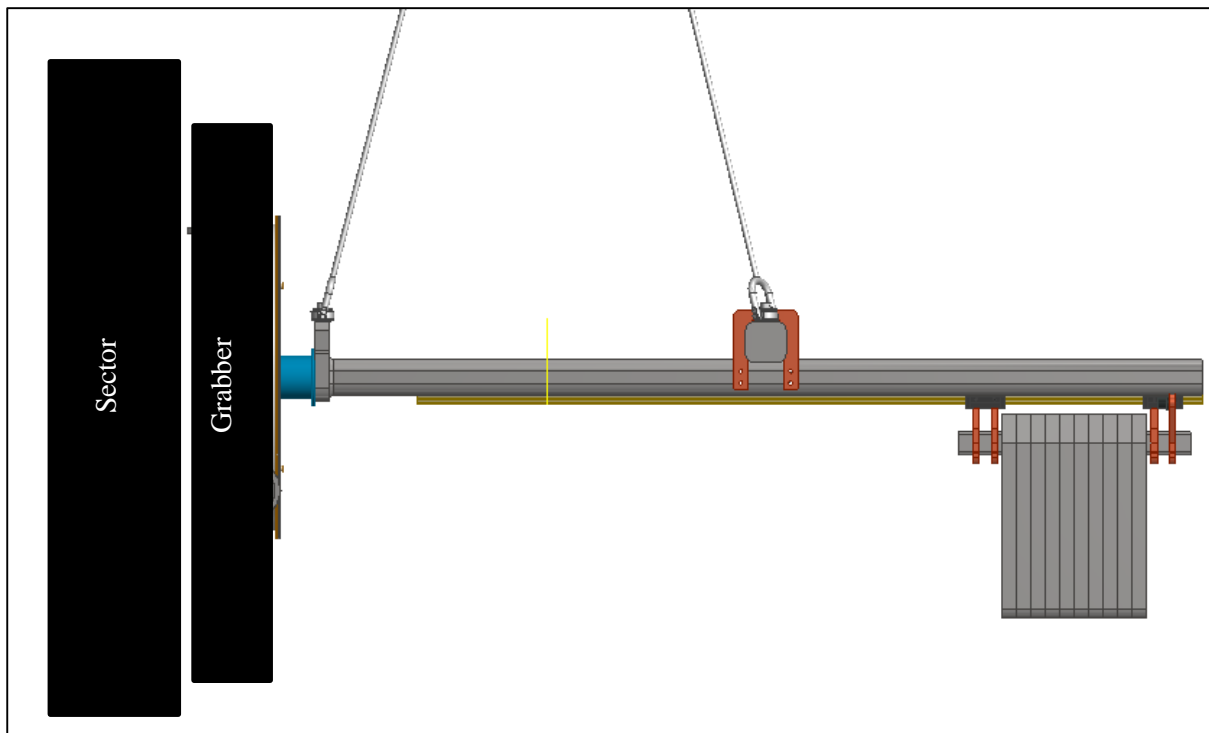


Figure 4-12. Main beam tooling concept with forward-biased hoist point.

4.6 Sector rotational orientation mechanism

A functional requirement of the NSW Installation Tooling in addition to balancing is the need for the sector to be rotated to a desired orientation. The Wisconsin Tooling used a simple yet effective trunnion assembly. This would be beneficial for the new tooling as well, especially for the compact size. This trait is important as it decreases the moment arm that the sector has about the effective hoist point. An

obvious difference between the new tooling and the old tooling was the difference in load that the trunnion assembly would have to support. To make a decision on the trunnion shaft diameter, a program was coded to compute the bend stress and deflection. A concept was made based on the initial outputs of the program. It was decided to also switch to metric sizes to comply with locally available bearings. Figure 4-13 shows the new concept for the NSW trunnion assembly which would look similar to the previous trunnion design, yet with different dimensions.

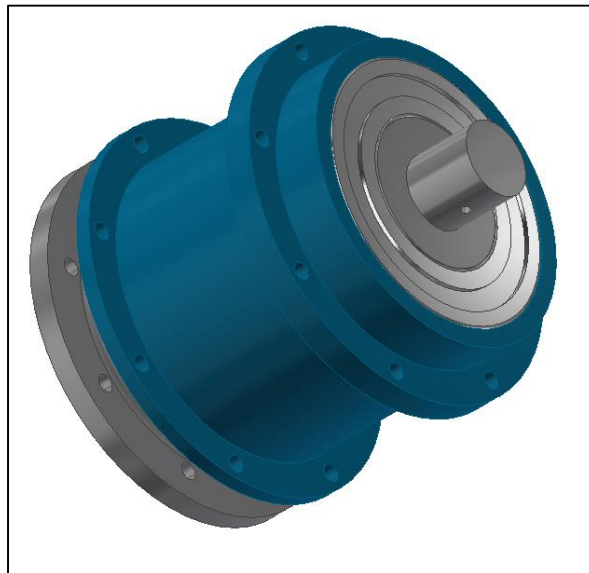


Figure 4-13. Modified trunnion assembly concept.

4.7 Rotation-locking mechanism:

A functional requirement for the rotational system is the ability to lock the tooling in position so that sector or spoke can be translated off its centre of gravity without it rotating out of position. This is both necessary for precision of installation as well as safety of the installation technicians.

The Wisconsin Tooling used a two wheel system with three locking pins as previously described. There were three main issues with this system. The first point is that due to manufacturing inaccuracies and deformations under load, the 3 pins never all lined up to allow easy locking. This resulted in only two pins being locked and therefore tooling was never operated under designed parameters. The next issue is the coarse and finite resolution that this method offered. Holes were positioned at 2° increments. This would not be suitable for the precision required in multiples of 22.5° for the NSW sector assembly. The last point of concern is the lack of a redundant locking system as required for the new tooling.

The objective with the initial concept was to address these three issues individually. The first consideration was the implementation of a frictional locking system instead of a pin-lock system. This would immediately address the first two issues. A frictional locking system would offer an infinite resolution of rotation making it suitable for the NSW sector and spoke orientations. A frictional locking system would also not rely on individual pins locking into similar sized holes and therefore can allow

for deformation and manufacturing inaccuracies without restricting locking ability. As for the redundant system, a modified pin lock system could still be implemented. Unlike the Wisconsin Tooling, the pins would instead lock into slotted holes that allow for rotation in either direction should the primary friction system fail.

Like the Wisconsin Tooling, a double wheel system would be used. This allows the locking points to have a significant torque arm therefore minimising locking force. The new wheels have a 1200 mm diameter to accommodate the locking interface. Figure 4-14 shows the two wheels, with the rotating wheel slightly larger to accommodate for easy rotation. The rotating wheel has handles along its perimeter to assist in rotating the sector. This was done to allow a greater degree of control versus the old system that used bent tube along the entire perimeter. A second advantage of the handles is that by avoiding the tube, manufacture is far simpler and the stationary wheel will not be at much risk of experiencing large welding deflection that may be caused by the tube type grip.

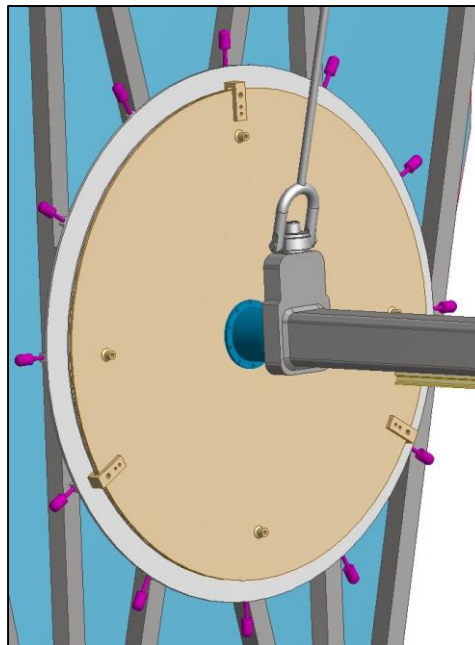


Figure 4-14. Rotating and stationary wheel concept.

The most effective method of frictional locking with the slimmest profile is a clamping system. A simple clamping system of a threaded pin tightened directly onto an appropriate lip was conceptualised. Figure 4-15 shows a detailed view of the clamp bracket which will house a threaded pin.

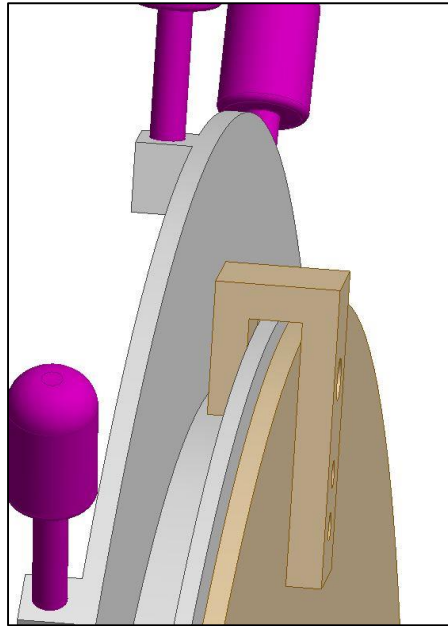


Figure 4-15. Concept of threaded pin frictional locking system.

The clamps will be attached to the stationary wheel on the tool-side. This will then clamp onto the lip of the grabber-side wheel that rotates with the sector or spoke. When the correct orientation of the wheel is set, the 3 clamps can be tightened by hand and the locking pins can be inserted into the slots. The locking pins will have slots positioned at 16 positions on the rotating wheel to correspond to the 16 different positions that the large and small sectors accommodate. Figure 4-16 shows these slots which allow for 5° of rotation in either direction of the clamped position.

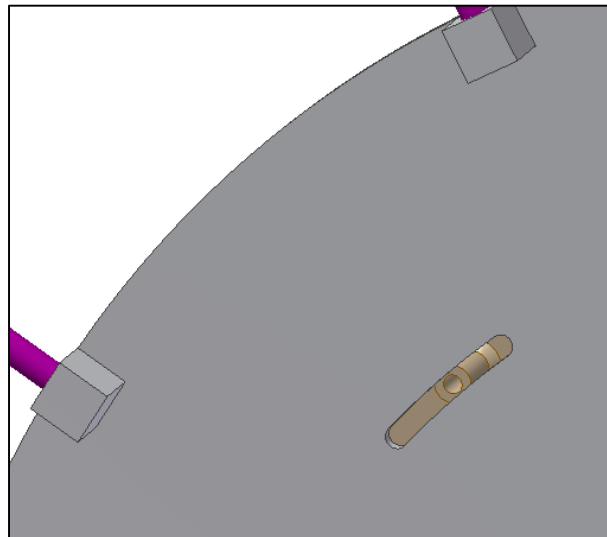


Figure 4-16. Modified pin locking fail safe concept with 5° leeway.

The first concept addressed the functional requirements for the new tooling, however it presented some new concerns. The first issue is that to apply the necessary force, it was calculated that a large torque will have to be applied to each clamping pin. In order to achieve this sort of torque by hand, the hand

T-piece would have to be excessively long. This both causes interference with the locking pins as well as requiring two hands to operate. The next concern is determining the required torque for complete locking. It will not be simple for the installation technician to determine when the required pin torque has been reached and it will also not be efficient to lock the wheel in a time efficient manner.

To address these issues, a different clamping system was conceptualised. The new concept makes use of toggle clamps. Toggle clamps may occupy more space than the threaded T-piece, however addresses all the concerns of that concept. Firstly, the toggle clamp can be adjusted to the correct locking force and it will always provide this exact force every time the clamp is actuated. The next benefit of this concept is that the clamp simply needs to be snapped into place requiring no unknown number of rotations or setting force. Due to the lever setup of the toggle clamp, enough mechanical advantage exists to offer minimal force input from the user. To provide a sufficient frictional surface, a neoprene pad will be mounted on the opposing side of the toggle clamp piston that already comes with a neoprene head. The neoprene ensures the correct coefficient of friction is met against the steel wheels for the particular force ratings. Figure 4-17 shows the toggle clamp with a modified clamping bracket and neoprene pad visible on opposing side.

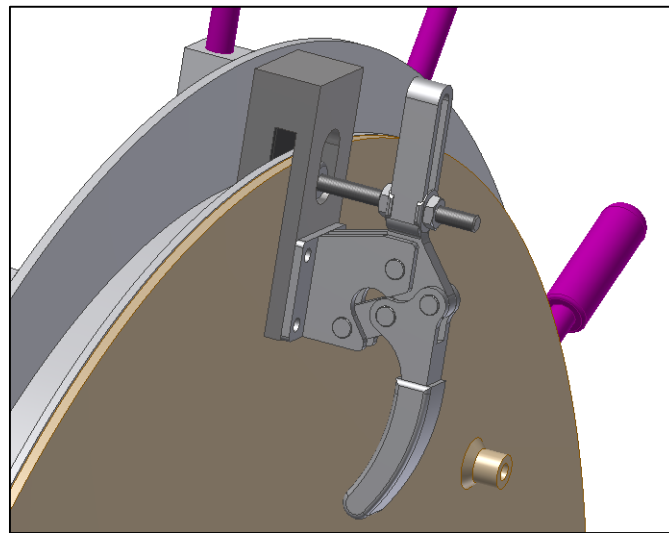


Figure 4-17. Toggle clamp locking concept.

4.8 COG translation mechanism

The translation adjustment capability of the Wisconsin Tooling achieved two main areas of use. It provided an efficient method for the installation technician to adjust the COG of the sector to aid in achieving effortless rotation by hand and once the sector was locked in an orientation, it could be used to make fine positional adjustments when installing. The linear guide system and utilisation of hand operated worm gearboxes was therefore implemented in the concept for the NSW Installation Tooling translation system. It was decided to increase the adjustment range in either direction from 40 mm to 100 mm. This offers a greater range for sectors that may be asymmetric in weight distribution or

inaccurate in manufacture. It also allows a greater degree of adjustment in the correct two directions when the correct rotational orientation has been met during installation. Instead of using worm gearboxes with screw actuators to the side of the linear guide plates, it was decided to position worm gearboxes with telescopic actuators in the middle of the plates. This would reduce the torques and stresses induced by pushing the load from a remote location. Figure 4-18 shows the concept for the new translation system. Appropriately sized gearboxes had to be selected for the large load of the sector and grabber.

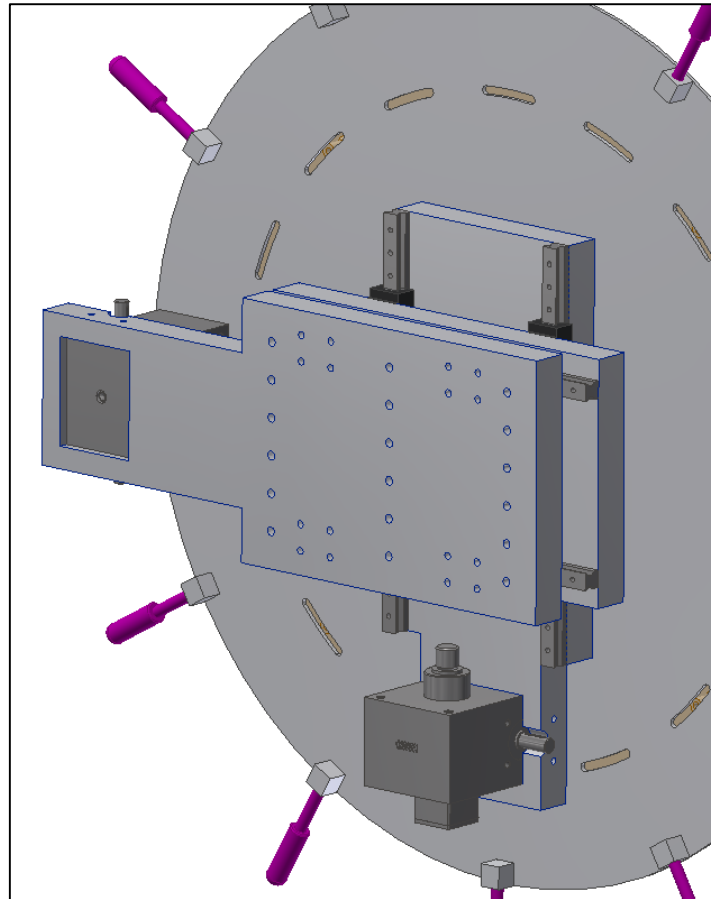


Figure 4-18. Concept for the COG adjustment translation system for the NSW Installation Tooling.

4.9 Small sector grabber

The SS grabber was conceptualised by taking into account all the consideration for the LS grabber. It was decided to utilise the same grabber arm design for the SS to simplify manufacture and compatibility of parts. The only change would occur dimensionally as the SS would have different grabber mounting points. Like the LS, grabber mount positions were analysed on available space when sTGC and sector kinematic mounts were taken into account as well as general space around the Small sector. Figure 4-19 shows the Small sector in the NSW assembly.

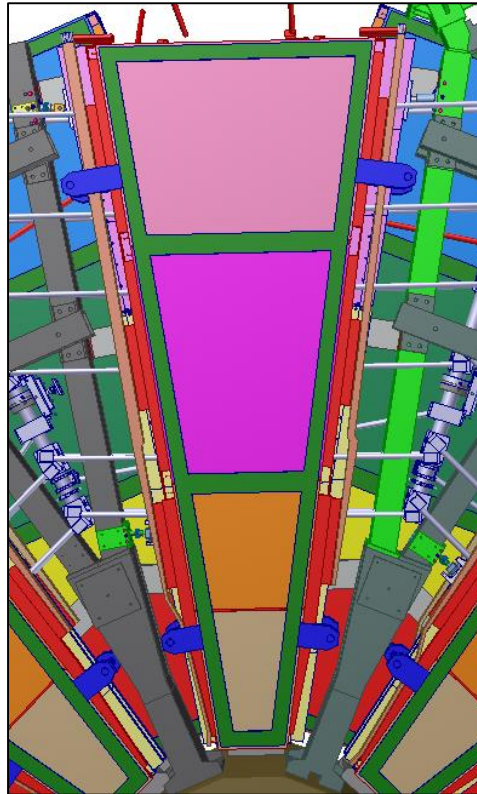


Figure 4-19. Small sector in NSW assembly (Pinnell, 2015).

Once the sTGC mount positions were known, the layout could be studied in order to determine suitable grabber mount positions. The available area around the SS differed quite significantly from the LS. In addition to this it was found that the areas around the foot spoke were even more compact. It was therefore decided to design the mount locations to satisfy the spatial requirements of the foot spoke and hence would satisfy the requirements of all normal small spokes as well. Figure 4-20 shows the grabber mount locations accounted for in the SS spacer frame. Notice that unlike the LS, the grabber mounts always lie between the sTGC and sector kinematic mounts. These positions therefore resulted in a larger grabber being required. Thus the SS grabber would be larger than the LS grabber.

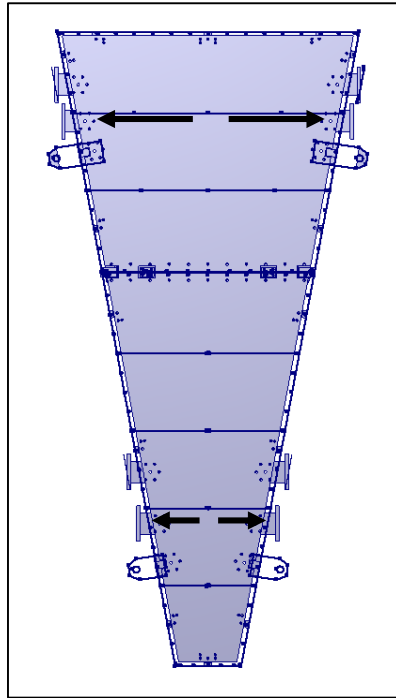


Figure 4-20. SS grabber mount positions (Schweiger, 2015).

Once these mount positions were finalised, the SS grabber CAD model was drawn in the same flexible manner as the LS grabber. For the reason of consistency, the same section profiles were used as the LS grabber. Figure 4-21 shows the concept developed for the SS grabber. Due to the larger size and need for the tooling mount interface to be the same, the vertical profile arrangement differs from the LS grabber. The gusset plates to be welded in utilise the same dimensions as the LS design.



Figure 4-21. SS grabber concept.

4.10 Foot spoke grabber

The Foot spoke grabber was conceptualised last due to its unique shape and weight. There are only two foot spokes per NSW and they are asymmetric about their centres. This presented a unique challenge when conceptualising the foot spoke grabber. Aside from the asymmetry, each foot spoke has the heavy alignment bar biased towards the bottom of the NSW assembly meaning that their COGs were not in a similar position on each spoke. It was however decided to design one grabber that could work for both foot spoke orientations. The asymmetry in the weight would be accounted for with the COG translation adjustment. Figure 4-22 shows the foot spoke and the mounting plates used to fix them onto the LS spokes. Since the foot spokes do not contain any delicate detectors or sensors and are to be manufactured from stainless steel and aluminium, they are not as sensitive as the sectors. Hence there is no need to design specialised mounts to resist stress and deflection as the LS spoke mounts are sufficient for installation.

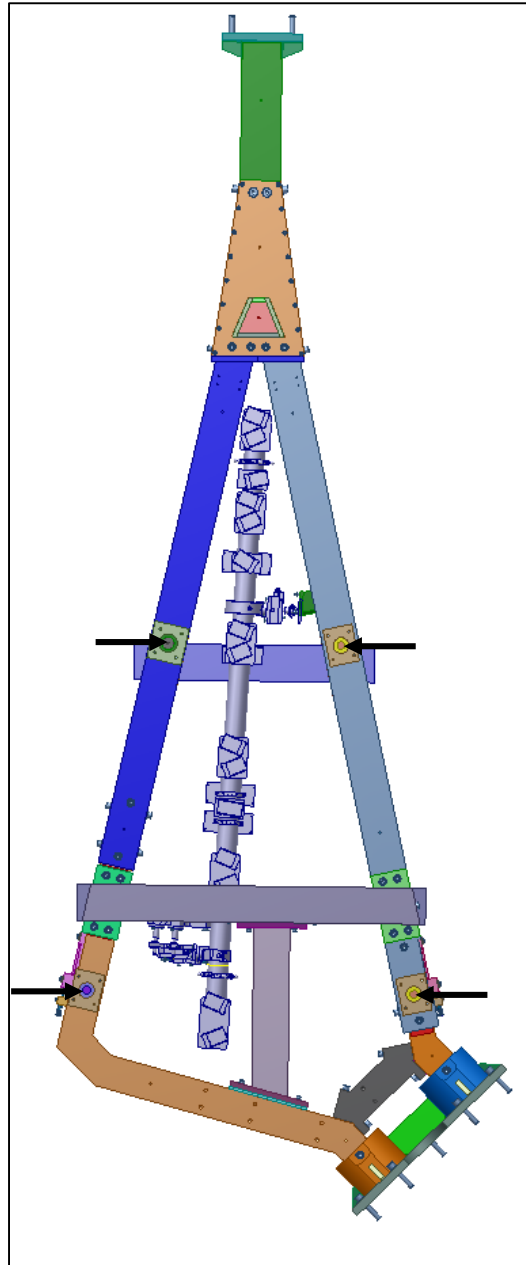


Figure 4-22. Foot spoke with mounting plates for LS spokes (Ciapetti, et al., 2015).

The idea for the concept was to design a symmetrical tooling that would have two separate mounting locations to account for the offset of COG of each foot spoke. These individual COGs could be determined by the COG tool in the Autodesk Inventor package. Another complication with the foot spoke is that the mounting plates are asymmetrical as well, with one of the plates sitting 5 mm lower. To account for this the bottom two mount plates of the grabber would have slotted holes. In addition to this, to avoid issues with misalignment from welding deformation, all mounting holes would be made with a larger diameter than the foot spoke mounting holes. Figure 4-23 shows the concept for the foot spoke grabber.

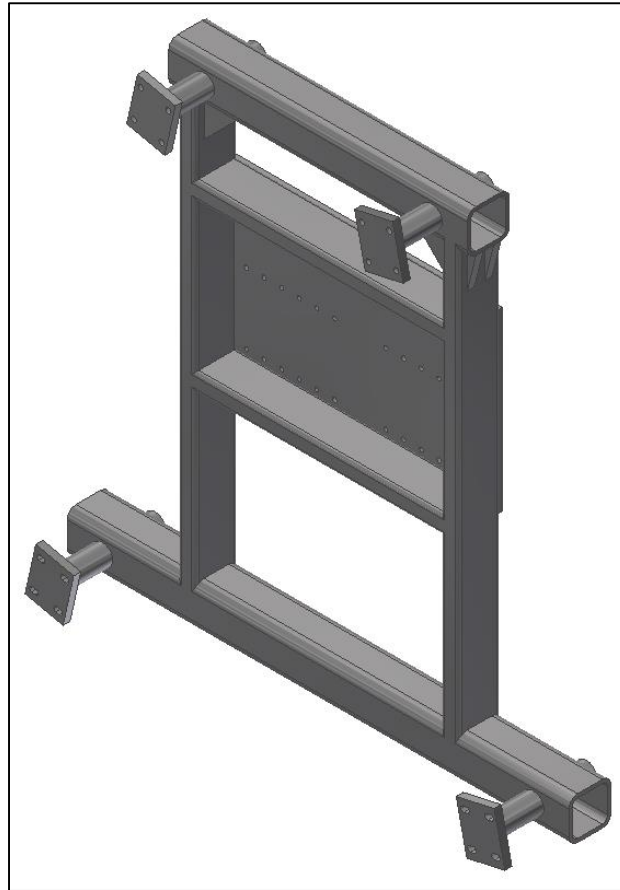


Figure 4-23. Universal foot spoke grabber with two mount positions.

The mounting plate strokes could be welded onto the main structure in the same manner as the LS and SS grabber arms. The larger mounting plate accommodates the two positions that the grabber can be attached to the tooling. The slight difference in asymmetric weight will be accounted for by the slight adjustment of the COG translator with the dimensions of this design. A last consideration for the design was that not all the mounting plates on the foot spoke lie on the same horizontal plane. This issue would be accounted for by designing the grabber with all the mounts in the same plane and including spacer shims of thickness 10 mm to offset the affected plates.

4.11 Tooling storage stand

The storage tooling serves to allow the tooling to be stable and securely supported when not in use. An added capability of the stand would be enough clearance from the ground and support to attach any of the grabbers to the tooling while on the stand and still maintaining balance. The first consideration when approaching this design was maintaining stability of the tooling. It was therefore decided to opt for a T-piece leg stand that would offer maximum stability to prevent sideways tipping. The next consideration was supporting the tooling in the correct locations. The obvious decision was to support the counter weight carriage directly as this would alleviate the entire load of the main beam and prevent static bending. The final consideration was ensuring enough clearance for the mounting plate of the tooling

to connect the various grabbers while on the storage stand, without jeopardising stability. To account for this the tooling stand was conceptualised high enough for the SS grabber to be attached in a horizontal position as the LS grabber occupies a smaller envelope when vertical. With the required clearance of the SS grabber, the remaining two grabbers easily attach while on the stand. Figure 4-24 shows a concept of the storage stand. A large counter weight carriage platform is incorporated to store the tooling in various different positions. This will also allow the tooling to be adjusted while on the stand.

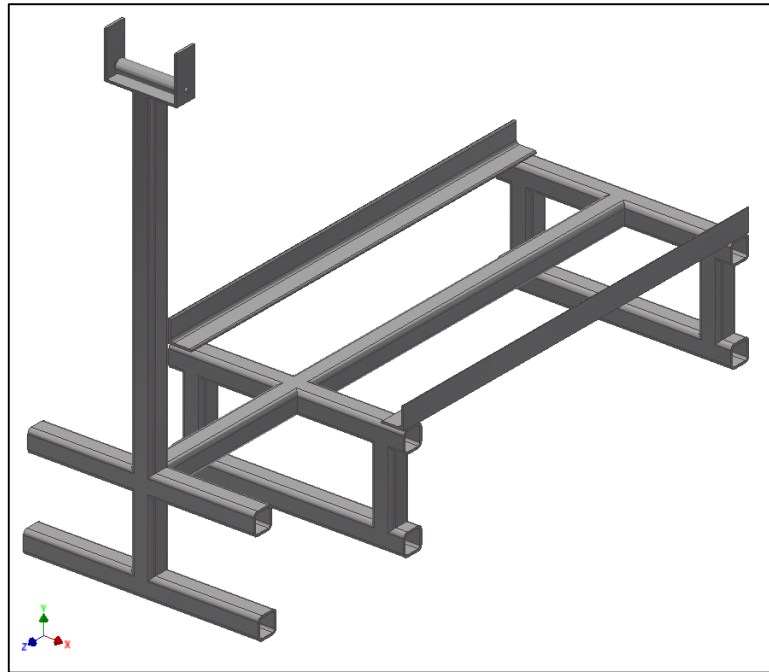


Figure 4-24. NSW Installation Tooling storage stand.

4.12 Counter weight adjustment motor

Like the Wisconsin Tooling, the NSW Installation Tooling concept utilised a motor drive for the adjustment of the CW. The concept of using a worm gearbox to drive the screw provided the necessary torque gain resulting in a smaller motor being needed, but also ensured self-locking when the CW tried to move along guides if the tooling tilted. To simplify the arrangement used on the Wisconsin Tooling, a motor with an incorporated worm gearbox was investigated. Correct ratio of the gearbox would ensure a small motor could still be selected. The best choice of motor was then found to be a DC permanent magnet motor for its high power to weight/size ratio. For purposes of availability in both countries of manufacture, it was decided to select a WEG EPG motor with single reduction worm gearbox.

Chapter: 5 Final design and simulation of the NSW Tooling

This chapter focuses on two primary aspects; explaining the various FEA procedures and finalising the design based on the results of these analyses. Critical and complex components are specifically described with minor more straight forward calculations carried out in Appendix A. Included in this chapter are suggestions or changes to the functional requirements of the NSW Installation tooling. A safety factor of 2 was applied to all stress calculations to comply with the specific Eurocodes mentioned in Chapter 2.

5.1 Large sector grabber and spacer frame

The large and small sector grabber behaviour under stress formed perhaps the most important aspect of the installation tooling design. This was primarily because the grabbers had to be able to support the sector as well as not induce more than 70 MPa in the sector spacer frame. Any modifications to the concept would also have to fall within the suggested sector envelope with 30 mm clearance from any other part of the NSW assembly. Another specification was that the spacer frame should not experience more than 1 mm of deflection between the 2 grabber mounts.

The first simulation carried out on the LS grabber did not include the spacer frame. This was to analyse what stresses and deflections the grabber would experience if the loads were individually added to the grabber pins of each grabber arm. The boundary conditions used were fixed body-to-ground contacts on each pin. To investigate the worst case scenario, the grabber was simulated in each of its orientations. This was done for two reasons. Firstly the shape of the grabber is only symmetrical about one axis meaning its strength qualities vary with orientation. The second reason is that the grabber mount positions were chosen based on available space and therefore not equally spaced from the sector centre of gravity. This results in different forces experienced by each set of grabber pins. After conducting these simulations the worst case orientation was the 0° upright position. This was mainly due to the grabber arms having the least amount of torque arm relative to the grabber frame. The force at each pin was twice the weight of the LS (safety factor) divided by 4 as all loading was equal in this orientation. Figure 5-1 shows the resulting FEA with the maximum Von Mises stress located at the highlighted point with a magnitude of 560.81 MPa. Considering that the selected material was S355 with a yield strength of 355 MPa, the design was not compliant.

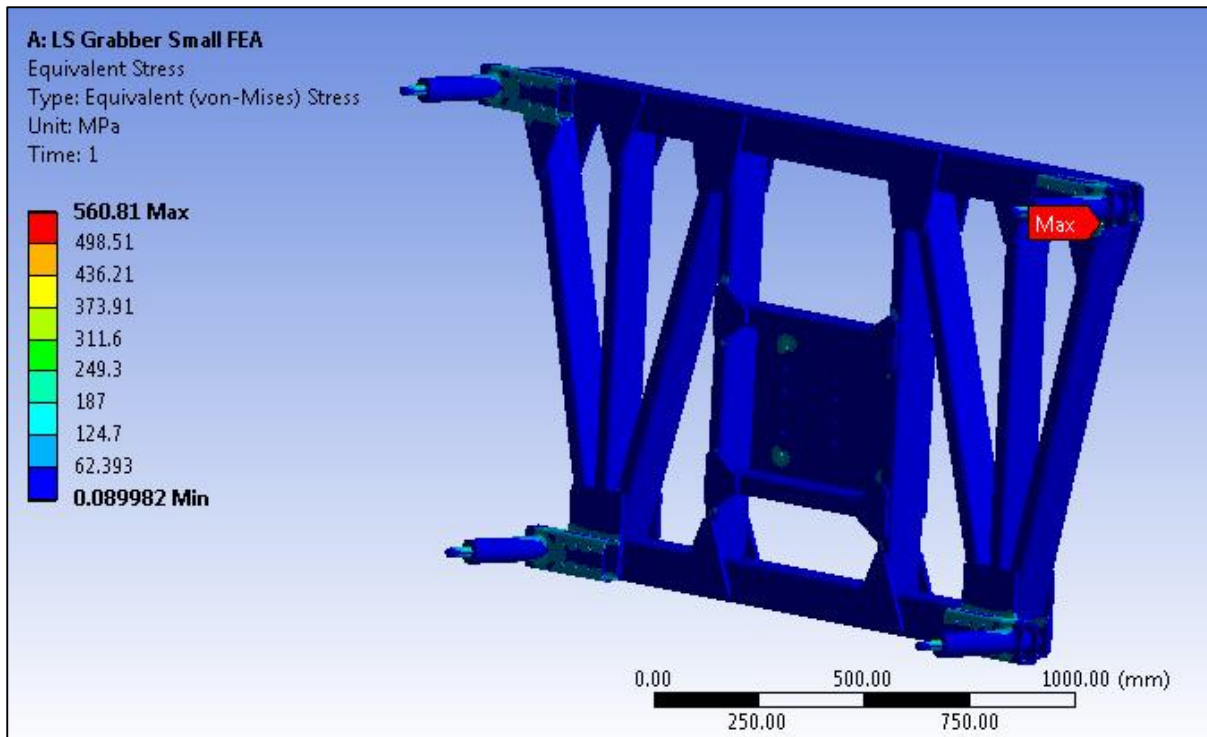


Figure 5-1. LS grabber simulation at 0° without spacer frame.

This was not an immediate concern as it was predicted a higher stress would occur without the support of the spacer frame. A point of interest with this simulation was to see what deflection the grabber arms were experiencing relative to each other. Any difference in the deflection of the top arm relative to the bottom arm would result in a bending stress the spacer frame would experience in order to resist this change in deflection. In essence the spacer frame would be twisted about the grabber mount points if these deflections were too large. Figure 5-2 shows the individual deflections (referred to as deformations in figure) that the top and bottom grabber arms experienced at their ends.

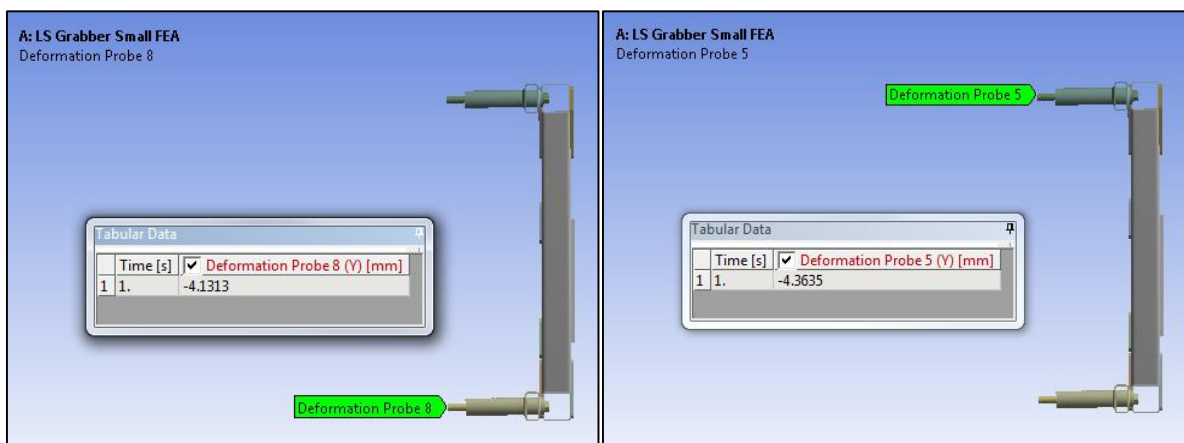


Figure 5-2. Deformation probe comparison of top and bottom grabber arm.

The difference of these two deflections was 0.2322 mm. This placed the deflection in the suggested limit of 1 mm. To study the real significance of this deflection and obtain a realistic stress experienced

by the LS grabber a simulation incorporating the spacer frame was conducted. During this simulation it would also be possible to verify whether the spacer frame stresses fell under the 70 MPa limit suggested by the spacer frame design engineer.

The FEA involving the spacer frame was set up in a similar fashion to the previous simulation except here the entirety of the force, still incorporating the safety factor of 2, was applied to the spacer frame (Force was doubled to apply the safety factor of 2). This acts to simulate the full weight of the LS without the unrealistic individual pin forces of the previous simulation. Figure 5-3 shows the Von Mises stresses on the LS grabber when the spacer frame is introduced.

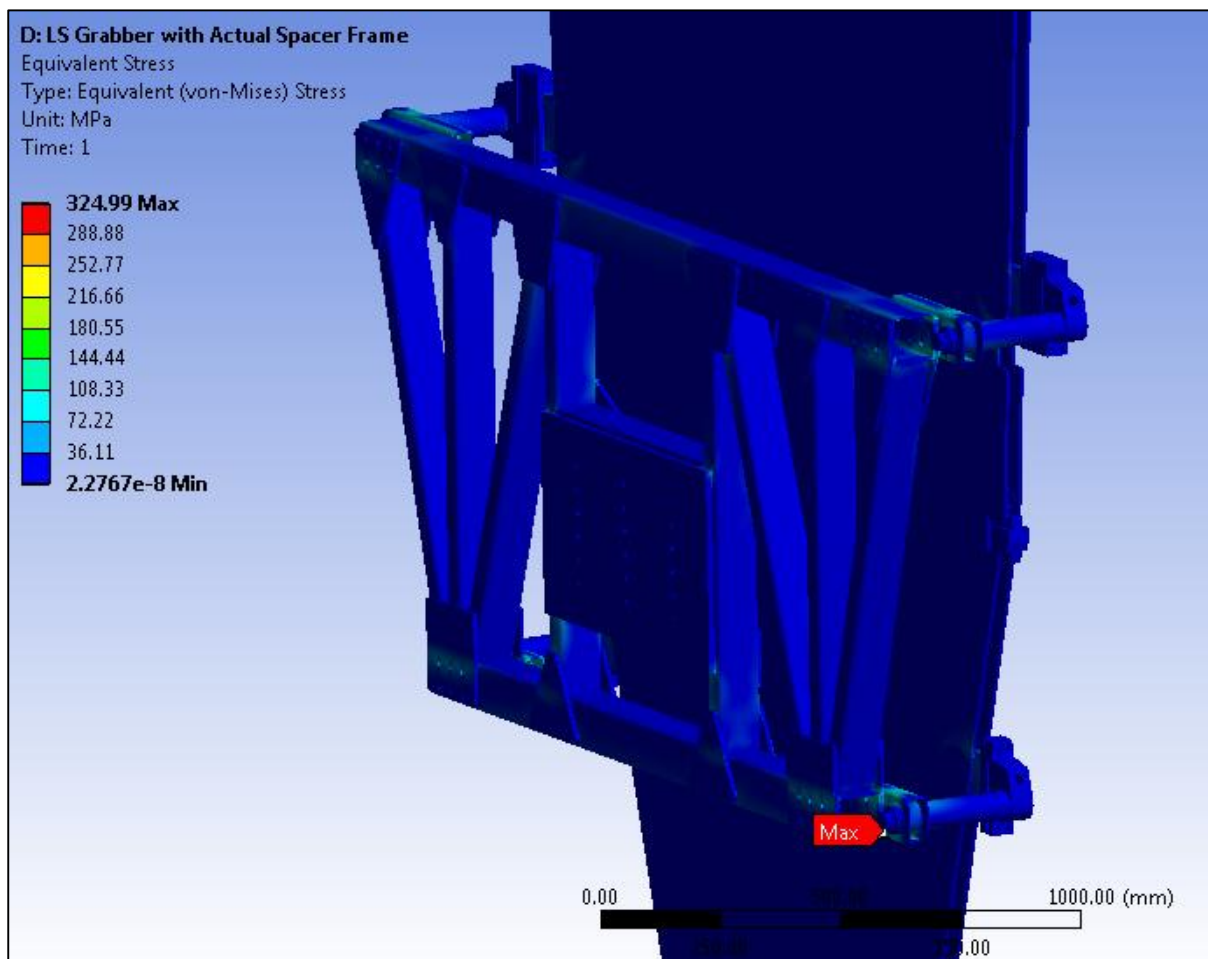


Figure 5-3. Von Mises stresses of LS grabber with spacer frame.

The stress experienced in the LS grabber reached a maximum of 324.99 MPa, therefore falling within the required 355 MPa yield point of the material. This represented a large reduction in stress compared to when the spacer frame was not taken into account, as expected. Figure 5-4 shows the stresses experienced by the aluminium spacer frame.

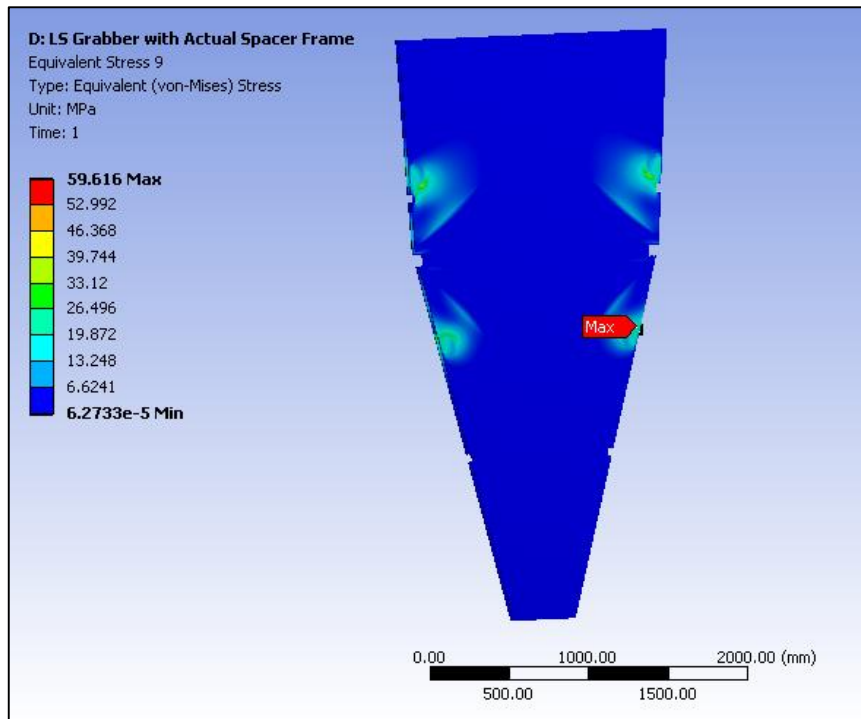


Figure 5-4. Von Mises stress result of worst stressed LS spacer frame panel.

The maximum stress was experienced on the spacer frame panel closest to the grabber. It reached its maximum stress close to the grabber mount point at 59.616 MPa. This also fell within the required 70 MPa limit and significantly within the yield point of the aluminium 6061 material. At this point the functional requirements of the LS grabber had been met and the design was deemed finalised.

5.2 Small sector grabber and grabber mounts

The SS grabber was simulated in a similar fashion to the LS grabber. Here the 90° horizontal orientation was found to give the highest stress. The pin forces were applied as seen in Appendix A – 3.2.2. Figure 5-5 shows the SS grabber experiencing a maximum Von Mises stress of 313.07 MPa.

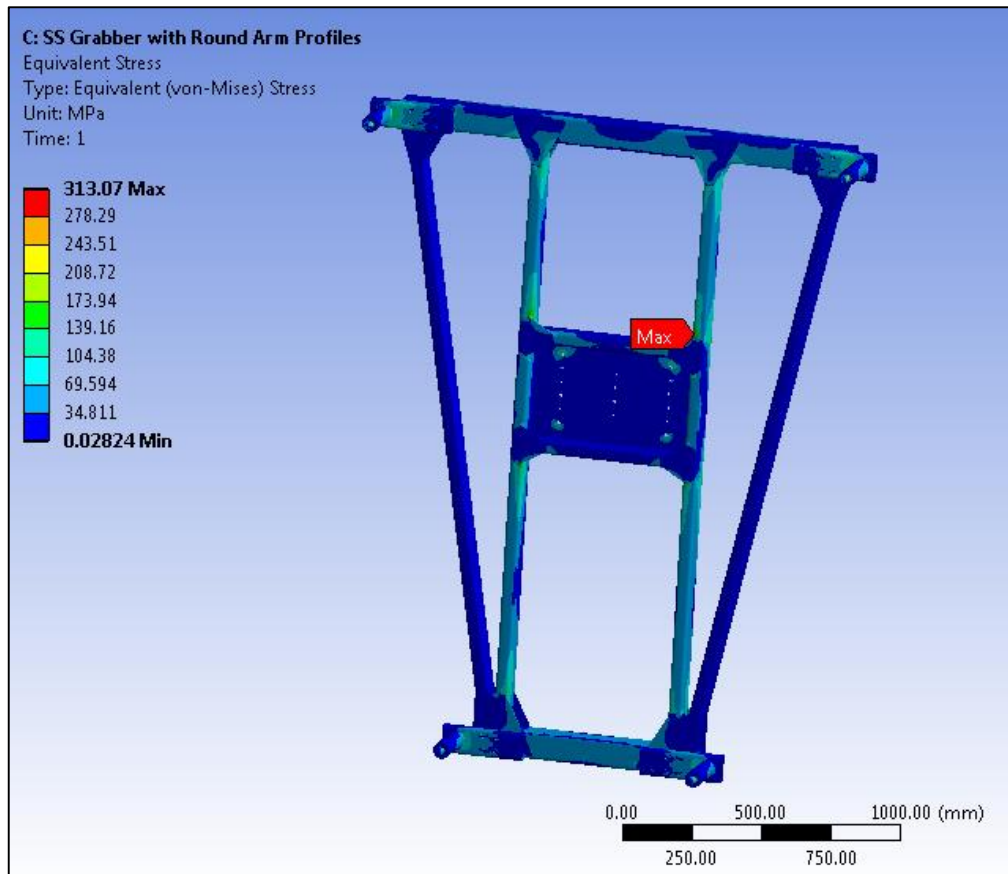


Figure 5-5. SS grabber Von Mises stresses at 90°.

This value, like the LS grabber, fell within the 355 MPa limit. The SS spacer frame also coped acceptably with its stress not exceeding the 70 MPa limit, at 62.13 MPa. The process of finalising the SS grabber progressed much faster as the main complications and areas of optimisation had already been dealt with in the finalisation of the LS grabber.

The grabber mounts were also simulated in this assembly to ensure both they and the aluminium insert between the spacer frame sheets did not exceed their respective yield points. Figure 5-6 shows the worst stressed grabber mount and aluminium insert peaking at 77.65 MPa, significantly below either materials yield point of 275 MPa for aluminium and 690 MPa for the T690 steel.

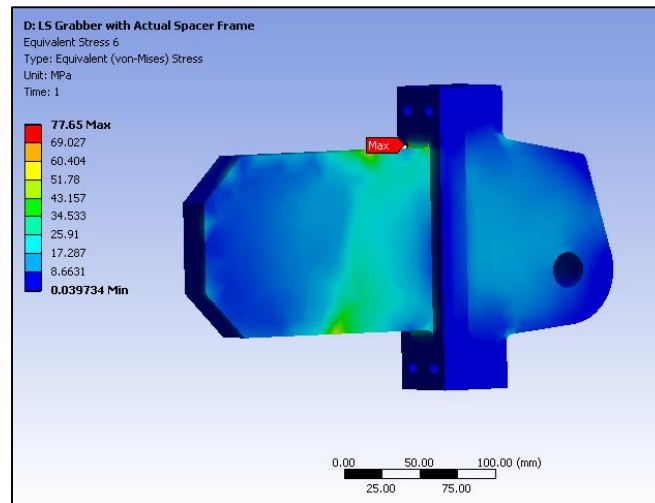


Figure 5-6. LS grabber mount and aluminium insert FEA Von Mises plot.

5.3 Foot spoke grabber

The foot spoke grabber simulation was again carried out under similar conditions to the LS and SS grabbers. Since the foot spoke itself was of a robust nature, it was unnecessary to include it in the simulation. Another simplification with the foot spoke grabber FEA was that it only had to be done in two positions, therefore reducing the number of simulations. The foot spokes each sit at 45° in the NSW assembly and therefore this had to be taken into account in the simulations. Figure 5-7 shows how the forces were divided into vertical and horizontal components to account for this angle.

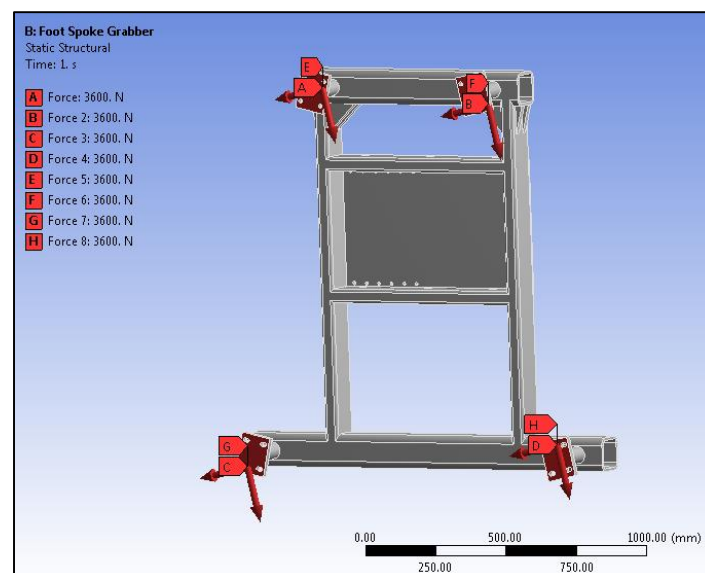


Figure 5-7. Forces applied to foot spoke grabber in simulation.

Since the foot spoke grabber is essentially one component, the simulation required these forces and a fixed constraint on the tooling mount holes. Figure 5-8 shows the Von Mises results of the simulation under these conditions.

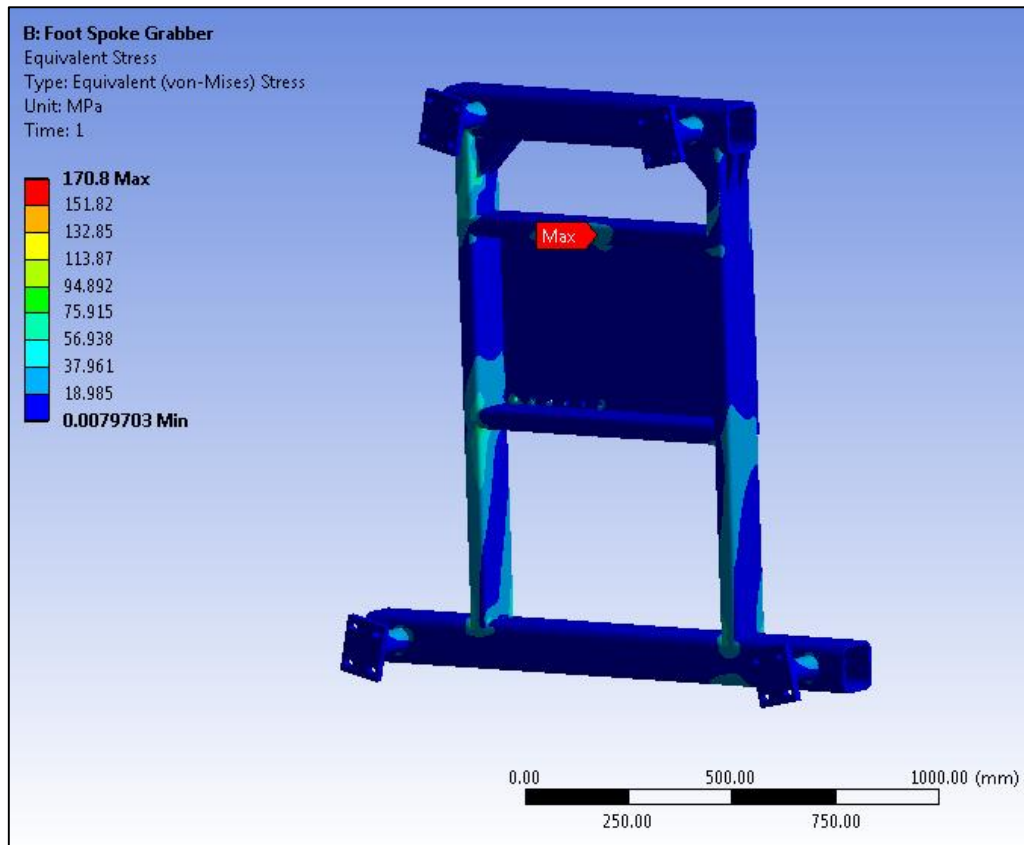


Figure 5-8. Von Mises stress experienced by foot spoke grabber.

The stress reached a maximum of 170.8 MPa at a bolt hole that fixes the grabber to the tooling. This fell below the 355 MPa allowed limit, yet due to the foot spoke grabber and foot not exceeding the weight of the LS and LS grabber, there was no need to weight optimise the structure. Weight optimisation would have led to a more complex design resulting in increased manufacturing costs and number of simulations. The foot spoke grabber was therefore compliant and finalised.

5.4 Main beam

5.4.1 Main beam balance and bending

The main beam profile was designed purely to withstand the applied stresses. To determine this stress and the deflection, an important consideration for the linear guides, a program was written to calculate these points of interest. The main beam was treated as a cantilever with the effective counter weight load accurately positioned away from the end of the beam. The inputs for the program are as follows:

$length$ – length of main beam

F – force of counter weight

a – distance from main beam centre to counter weight centre

b – distance from beam end to counter weight centre

E – Young's Modulus of main beam material

I – Moment of Inertia of beam profile

By using relevant deflection and bending stress calculations the desired output is obtained. After the sector and spoke weights had increased it was necessary to increase the main beam profile from 120 mm x 120 mm x 12 mm to a square profile with dimensions of 140 mm x 140 mm x 10 mm. This was based on the stress value output from the program being higher than the allowable 355 MPa. The new profile had a higher moment of inertia of 1312 mm⁴ and was found to be suitable based on the program output. Appendix D - 1 shows the program for the bending deflection and stress; giving results of 5 mm and 212.479 MPa respectively.

The main beam dimensions and counter weight size was dependant on the requirements for the tooling to be balanced. As other aspects of the tooling were finalised the program provided a progressively more accurate result for the required dimensions and size of the beam and counter weight respectively. The program was based on the dimensions seen in Appendix D - 2. The input variables were as follows, with the front of the main beam as the reference:

x_f – distance to effective pivot/hoist point

x_{sector} – distance to centre of sector

$x_{grabber}$ – distance to centre of grabber

x_{wheel} – distance to rotating wheel assembly centre

$x_{bearing}$ – distance between the trunnion bearings

W_{sector} – mass of desired sector

$W_{grabber}$ – mass of corresponding grabber

W_{wheel} – mass of rotating wheel assembly

These inputs were then manipulated into moment equations that would act to determine the required distance away from the tooling reference that the counter weight would have to be positioned at for a given counter weight size. By analysing this it can be determined whether the counter weight would fall within the desired tooling length to obtain tooling balance. The counter weight size can then be tweaked to allow for a safety allowance and for optimising its weight. Appendix D – 2 shows the Tooling Balance Program written in Matlab. This shows the details of the final design and the output value of x was 1.674 m. This would result in a safety allowance of 167 mm beyond which the counter weight can travel

if there is an inaccuracy with any component weight for a 3 m main beam and 1732 kg counter weight. To achieve this counter weight the carriage would have to include 12 full slices and 2 add on slices.

Based the finalised weights of all tooling components, the counter positions in Table 5-1 shows the position that the centre point of the counter weight carriage would need to be away from the front end of the beam to maintain balance for each of the listed lifting permutations.

Table 5-1. Counter weight positions for tooling balance.

Attachment	Position from front of tool (m)
No attachment	0.814
SS grabber	1.0
SS grabber and SS	2.08
LS grabber	1.031
LS grabber and LS	2.455
Foot spoke grabber	0.969
Foot spoke grabber and foot spoke	1.951
Beam length	3

5.4.2 Main beam weld

The main beam connects to the front hoist point by means of a fillet weld as seen in Figure 4-14. To accurately simulate this weld a particular FEA procedure must be implemented. Since the weld material is different to the base material, the particular material properties must be entered into the simulation material library. A welded component however is still a single part yet it is a mix of weld material and base material. To accurately represent a weld in ANSYS the geometry needs to be spliced to separate the weld from the base material. The simplest method of going about this is drawing the entire component as one body in the CAD environment. The 3D model must then be exported into the ANSYS Workbench where the 3D model can then be opened in the Design Modeller. Here the weld area can be spliced to separate it from the parts intended to be welded. Once the model is separated the user can return to the Workbench and enter the material library. The base material and weld material should be included at this point. If the weld material is not in the ANSYS standard material library then it can be manually added by inputting the UTS, Modulus of Elasticity and the Poisson's ratio. Additional cyclic information is required if fatigue simulations are intended to be done. Once the materials are assigned the Mechanical environment can be entered. By opening the geometry tab every individual body in the assembly should be present. Here the spliced weld and base geometry will be seen as different bodies. The materials selected from the library can then be assigned to the respective parts. In reality a weld penetrates into the base material. To achieve this in ANSYS the separate bodies can then be combined. By simply highlighting the base body and weld body, the context menu can then be used to display the

“Form New Part” function is seen in Figure 5-9. By selecting this ANSYS recognises these two bodies as a single entity, however they still maintain their separately assigned materials (Sciuccati, 2015).

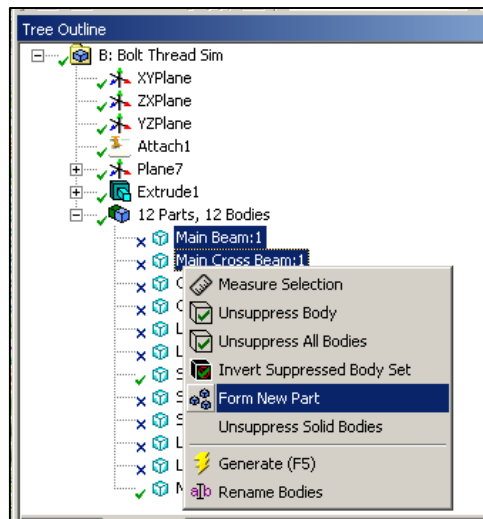


Figure 5-9. Combining bodies with separate material properties.

The next step was to mesh the welded component. Since ANSYS sees this as one body, meshing will create elements that flow through these two originally separate bodies. The highlighting order determines which element will grow into which body and therefore the weld properties can be chosen for the desired outcome. The growth ratio of the mesh is also important in ensuring consistent elements across the weld-base interface. Once the model is meshed the rest of the simulation process can be carried out as normal. The results will take the material properties into account when solving for stresses, strain and deflections yet also treat the component as one body. By adjusting the mesh size, growth ratio and selection order the weld penetration can be adjusted (Sciuccati, 2015).

The main beam weld simulation was carried out in the same manner as above. The main beam drawing was imported directly from Inventor into the Workbench environment. It was necessary to add the materials properties of the weld material. Once the Mechanical environment had been entered and the geometry was prepared and set with the above procedure, the constraints for the loading and fixtures could be added. Figure 5-10 shows the loads applied to the beam and its direction and location. The sector, grabber and rotating head forces had been simplified into a moment as calculated in Appendix A – 3.4.2. All loads were rounded up to the nearest 1000 N.

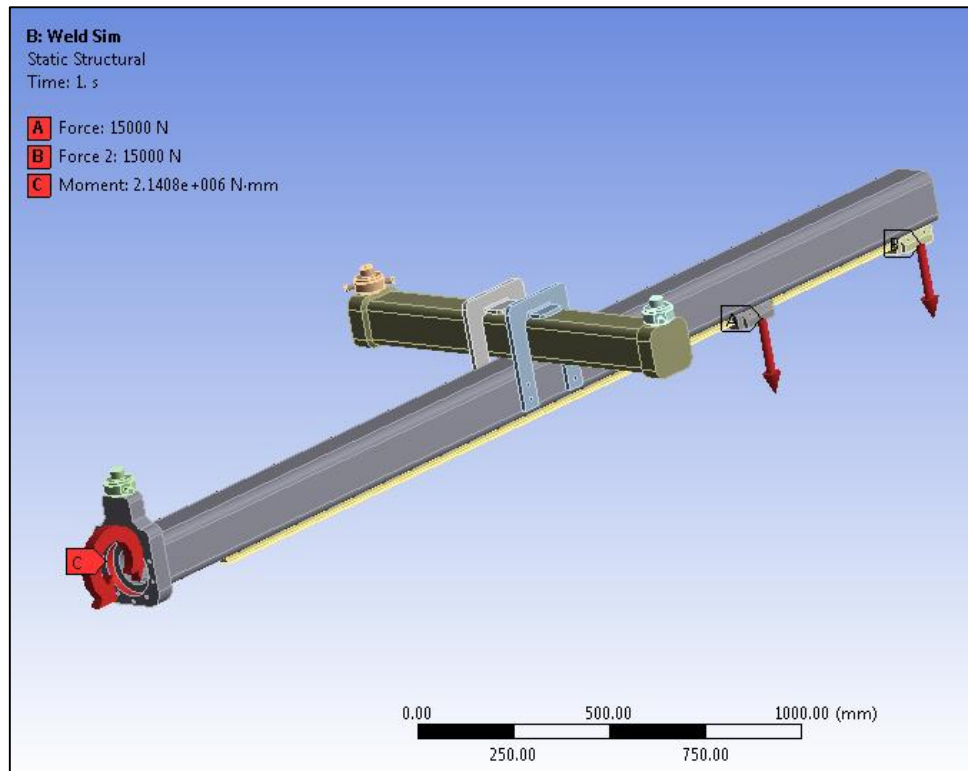


Figure 5-10. Loads applied to main beam.

Fixed ground constraints were applied to the 3 hoist points, however rotation about the axis parallel to the cross was free. This would not offer inaccurate strength during main beam deflection. The simulation was then run and due to the dense and irregular mesh by the penetrating weld, the simulation had to complete 9 iterations before converging. Figure 5-11 shows the Von Mises stresses experienced by the assembled main beam and cross beam. The stress reached a maximum of 272.42 MPa at the cross beam to main beam bracket hole. The stress pattern shown confirms the expected behaviour of the main beam profile. The counter weight applied a load causing a cantilever effect. The hoist point at the front effectively supported a significant portion of the sector, grabber and rotation head load and hence not much stress was experienced in the beam immediately after this point. The cross beam hoist points therefore acted as the main resisting point in the beam and the beam deflected about this point resulting in the highest stresses being in this region.

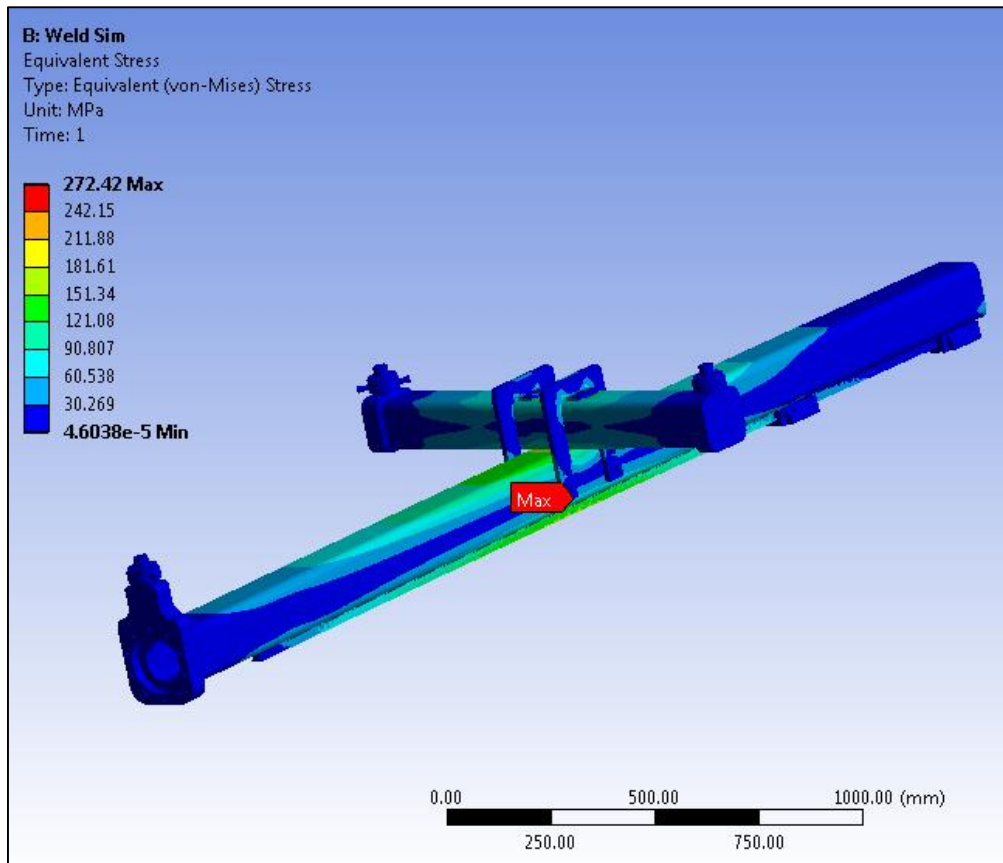


Figure 5-11. Main beam assembly Von Mises stress plot.

Figure 5-12 shows the stresses experienced by the weld joining the front plate to the main beam. A tool that allows certain stress magnitudes to be shown, capped iso-surfaces, was used to display the specific stresses in the areas where the weld penetrated. Since the front region of the main beam was not highly stressed due to the front hoist point, the maximum stress in the weld material reached a maximum of approximately 23.5 MPa. This value is significantly lower than the weld calculation in Appendix A – 3.5.2 of 120.3 MPa. The main difference for this case to the FEA is that there a worst case scenario was assumed where all the weight of the sector, grabber and rotation head was completely supported by the weld.

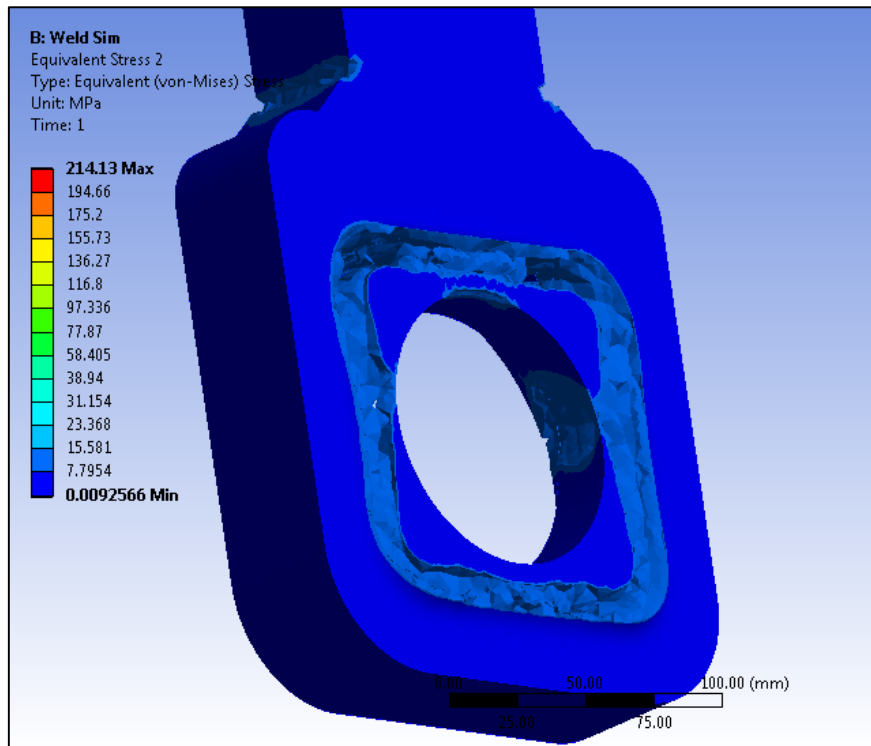


Figure 5-12. Weld penetration stresses of main beam.

5.4.3 Main beam hoist thread

The three hoist rings of the tooling are connected to the 50 mm end plates by means of an M24 threaded hole. It was of interest to accurately simulate what internal stresses would be experienced by these threads during operation.

The procedure for simulating threaded holes has been rather streamlined in ANSYS 15. The first step is preparing the geometry correctly. The hole and bolt diameter must be drawn equal, according to the outer thread size. Therefore for an M24 thread like the hoist rings, a 24 mm diameter will be selected. This geometry can then be imported into the Workbench environment. After entering the Mechanical environment, the body surfaces must be constrained. The outer cylindrical surface of the bolt must be constrained with a Frictional Surface Constraint to the inner cylindrical surface of the hole. To achieve this the bolt or body with the threaded hole can be temporarily hid in the geometry menu by accessing the context menu and selecting “Hide body” in order to view said surfaces. Once the frictional surface is constrained the Geometric Modification tab should be selected on in the Contacts menu (Sciuccati, 2015).

Next the drop down menu under Contact Geometry Correction should be changed to Bolt Thread. This in turn will open a new drop down list where the mean pitch diameter, pitch distance, thread angle, thread type and thread direction can be inputted as in Figure 5-13.

Details of "Frictional - Main Beam:1 To 5W3dP5-23374_23374-1.1"	
Advanced	
Formulation	Program Controlled
Detection Method	Program Controlled
Penetration Tolerance	Program Controlled
Elastic Slip Tolerance	Program Controlled
Normal Stiffness	Program Controlled
Update Stiffness	Program Controlled
Stabilization Damping Factor	0.
Pinball Region	Program Controlled
Time Step Controls	None
Geometric Modification	
Interface Treatment	Add Offset, No Ramping
<input type="checkbox"/> Offset	0. mm
Contact Geometry Correction	Bolt Thread
Orientation	Program Controlled
<input type="checkbox"/> Mean Pitch Diameter	20.75 mm
<input type="checkbox"/> Pitch Distance	3. mm
<input type="checkbox"/> Thread Angle	60. °
Thread Type	Single-Thread
Handedness	Right-Handed

Figure 5-13. Geometric modification details for bolt thread simulation.

Once this step is complete the components are ready to be meshed. Allowing ANSYS to automatically generate the mesh will then generate the threads as a result of selecting the specialised contact. However to accurately simulate the threads the following modifications to the standard settings were completed. In the Mesh details menu a MultiZone method should be added and applied to the bolt shank. This help develop the detailed mesh for the cylindrical shape. Next a mesh sizing should be applied to both the shank and internal cylindrical face of the hole. Table 5-2 shows the following changes that should be made from standard and program controlled settings (Sciuccati, 2015):

Table 5-2. Changes to Sizing Details for accurate Bolt Thread simulation in ANSYS.

	Standard Setting	Required Setting
Use Advanced Size Function	Off	On curvature
Relevance Center	Coarse	Medium
Initial Size Seed	Active Assembly	Active Assembly
Smoothing	Medium	Medium
Transition	Fast	Slow
Span Angle Center	Coarse	Medium

A modification that greatly helps accuracy and more importantly achieving convergence is choosing a mesh element size that is one quarter the size of the pitch. This ensures that there are sufficient elements per thread. Failure to do achieve this critical element size could result in the solution diverging.

To conduct this simulation for the hoist ring on the front of the main beam the existing main beam simulation could be utilised. The hoist ring uses an M24 thread with a 3 mm pitch. This would mean selecting a 0.75 mm mesh to achieve the required accuracy of the threads. With an element size as small as this, the number of elements generated in just the thread region would grow significantly. This

included with the remaining elements through the rest of the main beam would cause the computational time and required memory to increase immensely. To avoid this computationally expensive exercise a procedure known as sub-modelling was used.

To utilise sub-modelling an initial model must be completed. Here the simulation for the main beam bending and weld was used. Next the Static Structural simulation for the initial model must be duplicated in the Workbench environment and a linked must be made to feed the Solution Function of the original model into the Setup function of the duplicated simulation as seen in Figure 5-14.

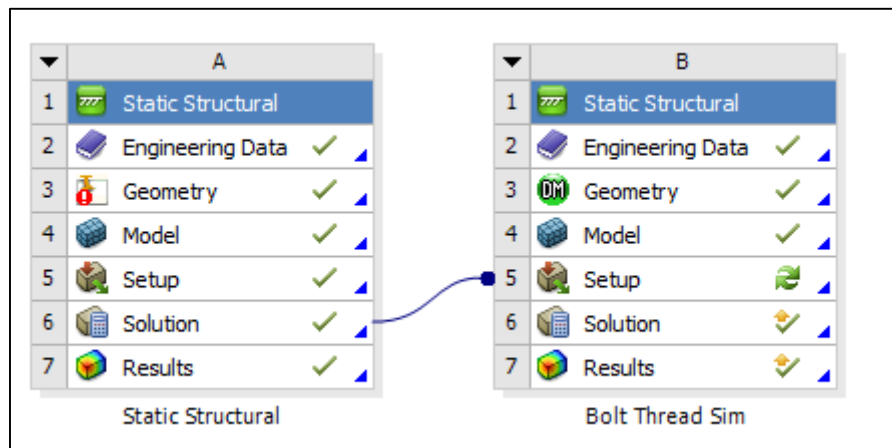


Figure 5-14. Connecting 'Solution' to 'Setup' for Sub-modelling.

Once the link is created the Design Modeller must be accessed in the new model. Here the geometry must be spliced in order to separate a portion of the detailed area of simulation from the rest of the component. Once this is complete the ANSYS Mechanical environment can be accessed. Here the component will now appear as two separate bodies. The body that is not of interest can be suppressed by accessing the Geometry menu and selecting Suppress Body. Only the portion of the body that requires the detailed meshed will remain. The main beam was spliced to display just the top of the welded plate with the threaded bolt hole as seen in Figure 5-15.

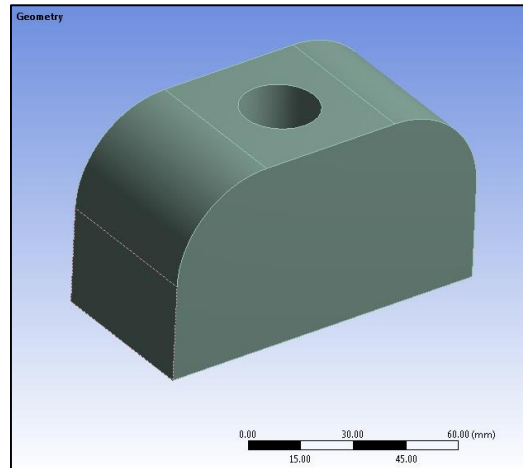


Figure 5-15. Sliced portion of main beam with hoist bolt hole.

After this step the results of the previous simulation were linked to the simplified portion by adding a Sub-modelling study in the Static Structural menu. Here an Import Cut Boundary Constraint was created. The face that the body was sliced on was selected for this constraint. By doing this the exact loads, deflection and strains of the original full model were applied to the plane in question as seen in Figure 5-16. This procedure ensured that all the necessary results of the full solution was carried over to the simplified body without the need of re-simulating the rest of the entire body (Sciuccati, 2015).

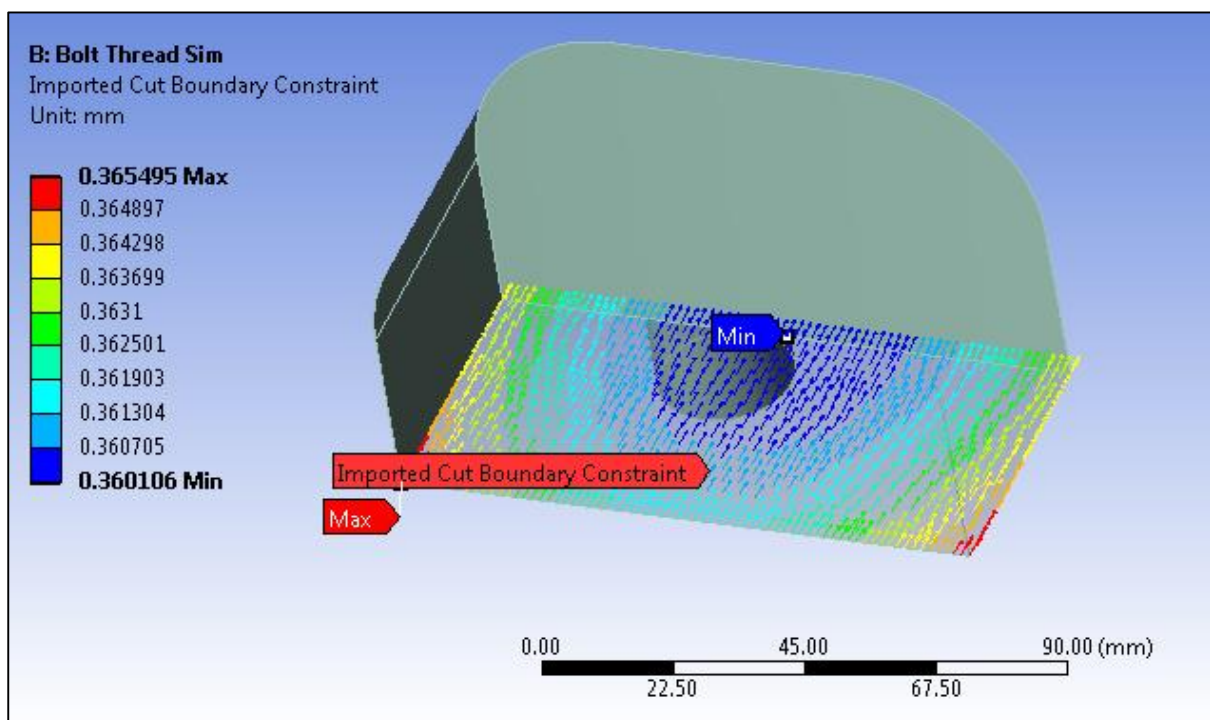


Figure 5-16. Imported Cut Boundary Constraint to adopt full model solution for sub-modelling.

After this the bolt hole was meshed using the proposed methods and settings. An element size of 3 mm was used for the entire volume while a contact sizing of 0.75 mm was used to satisfy the critical thread element size. The generated mesh can be seen in Figure 5-17. The fine mesh covered the entire surface

where contact was made with the hoist bolt, including the washer area on top. A noticeable trait is that the fine mesh stopped just before the bottom of the hole. This is due to the fact that the leading portion of the bolt is tapered and makes no contact with the threads of the hole, hence no additional detail was required in that region.

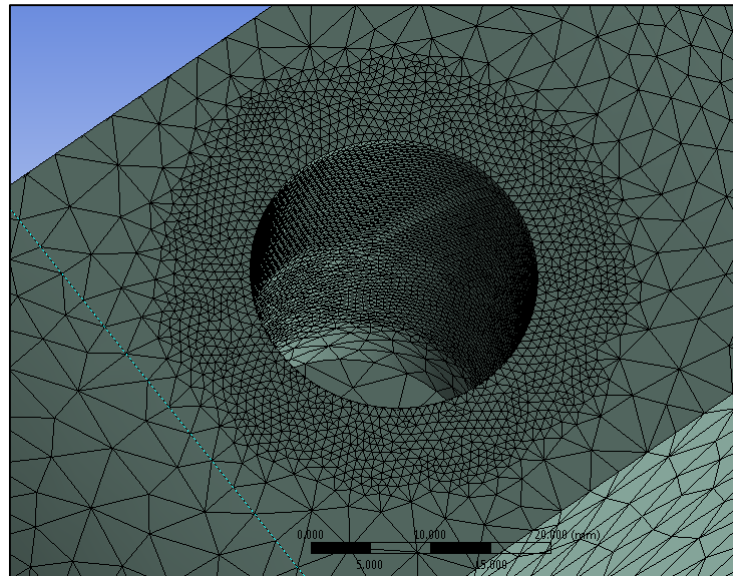


Figure 5-17. Finer mesh required for accuracy of threaded hole.

Since the entire model was a duplication of the previous full model simulation in Chapter 5.4, it was not necessary to remodel any of the other constraints or loads. Unnecessary constraints for the suppressed geometry were also suppressed. The model was run and due to the fine mesh it required 22 iterations to converge. Figure 5-18 shows the induced stresses at the individual threads reaching a maximum of 285.76 MPa.

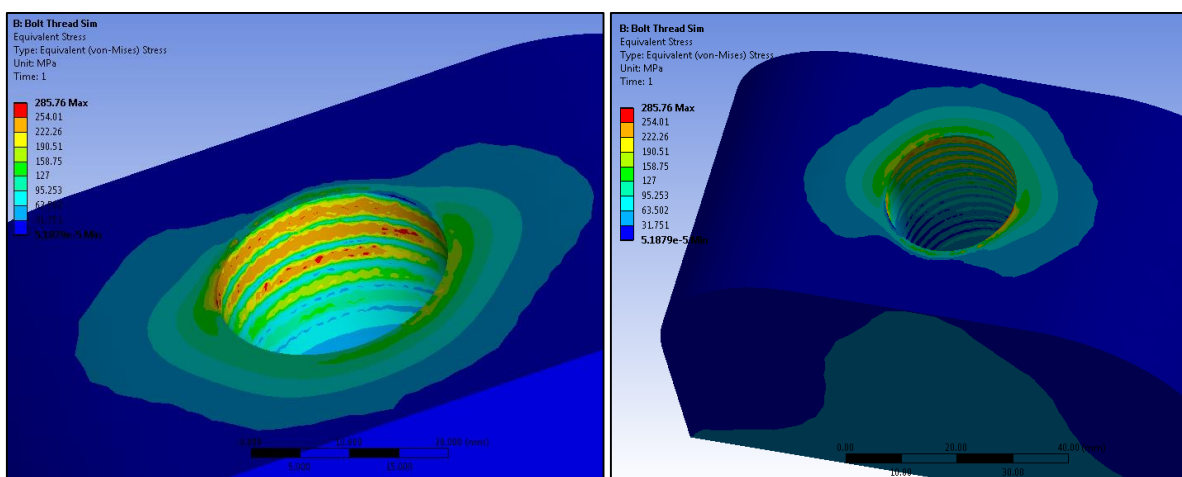


Figure 5-18. Thread Von Mises stresses of front hoist point hole.

From these various simulations the main beam assembly was successful in not exceeding the 355 MPa limit when experiencing loads with a safety factor of 2 and was therefore finalised.

5.5 Trunnion shaft study

The trunnion shaft is responsible for supporting the entire load of the sector, grabber and rotation head between two bearings and its mounting plate. In order to get an estimate of the dimensions the Trunnion Shaft Program was written to compute the bending stresses that the shaft would experience. This program is based directly on the bend stress calculation and force distribution diagram in Appendix A – 3.4.2.

After initial results were obtained using the dimensions of the previous tooling shaft it became evident that the diameter would need to increase significantly for two reasons. The first reason was that the shaft would fail under bending, even if a strong shaft material like En 9(S) were to be utilised. En 9(S) has a yield point of 555 MPa and is readily available in both South Africa and Europe in diameters up to 250 mm. The second reason was that the bearings of that size would not withstand the forced exerted on the more highly loaded side. The Trunnion Shaft Program was then used to find the next suitable size going up in increments of standard bearings sizes. It was found that a shaft size of 100 mm would be sufficient for a bearing of that size to support the load, however the shaft was still slightly beyond the yield point at the bearing abutment. A trunnion shaft with a diameter of 100 mm would require a trunnion coupling of 250 mm. Since this was the largest size profile offered by standard suppliers, it was decided to optimise the shaft using stress relief methods as a larger size would be restricted by the trunnion coupling.

A stress relief method investigated was the utilisation of stress relief grooves. These are strategically machined grooves of a various shape and size that causes force lines to move away from sharp bearing abutments.

In order to determine the critical size, shape and position of such a groove on the trunnion shaft, it was decided to approach the problem in two separate ways. One approach was utilising the Trunnion Shaft Program and including the stress concentration factors as per the relevant graphs in Appendix E. The second approach was to conduct a series of FEAs where each model has the groove in different shapes and positions.

Since the analytical approach would not have displayed the effect of changing the groove position, the FEA approach was carried out first. The analytical approach merely applies a factor to the stress calculation and therefore no detail regarding its position or interaction with other geometric features affect the result.

Each model included features referred to by the symbols per Figure 5-19.

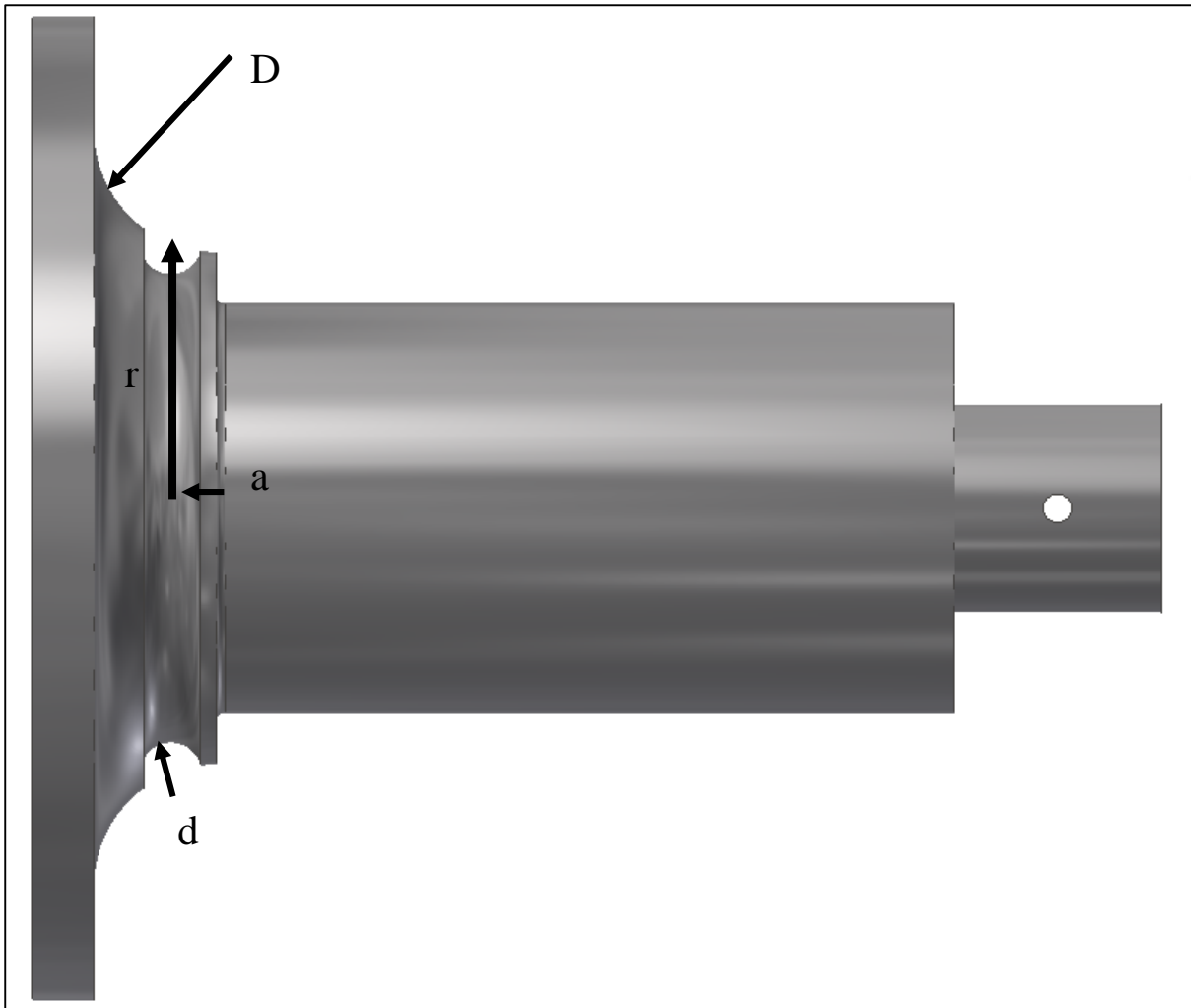


Figure 5-19. Trunnion shaft groove symbol diagram.

The symbols are as follows:

D – large shoulder diameter

d – groove diameter

a – axial distance from shoulder to centre of groove diameter

r – radial distance from shaft axis to centre of groove diameter

The results of various setups were as follows:

Table 5-3. Peak Von Mises stresses for different relief groove permutations.

D (mm)	d (mm)	a (mm)	r (mm)	Peak Stress (MPa)
20 (no groove)	0	0	0	599.23
30 (no groove)	0	0	0	572.82
30	8	7.5	55	786.34
30	15	10	55	545.15
30	6	10	50	612.85
30	20	10	55	563.84
30	15	10.5	62.5	496.75
30	15	8	62.5	523.91
30	15	15	62.5	511.36
30	15	12	62.5	502.66
30	15	12	67.5	509.48
30	15	11.4	65	490.42

Multiple simulations were conducted and Table 5-3 shows a selection of these simulations. The first parameter investigated was the effect of increasing the major radius of the shaft. When the radius was increased from 20 mm to 30 mm, the peak stress reduced by 26.41 MPa. The radius could not be increased any more than this as it would interfere with the holes that mount the shaft to the rotation head; there would not be a flat clamping area for the bolt. The next step was the inclusion of a relief groove. The first groove had a diameter of 8 mm. This caused the stress to increase significantly, hence a stress concentrator was developed instead of a relief groove. Next groove diameters of 15 mm, 6 mm, 20 mm and 15 mm were chosen. The effect of these groove diameters were not proportional to their magnitude. A smaller groove diameter of 6 mm caused a peak stress significantly lower than the 8 mm diameter, yet still higher than the shaft without a groove. A groove diameter of 20 mm was then chosen and stress was reduced below the un-grooved shaft, hence this acted as a relief groove. An optimum groove diameter of 15 mm was found to offer the lowest peak stress at 545.15 MPa, 27.67 MPa below the un-grooved shaft. Once a suitable relief groove size was determined, the next step carried out was to find the optimum position of the groove on the shaft to obtain the most favourable peak stress. By altering the a and r values an optimum position was determined that offered a peak stress at only 490.42 MPa, a full 82.4 MPa lower than the un-grooved shaft. Like the relief groove diameter, the a and r values did not display a linear relation to the peak stress.

Figure 5-20 shows the stress distribution on the trunnion shaft with a maximum stress value of 490.42 MPa at the centre of the groove. The optimum stress relief groove was therefore found to be a precise balance between the three dimensional parameters. Introducing a groove with too small a diameter resulted in a greater stress concentration being included. A diameter too large caused a similar scenario

as too much material was taken away. The best combination was found to be a groove with a 15 mm diameter at a distance of 65 mm away from the shaft axis. This ensured that the force flow lines were sufficiently deflected, but also that the groove was not too close to the force lines. After that it was found that moving the groove slightly away from the shoulder optimised the relief further.

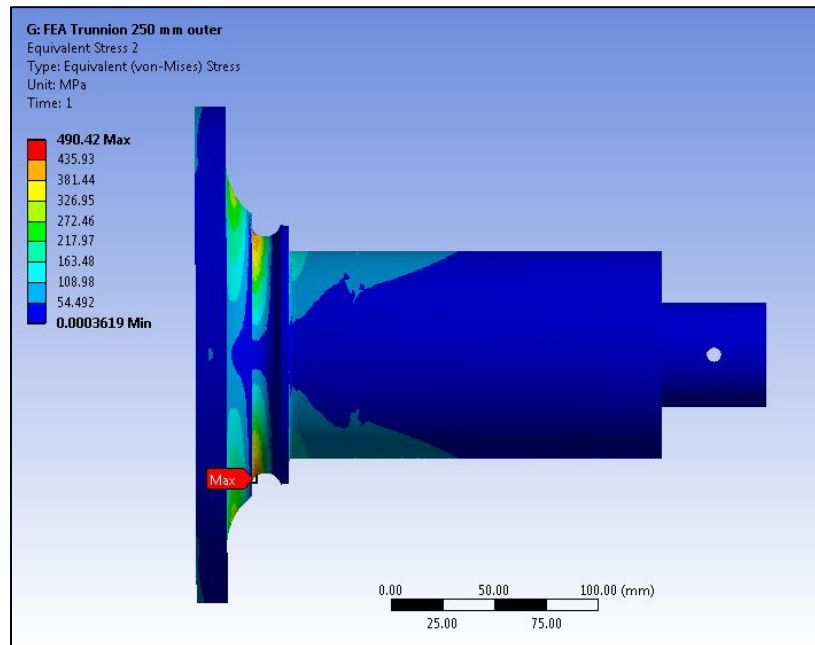


Figure 5-20. Stress experienced by trunnion shaft with stress relief groove.

Once it was determined that the stress could be reduced significantly below the 555 MPa limit of the shaft material by using a particular diameter and position, the Trunnion Shaft Program was used to verify these results. The stress concentration factors, K_t , were obtained from the notch sensitivity tables in Appendix E and utilised in the Trunnion Shaft Program. Two separate methods were used to calculate the bend stress in the program. The first method calculated the moment term for the bend stress by using the reaction force exerted by the bearing and the second method used a summation of all the moments experienced by the shaft. The reason for using these two methods were to verify that the stress at the bearing with the highest reaction force corresponded to the moment about the bearing abutment. Appendix D - 3 shows the program with both methods indicated as well as chosen average K_t value of 2.2. The analytical method displayed a final stress of 491.56 MPa. This was similar to the FEA result of 490.42 MPa and therefore the design for the trunnion shaft was finalised with these dimensions. The inclusion of a stress relief groove therefore caused a vast improvement over the shaft without a relief groove that peaked at 572.82 MPa.

5.6 Hoisting and spatial consideration of final tooling

An area of consideration when designing the overall tooling was adherence to spatial awareness to avoid interaction with any other part of the NSW assembly when installing sectors or spokes. As mentioned in the LS and SS grabber design details, the suggested allowance gap around any part of the grabber

envelope should be at least 30 mm. Figure 5-21 shows the gaps between the respective sector and its spoke. The SS grabber had a minimum clearance of 35.12 mm while the LS grabber had a 30.03 mm gap.

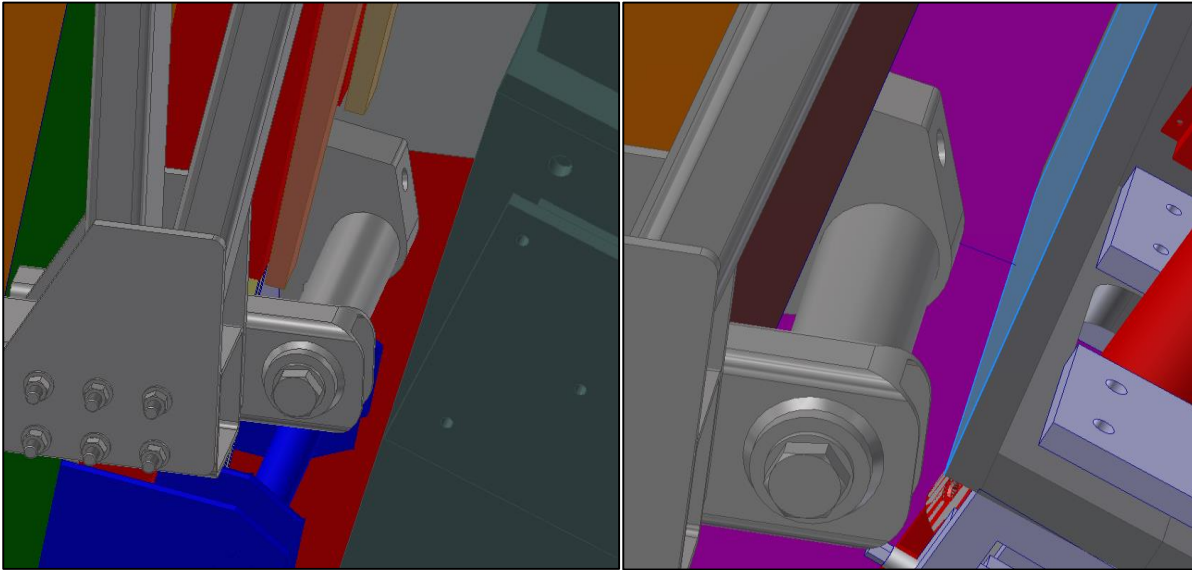


Figure 5-21. Minimum SS grabber clearance (left) and LS grabber clearance (right) (Singh, 2015).

The next spatial consideration was that of the overhead crane. The overhead 140 ton crane in Building 191 at the Meyrin site of CERN comprises a large hoisting hook with a rectangular pulley box that moves with the hook. The tooling hoist point was designed at the correct dimension to ensure that this box would not come into contact with the protruding NSW hub when the bottom Small sectors are installed as this scenario would be the worst case. Figure 5-22 shows this scenario in a 3D model with sufficient clearance between the crane pulley box and the hub.

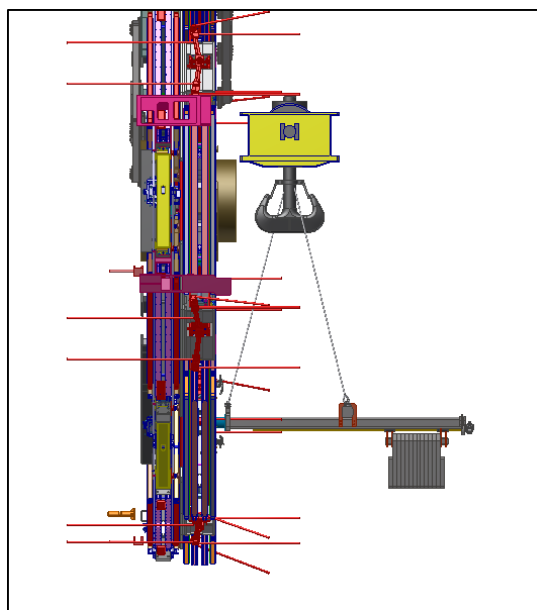


Figure 5-22. Overhead crane clearance when installing Small sector (Singh, 2015).

5.7 Final design specifications

Figure 5-23 shows the completed design for the NSW Installation Tooling with LS grabber attached.

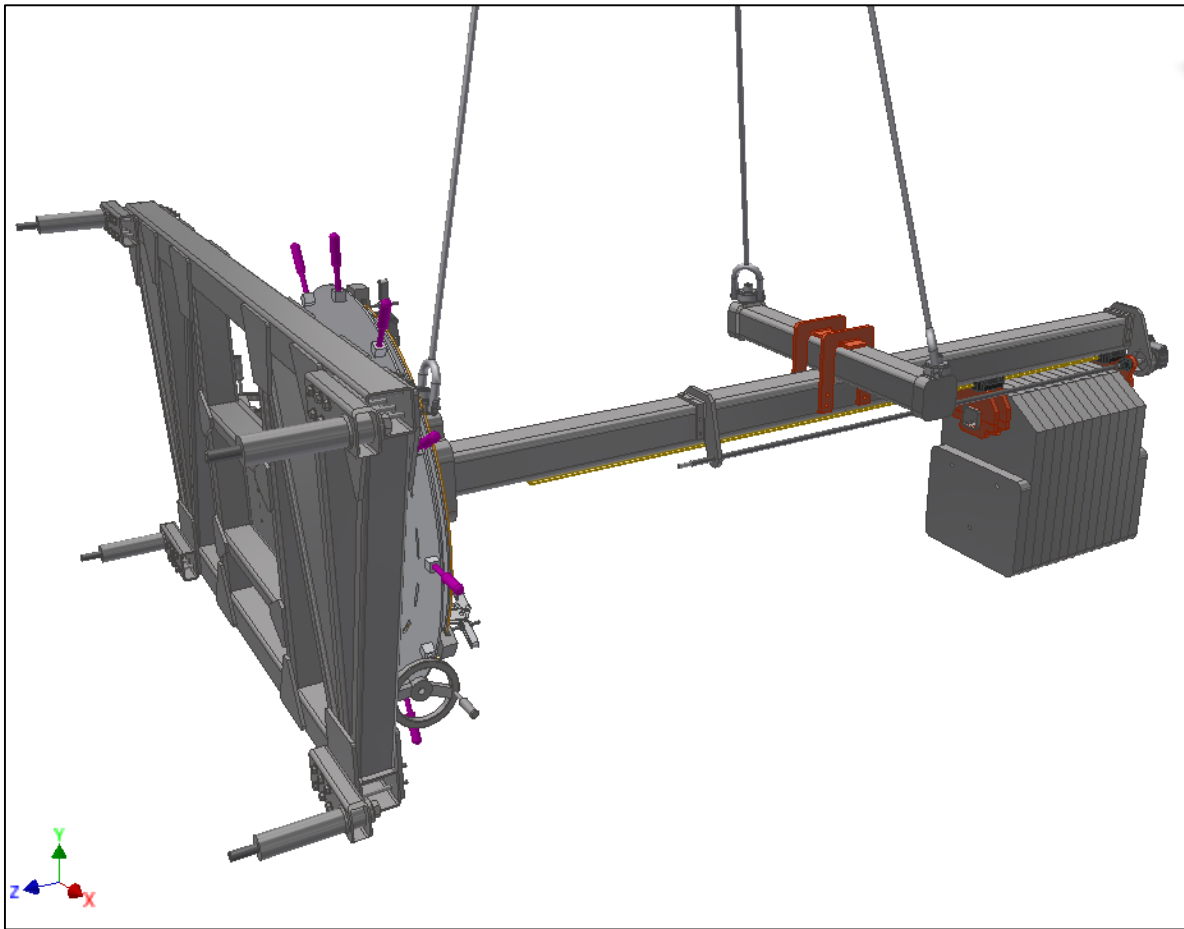


Figure 5-23. Full NSW Installation Tooling with LS grabber.

All remaining stress and deflections calculations to determine the dimensions shown in Table 5-4 are shown in Appendix A, the Tooling Safety Document required by CERN to verify the legitimacy of the design. All manufacturing drawings for final design appear in Appendix C.

Table 5-4. Final NSW Installation Tooling design specifications.

Component	Description
Total tooling weight (No grabbers or sectors)	2276 kg
No. of CW slices	12 slices + 2 add-on slices
CW slice material	T690 steel alloy
Motor selection (Model, power, max torque)	WEG EPG 233 Type 14, 350 watt, 25 Nm
Main beam length	3050 mm
Main and Cross beam material	S355 steel
Hoist ring size	M26
Total tooling length (Grabber pin to motor)	4017.5 mm
Beam linear guide type and length	Thomson Linear 512 B, 2700 mm
COG translator linear guide type and length	Thomson Linear 512 D, 553.4 mm
Hoist rope length	3000 mm
Trunnion shaft material	En 9(S)
Trunnion bearing type	SNR NTN
Grabber pin bolt	M24 x 340 mm

Chapter: 6 Design evaluation and discussion

6.1 Comparison of NSW Installation Tooling to Wisconsin Tooling

The most significant change between the toolings is the relative counter weight mass compared to the sector mass. The Wisconsin Tooling had a maximum lifting capability of 400 kg which included the sector/chamber and grabber. Its counter weight had a mass of 1144 kg. This means that the counter weight mass is 2.86 times heavier than sector/chamber and grabber mass. Since the NSW Installation Tooling has a forward biased hoist point, the counter weight is only 1732 kg in order to support a 1450 kg sector and a 280 kg grabber (combined mass of 1730 kg). The counter weight mass is therefore approximately a one to one ratio with the mass of the supported components. This therefore represents a significant improvement in the mass optimisation of the new tooling. Figure 6-1 shows a visual size comparison of the Wisconsin Tooling to the NSW Installation Tooling. It is evident that NSW Installation Tooling is more efficiently designed from a size perspective considering it is designed to handle a load by a factor of 4.325 times larger than the Wisconsin Tooling.

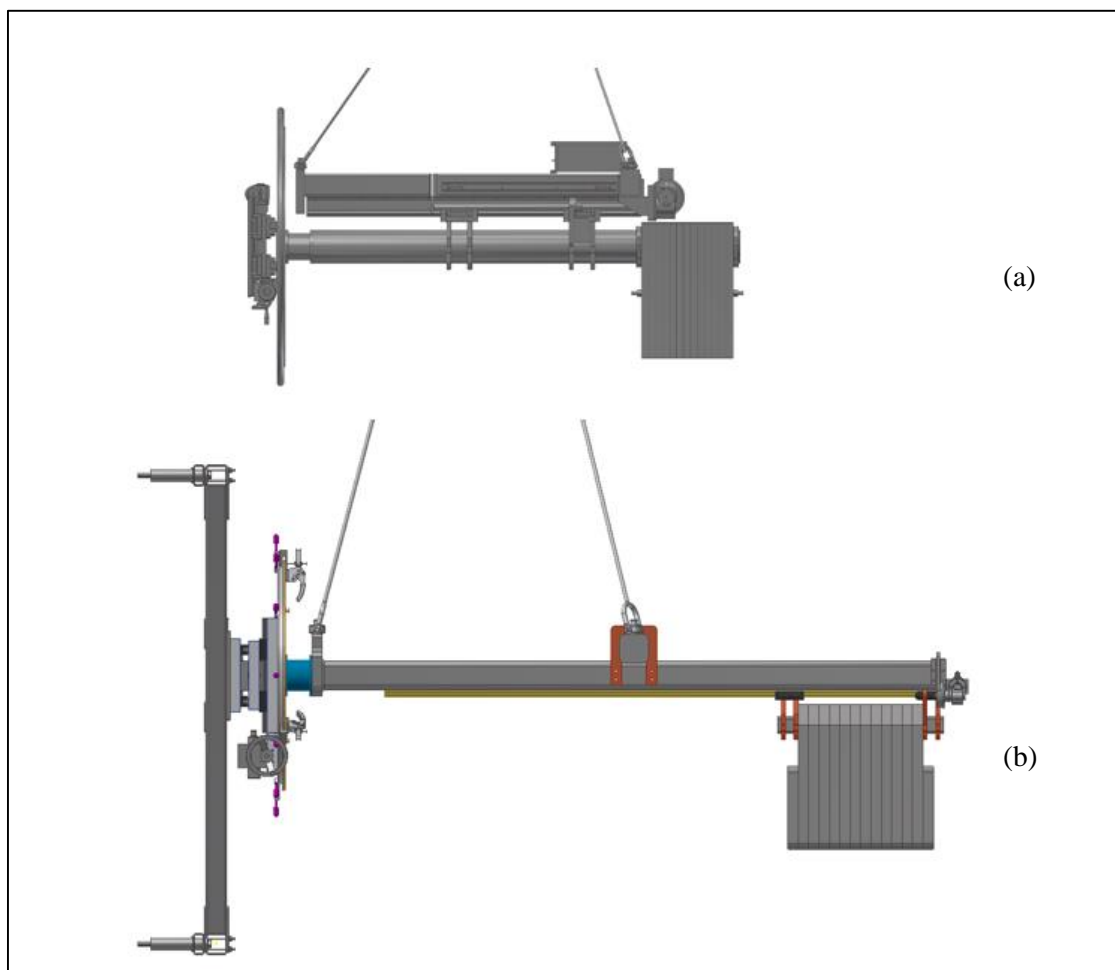


Figure 6-1. Size comparison of Wisconsin Tooling (a) to NSW Installation Tooling (b) (Singh, 2015).

6.2 Specialised FEA procedures

An area of research across all simulations for this dissertation was to implement the best procedure for efficient and accurate convergence of final results, especially for non-linear simulations. The most critical contributor to achieving convergence, or allowing initial configuration to be inside the radius of convergence, was found to be the application of the mesh. A general rule of thumb when trying to achieve convergence and faster computing times is utilising a large element size for the mesh while only sacrificing accuracy. This was found to not be the case when working with non-linear simulations involving frictional surface constraints. Not constructing the mesh to meet small geometric features resulted in much longer periods for the solution to converge and often convergence was not achievable. It is however not feasible to mesh an entire component based on the smallest geometric feature mesh size so it was found that surface and feature mesh refinement was a valuable tool and significant effort was applied to implementing this in the best possible manner.

The bolt thread simulation feature in ANSYS 15 has streamlined the process for achieving accurate results. Previously the bolt and threaded hole would need to be prepared in the CAD model which resulted in having to constrain a number of surfaces resulting in a computationally expensive and non-linear simulation. Alternatively the simulation can be done without thread at the cost of accuracy. The inclusion of bolt thread simulation serves as a compromise between these two methods by offering a significantly high level of accuracy at an efficient solution run time. It is also more convenient as no separate CAD preparation of the threads are necessary.

Weld simulations are often simplified due to the complex nature of a welded part and its make-up. With the geometry controls of ANSYS a detailed and accurate simulation is possible with the few steps utilised in this dissertation. The correct simulations of welds are essential in achieving optimal weld sizes for complex welds that cannot be achieved analytically or by weld tables.

6.3 Manufacture of NSW Installation Tooling

As mentioned, the NSW Installation Tooling will be manufactured in either South Africa at UKZN or in Europe at one of CERN's local or contractual workshops. It was for this reason that special attention had to be given when selecting materials and components to ensure availability in both regions. Another consideration when developing the concepts was the need for simple manufacture and assembly. This would be necessary considering that if the tooling is manufactured in South Africa, it will be disassembled and shipped to CERN.

All of the main tooling components bolt together with metric fasteners. Certain components require precision installation, such as the linear guides onto the rails. The manufacturing processes required to prepare the tooling for this assembly are made up of 4 different procedures. Laser cutting will be used

for all counter weight slices, hoist point end plates, brackets and rotating wheels. The trunnion shaft and coupling will be CNC turned. The main and cross beams as well as the fictional clamp disk will be welded together. The last of the procedures procedure will involve threads being cut into the hoist point end plates. Other minor components will be manufactured by common methods.

6.4 Practical stress analysis

A good point of comparison when confirming stresses and deflections of the tooling components was verifying the FEA result with an analytical calculation where ever possible. This ensured that the FEA model was set up accurately without incurring common problems such as over constraining a model, applying loads incorrectly and introducing artificial strength.

The next step to fully confirm the stresses of the tooling components would be to conduct practical stress analyses on the manufactured tooling. The complication with carrying out conventional stress tests is that components are normally loaded till failure occurs to achieve an accurate confirmation of limits. Other conventional non-destructive methods also do not provide accurate stress results and are mainly used to confirm deflections. Usually a component is strain-gauged at various critical locations and these are compared to the model in the elastic range. A good form of analysis to carry out on the manufactured tooling would therefore be photostress analysis. Photostress analysis consists of spraying the component with a coating that allows a specialised detection unit to monitor displacements and strains. These strains can be used to directly calculate the resulting stresses by applying the material properties (Dantec Dynamics, 2013).

6.5 Refinement of flexible analysis programs

A principle objective of this thesis, aside from the NSW Installation Tooling design, was achieving a flexible design strategy for large scale projects with volatile requirements. A significant aspect in the design methodology in achieving this was implementing simple Matlab programs so that analytical calculations for component dimension and balance were achieved immediately.

These programs proved to be critical with regards to find suitable tooling balance and determining component dimensions. The programs were only coded to find stress and deflection for one critical portion of the components. The programs could be refined and made to include other aspects, thus optimising their effect. The aim would be to use only the programs through the entire design period and only require only a few final FEAs to be conducted before manufacture, without having to repeat the analysis numerous times. Programs can be further improved by including look-up tables for stress concentrations and include if conditions to display any parameter that is exceeded.

Another improvement would be to instead code the program in C++ or Java instead of Matlab. This would allow a GUI where inputs can be updated in a more user friendly manner. This would also offer

more complex aspects of the flexible design feedback loops to be coded in a more widely understood language. Essentially the restrictions of Matlab could be avoided completely.

6.6 Final tooling certification

Since the NSW Installation Tooling will be operated in Switzerland, the final requirement would be the CE safety certification. This involves testing the equipment at 1.5 times the normal load after which the tooling can be stamped with the official CE logo and CE maximum operating weight. This test will be conducted at the CERN premises in Meyrin and will require the necessary safety documents, FEA results and the presence of the author as the design engineer.

6.7 Trunnion shaft study findings

A significant finding during the dissertation was the outcome of the stress relief groove effect on the trunnion shaft in Chapter 5.5. The final groove implemented decreased the stress experienced at the shoulder by 82.4 MPa. This represented a 14.38% reduction in stress. The study showed the significant effect of such a groove.

A further area of optimising the groove would be to observe the effect of different groove shapes instead of only constant diameter grooves. Another area of research could investigate the introduction of multiple grooves along the shaft shoulder. The ideal method for going about this research would be to improve the stress program instead of repeating numerous FEAs. The comparison between FEA and analytical results verified the validity of the FEA calculation. A significant way that the program might be improved is mapping the stress concentration notch sensitivity graphs. This could either be done by introducing lookup tables in the code or inputting the actual graphs for Matlab to interpolate.

Once the tooling components are completed, a final practical analysis using photostress can be used to offer a second method of validation for the FEA result. The results from such strain-gauge testing would also validate the program.

Chapter: 7 Conclusion

The NSW Installation Tooling is a significant improvement over the previous Wisconsin Tooling. It adheres to all functional requirements. This was achieved by specifically addressing the issues that restricted the Wisconsin Tooling from meeting the functional requirements and also by improving its user friendliness. The largest contributor to user efficiency is the use of a moving counter weight carriage. The implementation of this simplified the intended installation process, the time taken and the mechanical stresses experienced by the linear guides. The decision to opt for a stationary hoist point and moving counter weight carriage allowed for the principle of operation to be changed. Operation of the tooling requires just one operator and therefore also decreases the necessary man power and need for precise synchronisation.

The specialised grabbers designed for the LS and SS both ensured that the internal stress limit of the spacer frame was not exceeded. The grabber was also optimised and modified based on outcomes of the FEA to ensure its structural integrity during operation. In addition the design allowed for removable grabber mounts on the spacer frame meaning all magnetic effects could be ignored.

The study of the stress relief grooves on the trunnion shaft resulted in significant optimisations in the shaft design. The analytical calculation aspect of the Trunnion Shaft Program was used to validate the FEA result, showing the benefit and opportunity for optimal design by using only simply coded programs.

The utilisation of dimension-adjustable CAD models and stress-deflection/balance programs lead to achieving flexible and efficient design for the regular change in functional requirements that occurs in the CERN design environment. The design methodology developed allowed for efficient generation and finalisation of concepts even when functional requirements were changed throughout the process.

The work provides a suitable design for the NSW Installation Tooling for manufacture and use in 2017, a flexible design and simulation methodology and significant results in the utilisation of stress relief grooves.

References

ANSYS Inc, 2013. *ANSYS Mechanical General Procedures*

ANSYS Inc, 2013. *ANSYS Mechanical Introduction to Structural Nonlinearities*

ATLAS Collaboration, 2008. The ATLAS Experiment at the CERN Large Hadron Collider. 1(1), pp. 1-97.

ATLAS Collaboration, 2013. ATLAS New Small Wheel Technical Design Report. 1(1), pp. 1-27.

BAHRNS, 2010. *HERCULES Standard Telescoping Booms*. [Online]
Available at: <http://www.bahrns.com/HERCULES-Standard-Telescoping-Booms-id55604.html>
[Accessed 08 October 2015].

Betty, A., 2012. *Strangeness at the new energy frontier, from pp to PbPb*. [Online]
Available at: http://alicematters.web.cern.ch/?q=abelevbetty_strangeness
[Accessed 06 December 2015].

Bini, C., 2013. *Properties and spectroscopy of b-hadrons with the ATLAS detector*, Rome: Sapienza University.

Cattai, A., Ciapetti, M. & Seletskiy, A., 2014. *Small Wheel Different Manufacturing Options*. Geneva, Indico 376888.

Ciapetti, M. & Ponsot, P., 2015. Geneva

Ciapetti, M. & Spigo, G., 2014. *NSW Structure and envelopes*, Geneva

Ciapetti, M. et al., 2015. *New Small Wheel & New JD*, Geneva: Indico 395479.

Dantec Dynamics, 2013. *Q-400 DIC - Digital Image Correlation System - Measurement of Shape, Displacement and Strain*. [Online]

Available at: <http://www.dantecdynamics.com/q-400-dic>
[Accessed 08 December 2015].

European Committee for Standardization, 2005. *Eurocode 3*, Brussels: s.n.

OZENINC, n.d. *ANSYS Mechanical*. [Online]
Available at: http://www.ozeninc.com/images/r12_features2_sm.jpg
[Accessed 05 October 2015].

Peterson, R. E., 1953. In: *Stress Concentration Design Factors*. s.l.:John Wiley & Sons.

- Pinnell, J., 2015. *NSW Simplified foe MMsTGC Grabbers*, Geneva
- Pitot, J., 2011. *Engineering Computational Methods*. Durban: s.n.
- Ponsot, P., 2014. *ATLAS-NSW Layout and Mechanics with a new JD*. Geneva
- Ponsot, P. & Ciapetti, M., 2015. *Proposal for MSc Engineering thesis - Design/FEA*. Geneva
- Ponsot, P. & Spigo, G., 2015. *Specifications for the sector installation tooling of the New Small Wheel*, Geneva
- Schwalb, N., 2014. *Stress Concentration*. Kharagpur: IIT Kharagpur.
- Schweiger, H., 2015. *Spacer frame Prototypes*, Geneva: s.n.
- Sciuccati, A., 2015. *ANSYS 15 layout, features and simulations* [Interview] (09 March 2015).
- Sinclair, P., 2015. *NSW Sector Transport, Assembly and Storage*. Geneva: Indico 395479.
- Singh, S., 2015. *NSW Sector and Foot Spoke Installation Tooling*, Geneva: Indico 395479.
- Spigo, G., 2015. *Stress Relief Grooves* [Interview] (10 June 2015).
- The British Standard Institution, 2010. *Cranes - Safety - Non-fixed load lifting attachments*, La Plaine Saint-Denis Cedex: Boutique AFNOR.
- University of Wisconsin, 2001. *Muon Chamber Lifter/Positioner*. 1(1), pp. 1-34.

Appendix A

Tooling Safety Document

Mechanical calculations and simulations for the New Small Wheel Sector and Foot spoke Installation Tooling and Grabbers for assembly of the New Small Wheel in Building 191

1. Summary

The following document covers the relevant safety calculations for the NSW sector and foot spoke installation tooling and respective grabbers. It deals specifically with the critical components of the tooling and describes the various assumptions, factors and analytical procedures conducted in order to conform to the relevant Eurocode and accompanying standards.

2. Document Introduction

The mechanical integrity of the NSW sector and foot installation tooling is vital for the design to be of any value. In order to maintain the required integrity and safety margin, the Euro code has been satisfied for all tooling components. Since steel is the material used in all stressed parts of the tooling, Eurocode 3 has to be consulted; European Standard EN 1993-1-1. In addition to the Eurocode, the standards of BS EN 13155:2003+A2 will be complied with specifically for Cranes-Safety-Non-fixed load lifting attachments. The specific requirement that has been addressed from the document is from chapter 5 for Safety requirements and/or measures where under point 5.1.1.1 it states, “the attachment shall be designed to withstand a static load of two times the working load limit without permanent deformation.” In order to satisfy this requirement, all forces and masses are first multiplied by a factor of 2 before stress calculations are done. In this way the maximum stress needs only to fall below the yield stress of the material to be in accordance with the safety requirements.

3. Installation tooling descriptions and calculations

a. Large Sector Grabber

i. Description

The Large Sector Grabber will attach to the Large Sector to position and orientate during NSW assembly. The LS Grabber is to be made of a combination of 100 x 100 x 5 mm square steel profiles and 100 x 50 x 5 mm rectangular steel profiles. These profiles are cut and welded to realise the shape below. Separate grabber arms are bolted onto the main grabber frame to offer the connection point to the large sector. The material intended to be used is S355 which yields at 355 MPa and has a modulus of elasticity of 210 GPa. S355 also has a UTS of 470 MPa. The Large Sector grabber is a trapezoidal shape that has 4 protruding arms as seen below.

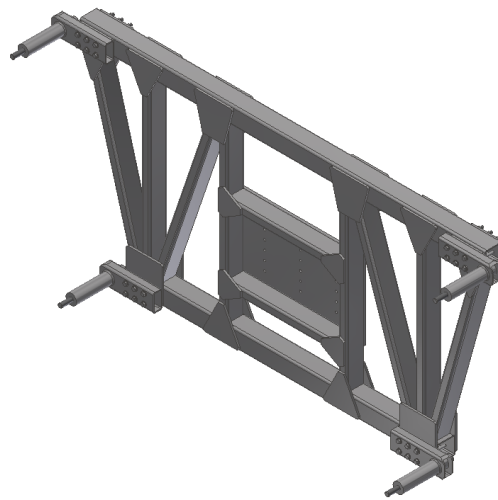
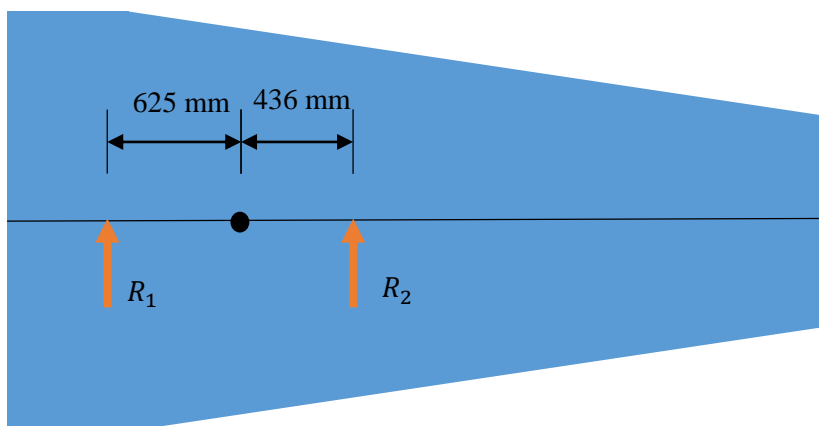


Figure 2 - Large Sector Grabber

ii. Calculations

Forces on Grabber pins:

Assume worst case scenario; sector is orientated to horizontal position where forces on grabber pins are highest due to dissimilar positions away from centre of gravity of the sector.



$$W_{LS} = 1450 \text{ kg} = 14224.5 \text{ N}$$

with SF of 2, $W_{LS} = 28449$ N

$$R_1 + R_2 = 28449 \text{ N} \quad \therefore R_2 = 28449 - R_1$$

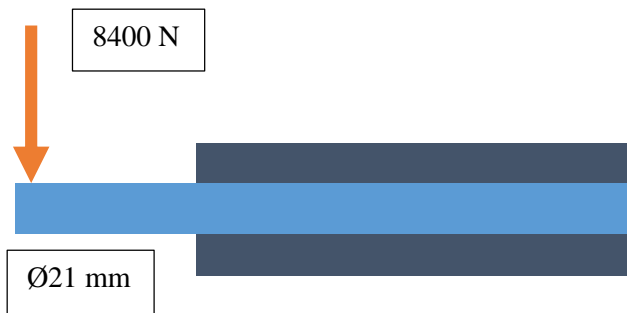
$$\Sigma_{R_1} = 0 \quad \therefore -W_{LS} (0.625) + R_2 (0.625 + 0.436) = 0$$

$$-(28449)(0.625) + (28449 - R_1)(0.625 + 0.436) = 0$$

$$\therefore R_1 = 11690.64 \text{ N}, \quad \text{so for each pin: } \frac{R_1}{2} = \frac{11690.64}{2} = 5845.32 \text{ N, say } R_1 = \mathbf{5900 \text{ N}}$$

$$\therefore R_2 = 16758.36 \text{ N}, \quad \text{so for each pin: } \frac{R_2}{2} = \frac{16758.36}{2} = 8379.18 \text{ N, say } R_2 = \mathbf{8400 \text{ N}}$$

Grabber pin shear:

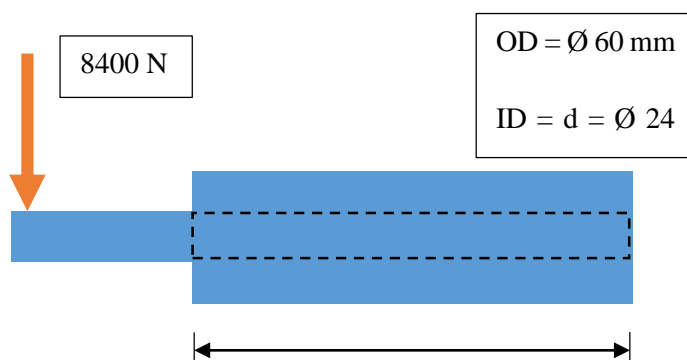


$$\tau = \frac{F_s}{A} \times \frac{4}{3} = \frac{F_s}{\frac{\pi \times d^2}{4}} \times \frac{4}{3} = \frac{8400}{\frac{\pi \times 0.021^2}{4}} \times \frac{4}{3} = 32.34 \text{ MPa}$$

$$32.34 \text{ MPa} \leq 205 \text{ MPa}$$

\therefore Design is compliant

Grabber arm round profile bending:



$$\sigma_b = \frac{32M}{\pi d^3} = \frac{32 \times (8400 \times 0.232) + 0.06}{\pi \times (0.06^3 - 0.024^3)} = 94.31 \text{ MPa}$$

$$94.31 \text{ MPa} \leq 355 \text{ MPa}$$

∴ Design is compliant

$$\delta = \frac{1}{3} \frac{Fl^3}{EI} = \frac{1}{3} \frac{Fl^3}{E x \frac{\pi x d^4}{64}} = \frac{1}{3} \frac{4200 x 0.232^3}{206 x 10^9 x \frac{\pi x (0.06^4 - 0.024^4)}{64}} = 0.14 \text{ mm}$$

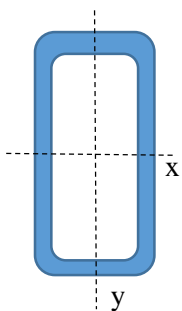
$$\alpha = \frac{Fl^2}{2EI} = \frac{Fl^2}{2 x E x \frac{\pi x d^4}{64}} = \frac{4200 x 0.232^2}{2 x 206 x 10^9 x \frac{\pi x (0.06^4 - 0.024^4)}{64}} = 0.885 \text{ m rad} = 0.051^\circ$$

The deflection is of great concern as the grabber arms connect directly to the sector. This deflection translates to stress on the actual spacer frame when the spacer frame is taken into account. It is therefore vital that this value be small. See FEA which shows the stresses induced in the spacer frame when it is taken into account.

Assume all bending force applied to 4 vertical uprights.

$$\text{Therefore } \frac{28449}{4} = 7112.25 \text{ N say } 7200 \text{ N}$$

Frame bending:



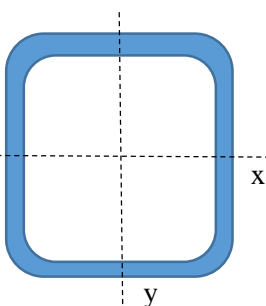
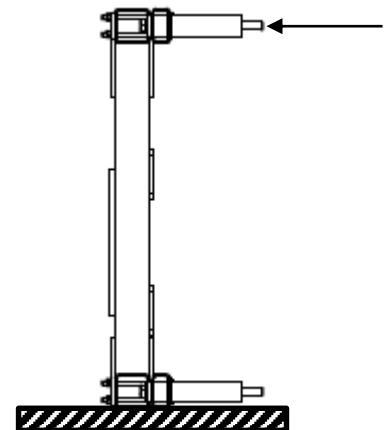
Rectangular cross section: 100 x 50 x 5 mm

$$I_{xx} = 158.19 \text{ cm}^4$$

$$\sigma_b = \frac{My}{I} = \frac{2 x 7200 x 0.342 x 0.05}{8 x 158.19/100^4} = 19.46 \text{ MPa}$$

$$19.46 \text{ MPa} \leq 355 \text{ MPa}$$

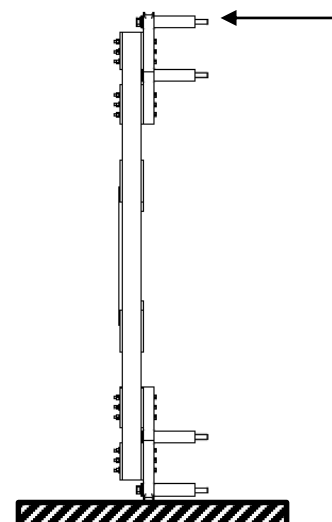
∴ Design is compliant



Square cross section: 100 x 50 x 5 mm

$$I_{xx} = 271 \text{ cm}^4$$

$$\sigma_b = \frac{My}{I} = \frac{2 x 8400 x 0.342 x 0.05}{2 x 271/100^4} = 53 \text{ MPa}$$



53 MPa \leq 355 MPa

\therefore Design is compliant

iii. FEA

The FEA below shows the stresses induced when applying 2 times the force induced by the weight of the large sector on the large sector grabber frame. The frame is fixed to ground at the tool interface holes and the force is applied to the spacer frame. The stresses peak at 205.21 MPa at the point where the grabber arms edge touches the grabber frame gusset plate. This value of 205.21 MPa is below the yield point of S355 steel and therefore the Eurocode is satisfied and the design is compliant.

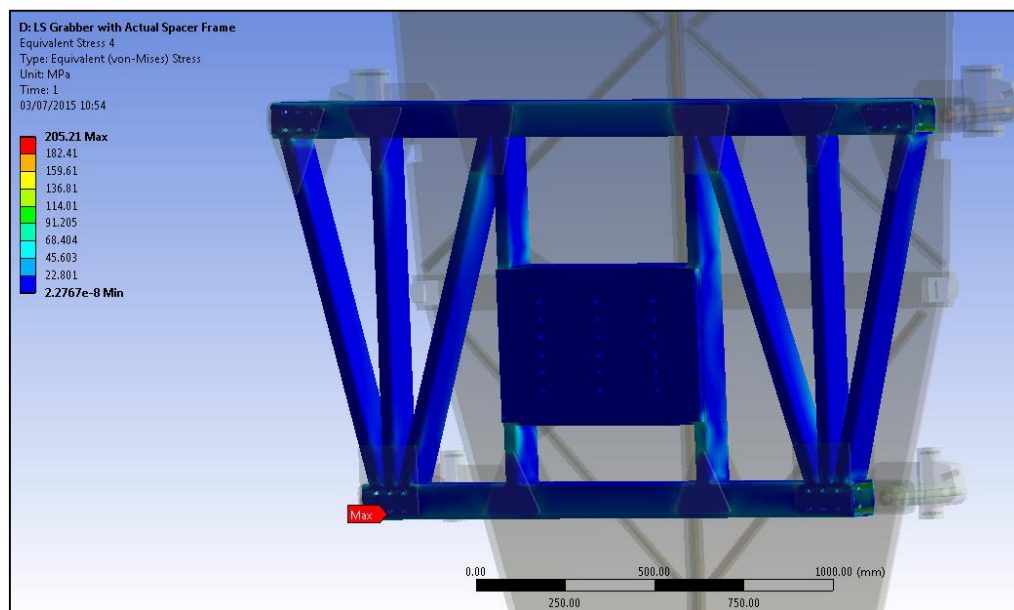


Figure 3 - FEA of LS Grabber Frame with Spacer Frame attached

This FEA shows the stresses induced on the spacer frame when it is attached to the grabber as a result of the deflection of the grabber arms. The FEA also included the force multiplied by a factor of 2 to comply with the required Eurocode and peaks at 43.38 MPa at the grabber point interfaces. This value is comfortably below the yield point of 240 MPa for 6082-T6 aluminium and therefore the design is compliant.

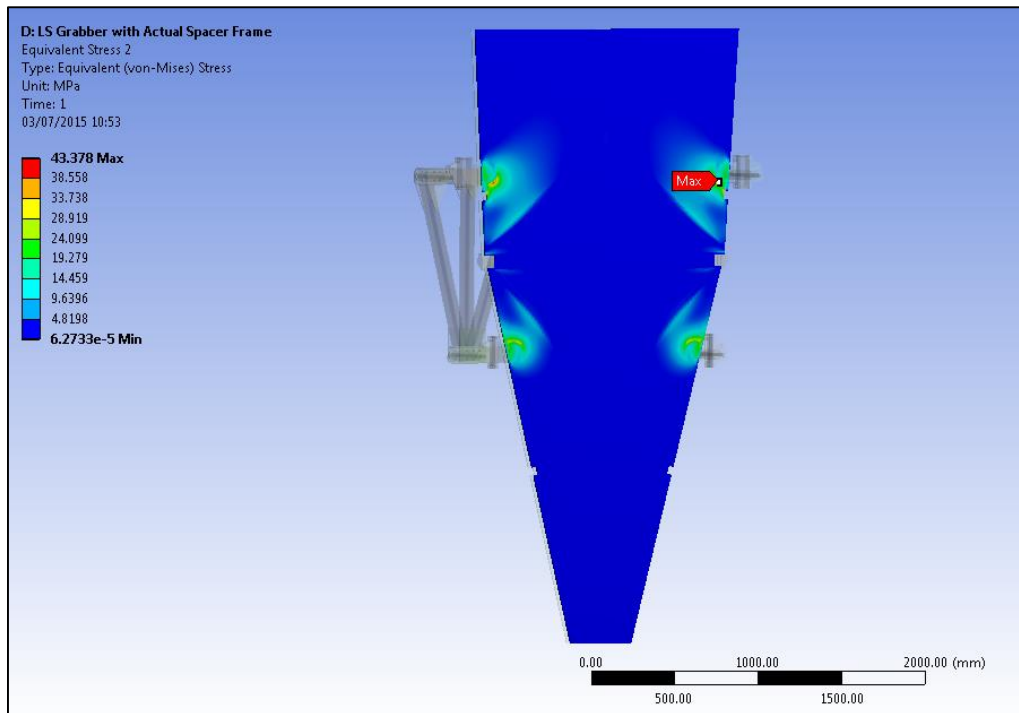


Figure 4 - Stresses induced on Spacer Frame as a result of Grabber arm deflection

The grabber arms seen below experienced 227.1 MPa at the point where its edge touches the grabber frame gusset plate. This again is below the yield point of 355 MPa of S355 steel. The design is therefore compliant.

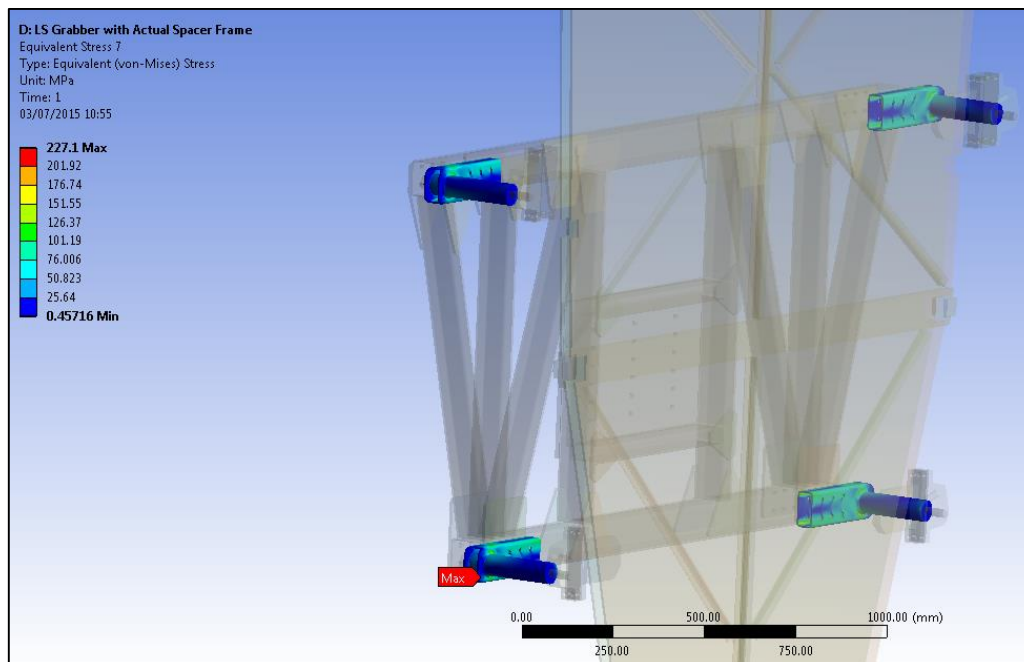


Figure 5 - Grabber arm bracket stresses during loading

b. Small Sector Grabber

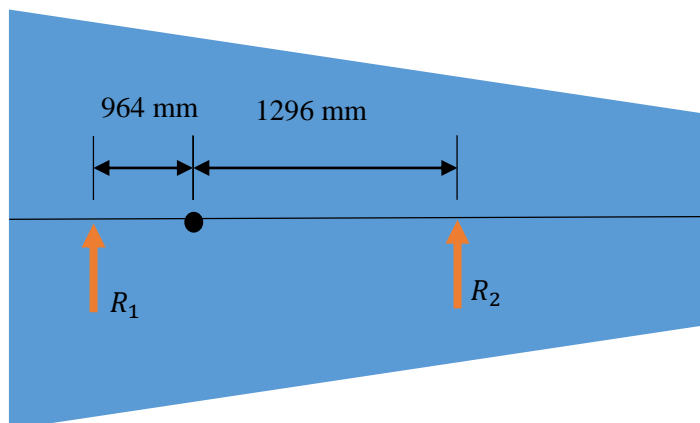
i. Description

The Small Sector Grabber serves the same purpose as the LS Grabber except that it is optimized for the dimensions and weight of the Small Sector. It uses the same profiles as the LS Grabber made of S355 steel. This geometry conforms to the available grabbing points on the assembled small sector as seen below.



ii. Calculations

Forces on Grabber pins:



$$W_{SS} = 1100 \text{ kg} = 10791 \text{ N}$$

$$\text{with SF of 2, } W_{LS} = 21582 \text{ N}$$

$$R_1 + R_2 = 21582 \text{ N} \quad \therefore R_2 = 21582 - R_1$$

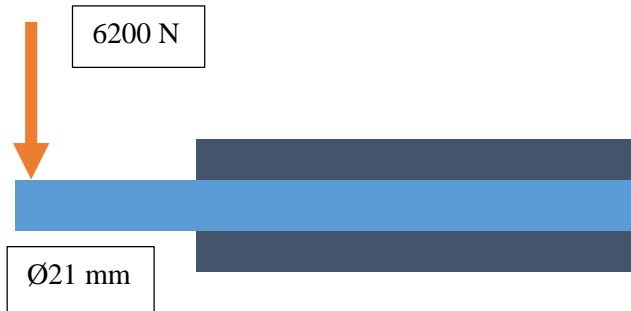
$$\Sigma_{R_1} = 0 \quad \therefore -W_{SS} (0.964) + R_2 (0.964 + 1.296) = 0$$

$$-(21582)(0.964) + (21582 - R_1)(0.964 + 1.296) = 0$$

$$\therefore R_1 = 12376.23 \text{ N, so for each pin: } \frac{R_1}{2} = \frac{12376.23}{2} = 6188.12 \text{ N, say } R_1 = \mathbf{6200 \text{ N}}$$

$$\therefore R_2 = 9205.77 \text{ N, so for each pin: } \frac{R_2}{2} = \frac{9205.77}{2} = 4602.89 \text{ N, say } R_2 = \mathbf{4650 \text{ N}}$$

Grabber pin shear:

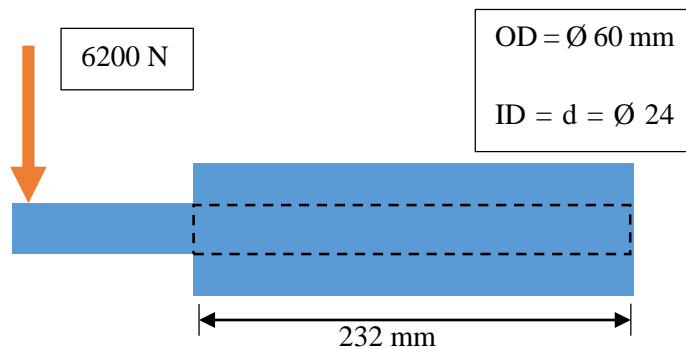


$$\tau = \frac{F_s}{A} \times \frac{4}{3} = \frac{F_s}{\frac{\pi \times d^2}{4}} \times \frac{4}{3} = \frac{6200}{\frac{\pi \times 0.021^2}{4}} \times \frac{4}{3} = 23.87 \text{ MPa}$$

$$23.87 \text{ MPa} \leq 355 \text{ MPa}$$

\therefore Design is compliant

Grabber arm round profile bending:



$$\sigma_b = \frac{32M}{\pi d^3} = \frac{32 \times (6200 \times 0.232) + 0.06}{\pi \times (0.06^3 - 0.024^3)} = 69.61 \text{ MPa}$$

$$69.61 \text{ MPa} \leq 355 \text{ MPa}$$

\therefore Design is compliant

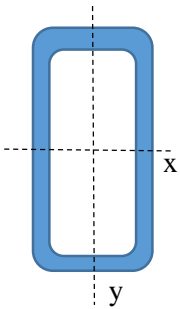
$$\delta = \frac{1}{3} \frac{FL^3}{EI} = \frac{1}{3} \frac{FL^3}{E \times \frac{\pi \times d^4}{64}} = \frac{1}{3} \frac{3100 \times 0.232^3}{206 \times 10^9 \times \frac{\pi \times (0.06^4 - 0.024^4)}{64}} = 0.1 \text{ mm}$$

$$\alpha = \frac{FL^2}{2EI} = \frac{FL^2}{2 \times E \times \frac{\pi \times d^4}{64}} = \frac{3100 \times 0.232^2}{2 \times 206 \times 10^9 \times \frac{\pi \times (0.06^4 - 0.024^4)}{64}} = 0.653 \text{ m rad} = 0.037^\circ$$

Assume all bending force applied to 4 vertical uprights.

Therefore $\frac{21582}{4} = 5395.5 \text{ N}$ say 5400 N

Frame bending:



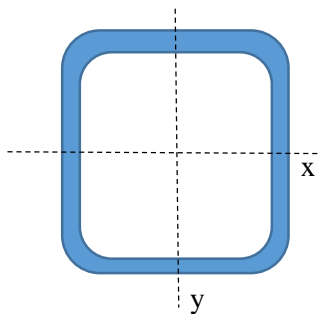
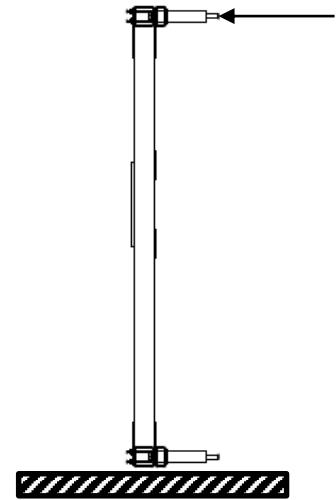
Rectangular cross section: 100 x 50 x 5 mm

$$I_{xx} = 158.19 \text{ cm}^4$$

$$\sigma_b = \frac{My}{I} = \frac{2 \times 5400 \times 0.342 \times 0.05}{4 \times 158.19/100^4} = 29.19 \text{ MPa}$$

$$29.19 \text{ MPa} \leq 355 \text{ MPa}$$

∴ Design is compliant



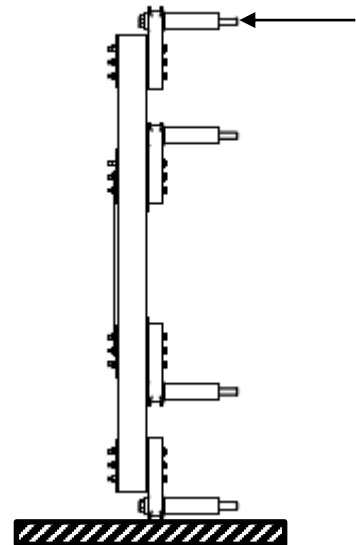
Square cross section: 100 x 50 x 5 mm

$$I_{xx} = 271 \text{ cm}^4$$

$$\sigma_b = \frac{My}{I} = \frac{2 \times 6200 \times 0.342 \times 0.05}{2 \times 271/100^4} = 39.12 \text{ MPa}$$

$$39.12 \text{ MPa} \leq 355 \text{ MPa}$$

∴ Design is compliant



iii. FEA

The FEA for the Small Sector Grabber was conducted using the weight of the Small Sector multiplied by 2 to conform to the relevant Eurocode. Unlike the LS grabber, this simulation

had individual forces applied to each grabber arm to determine the induced stresses under this worst case scenario. The stresses rose to 313.07 MPa at the weld between the centre interface plate and the main frame uprights. This is below the yield point of S355 steel and therefore the design is compliant.

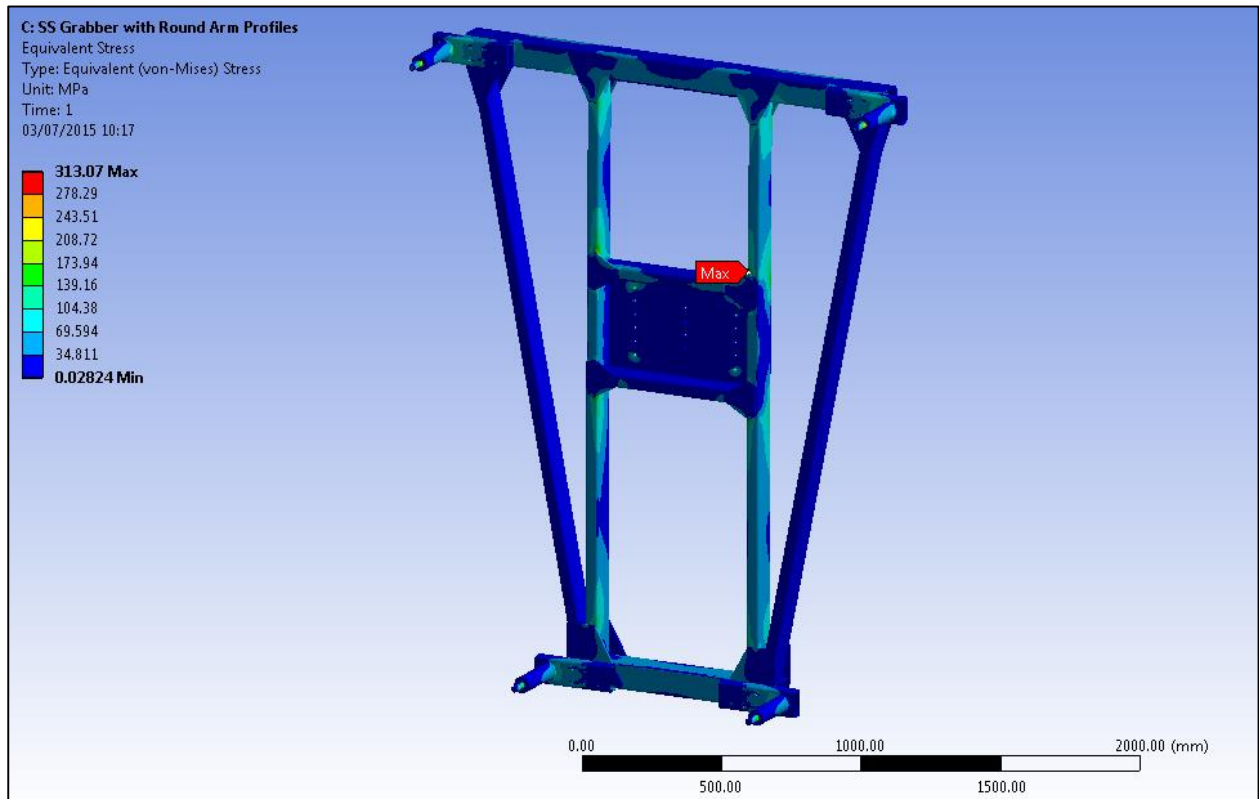


Figure 6 - FEA of Small Sector Grabber with forces applied on individual arms

c. Foot Spoke Grabber

i. Description

The Foot Spoke Grabber is designed to pick up and position both left and right Foot Spokes of the NSW. It is made up of 100 x 100 x 5 mm square and 100 x 50 x 5 mm rectangular S355 steel profiles. The interface points are made up of 60 mm diameter rods that are welded to the main grabber frame. The tool interface plate has two separate connection positions to account for the different centre of gravities of the left and right foot spoke as seen below.

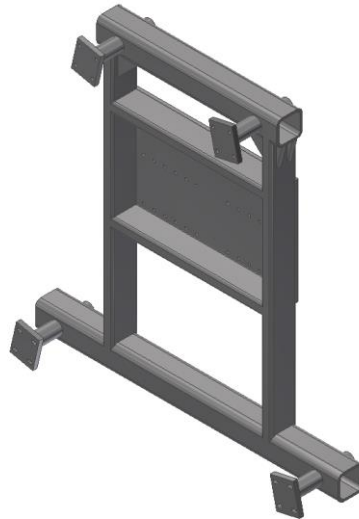


Figure 7 - Foot Spoke Grabber designed for left and right Foot Spokes

ii. Calculations

$$\tau = \frac{F_s}{A} \times \frac{4}{3} = \frac{F_s}{\frac{\pi \times d^2}{4}} \times \frac{4}{3} = \frac{5000}{\frac{\pi \times 0.06^2}{4}} \times \frac{4}{3} = 2.36 \text{ MPa}$$

$$\sigma_b = \frac{32M}{\pi d^3} = \frac{32 \times (5000 \times 0.15)}{\pi \times (0.06^3)} = 35.37 \text{ MPa}$$

$$35.37 \text{ MPa} \leq 355 \text{ MPa}$$

∴ Design is compliant

$$\delta = \frac{1}{3} \frac{Fl^3}{EI} = \frac{1}{3} \frac{Fl^3}{E \times \frac{\pi \times d^4}{64}} = \frac{1}{3} \frac{2500 \times 0.15^3}{206 \times 10^9 \times \frac{\pi \times (0.06^4)}{64}} = 0.022 \text{ mm}$$

iii. FEA

The peak stresses of the foot spoke grabber occurred at the interface holes where the grabber connects to the tool. The simulation as seen below was done at the 45° angle of the foot spoke when installed. As proved in the analytical calculations, the rest of the tooling experiences relatively low stresses due to the robust design. The peak stress is 170.8 MPa which is below the yield of 355 MPa and therefore the design is compliant.

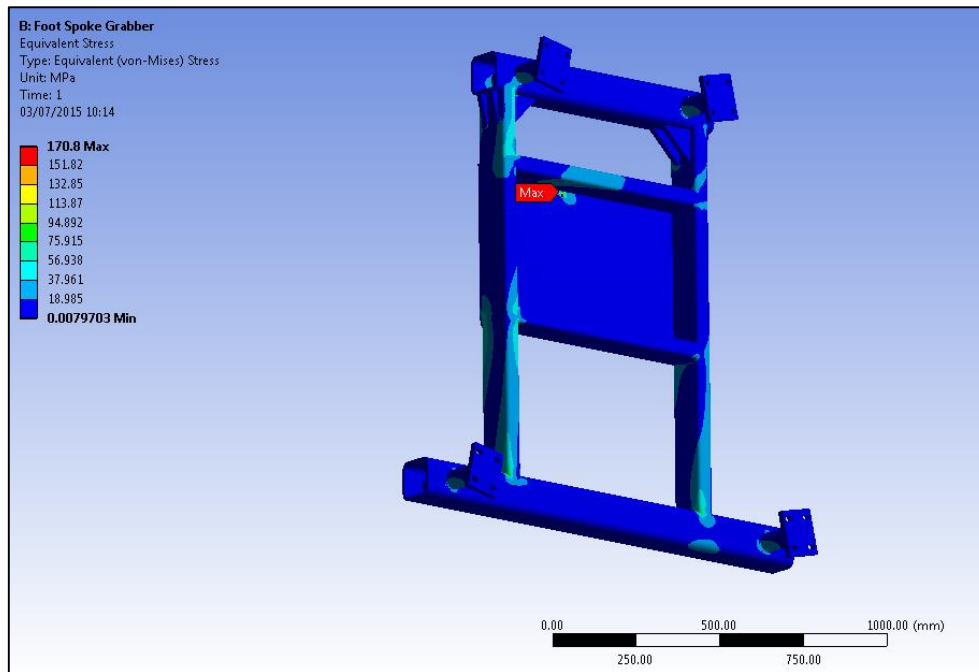


Figure 8 - FEA of the Foot Spoke Grabber at installation angle

d. Trunnion assembly

i. Description

The trunnion bearing assembly is made up of 3 main components; the trunnion shaft, the trunnion coupling and the trunnion bearings. The trunnion shaft and coupling are to be manufactured from high strength steel alloy, En9(S), with a yield point of 555 MPa. These 2 parts are to be machined from solid rod profiles of 250 mm diameter.

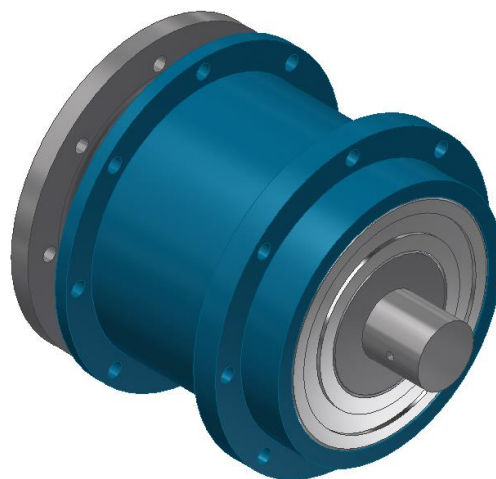
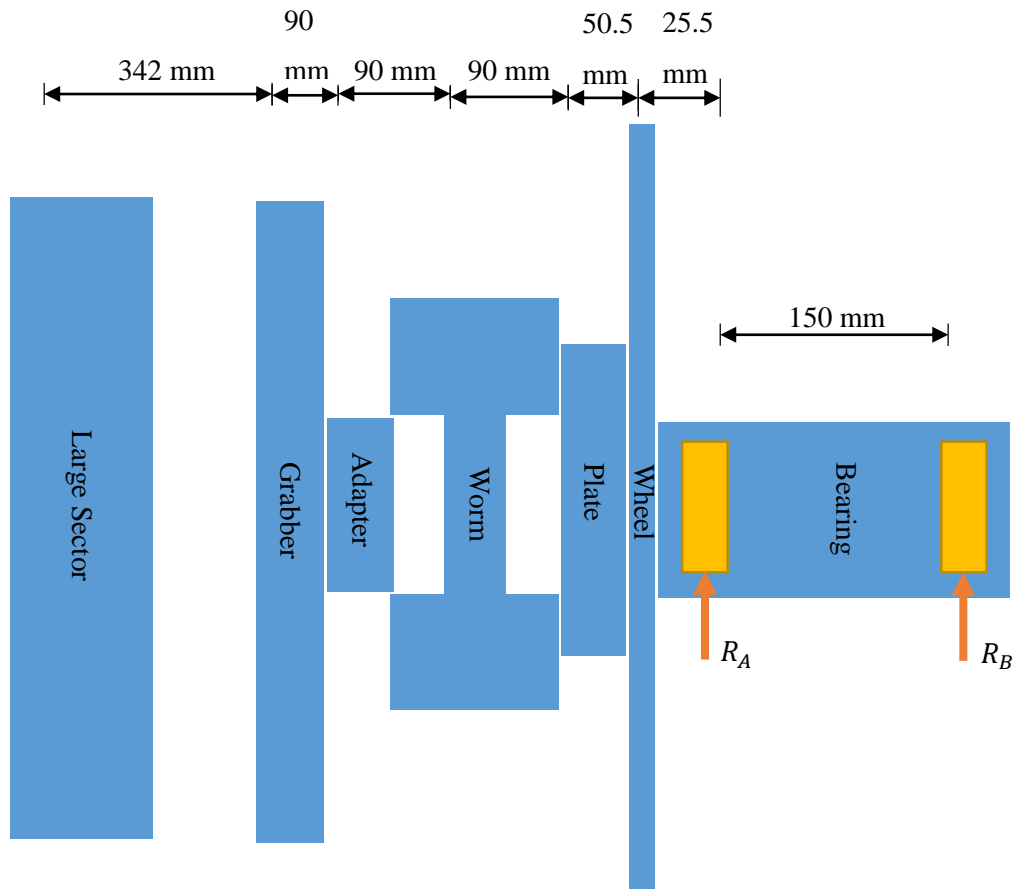


Figure 9 - Trunnion Assembly made up of Trunnion shaft, Trunnion coupling and Roller bearings

ii. Calculations



$$W_{LS} = 1450 \times 9.81 = 14224.5 \text{ N}, \therefore \text{with SF of 2: } W_{LS} = 28449 \text{ N}$$

$$W_{grabber} = 280 \times 9.81 = 2746.8 \text{ N}, \therefore \text{with SF of 2: } W_{grabber} = 5493.6 \text{ N}$$

$$W_{adapter} = 30.5 \times 9.81 = 299.21 \text{ N}, \therefore \text{with SF of 2: } W_{adapter} = 598.42 \text{ N}$$

$$W_{worm} = 65 \times 9.81 = 637.65 \text{ N}, \therefore \text{with SF of 2: } W_{worm} = 1275.3 \text{ N}$$

$$W_{plate} = 25.5 \times 9.81 = 250.16 \text{ N}, \therefore \text{with SF of 2: } W_{plate} = 500.32 \text{ N}$$

$$W_{wheel} = 118 \times 9.81 = 1157.58 \text{ N}, \therefore \text{with SF of 2: } W_{wheel} = 2315.16 \text{ N}$$

Span distances

$$X_{LS} = 688 \text{ mm}$$

$$X_{grabber} = 346 \text{ mm}$$

$$X_{adapter} = 256 \text{ mm}$$

$$X_{worm} = 166 \text{ mm}$$

$$X_{plate} = 76 \text{ mm}$$

$$X_{wheel} = 25.5 \text{ mm}$$

$$X_{bearing} = 150 \text{ mm}$$

$$R_A + R_B = 38631.8 \text{ N} \quad \therefore R_A = 38631.8 - R_B$$

$$\Sigma_{R_A} = 0 \quad \therefore W_{LS} (0.688) + W_{grabber} (0.346) + W_{adapter} (0.256) + W_{worm} (0.166) + W_{plate} (0.076) + W_{wheel} (0.0255) + R_B (0.15) = 0$$

$$\therefore R_B = -146.24 \text{ kN (including SF = 2)}$$

$$\therefore R_A = 184.87 \text{ kN (including SF = 2)}$$

From graph showing stress concentration for bending case of a shaft with a shoulder fillet:

$$K_t = 2.2 \text{ (largest between abutment fillet and relief groove)}$$

$$\sigma_b = K_t \frac{32M}{\pi d^3} = K_t \frac{32 \times (R_b \times X_{bearing})}{\pi d^3} = 2.2 \times \frac{32 \times (146.24 \times 10^3 \times 0.15)}{\pi \times 0.1^3} = 491.56 \text{ MPa}$$

$$491.56 \text{ MPa} \leq 555 \text{ MPa}$$

\therefore Design is compliant

$$\delta = \frac{1}{3} \frac{Fl^3}{EI} = \frac{1}{3} \frac{Fl^3}{E \times \frac{\pi \times d^4}{64}} = \frac{1}{3} \frac{73.12 \times 10^3 \times 0.15^3}{206 \times 10^9 \times \frac{\pi \times (0.1^4)}{64}} = 0.081 \text{ mm}$$

iii. FEA

The trunnion shaft FEA was carried out by applying the torque induced by the various components as well as applying the related shear force. The safety factor of 2 was also introduced for these loads to analyse whether Eurocode compliance. The introduction of a relief groove as seen below dramatically decreased the peak stress of the trunnion shaft. The FEA result which peaked at 490.42 MPa matches very closely to the analytical result of 491.56 MPa. This confirms the accuracy of the FEA and both these stresses fall below the yield strength of 555 MPa of En9(S). The trunnion design is therefore compliant with the relevant Eurocode.

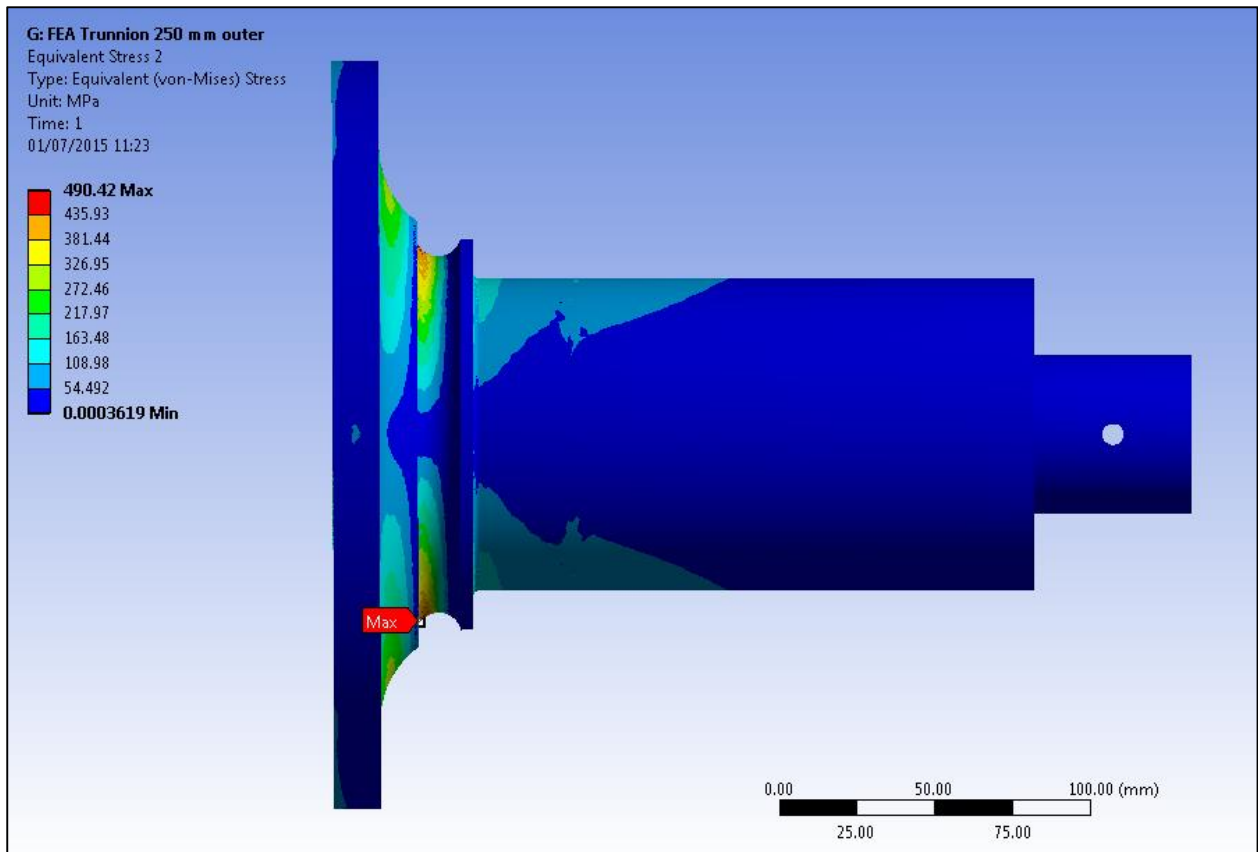
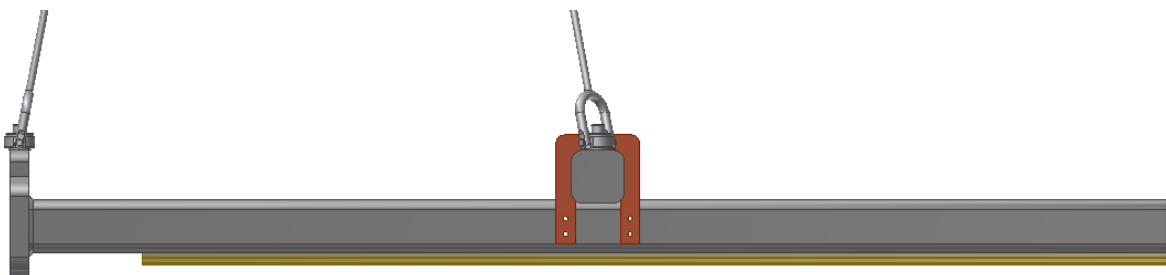


Figure 10 - FEA showing peak stress experienced in optimised relief groove on the Trunnion shaft

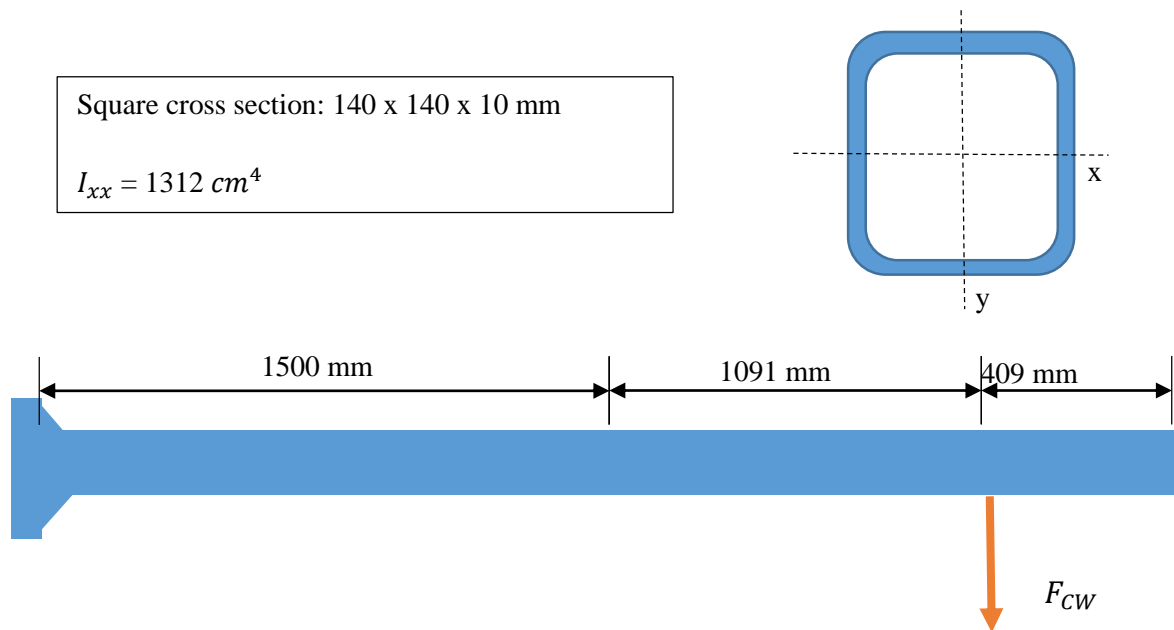
e. Main beam

i. Description

The Main beam of the tooling is made up of a 140 x 140 x 10 mm square steel tubing welded to a 50 mm thick steel plate for the trunnion interface. The main beam profile will also have holes drilled into the bottom and side faces for the linear guide and cross beam attachment respectively.



ii. Calculations

Beam bending:

$$F_{CW} = 1732 \times 9.81 = 16990.92 \text{ N, say } F_{CW} = 17 \text{ kN}$$

$$\therefore \text{with SF of 2, } F_{CW} = 34 \text{ kN}$$

For worst case scenario, assume cantilevered beam fixed at midpoint (cross beam hoist point).

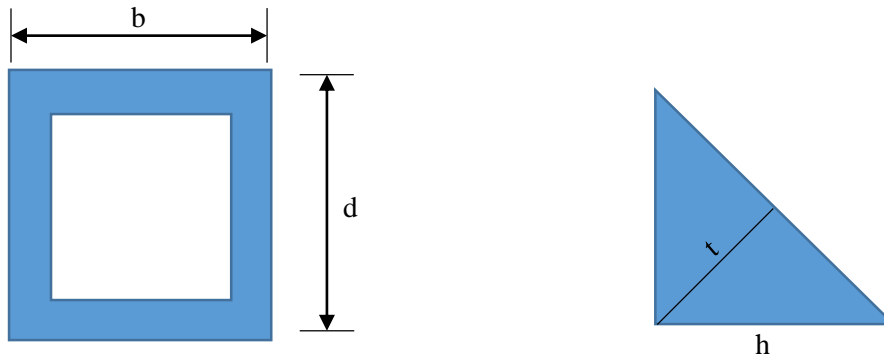
$$\sigma_b = \frac{My}{I} = \frac{34 \times 10^3 \times 1.091 \times 0.07}{1312/100^4} = 197.91 \text{ MPa}$$

$$197.91 \text{ MPa} \leq 355 \text{ MPa}$$

\therefore Design is compliant

$$\delta = \frac{1}{3} \frac{Fa^3}{EI} \left(1 + \frac{3b}{2a}\right) = \frac{1}{3} \frac{17 \times 10^3 \times 1.091^3}{206 \times 10^9 \times 1312/100^4} \left(1 + \frac{3 \times 0.409}{2 \times 1.091}\right) = 4.25 \text{ mm}$$

Beam weld:



$$t = 0.707 h$$

$$A_w = 0.707 \times 2 \times h (b+d) = 0.707 \times 2 \times 0.01 \times (0.14 + 0.14) = 3.9592 \times 10^{-3} \text{ m}^2$$

$$\tau_{\parallel} = \frac{F}{A_w} = \frac{38631.8}{3.9592 \times 10^{-3}} = 9.76 \text{ MPa}$$

$$I = \frac{d^2}{6} (3b + d) t = \frac{0.14^2}{6} \times (3 \times 0.14) + 0.14 \times (0.707 \times 0.01) = 1.2935 \times 10^{-5} \text{ m}^4$$

$$\sigma_b = \frac{My}{I} = \frac{22000 \times d/2}{1.2935 \times 10^{-5}} = \frac{22000 \times 0.07}{1.2935 \times 10^{-5}} = 119.06 \text{ MPa}$$

$$\sigma = \sqrt{\sigma_b^2 + 3(\tau_{\parallel}^2 + \tau_{\perp}^2)} = \sqrt{(119.06 \times 10^6)^2 + 3((9.76 \times 10^6)^2 + 0)} = 120.3 \text{ MPa}$$

$$\text{To satisfy Eurocode; } \sigma = \sqrt{\sigma_b^2 + 3(\tau_{\parallel}^2 + \tau_{\perp}^2)} \leq \frac{f_u}{\beta_w \gamma_{Mw}} = 470 \text{ MPa} \quad \text{as } f_u \text{ is UTS}$$

$$\text{For steel: } \beta_w = 0.8$$

$$\gamma_{Mw} = 1.25$$

$$\therefore \sigma \leq \frac{470 \times 10^6}{0.8 \times 1.25} = 470 \text{ MPa (Using a one to one weld filler material)}$$

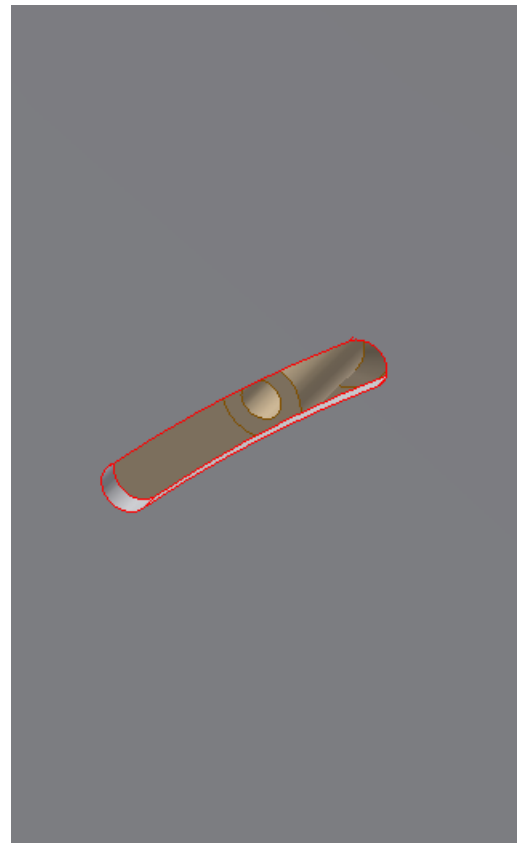
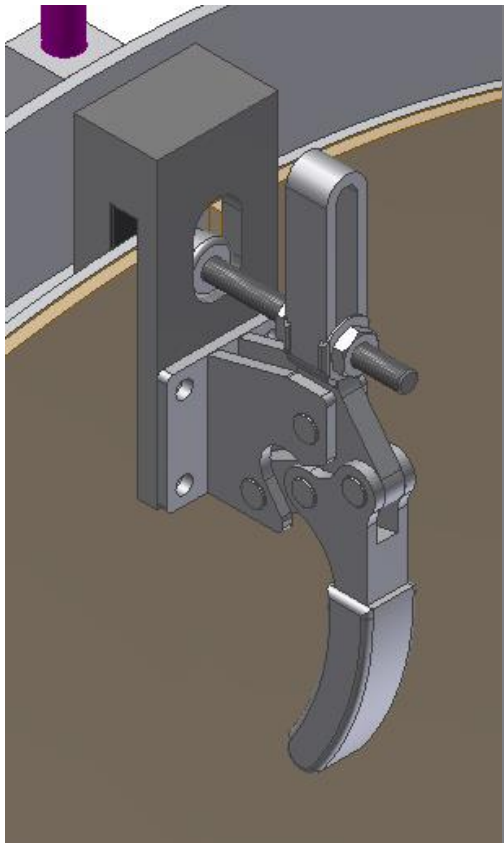
$$120.3 \text{ MPa} \leq 470 \text{ MPa}$$

\therefore Design is compliant

f. Toggle clamp and safety pins

i. Description

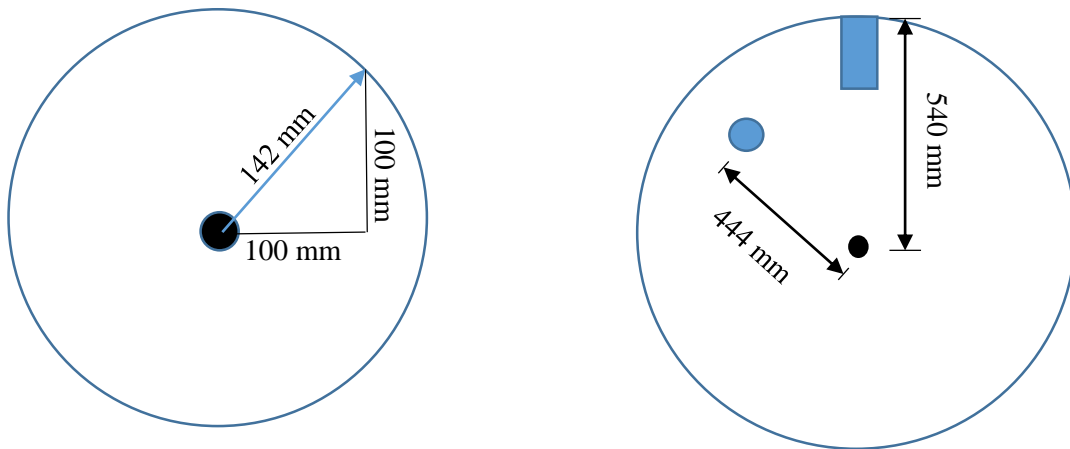
The rotation wheel uses two main locking mechanisms to prevent grabber from rotating when correct angle is obtained. These two mechanisms comprises the toggle clamp and safety pins. The toggle clamps specifically have to comply with point 5.2.7.1 which states, “The holding force of clamps holding by friction to prevent the load from slipping shall be at least 2 times the working load limit.”



ii. Calculations

Toggle clamps:

Worst case scenario; translate LS 100 mm horizontally and vertically



$$M_t = (1450 + 280) \times 9.81 \times 0.142$$

$$= 2409.92 \text{ Nm}$$

with SF of 2, $M_t = 4819.85 \text{ Nm}$

So force required at each clamp: $\frac{M_t}{\text{clamp radius} \times \text{No. of clamps}} = \frac{4819.85}{0.54 \times 3} = 2975.22 \text{ N}$

So to calculate the clamp force required, frictional grip needs to be considered.

$$\frac{F}{N} = \mu \text{ (stainless steel on neoprene)}$$

$$\therefore N = \frac{F}{\mu} = \frac{2975.22}{1.3} = 2288.63 \text{ N (oily/greasy surface)}$$

$$\therefore N = \frac{F}{\mu} = \frac{2975.22}{2.2} = 1352.37 \text{ N (dry surface)}$$

Safety pins:

From previous, force required at each pin: $\frac{M_t}{\text{pin radius} \times \text{No. of pins}} = \frac{4819.85}{0.444 \times 4} = 2713.88 \text{ N}$

$$\tau = \frac{F_s}{A} \times \frac{4}{3} = \frac{F_s}{\frac{\pi \times d^2}{4}} \times \frac{4}{3} = \frac{2713.88}{\frac{\pi \times 0.01^2}{4}} \times \frac{4}{3} = 46.07 \text{ MPa}$$

$$\sigma_b = \frac{32M}{\pi d^3} = \frac{32 \times (2713.88 \times 0.039) + 0.02}{\pi \times (0.02^3 - 0.01^3)} = 143.74 \text{ MPa} \quad \text{bending of pin collar}$$

$$143.74 \text{ MPa} \leq 355 \text{ MPa}$$

∴ Design is compliant

$$\sigma_b = \frac{32M}{\pi d^3} = \frac{32 \times (2713.88 \times 0.007)}{\pi \times (0.01^3)} = 193.50 \text{ MPa} \quad \text{bending of safety pin}$$

$$193.50 \text{ MPa} \leq 355 \text{ MPa}$$

∴ Design is compliant

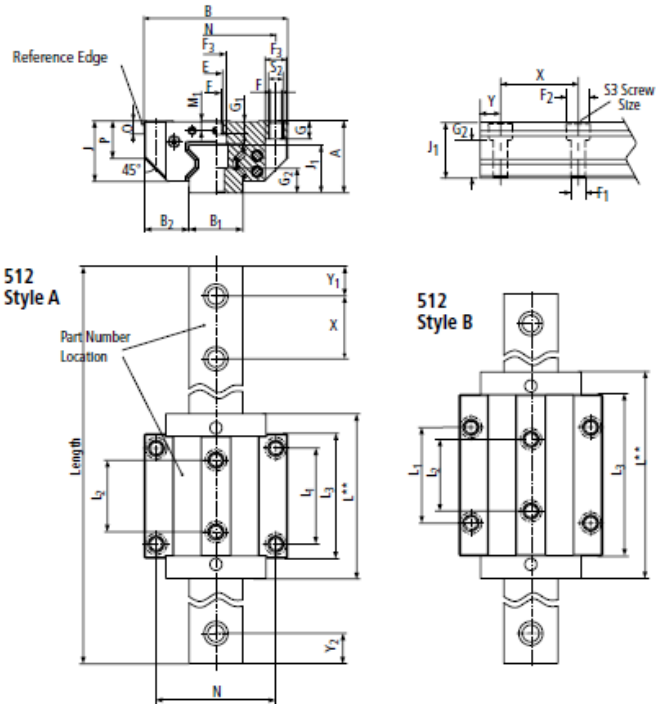
4. Conclusions

The critical components of the NSW Installation Tooling all comply with the relevant Eurocode static load compliances of two times the working limit of EN 1993-1-1 and BS EN 13155:2003+A2. This serves to prove that the tooling design is safe to use for all required functional actions for the installation of the various sectors and spokes.

Appendix B

Catalogue Components

512 Style A and B



512 Style A – Standard Roller

Size	Dimensions (mm)							L**	L ₁	L ₂	L ₃	X	N	S ₂	S ₃	F	F ₁	F ₂	F ₃	Roller						
	A	B	B ₁ * ±0.05	B ₂	J	J ₁	∅													G	G ₁	G ₂	M ₁	O	P	
25	36	70	23	23.5	29.5	24.5	81	45	40	60	30	57	M8	M6	6.8	7	11	11	3.2	9	6.5	13	5.5	7.5	17.5	
35	48	100	34	33	40	32	109	62	52	80	40	82	M10	M8	8.5	9	15	15	4.5	12	10	15	7	8	23	
45	60	120	45	37.5	50	40	137.5	80	60	104	52.5	100	M12	M12	10.5	14	20	18	5	15	11	21	8	10	30.5	
55	70	140	53	43.5	57	48	163.5	95	70	120	60	116	M14	M14	12.5	16	24	20	6	18	13.5	26	9	12	34.5	

512 Style B – Standard Long Roller

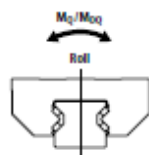
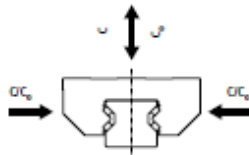
Size	Dimensions (mm)							L**	L ₁	L ₂	L ₃	X	N	S ₂	S ₃	F	F ₁	F ₂	F ₃	Roller						
	A	B	B ₁ * ±0.05	B ₂	J	J ₁	∅													G	G ₁	G ₂	M ₁	O	P	
25	36	70	23	23.5	29.5	24.5	103.4	45	40	79.4	30	57	M8	M6	6.8	7	11	11	3.2	9	6.5	13	5.5	7.5	17.5	
35	48	100	34	33	40	32	136	62	52	103	40	82	M10	M8	8.5	9	15	15	4.5	12	10	15	7	8	23	
45	60	120	45	37.5	50	40	172.5	80	60	135	52.5	100	M12	M12	10.5	14	20	18	5	15	11	21	8	10	30.5	
55	70	140	53	43.5	57	48	205.5	95	70	162	60	116	M14	M14	12.5	16	24	20	6	18	13.5	26	9	12	34.5	
65	90	170	63	53.5	76	58	251	110	82	201	75	142	M16	M16	14.5	18	26	25.5	7	23	19	32	13	15	51	

500 Series Roller

512 Style A and B

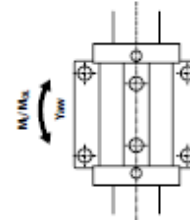
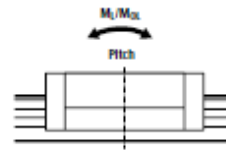
Dynamic Load and Moment Ratings

C = Dynamic load rating
 M_L = Dynamic pitch and yaw moment rating
 M_Q = Dynamic roll moment rating



Static Load and Moment Capacities

C_0 = Static load capacity
 M_{0L} = Static pitch and yaw moment capacity
 M_0 = Static roll moment capacity



Size & Style	Loading Capabilities		Moments				Weights	
	C_0 (N)	C (N)	M_{0Q} (Nm)	M_0 (Nm)	M_{0L} (Nm)	M_L (Nm)	Carriage (kg)	Rail (kg/m)
25A	49800	27700	733	408	476	265	0.7	
25B	70300	39100	1035	576	936	521	0.9	3.4
35A	93400	52000	2008	1118	1189	662	1.6	
35B	128500	71500	2762	1537	2214	1232	2.2	6.5
45A	167500	93400	4621	2577	2790	1556	3.2	
45B	229500	127800	6333	3527	5161	2874	4.3	10.7
55A	237000	131900	7771	4325	6650	2837	5.0	
55B	324000	180500	10624	5919	8745	4872	6.8	15.2
65B	530000	295000	20912	11640	17930	9980	13.5	22.5

1. The dynamic load and moment ratings are based upon 100 km travel life. When comparing these load ratings with other bearings take into consideration that some manufacturers dynamic and moment ratings are based on 50 km travel life. In order to compare with bearing dynamic and moment ratings based on 50 km travel life, divide the dynamic capacity of the bearing rated for 50 km by 1.23 to get an accurate comparison.

2. The static load and moment rating are the maximum radial load and moment load that should be applied to the bearing while there is no relative motion between the carriage and rail.

Bearing Travel Life Comparison

$$L = (C/F)^3 \times 100 \text{ km}$$

where:

L = travel life, km

C = dynamic load rating, N

F = applied dynamic load, N

$$C_{\text{min}} = F \left(\frac{L}{100} \right)^{1/3}$$

where:

C_{min} = minimum required

dynamic load rating, N

F = applied dynamic load, N

L = required travel life, km

Operating Parameters:

Maximum Velocity: 3 m/s

Maximum Acceleration: 50 m/s²

Temperature: Min: -40° C

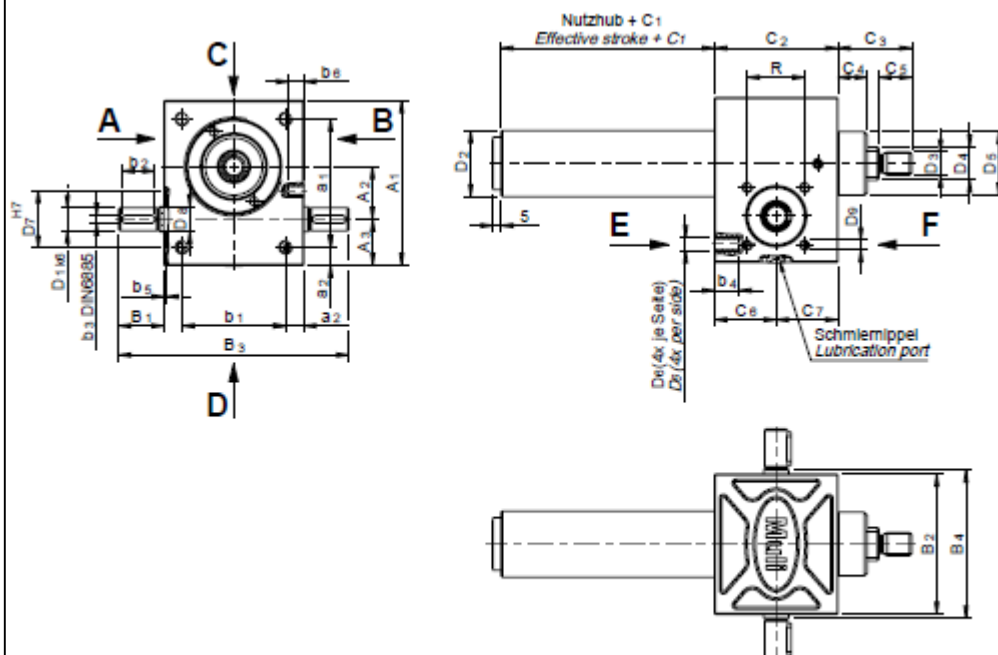
Max: 80° C

Max peak: 120° C short time*

*without bellows

THOMSON
Linear Motion. Optimized.

Ausführung N, V
Version N, V



Bei Aggregateinbau bitte Anbausite angeben (NB)! / If attachments are to be fitted, please specify on which side (NB)!



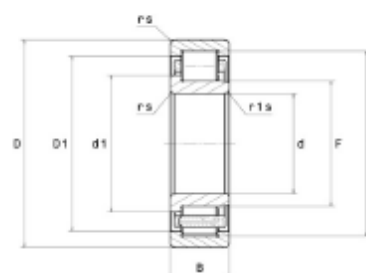
PDF technical sheet NJ.220.E.M.J30



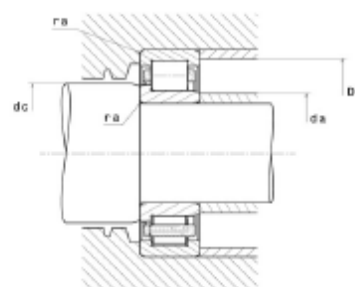
Single row cylindrical roller bearings

Single row cylindrical roller bearing, single direction for axial loads, separable, brass cage.

Product definition	
d	100 mm
D	180 mm
B	34 mm
E	163 mm
F	119 mm
d1	127.30 mm
D1	156.90 mm
rs min	2.10 mm
r1s min	2.10 mm
Radial clearance class	C3
Mass (without HJ ring)	3.83 kg
Brand	SNR



Product performance	
Dynamic load, C	251,000 daN
Static load, C0	308,000 daN
Fatigue limit load, Cu	33,900 daN
Nref	3,500 rpm
Nlim	5,900 rpm
Min operating temperature, Tmin	-40 °C
Max operating temperature, Tmax	120 °C
Characteristic cage frequency, FTF	0.42 Hz
Characteristic rolling element frequency, BSF	6.25 Hz
Characteristic outer ring frequency, BPF0	7.17 Hz
Characteristic inner ring frequency, BPF1	9.83 Hz



Abutment dimensions	
da min	111 mm
da max	117 mm
db min	122 mm
dc min	130 mm
Da max	169 mm
ra max	2 mm
r1a max	2 mm

PROTEX
BS EN 150 9001

TCH-BMAB-090-102

Toggle Clamp Horizontal Action

Base Mounted Adjustable

TCH-BMAB-090-102-MS

Material: Mild steel
Finish: Zinc plated (3 microns)
Weight: 0.90 Kgs
Supplied with: M10x80mm spindle
Ultimate force: 480 Kgf
Clamping force: See image

Accessories

Neoprene cap



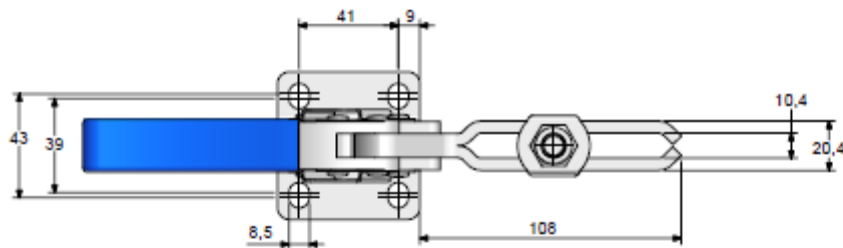
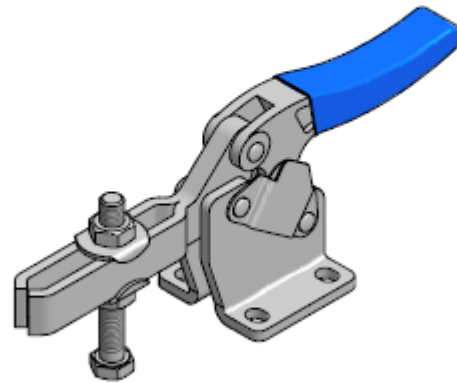
TCA-CAP-NEO-010

Accessories

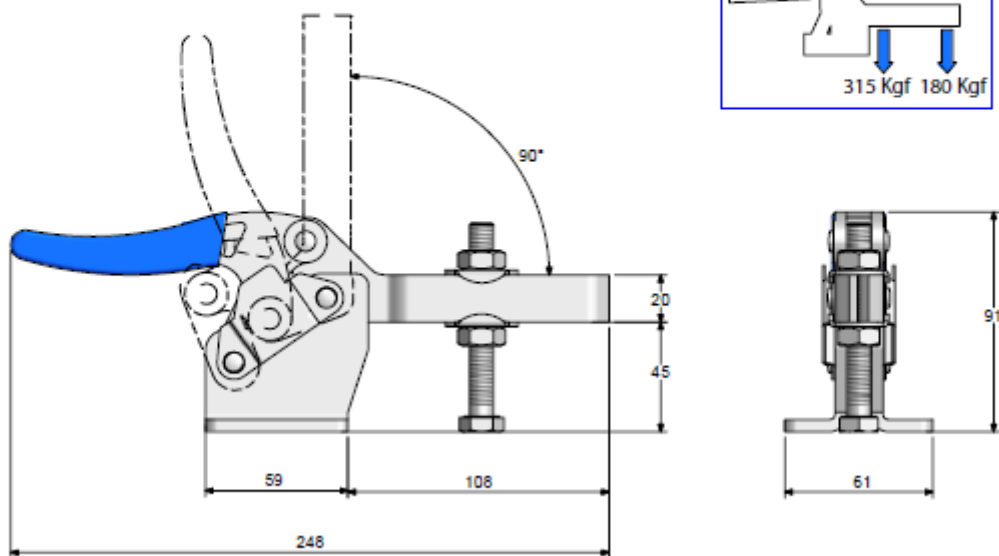
Neoprene spindle



TCA-ADSP-NEO-010-080



Clamping Force



EPG Permanenterregte Gleichstrommotoren

D. C. Permanent Magnet Motors

**Typ 14
25 Nm
mit Einfach-Schneckengetriebe**

with Single Reduction Worm Gear Unit

i	6,75:1	8:1	10:1	12:1	15:1	20:1	25:1	30:1	40:1	50:1	60:1	70:1	80:1
$n_1 = 3000 \text{ min}^{-1}$													
P [W]	350	220	220	220	220	170	170	170	120	120	120	120	120
n_2 [min^{-1}]	444	375	300	250	200	150	120	100	75	60	50	43	38
M_2 [Nm]	5,6	4,1	5,0	5,9	6,9	6,6	8,1	9,1	7,9	7,6	7,8	8,3	8,9
$n_1 = 2000 \text{ min}^{-1}$													
P [W]	250	250	250	170	170	170	120	120	120	80	80	80	80
n_2 [min^{-1}]	296	250	200	167	133	100	80	67	50	40	33	29	25
M_2 [Nm]	6,0	7,1	8,6	6,8	8,0	9,9	8,6	9,6	11,9	7,6	7,8	8,3	8,9

Die Motorleistungen sind empfohlene Werte für Dauerbetrieb, siehe Seite 12.

The motor outputs are recommended values for continuous operation, see page 12.

Motordrehzahl / Speed 3000 min^{-1}

Typ Type	P (FF 1,1) [W]	I (180 V) [A]	I_{max} (180 V) [A]
EPG 123	120	0,90	6,0
EPG 133	170	1,20	8,0
EPG 213	220	1,70	9,0
EPG 233	350	2,50	14,0

Angaben für 24 V siehe Seite 22/23.

Standardausführung:
mit Anschlusslitzen 350 mm lang.

Sonderausführungen:
mit Klemmkasten, Bremse, Digital-Tachogebler, Analog-Tachogebler.

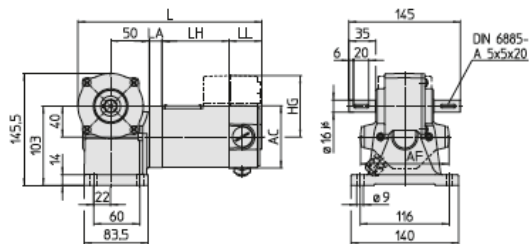
Motordrehzahl / Speed 2000 min^{-1}

Typ Type	P (FF 1,1) [W]	I (180 V) [A]	I_{max} (180 V) [A]
EPG 122	80	0,65	4,5
EPG 132	120	0,90	6,0
EPG 212	170	1,40	7,5
EPG 232	250	1,90	10,0

For data for 24 V refer to page 22/23.

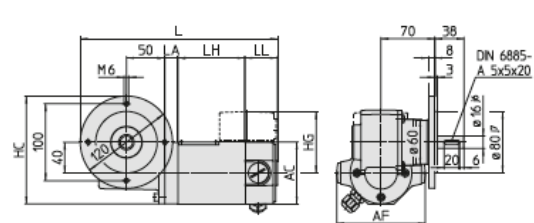
Standard version:
with flying leads 350 mm long.
Options:
with terminal box, brake, digital-tacho, analogue-tacho.

**Getriebe Typ GS 140 Fußausführung /
Gear unit type GS 140 Foot mounting**



▲ GS 140

**Getriebe Typ GF 140 Flanschausführung /
Gear unit type GF 140 Flange mounting**



▲ GF 140

Appendix C

Manufacturing Drawings

1. Counter Weight Assembly

1-1. Counter Weight Slice

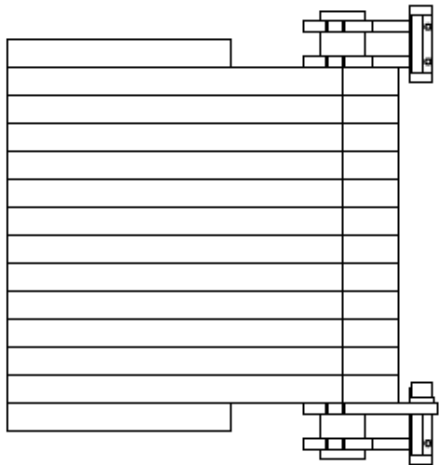
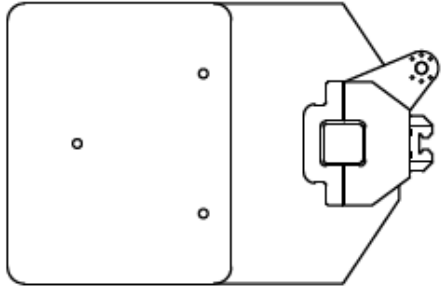
1-2. Counter Weight Add-on Slice

1-3. Counter Weight Beam

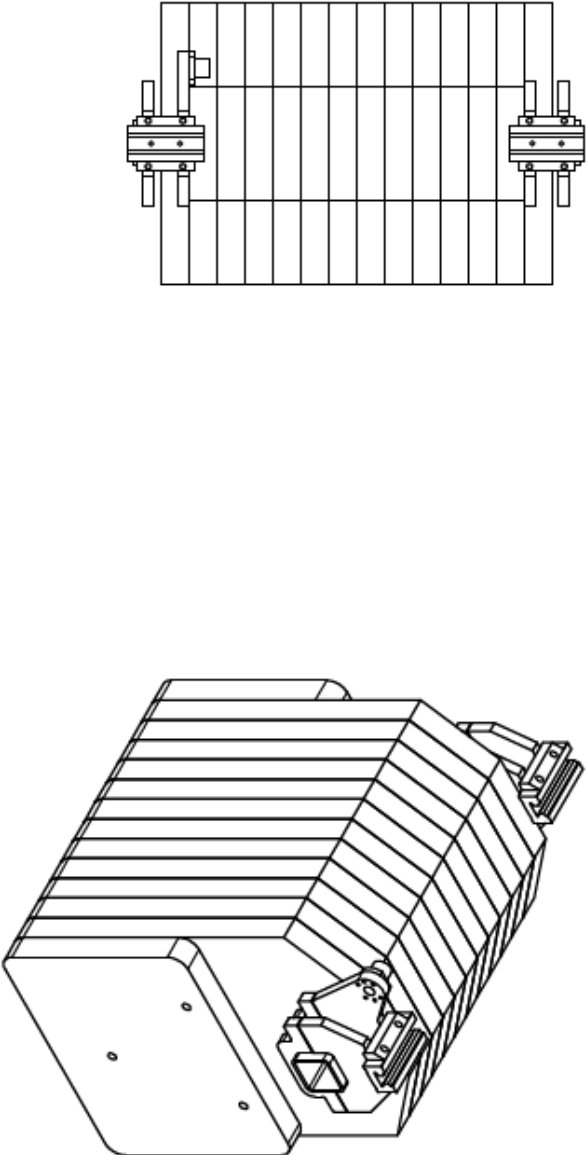
1-4. Counter Weight Bottom Bracket

1-5. Counter Weight Top Bracket

1-6. Counter Weight Top Drive Bracket



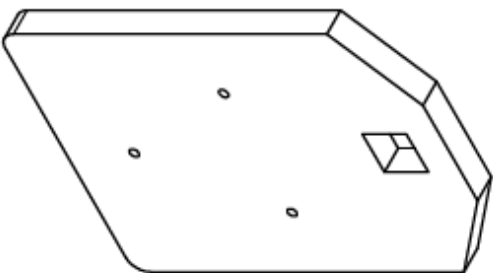
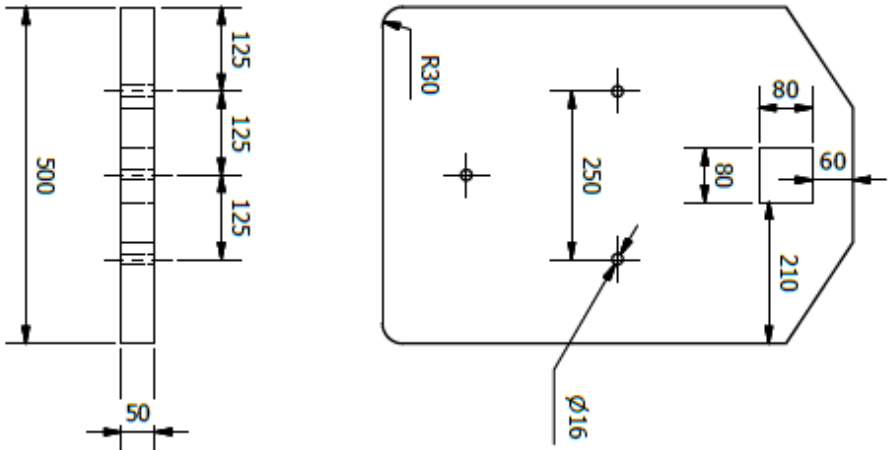
PARTS LIST				
ITEM	MATERIAL	PART NUMBER	QTY	
1	Steel, Mild	Counter Weight Beam	1	
2	Steel, Mild	Counter Weight Slice	12	
3	Steel, Mild	Carriage Bracket Bottom	4	
4	Steel, Mild	Carriage Bracket Top Non-drive	3	
5	Steel, Mild	Carriage Bracket Top for Drive	1	
6	Stainless Steel	Linear Guide Carriage	2	
7	Steel, Mild	Counter Weight Slice Add-on	2	
8	Stainless Steel	Ball Screw Nut 16 mm	1	



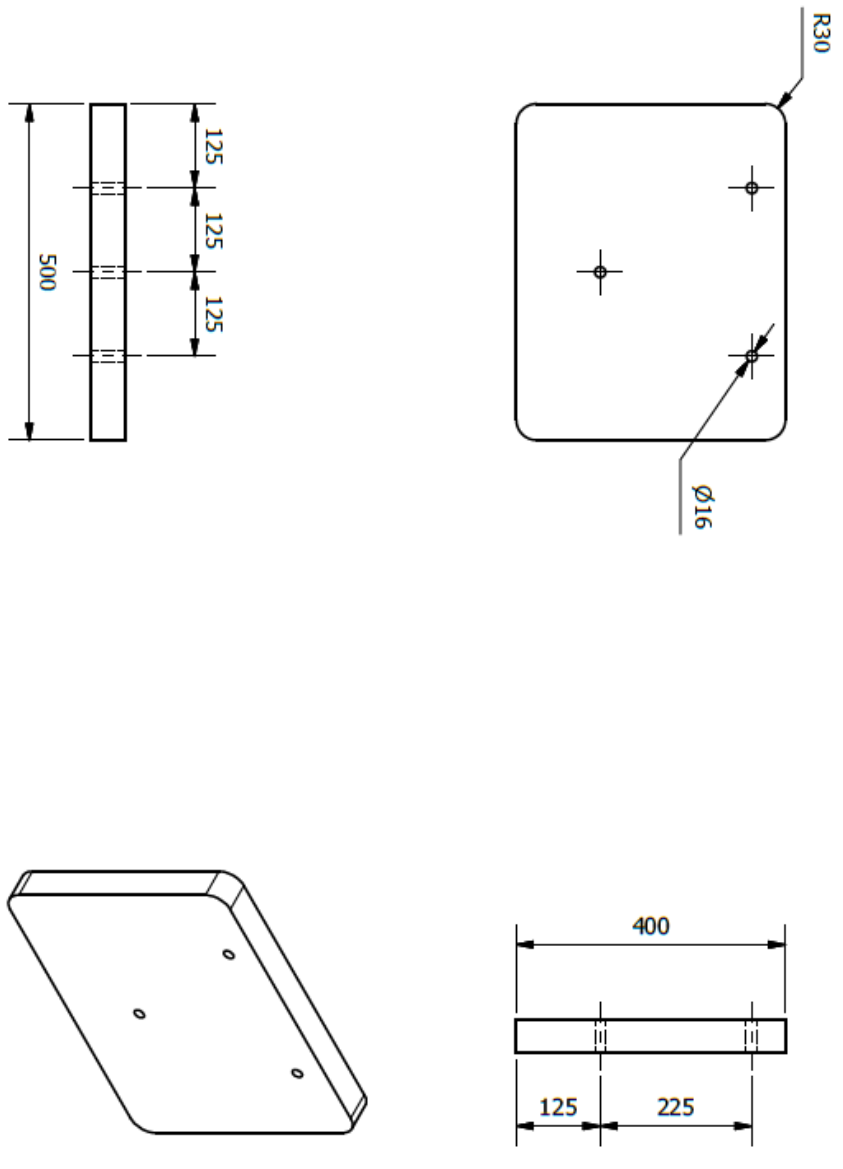
UNLESS OTHERWISE STATED GENERAL TOLERANCES: ± 0.05 mm ANGLES: $\pm 0.1^\circ$

 UNIVERSITY OF KWAZULU-NATAL SCHOOL OF ENGINEERING MECHANICAL ENGINEERING	MAT.: N/A		No. REQ.: 1	SCALE: 1:12	UNITS: mm	PROJECT: NSW INSTALLATION TOOLING	NO.:
	PROJECT SUPERVISOR	DATE	CHECKED	STUDENT NAME: SHUVAY SINGH			1
WORKSHOP TECHNICIAN			STUDENT No.: 211516515	E-MAIL: shuvaysingh@gmail.com		TITLE: COUNTER WEIGHT ASSEMBLY	
TECHNICAL OFFICER			TEL. NO.: +27 (0)945882810				

UNLESS OTHERWISE STATED GENERAL TOLERANCES: ±0.05 mm ANGLES: ±0.1 °




 UNIVERSITY OF KWAZULU-NATAL		SCHOOL OF ENGINEERING		MECHANICAL ENGINEERING	
MAT.: N/A		No. REQ.: 12		SCALE: 1:10	
PROJECT SUPERVISOR		CHECKED		STUDENT NAME: SHUVAY SINGH	
WORKSHOP TECHNICIAN		DATE		STUDENT No.: 211516515	
TECHNICAL OFFICER		No. REQ.: 12		E-MAIL: shuvaysingh@gmail.com	
TECHNICAL OFFICER		No. REQ.: 12		TEL. NO.: +27 (0)945882810	
PROJECT: NSW INSTALLATION TOOLING				NO.: 1-1	
TITLE: COUNTER WEIGHT SLICE					

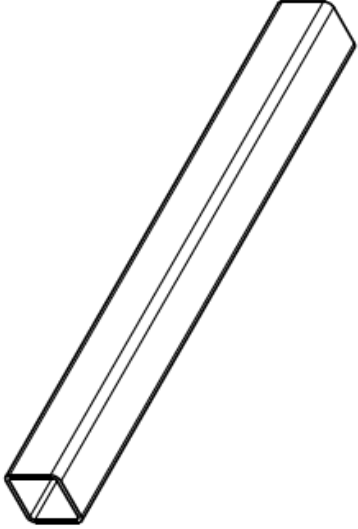
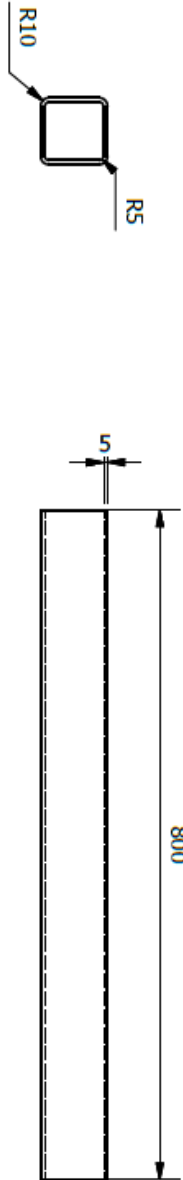


UNLESS OTHERWISE STATED GENERAL TOLERANCES: ±0.05 mm ANGLES: ±0.1 °



 UNIVERSITY OF KWAZULU-NATAL
 SCHOOL OF ENGINEERING
 MECHANICAL ENGINEERING

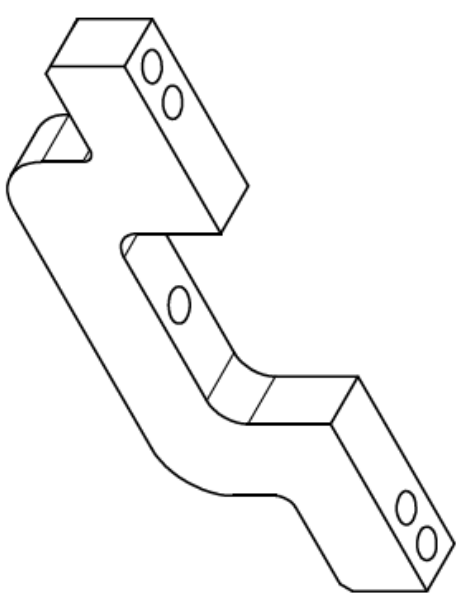
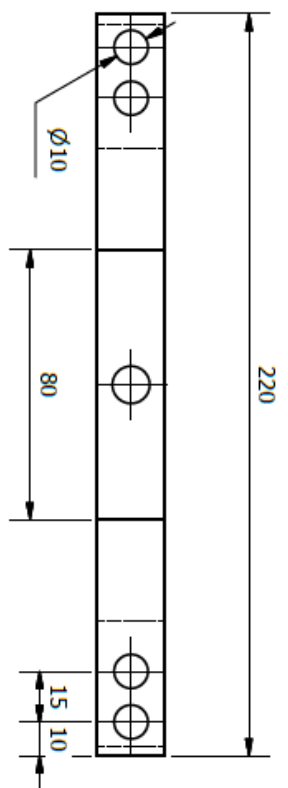
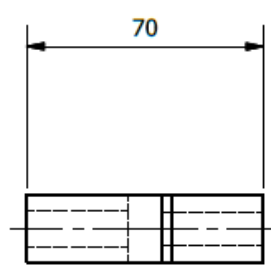
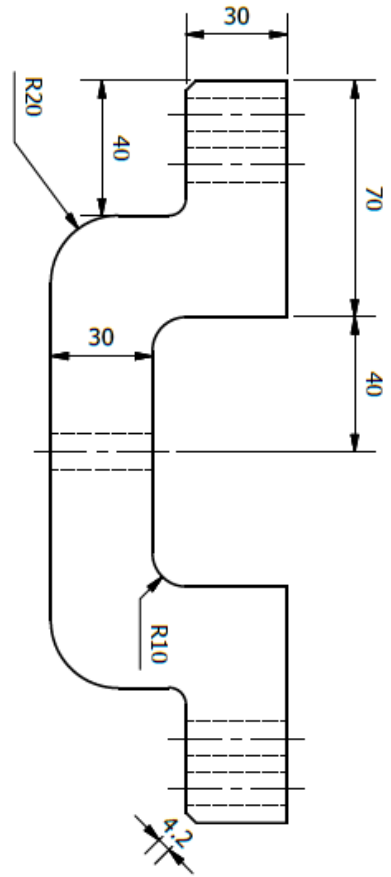
MAT.: MILD STEEL	No. REQ.: 2	SCALE: 1:10	UNITS: mm	PROJECT: NSW INSTALLATION TOOLING	NO.: 1-2
PROJECT SUPERVISOR	CHECKED	STUDENT NAME: SHUVAY SINGH		TITLE: COUNTER WEIGHT ADD-ON SLICE	
WORKSHOP TECHNICIAN		STUDENT No.: 211516515			
TECHNICAL OFFICER		E-MAIL: shuvaysingh@gmail.com			
		TEL. NO.: +27 (0)845882810			





UNLESS OTHERWISE STATED GENERAL TOLERANCES: ± 0.05 mm ANGLES: $\pm 0.1^\circ$

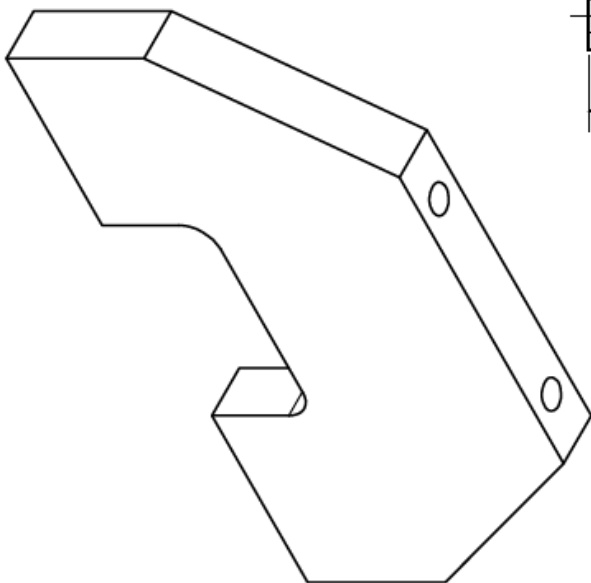
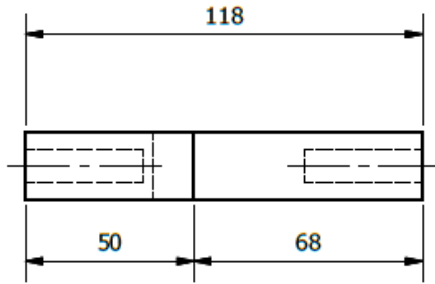
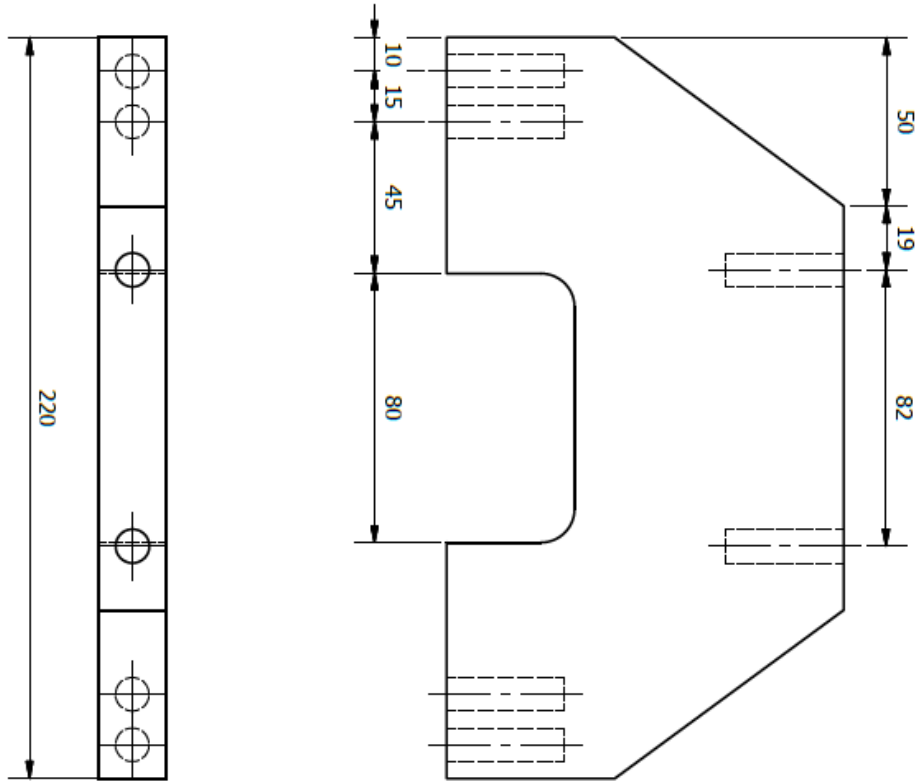
 UNIVERSITY OF KWAZULU-NATAL		SCHOOL OF ENGINEERING MECHANICAL ENGINEERING					
MAT.: S355 STEEL	DATE	No. REQ.: 1	CHECKED	SCALE: 1:8	UNITS: mm	PROJECT: NSW INSTALLATION TOOLING	NO.: 1-3
PROJECT SUPERVISOR				STUDENT NAME: SHUVAY SINGH			
WORKSHOP TECHNICIAN				STUDENT No.: 211516515		TITLE: COUNTER WEIGHT BEAM	
TECHNICAL OFFICER				E-MAIL: shuvaysingh@gmail.com			
				TEL. NO.: +27 (0)845882810			





UNLESS OTHERWISE STATED GENERAL TOLERANCES: ± 0.05 mm ANGLES: $\pm 0.1^\circ$


 UNIVERSITY OF KWAZULU-NATAL	SCHOOL OF ENGINEERING MECHANICAL ENGINEERING	MAT.: T690 STEEL	No. REQ.: 4	SCALE: 1:2	UNITS: mm	PROJECT: NSW INSTALLATION TOOLING	NO.: 1-4 
		PROJECT SUPERVISOR WORKSHOP TECHNICIAN TECHNICAL OFFICER	CHECKED	STUDENT NAME: SHUVAY SINGH	STUDENT No.: 211516515	E-MAIL: shuvaysingh@gmail.com	
		DATE		TEL. NO.: +27 (0)945882810			

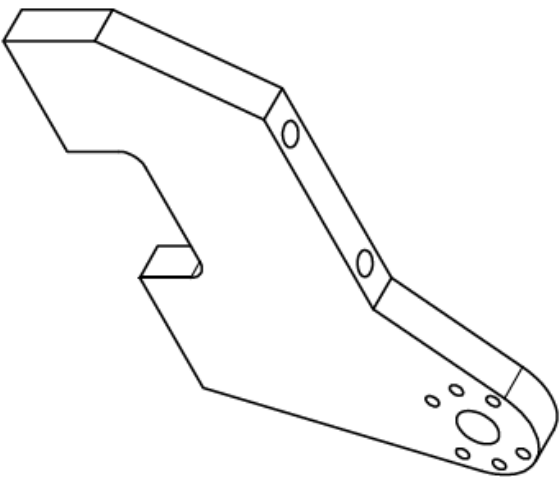
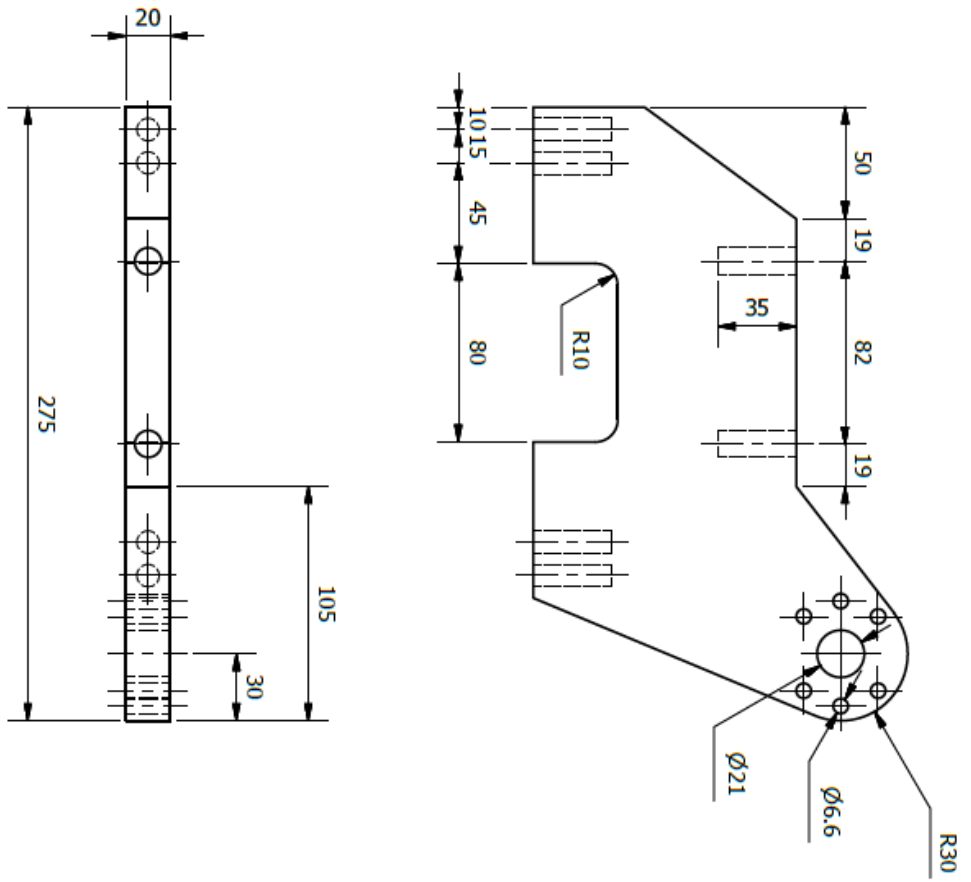


UNLESS OTHERWISE STATED GENERAL TOLERANCES: ± 0.05 mm ANGLES: $\pm 0.1^\circ$



 UNIVERSITY OF KWAZULU-NATAL
 SCHOOL OF ENGINEERING
 MECHANICAL ENGINEERING

MAT.: T690 STEEL	No. REQ.: 3	SCALE: 1:2	UNITS: mm	PROJECT: NSW INSTALLATION TOOLING	NO.: 1-5
PROJECT SUPERVISOR	CHECKED	STUDENT NAME: SHUVAY SINGH		TITLE: COUNTER WEIGHT TOP BRACKET	
WORKSHOP TECHNICIAN		STUDENT No.: 211516515			
TECHNICAL OFFICER		E-MAIL: shuvaysingh@gmail.com			
		TEL. NO.: +27 (0)845882810			




UNLESS OTHERWISE STATED GENERAL TOLERANCES: ± 0.05 mm ANGLES: $\pm 0.1^\circ$



 UNIVERSITY OF KWAZULU-NATAL
 SCHOOL OF ENGINEERING
 MECHANICAL ENGINEERING

MAT.: 1690 STEEL	No. REQ.: 1	SCALE: 1:3	UNITS: mm
PROJECT SUPERVISOR	CHECKED	STUDENT NAME: SHUVAY SINGH	
WORKSHOP TECHNICIAN		STUDENT No.: 211516515	
TECHNICAL OFFICER		E-MAIL: shuvaysingh@gmail.com	
		TEL. NO.: +27 (0)845882810	

PROJECT: NSW INSTALLATION TOOLING
 TITLE: COUNTER WEIGHT TOP DRIVE BRACKET

NO.: 1-6


2. Main Beam Assembly

2-1. Main Beam

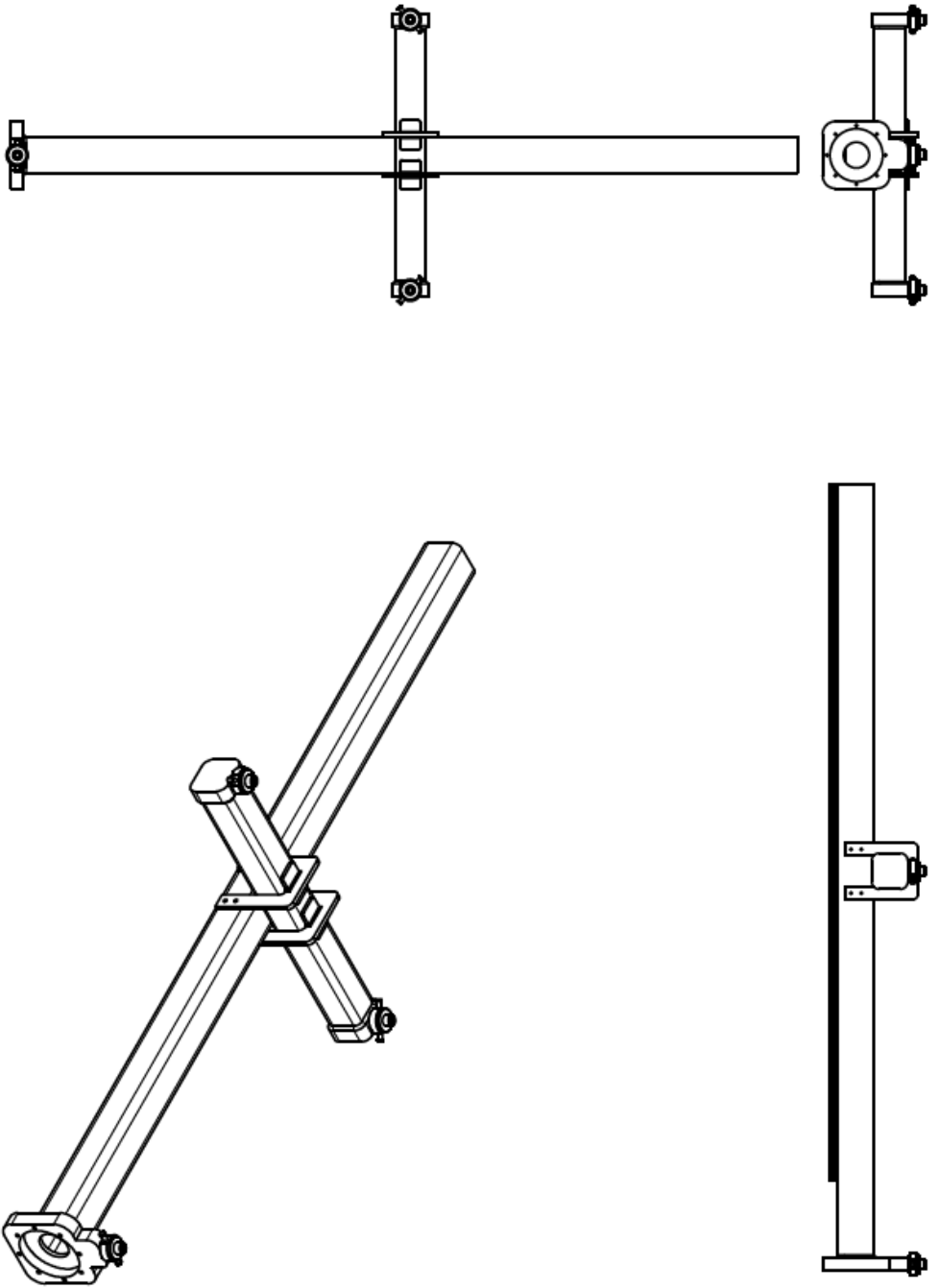
2-2. Cross Beam

2-3. Cross Beam Bracket

2-4. Ball Screw Mount

2-5. Motor Mount

2-6. Linear Guide Rail Clamping Bar




PARTS LIST			
ITEM	MATERIAL	PART NUMB	QTY
1	Steel, Mild	Main Beam	1
2	Steel, Mild	Cross Beam	1
3	Steel, Mild	Cross Beam Bracket	2
4	Generic	Hoist Ring	3
5	Stainless Steel	Linear Guide Rail	1
6	Steel, Mild	Linear Rail Clamping Bar	1

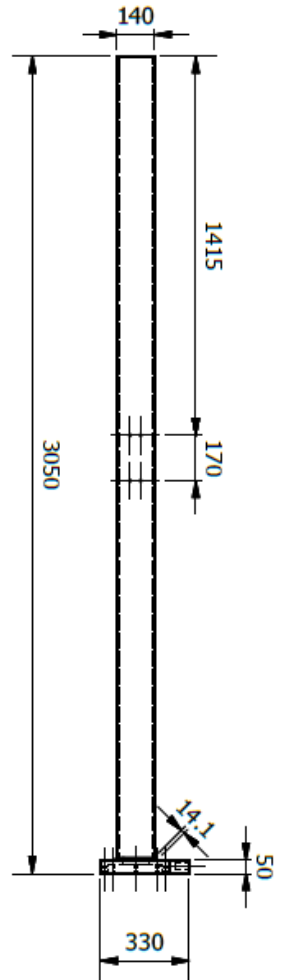
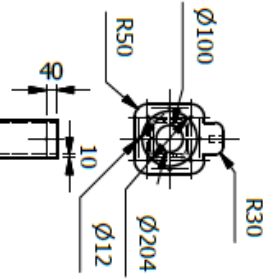
UNLESS OTHERWISE STATED GENERAL TOLERANCES: ±0.05 mm ANGLES: ±0.1 °


SCHOOL OF ENGINEERING
MECHANICAL ENGINEERING
 UNIVERSITY OF KWAZULU-NATAL

MAT.: N/A	No. REQ.: 1	SCALE: 1:25	UNITS: mm
PROJECT SUPERVISOR	CHECKED	STUDENT NAME: SHUVAY SINGH	
WORKSHOP TECHNICIAN		STUDENT No.: 211516515	
TECHNICAL OFFICER		E-MAIL: shuvaysingh@gmail.com	
		TEL. NO.: +27 (0)845882810	

PROJECT: NSW INSTALLATION TOOLING
 TITLE: MAIN BEAM ASSEMBLY
 NO.: 2


UNLESS OTHERWISE STATED GENERAL TOLERANCES: ±0,05 mm ANGLES: ±0,1 °



UNIVERSITY OF KWAZULU-NATAL

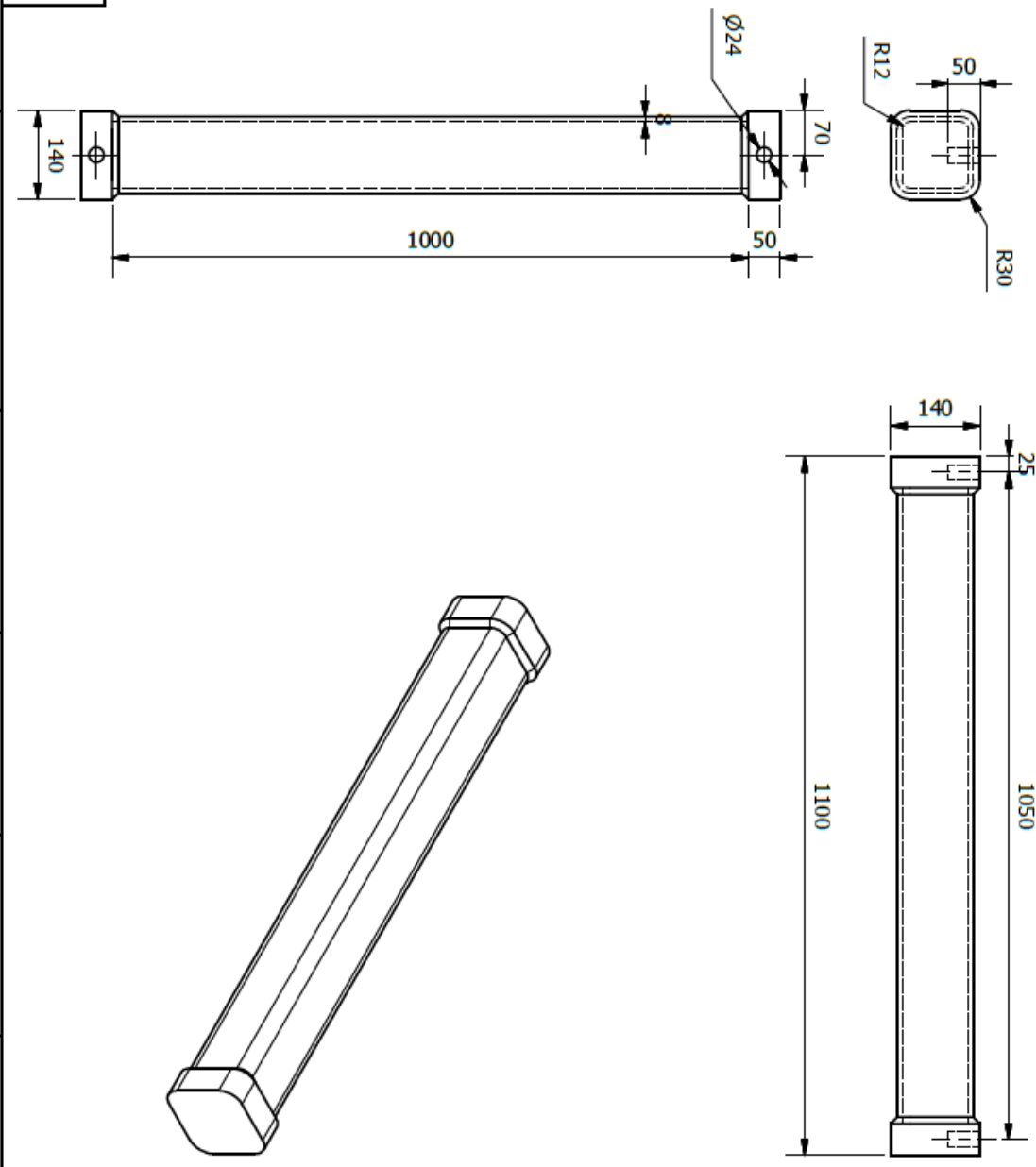
SCHOOL OF ENGINEERING
MECHANICAL ENGINEERING


MAT.: S355 and T690 STEEL	No. REQ.: 1	SCALE: 1:25	UNITS: mm
PROJECT SUPERVISOR	CHECKED	STUDENT NAME: SHUVAY SINGH	
WORKSHOP TECHNICIAN		STUDENT No.: 211516515	
TECHNICAL OFFICER		E-MAIL: shuvaysingh@gmail.com	
		TEL. NO.: +27 (0)945882810	

PROJECT: NSW INSTALLATION TOOLING
TITLE: MAIN BEAM

NO.: 2-1

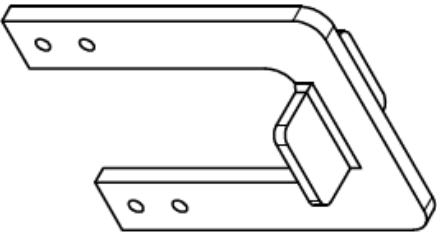
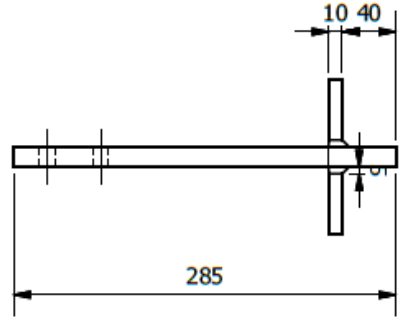
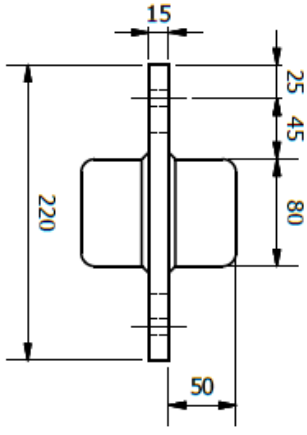
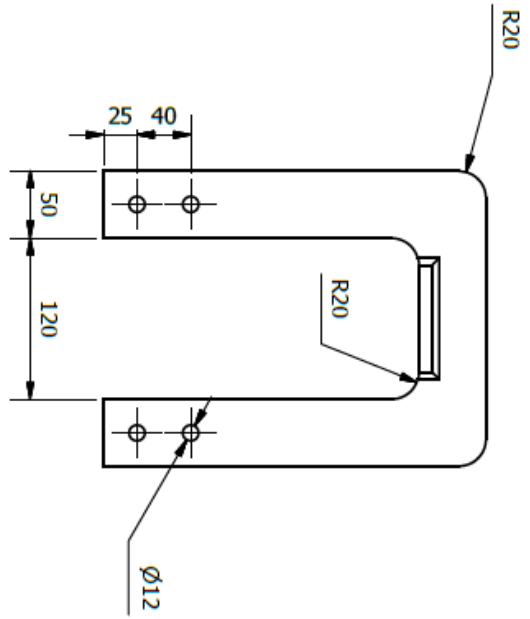
UNLESS OTHERWISE STATED GENERAL TOLERANCES: ±0.05 mm ANGLES: ±0.1 °



 <p>UNIVERSITY OF KWAZULU-NATAL</p>	SCHOOL OF ENGINEERING		MECHANICAL ENGINEERING	
	MAT.: S355 and T690 STEEL	No. REQ.: 1	SCALE: 1:10	UNITS: mm
	PROJECT SUPERVISOR	CHECKED	STUDENT NAME: SHUVAY SINGH	
	WORKSHOP TECHNICIAN		STUDENT No.: 211516515	
TECHNICAL OFFICER		E-MAIL: shuvaysingh@gmail.com		
		TEL. NO.: +27 (0)845882810		
PROJECT: NSW INSTALLATION TOOLING			TITLE: CROSS BEAM	
				NO.: 2-2




UNLESS OTHERWISE STATED GENERAL TOLERANCES: ±0.05 mm ANGLES: ±0.1 °

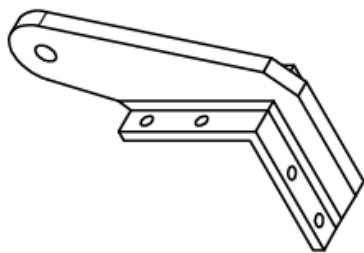
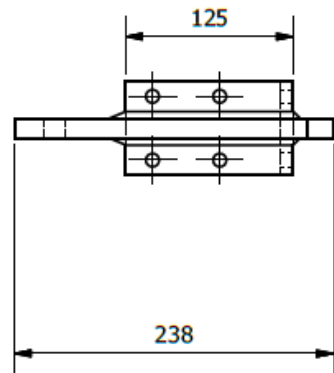
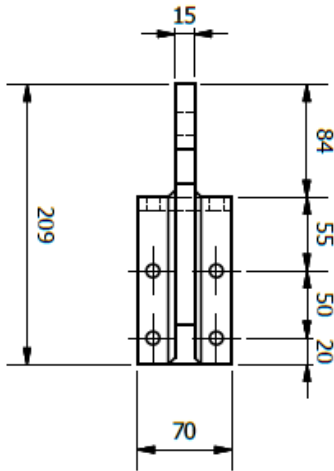
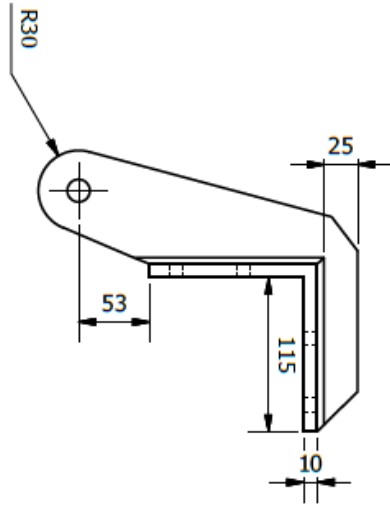


UNIVERSITY OF KWAZULU-NATAL

 SCHOOL OF ENGINEERING
 MECHANICAL ENGINEERING


MAT.: T690 STEEL	No. REQ.: 2	SCALE: 1:5	UNITS: mm
PROJECT SUPERVISOR	CHECKED	STUDENT NAME: SHUVAY SINGH	
WORKSHOP TECHNICIAN		STUDENT No.: 211516515	
TECHNICAL OFFICER		E-MAIL: shuvaysingh@gmail.com	
		TEL. NO.: +27 (0)845882810	

PROJECT: NSW INSTALLATION TOOLING	NO.:
TITLE: CROSS BEAM BRACKET	2-3
	




UNLESS OTHERWISE STATED GENERAL TOLERANCES: $\pm 0,05$ mm ANGLES: $\pm 0,1^\circ$

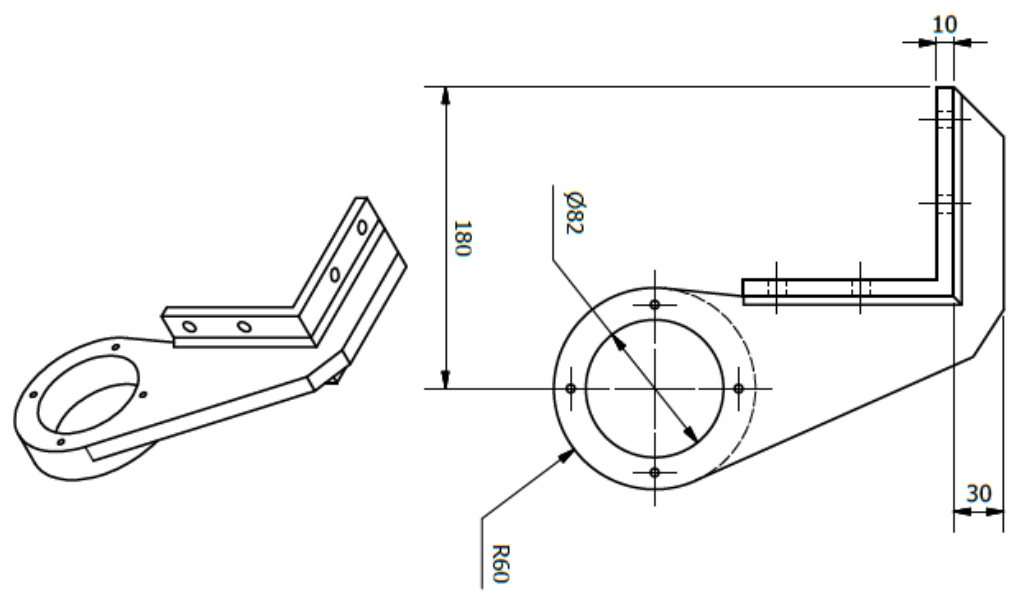
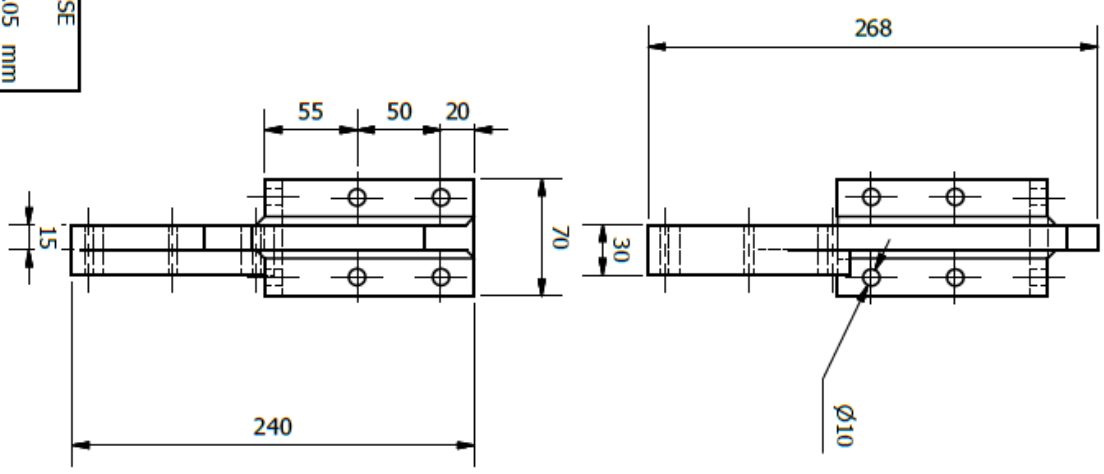
UNIVERSITY OF KWAZULU-NATAL





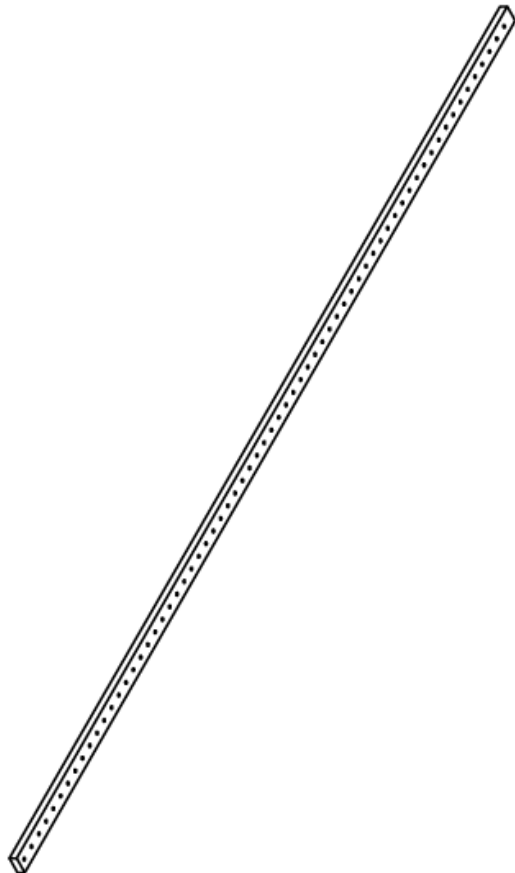
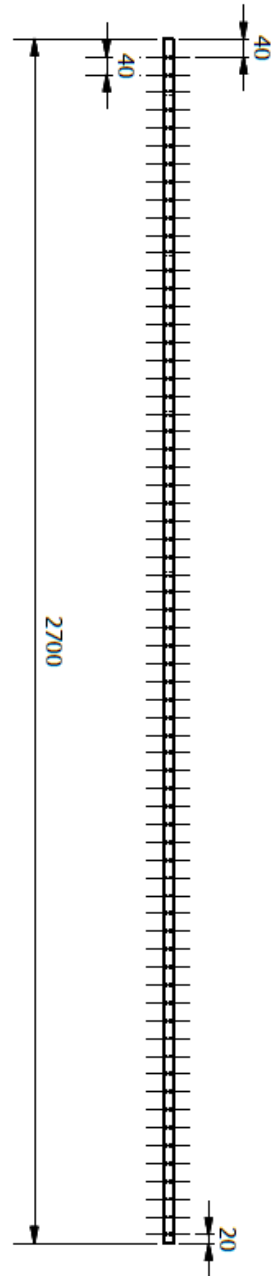
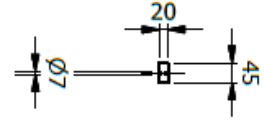
SCHOOL OF ENGINEERING
MECHANICAL ENGINEERING

MAT.: T690 STEEL	No. REQ.: 1	SCALE: 1:5	UNITS: mm	PROJECT: NSW INSTALLATION TOOLING	NO.: 2-4
PROJECT SUPERVISOR	CHECKED	STUDENT NAME: SHUVAY SINGH		TITLE: BALL SCREW MOUNT	
WORKSHOP TECHNICIAN		STUDENT No.: 211516515			
TECHNICAL OFFICER		E-MAIL: shuvaysingh@gmail.com			
		TEL. NO.: +27 (0)845882810			

UNLESS OTHERWISE STATED GENERAL TOLERANCES: ±0.05 mm ANGLES: ±0.1 °



 UNIVERSITY OF KWAZULU-NATAL		SCHOOL OF ENGINEERING		MECHANICAL ENGINEERING	
MAT.: T690 STEEL		No. REQ.: 1		SCALE: 1:4	
PROJECT SUPERVISOR		CHECKED		STUDENT NAME: SHUVAY SINGH	
WORKSHOP TECHNICIAN		DATE		STUDENT No.: 211516515	
TECHNICAL OFFICER		No. REQ.: 1		E-MAIL: shuvaysingh@gmail.com	
PROJECT: NSW INSTALLATION TOOLING		UNITS: mm		TITLE: MOTOR MOUNT	
NO.: 2-5		TEL. NO.: +27 (0)845882810			



UNLESS OTHERWISE
STATED GENERAL
TOLERANCES: ± 0.05 mm
ANGLES: $\pm 0.1^\circ$

UNIVERSITY OF
KWAZULU-NATAL

SCHOOL OF
ENGINEERING

MECHANICAL
ENGINEERING

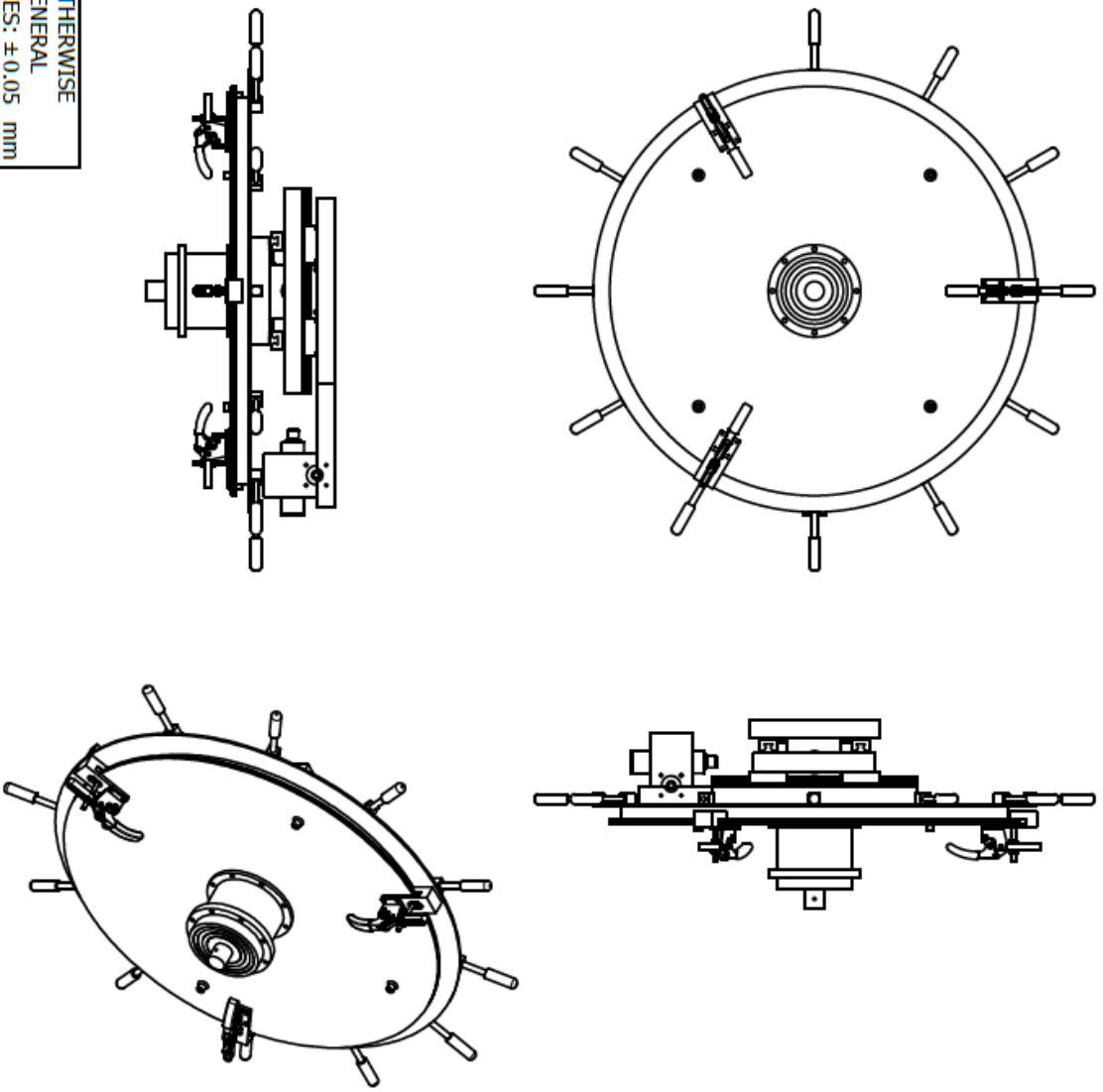
MAT.: MILD STEEL	No. REQ.: 1	SCALE: 1:15	UNITS: mm	PROJECT: NSW INSTALLATION TOOLING	NO.:
PROJECT SUPERVISOR	CHECKED	STUDENT NAME: SHUVAY SINGH		TITLE:	2-6
WORKSHOP TECHNICIAN		STUDENT No.: 211516515		LINEAR GUIDE RAIL CLAMPING BAR	
TECHNICAL OFFICER		E-MAIL: shuvaysingh@gmail.com			
		TEL. NO.: +27 (0)845882810			





3. Rotation Head Assembly

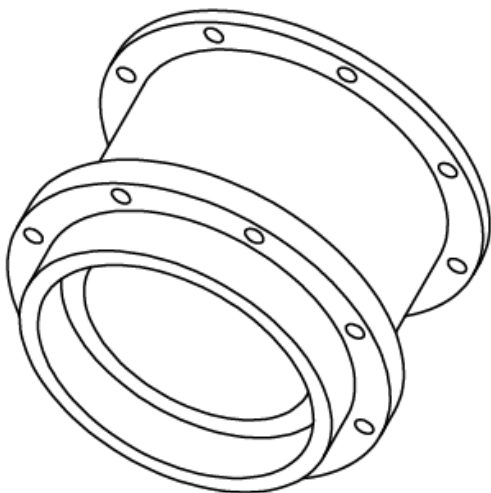
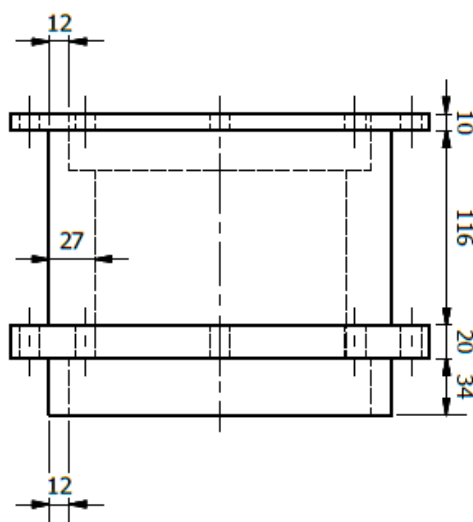
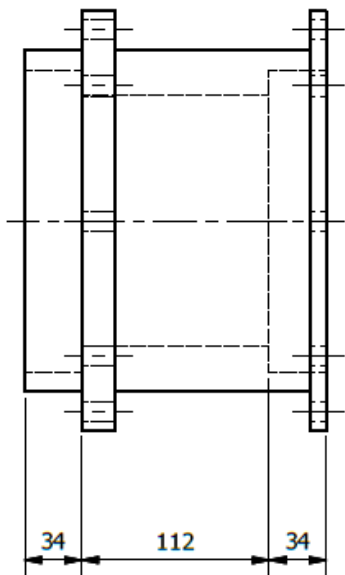
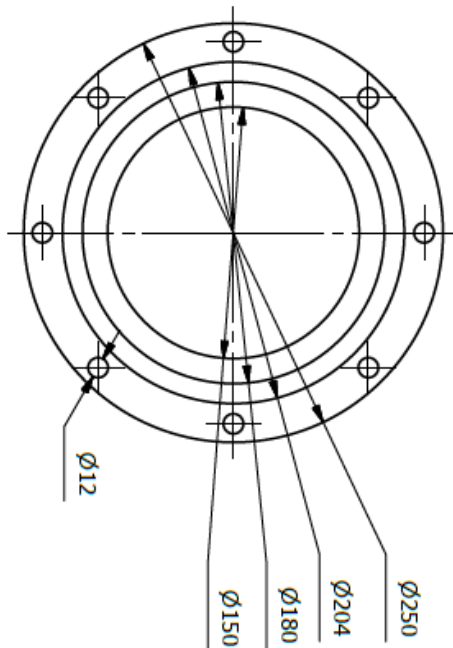
- 3-1. Trunnion Coupling
- 3-2. Trunnion Shaft
- 3-3. Non-Rotating Wheel
- 3-4. Rotating Wheel
- 3-5. Toggle Clamp Bracket
- 3-6. Rail Toolside Plate
- 3-7. Guide Carrying Plate
- 3-8. Grabber Adapter Plate

PARTS LIST			
ITEM	MATERIAL	PART NUMBER	QTY
1	Steel, Mild	Rotation Wheel Moving	1
2	Steel, Mild	Linear Guide Rail 25C 300mm	4
3	Stainless Steel	Linear Guide Carriage 25C	8
4	Aluminum 6061	Guide Carriage Plate	1
5	Aluminum 6061	Grabber Adapter Plate	1
6	Steel, Mild	Rotation Wheel Non-moving	1
7	Aluminum 6061	Rail Plate Toolside	1
8	Stainless Steel	Worm Gearbox Actuator	2
9	Generic	Hand Wheel Knob	11
10	Steel	Clamping Assembly	3
11	Steel, Mild	Trunnion Shaft 100 mm	1
12	Steel, Mild	Trunnion Coupling 100 mm	1
13	Stainless Steel	Trunnion Bearing 100 mm	2



UNLESS OTHERWISE
STATED GENERAL
TOLERANCES: ±0.05 mm
ANGLES: ±0.1 °

 UNIVERSITY OF KWAZULU-NATAL		SCHOOL OF ENGINEERING		MAT.: N/A		No. REQ.: 1		SCALE: 1:18		UNITS: mm		PROJECT: NSW INSTALLATION TOOLING		NO.: 3	
MECHANICAL ENGINEERING		PROJECT SUPERVISOR		DATE		CHECKED		STUDENT NAME: SHUVAY SINGH		STUDENT No.: 211516515		TITLE: ROTATION HEAD ASSEMBLY			
WORKSHOP TECHNICIAN		TECHNICAL OFFICER		E-MAIL: shuvaysingh@gmail.com		TEL. NO.: +27 (0)845882810		PROJECT:		TITLE:		NO.:		3	



UNLESS OTHERWISE STATED GENERAL TOLERANCES: $\pm 0,05$ mm ANGLES: $\pm 0,1^\circ$

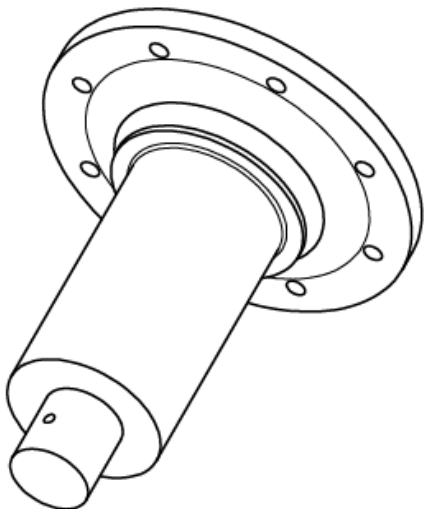
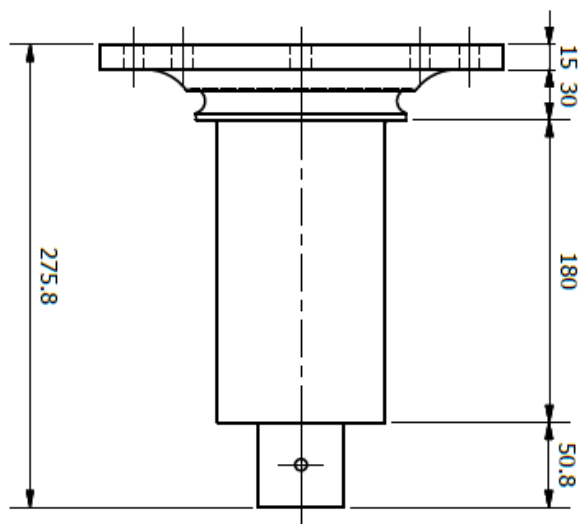
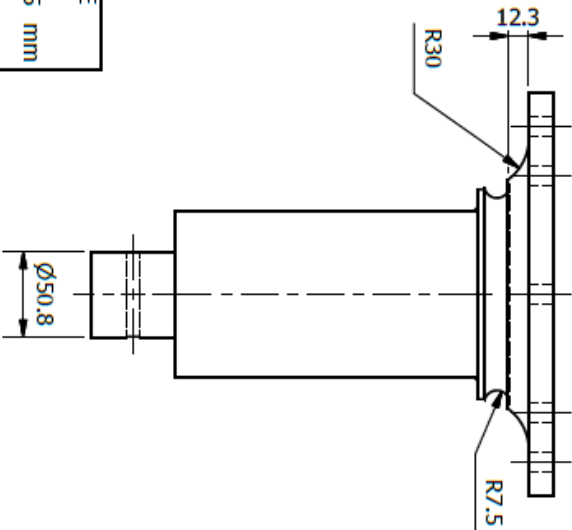
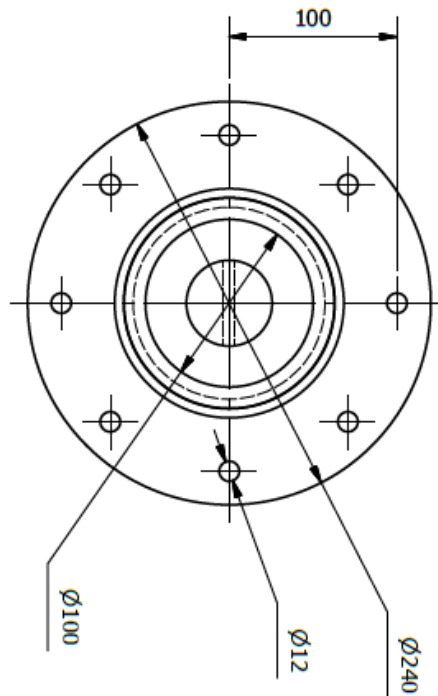



 UNIVERSITY OF KWAZULU-NATAL
 SCHOOL OF ENGINEERING
 MECHANICAL ENGINEERING

MAT.: En 9(S) STEEL	DATE	No. REQ.: 1	CHECKED	SCALE: 1:4	UNITS: mm	PROJECT: NSW INSTALLATION TOOLING	NO.: 3-1
PROJECT SUPERVISOR				STUDENT NAME: SHUVAY SINGH			
WORKSHOP TECHNICIAN				STUDENT No.: 211516515		TITLE: TRUNNION COUPLING	
TECHNICAL OFFICER				E-MAIL: shuvaysingh@gmail.com			
				TEL. NO.: +27 (0)845882810			

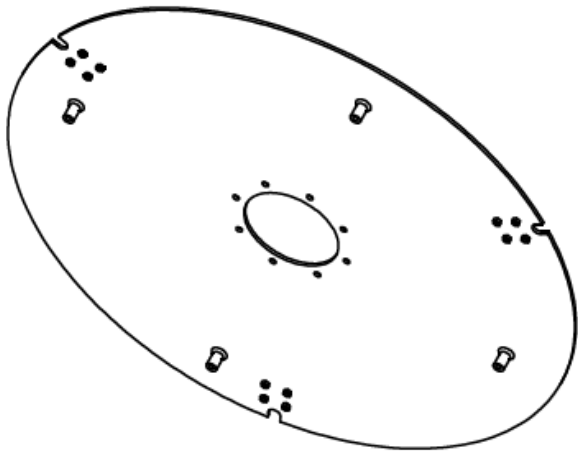
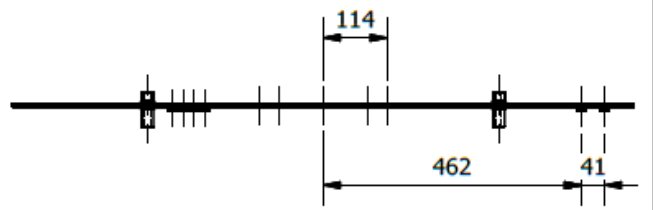
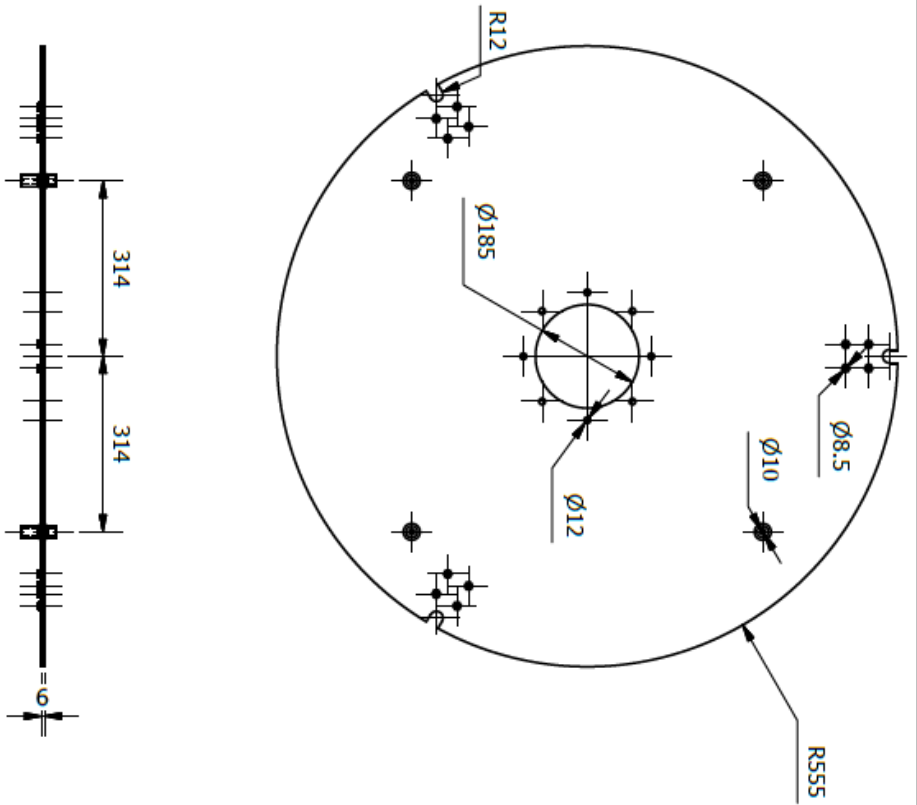


UNLESS OTHERWISE STATED GENERAL TOLERANCES: ±0.05 mm ANGLES: ±0.1 °



 UNIVERSITY OF KWAZULU-NATAL SCHOOL OF ENGINEERING MECHANICAL ENGINEERING	MAT.: En 9(S) STEEL	No. REQ.: 1	SCALE: 1:4	UNITS: mm	PROJECT: NSW INSTALLATION TOOLING	NO.: 3-2
	PROJECT SUPERVISOR	CHECKED	STUDENT NAME: SHUVAY SINGH			
WORKSHOP TECHNICIAN		STUDENT No.: 211516515	E-MAIL: shuvaysingh@gmail.com		TITLE: TRUNNION SHAFT	
TECHNICAL OFFICER		TEL. NO.: +27 (0)845882810				






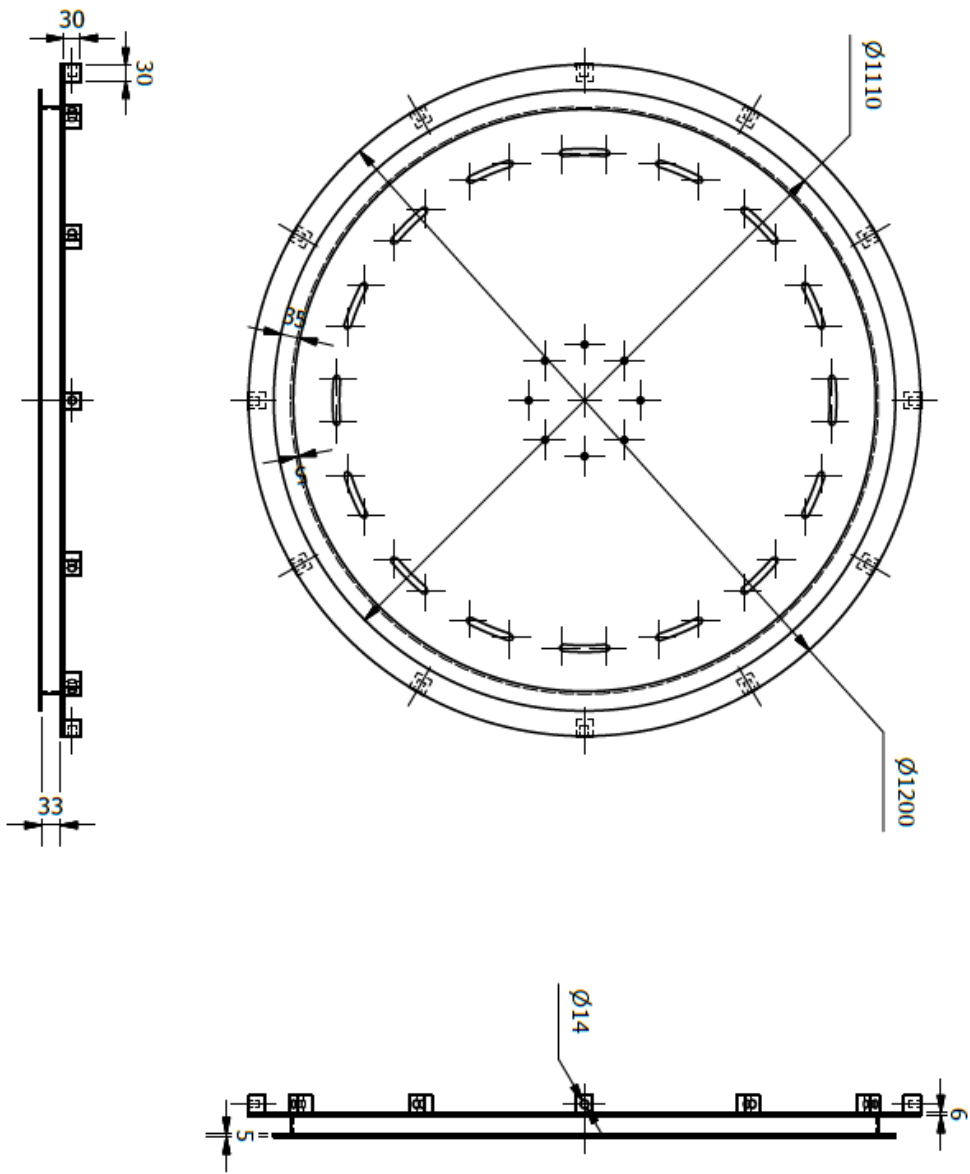
UNLESS OTHERWISE STATED GENERAL TOLERANCES: ± 0.05 mm ANGLES: $\pm 0.1^\circ$



 UNIVERSITY OF KWAZULU-NATAL
 SCHOOL OF ENGINEERING
 MECHANICAL ENGINEERING

MAT.: STAINLESS STEEL	No. REQ.: 1	SCALE: 1:12	UNITS: mm
PROJECT SUPERVISOR	CHECKED	STUDENT NAME: SHUVAY SINGH	
WORKSHOP TECHNICIAN		STUDENT No.: 211516515	
TECHNICAL OFFICER		E-MAIL: shuvaysingh@gmail.com	
		TEL. NO.: +27 (0)945882810	

PROJECT: NSW INSTALLATION TOOLING
 TITLE: NON-ROTATING WHEEL
 NO.: 3-3





UNLESS OTHERWISE STATED GENERAL TOLERANCES: ± 0.05 mm ANGLES: $\pm 0.1^\circ$

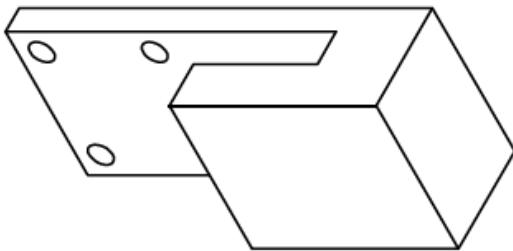
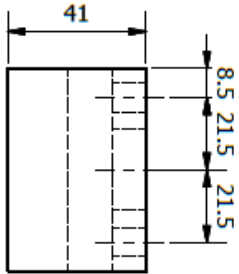
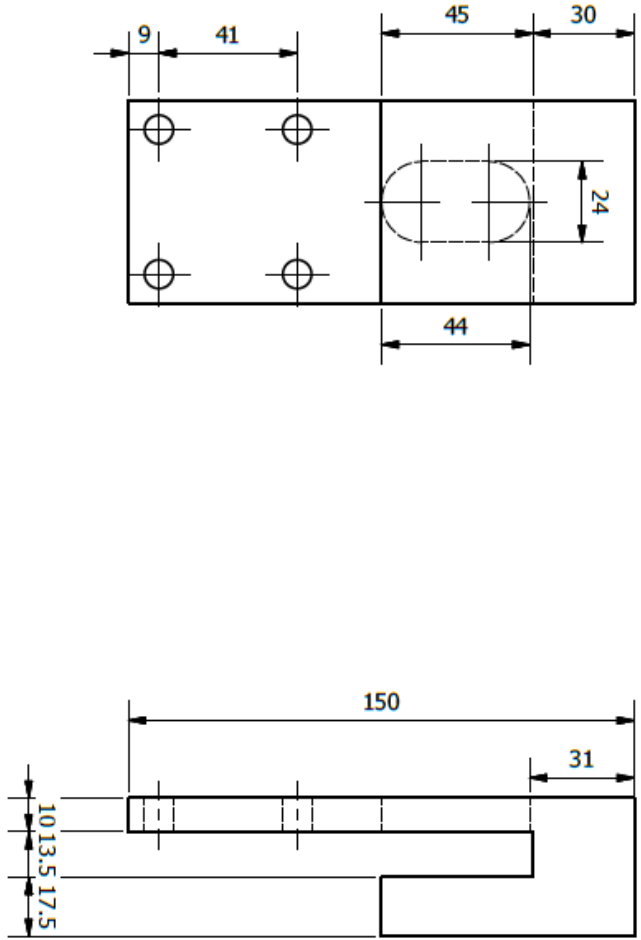


 UNIVERSITY OF KWAZULU-NATAL
 SCHOOL OF ENGINEERING
 MECHANICAL ENGINEERING

MAT.: STAINLESS STEEL	No. REQ.: 1	SCALE: 1:12	UNITS: mm
PROJECT SUPERVISOR	CHECKED	STUDENT NAME: SHUVAY SINGH	
WORKSHOP TECHNICIAN		STUDENT No.: 211516515	
TECHNICAL OFFICER		E-MAIL: shuvaysingh@gmail.com	
		TEL. NO.: +27 (0)945882810	

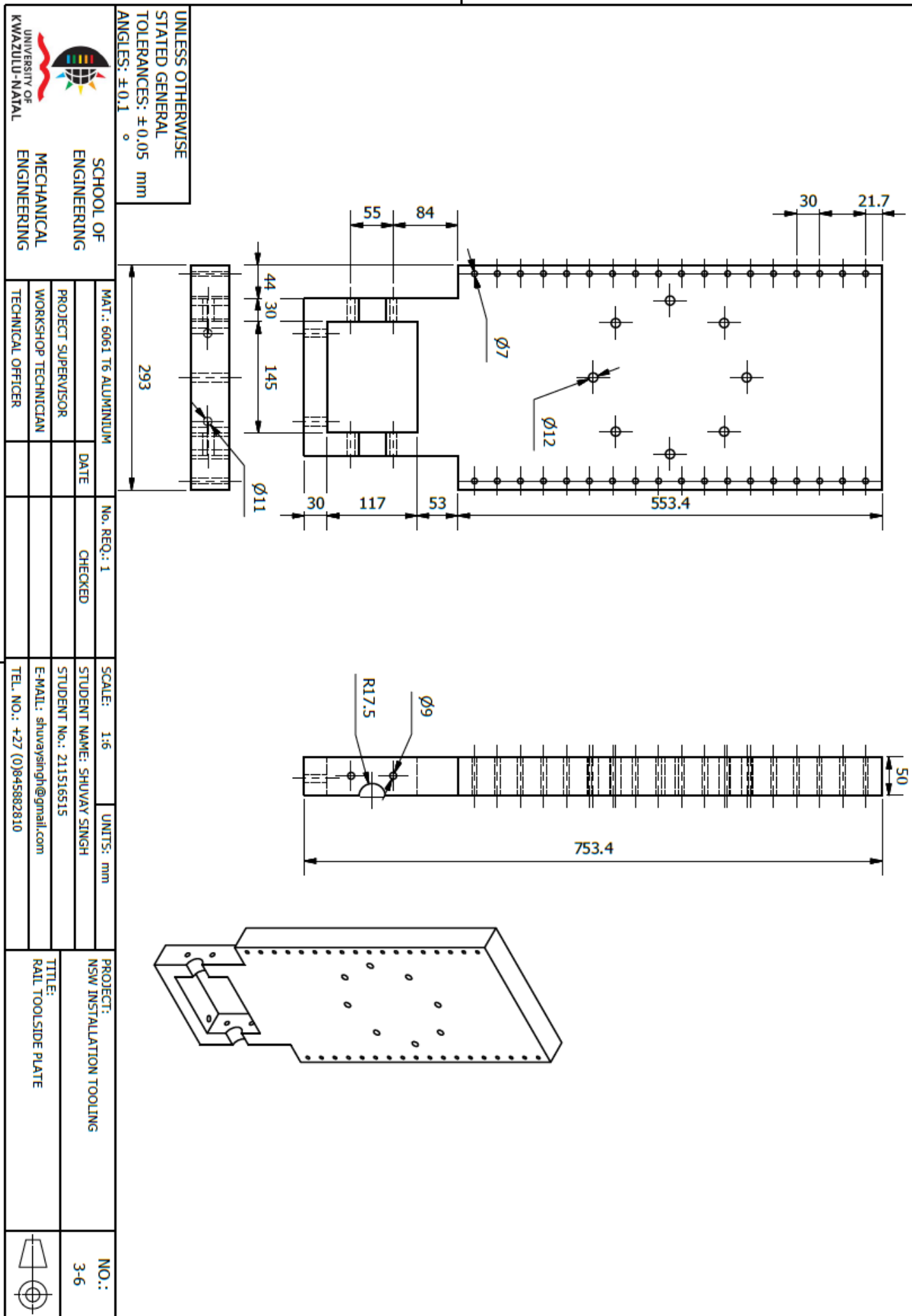
PROJECT: NSW INSTALLATION TOOLING
 TITLE: ROTATING WHEEL

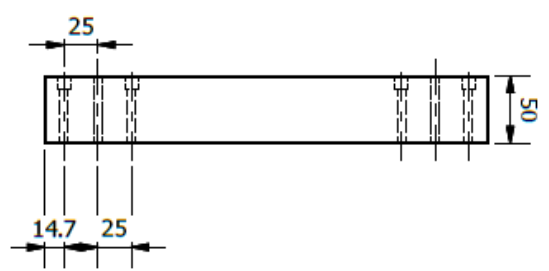
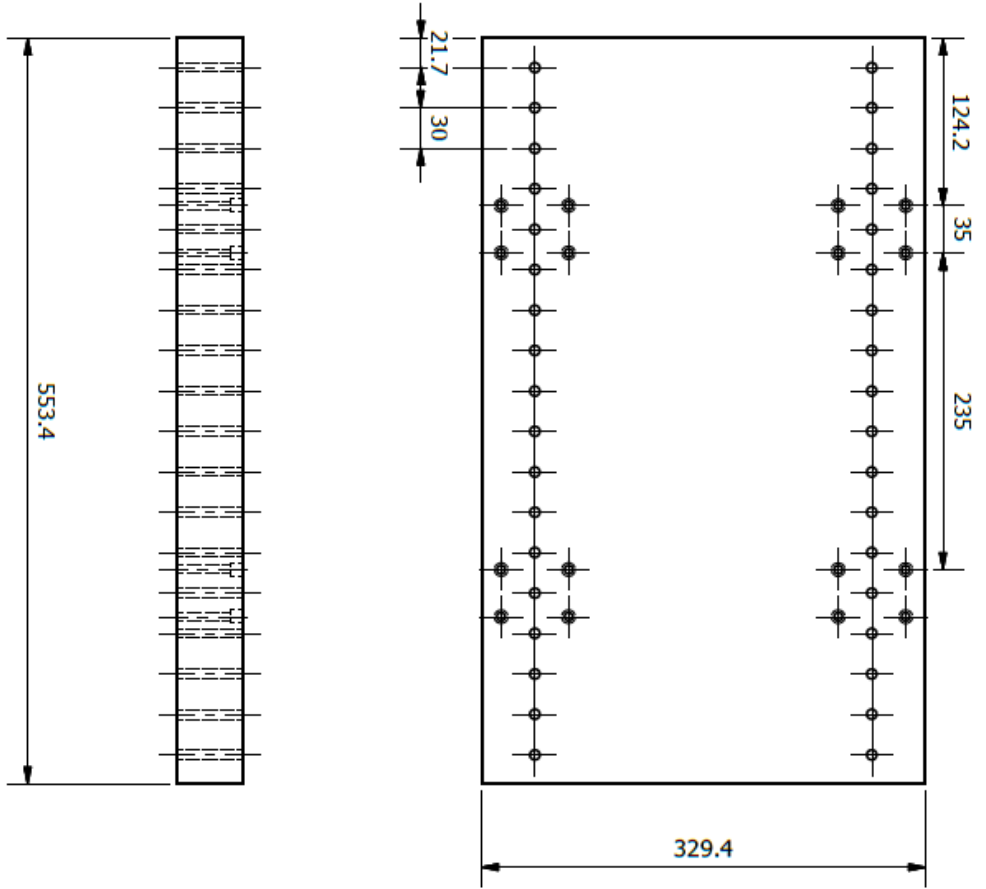
NO.: 3-4




UNLESS OTHERWISE STATED GENERAL TOLERANCES: ± 0.05 mm ANGLES: $\pm 0.1^\circ$

 UNIVERSITY OF KWAZULU-NATAL	SCHOOL OF ENGINEERING MECHANICAL ENGINEERING	MAT.: T690 STEEL	No. REQ.: 3	SCALE: 1:2	UNITS: mm	PROJECT: NSW INSTALLATION TOOLING	NO.: 3-5
		PROJECT SUPERVISOR WORKSHOP TECHNICIAN TECHNICAL OFFICER	CHECKED	STUDENT NAME: SHUVAY SINGH STUDENT No.: 211516515 E-MAIL: shuvaysingh@gmail.com TEL. NO.: +27 (0)845882810	TITLE: TOGGLE CLAMP BRACKET		





UNLESS OTHERWISE STATED GENERAL TOLERANCES: ±0.05 mm ANGLES: ±0.1 °

UNIVERSITY OF KWAZULU-NATAL



SCHOOL OF ENGINEERING

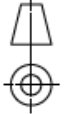
MECHANICAL ENGINEERING

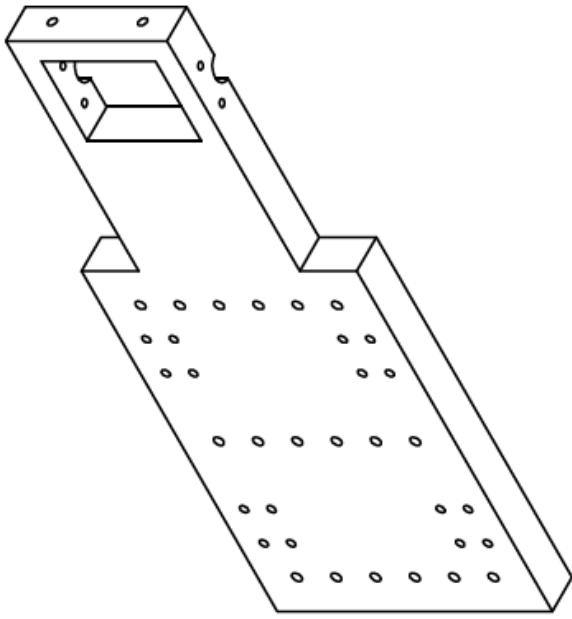
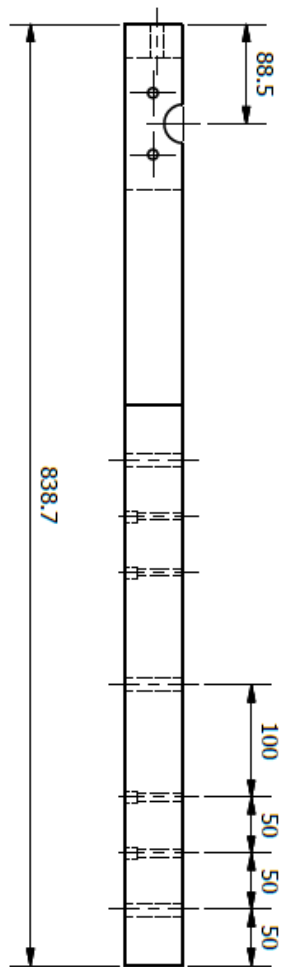
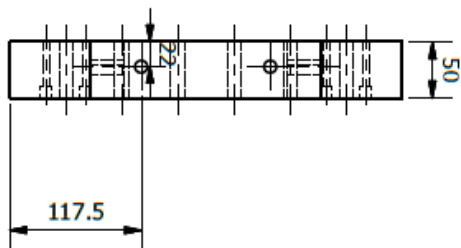
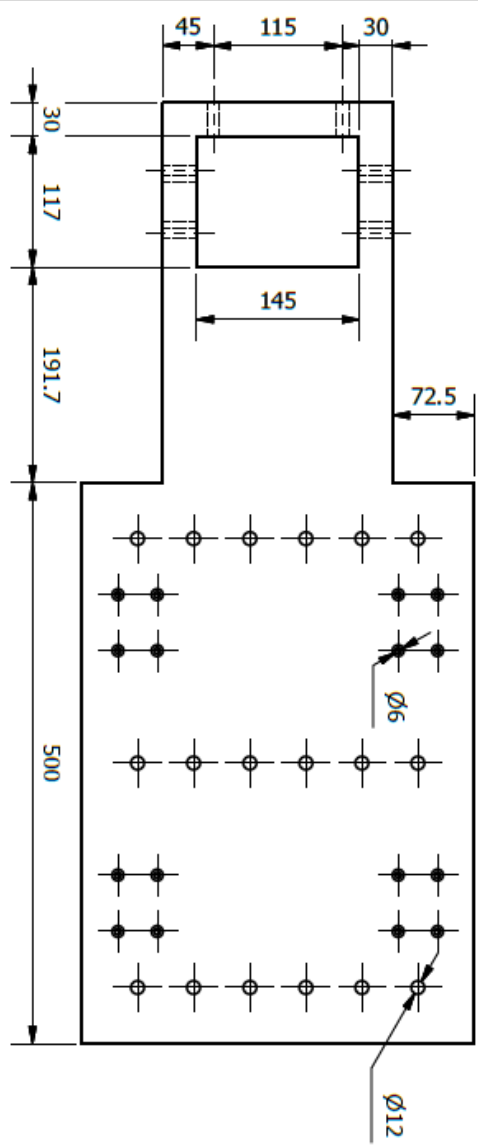
MAT.: 6061 T6 ALUMINIUM	No. REQ.: 1	SCALE: 1:5	UNITS: mm
PROJECT SUPERVISOR	CHECKED	STUDENT NAME: SHUVAY SINGH	
WORKSHOP TECHNICIAN		STUDENT No.: 211516515	
TECHNICAL OFFICER		E-MAIL: shuvaysingh@gmail.com	
		TEL. NO.: +27 (0)845882810	

PROJECT: NSW INSTALLATION TOOLING



TITLE: GUIDE CARRYING PLATE

NO.: 3-7





UNLESS OTHERWISE STATED GENERAL TOLERANCES: ±0.05 mm ANGLES: ±0.1 °

 UNIVERSITY OF KWAZULU-NATAL	SCHOOL OF ENGINEERING		MAT.: 6061 T6 ALUMINIUM	No. REQ.: 1	SCALE: 1:6	UNITS: mm	PROJECT: NSW INSTALLATION TOOLING	NO.: 3-8
	MECHANICAL ENGINEERING		PROJECT SUPERVISOR	CHECKED	STUDENT NAME: SHUWAY SINGH			
		WORKSHOP TECHNICIAN	TECHNICAL OFFICER		STUDENT No.: 211516515		E-MAIL: shuwaysingh@gmail.com	
					TEL. NO.: +27 (0)945882810		TITLE: RUBBER ADAPTER PLATE	

4 a. LS Grabber Assembly

4 b. SS Grabber Assembly

4-1. LS Grabber Frame

4-2. LS Upper Gusset Plate

4-3. LS Upper Gusset Plate Double

4-4. LS Lower Gusset Plate

4-5. SS Grabber Frame

4-6. SS Upper Gusset Plate

4-7. SS Lower Gusset Plate

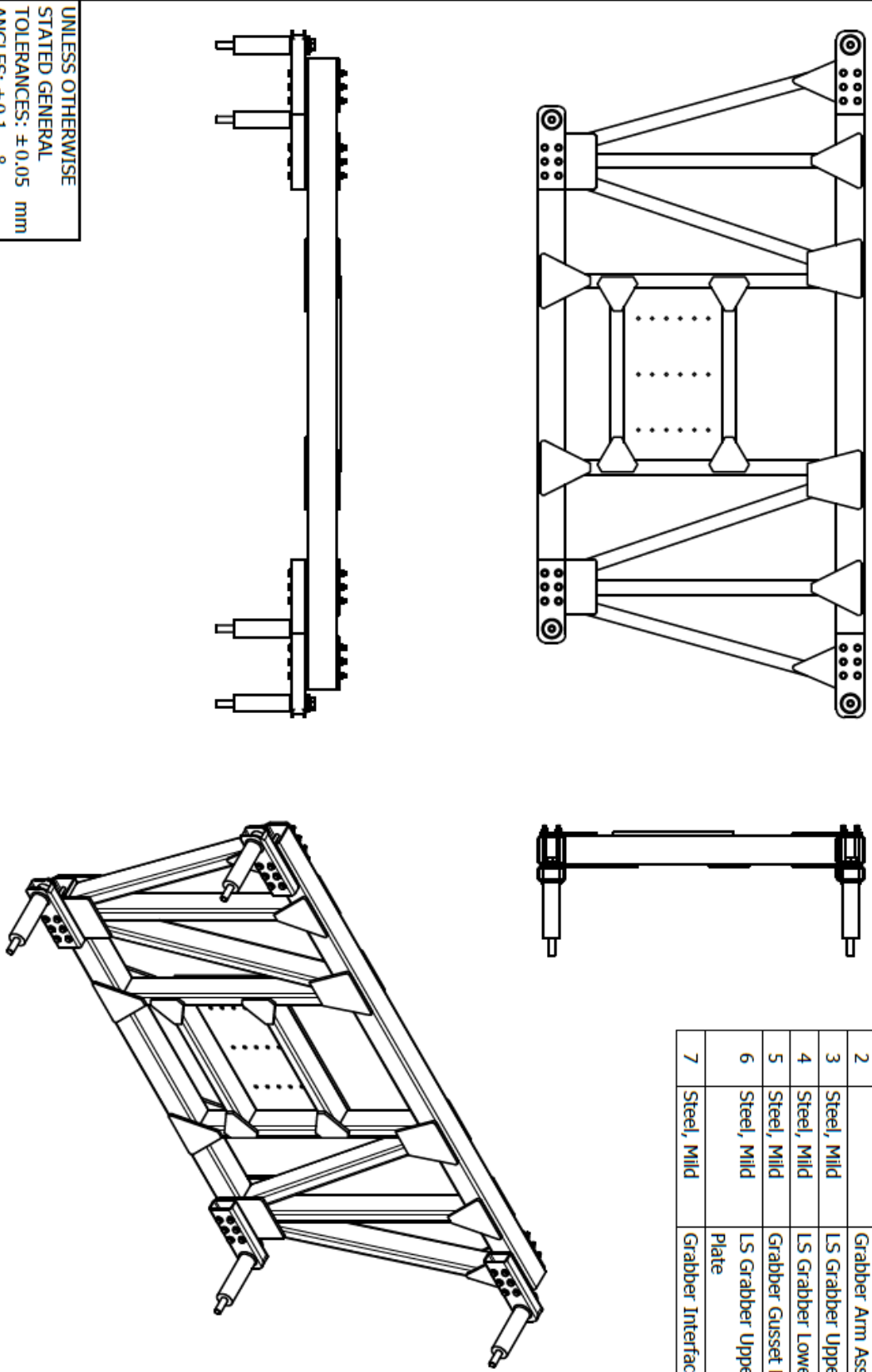
4-8. T-Joint Gusset Plate

4-9. Grabber Interface Gusset Plate

4-10. Grabber Arm

4-11. Foot Spoke Grabber

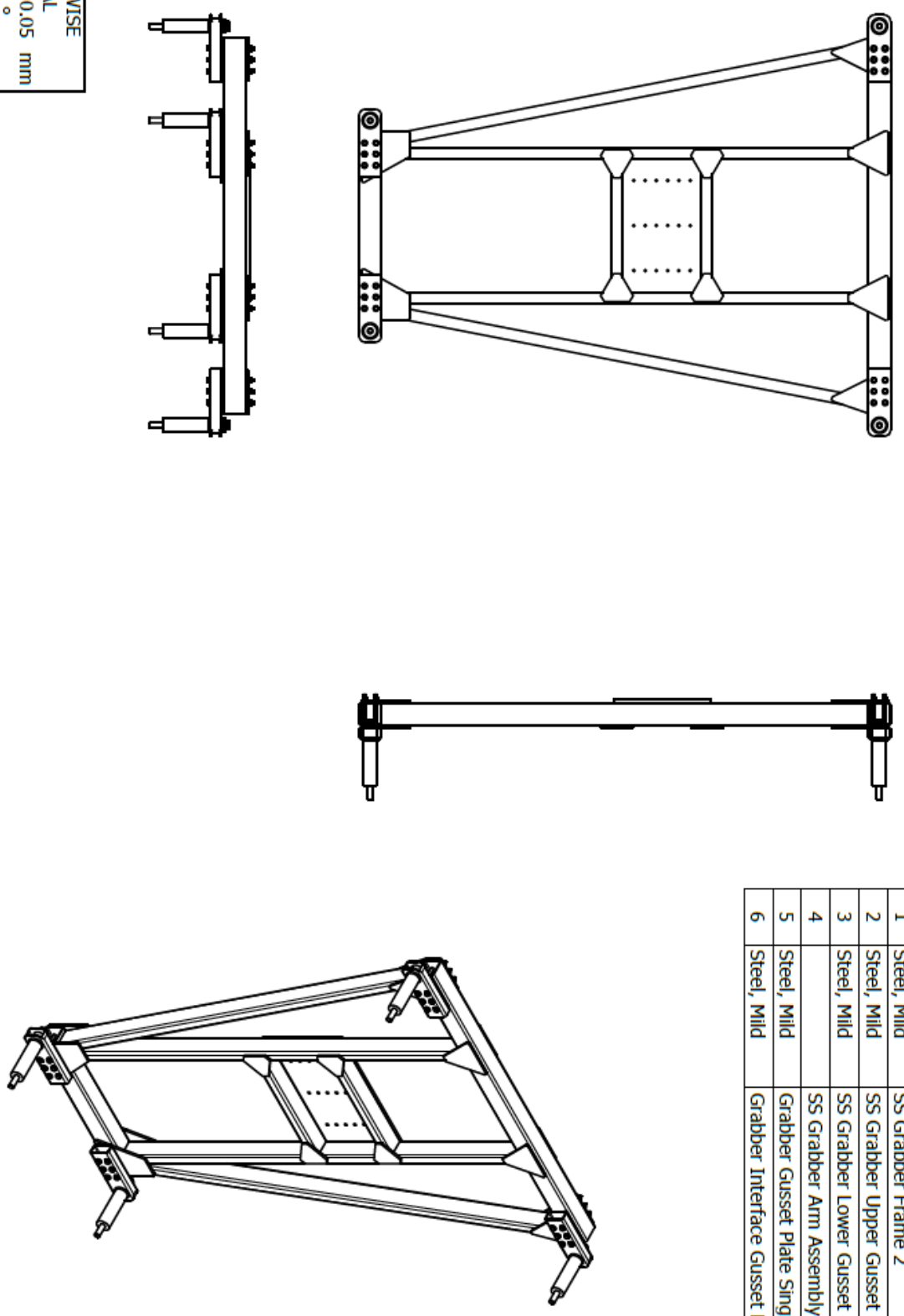
PARTS LIST			
ITEM	MATERIAL	PART NUMBER	QTY
1	Steel, Mild	LS Grabber Frame	1
2		Grabber Arm Assembly	4
3	Steel, Mild	LS Grabber Upper Gusset Plate	4
4	Steel, Mild	LS Grabber Lower Gusset Plate	4
5	Steel, Mild	Grabber Gusset Plate Single	8
6	Steel, Mild	LS Grabber Upper Gusset Double Plate	4
7	Steel, Mild	Grabber Interface Gusset Plate	4





UNLESS OTHERWISE STATED GENERAL TOLERANCES: ±0,05 mm ANGLES: ±0,1 °

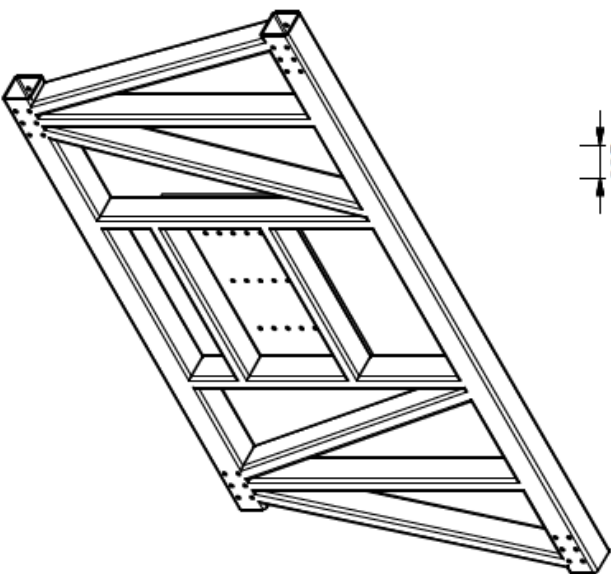
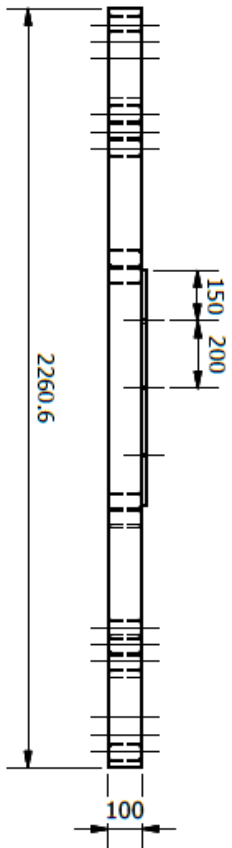
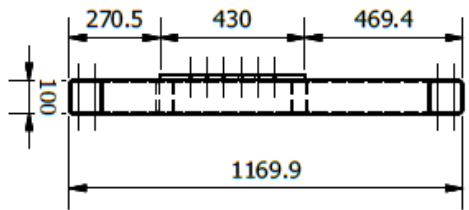
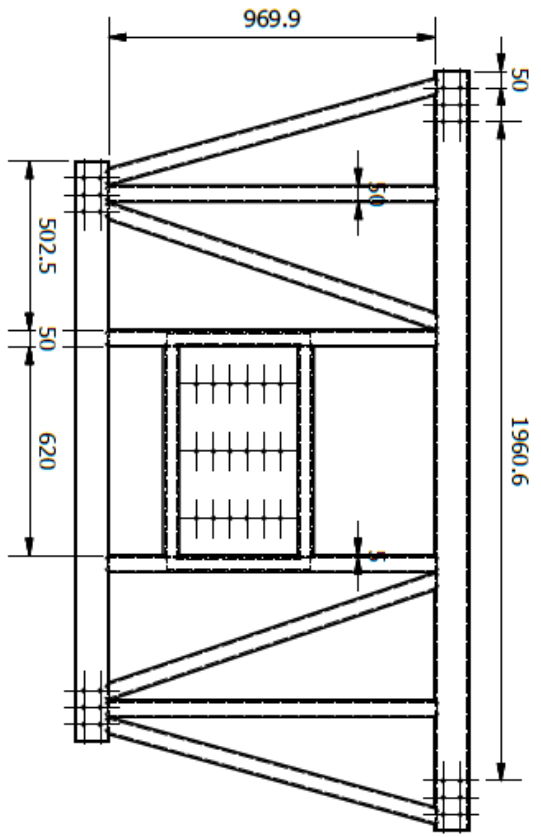
 <p>UNIVERSITY OF KWAZULU-NATAL</p>		<p>SCHOOL OF ENGINEERING</p>		<p>MAT.: N/A</p>		<p>No. REQ.: 1</p>		<p>SCALE: 1:20</p>		<p>UNITS: mm</p>		<p>PROJECT: NSW INSTALLATION TOOLING</p>		<p>NO.: 4 a</p>	
<p>MECHANICAL ENGINEERING</p>		<p>PROJECT SUPERVISOR</p>		<p>DATE</p>		<p>CHECKED</p>		<p>STUDENT NAME: SHUVAY SINGH</p>		<p>STUDENT No.: 211516515</p>		<p>TITLE: LS GRABBER ASSEMBLY</p>			
<p>WORKSHOP TECHNICIAN</p>		<p>TECHNICAL OFFICER</p>		<p>E-MAIL: shuvaysingh@gmail.com</p>		<p>TEL. NO.: +27 (0)845882810</p>									

PARTS LIST			
ITEM	MATERIAL	PART NUMBER	QTY
1	Steel, Mild	SS Grabber Frame 2	1
2	Steel, Mild	SS Grabber Upper Gusset Plate	4
3	Steel, Mild	SS Grabber Lower Gusset Plate	4
4		SS Grabber Arm Assembly	4
5	Steel, Mild	Grabber Gusset Plate Single	4
6	Steel, Mild	Grabber Interface Gusset Plate	4



UNLESS OTHERWISE STATED GENERAL TOLERANCES: ± 0.05 mm ANGLES: $\pm 0.1^\circ$

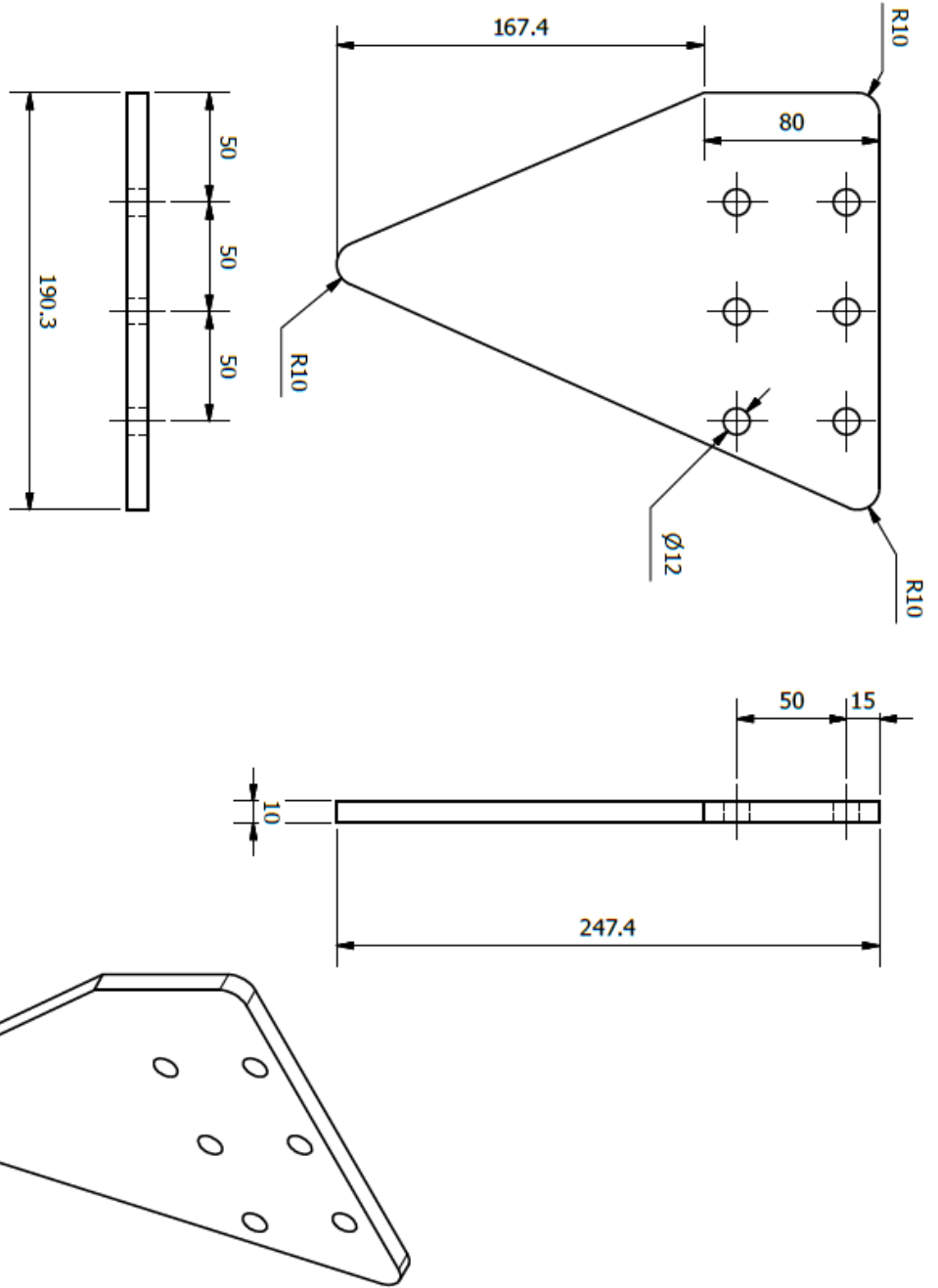
 UNIVERSITY OF KWAZULU-NATAL SCHOOL OF ENGINEERING MECHANICAL ENGINEERING	MAT.: N/A	No. REQ.: 1	SCALE: 1:25	UNITS: mm	PROJECT: NSW INSTALLATION TOOLING	NO.:
	PROJECT SUPERVISOR	CHECKED	STUDENT NAME: SHUVAY SINGH		TITLE: SS GRABBER ASSEMBLY	4 b
WORKSHOP TECHNICIAN		STUDENT No.: 211516515	E-MAIL: shuvaysingh@gmail.com			
TECHNICAL OFFICER		TEL. NO.: +27 (0)845882810				



UNLESS OTHERWISE STATED GENERAL TOLERANCES: ±0.05 mm ANGLES: ±0.1 °

 UNIVERSITY OF KWAZULU-NATAL	SCHOOL OF ENGINEERING		MAT.: S355 STEEL	No. REQ.: 1	SCALE: 1:20	UNITS: mm	PROJECT: NSW INSTALLATION TOOLING	NO.: 4-1
	MECHANICAL ENGINEERING		PROJECT SUPERVISOR	CHECKED	STUDENT NAME: SHUVAY SINGH			
		WORKSHOP TECHNICIAN			STUDENT No.: 211516515		TITLE: LS GRABBER FRAME	
		TECHNICAL OFFICER			E-MAIL: shuvaysingh@gmail.com			
					TEL. NO.: +27 (0)945882810			





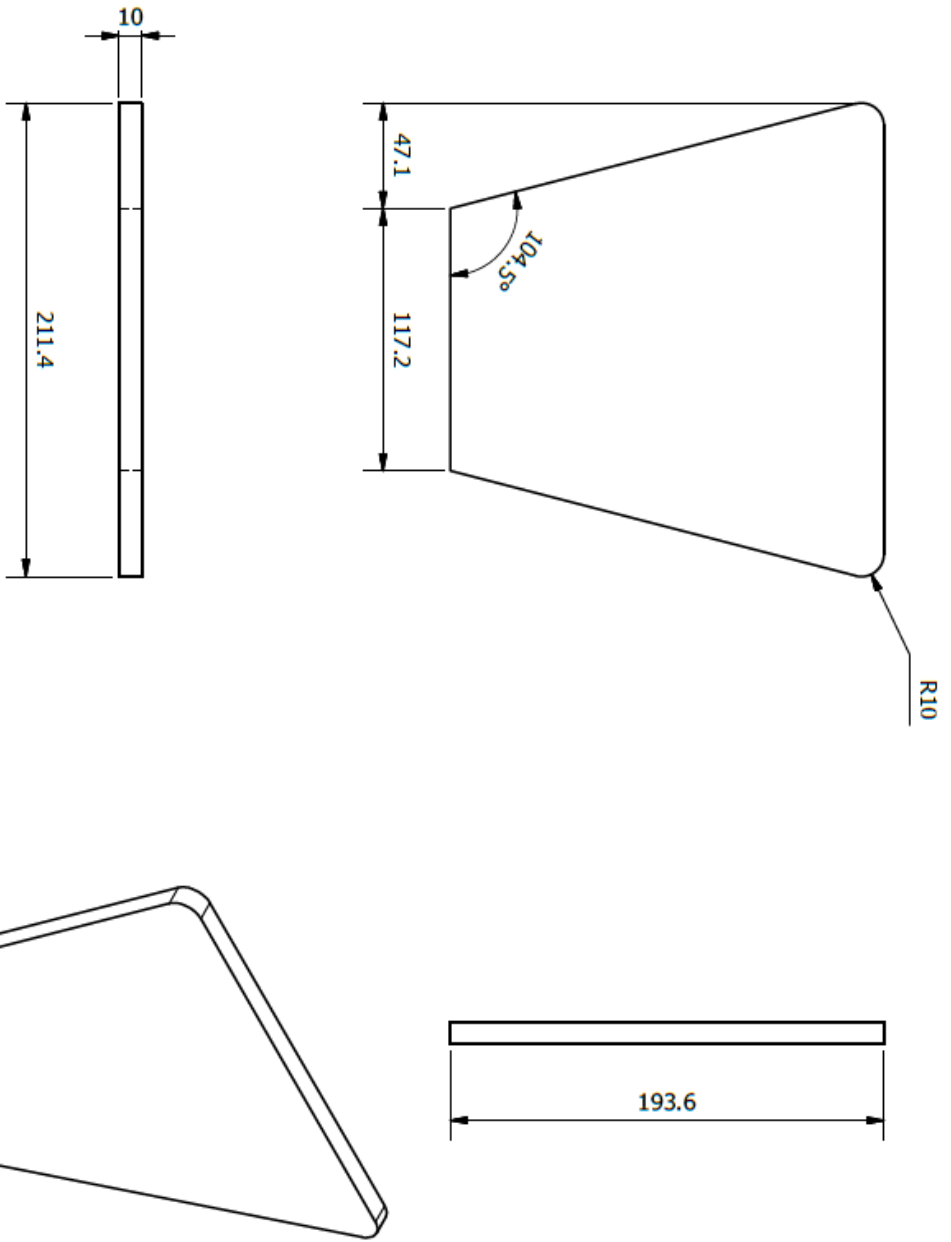
UNLESS OTHERWISE STATED GENERAL TOLERANCES: ±0.05 mm ANGLES: ±0.1 °



 UNIVERSITY OF KWAZULU-NATAL
 SCHOOL OF ENGINEERING
 MECHANICAL ENGINEERING

MAT.: T690 STEEL		No. REQ.: 4	SCALE: 1:3	UNITS: mm	PROJECT: NSW INSTALLATION TOOLING	NO.: 4-2
PROJECT SUPERVISOR	DATE	CHECKED	STUDENT NAME: SHUVAY SINGH			
WORKSHOP TECHNICIAN			STUDENT No.: 211516515		TITLE: LS GUSSET PLATE	
TECHNICAL OFFICER			E-MAIL: shuvaysingh@gmail.com			
			TEL. NO.: +27 (0)845882810			





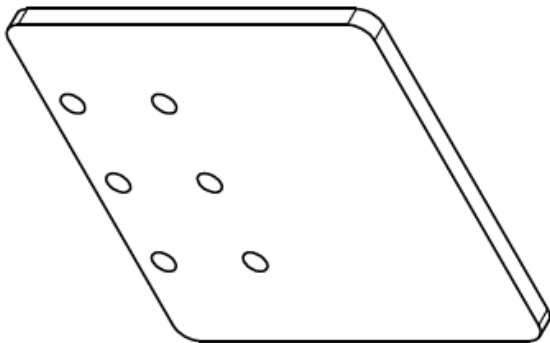
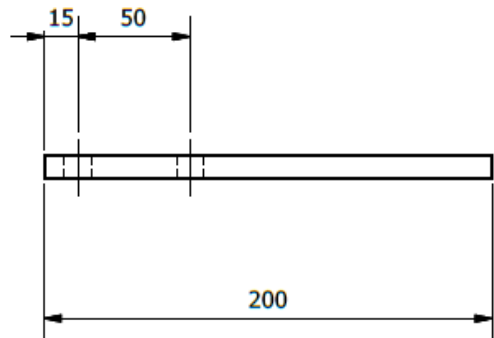
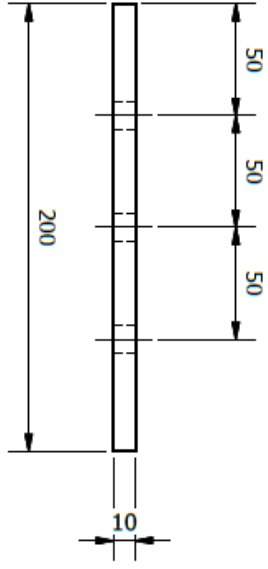
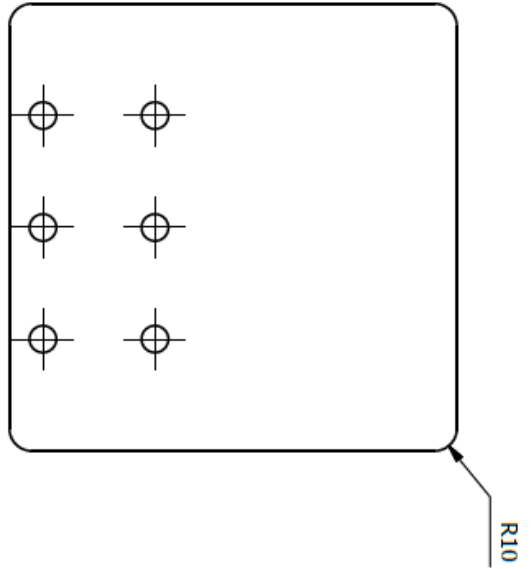
UNLESS OTHERWISE STATED GENERAL TOLERANCES: ±0.05 mm ANGLES: ±0.1 °



 UNIVERSITY OF KWAZULU-NATAL
 SCHOOL OF ENGINEERING
 MECHANICAL ENGINEERING

MAT.: T690 STEEL		No. REQ.: 4	SCALE: 1:3	UNITS: mm	PROJECT: NSW INSTALLATION TOOLING	NO.: 4-3
PROJECT SUPERVISOR	DATE	CHECKED	STUDENT NAME: SHUVAY SINGH			
WORKSHOP TECHNICIAN			STUDENT No.: 211516515			
TECHNICAL OFFICER			E-MAIL: shuvaysingh@gmail.com		TITLE: LS GUSSET PLATE DOUBLE	
			TEL. NO.: +27 (0)845882810			




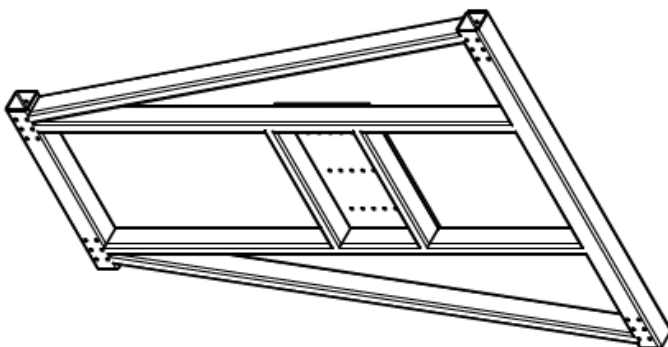
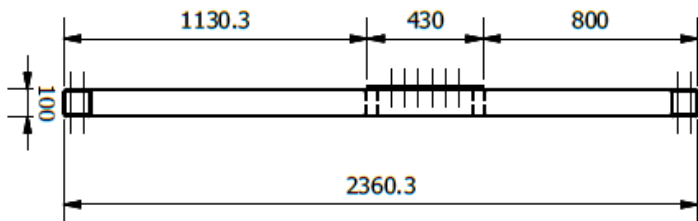
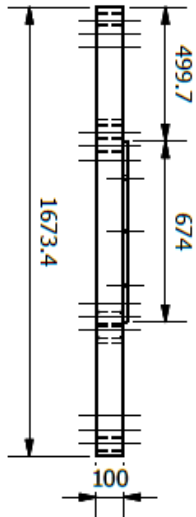
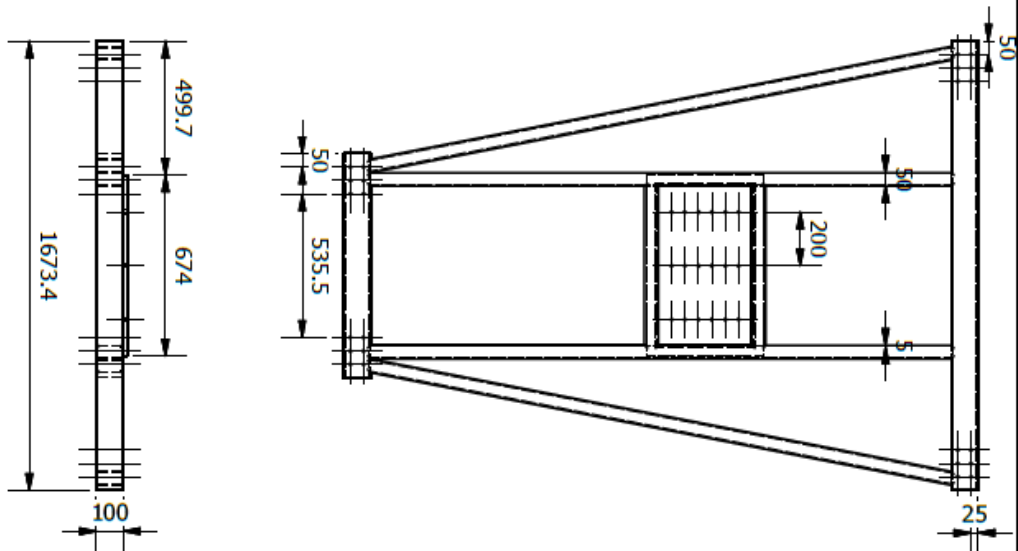


UNLESS OTHERWISE STATED GENERAL TOLERANCES: ± 0.05 mm ANGLES: $\pm 0.1^\circ$



 UNIVERSITY OF KWAZULU-NATAL
 SCHOOL OF ENGINEERING
 MECHANICAL ENGINEERING

MAT.: T690 STEEL	No. REQ.: 4	SCALE: 1:3	UNITS: mm	PROJECT: NSW INSTALLATION TOOLING	NO.: 4-4
PROJECT SUPERVISOR	CHECKED	STUDENT NAME: SHUVAY SINGH		TITLE: LS LOWER GUSSET PLATE	
WORKSHOP TECHNICIAN		STUDENT No.: 211516515			
TECHNICAL OFFICER		E-MAIL: shuvaysingh@gmail.com			
		TEL. NO.: +27 (0)845882810			



UNLESS OTHERWISE STATED GENERAL TOLERANCES: ± 0.05 mm ANGLES: $\pm 0.1^\circ$

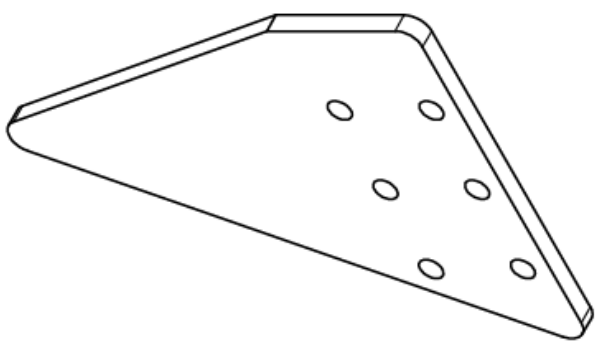
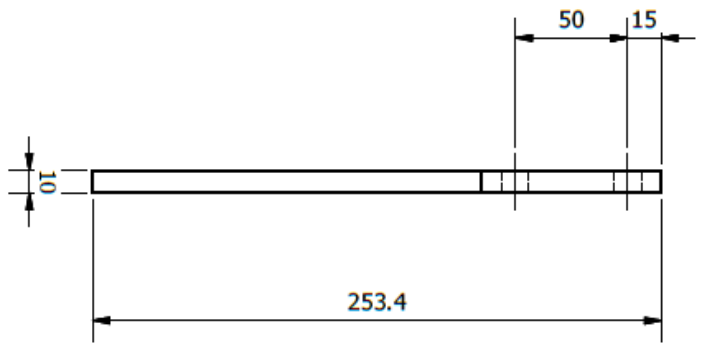
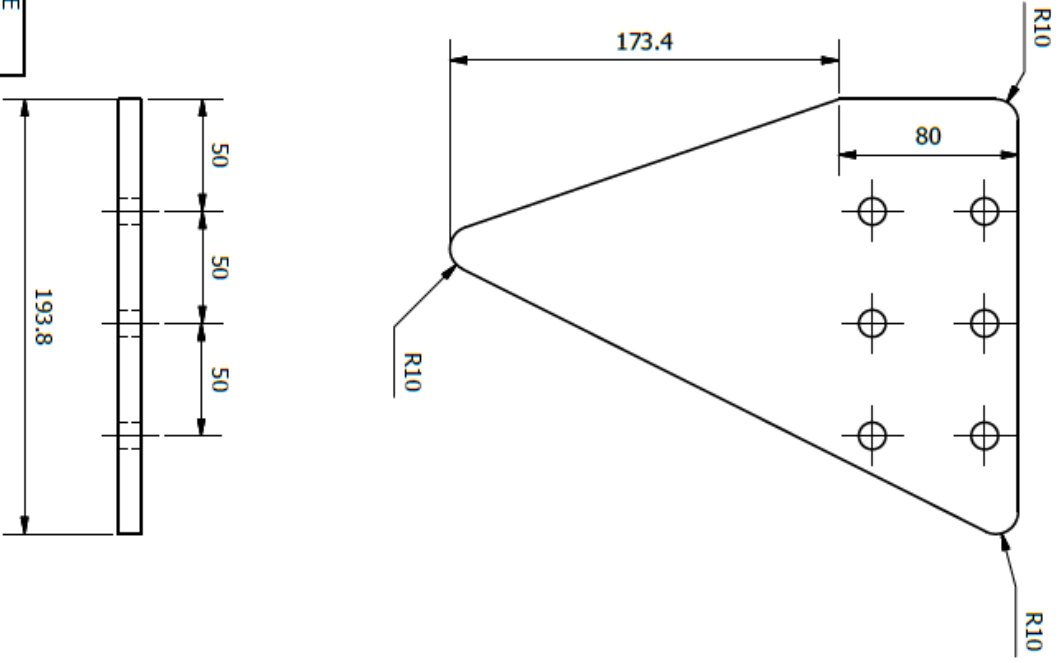


 UNIVERSITY OF KWAZULU-NATAL
 SCHOOL OF ENGINEERING
 MECHANICAL ENGINEERING


MAT.: S355 STEEL	No. REQ.: 1	SCALE: 1:25	UNITS: mm
PROJECT SUPERVISOR	CHECKED	STUDENT NAME: SHUVAY SINGH	
WORKSHOP TECHNICIAN		STUDENT No.: 211516515	
TECHNICAL OFFICER		E-MAIL: shuvaysingh@gmail.com	
		TEL. NO.: +27 (0)945882810	

PROJECT: NSW INSTALLATION TOOLING	NO.:
TITLE: S5 GRABBER FRAME	4-5






UNLESS OTHERWISE STATED GENERAL TOLERANCES: ± 0.05 mm ANGLES: $\pm 0.1^\circ$

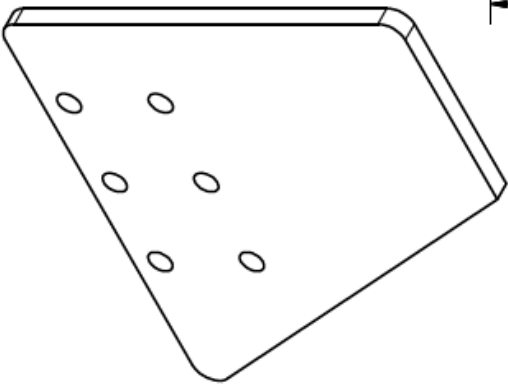
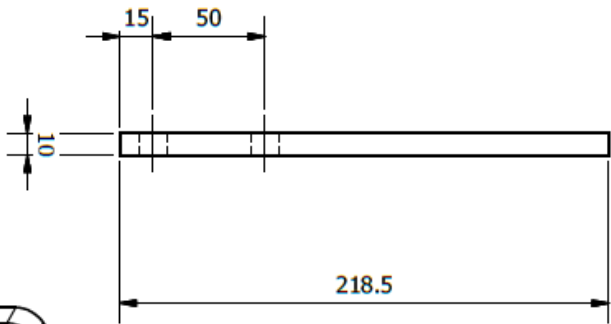
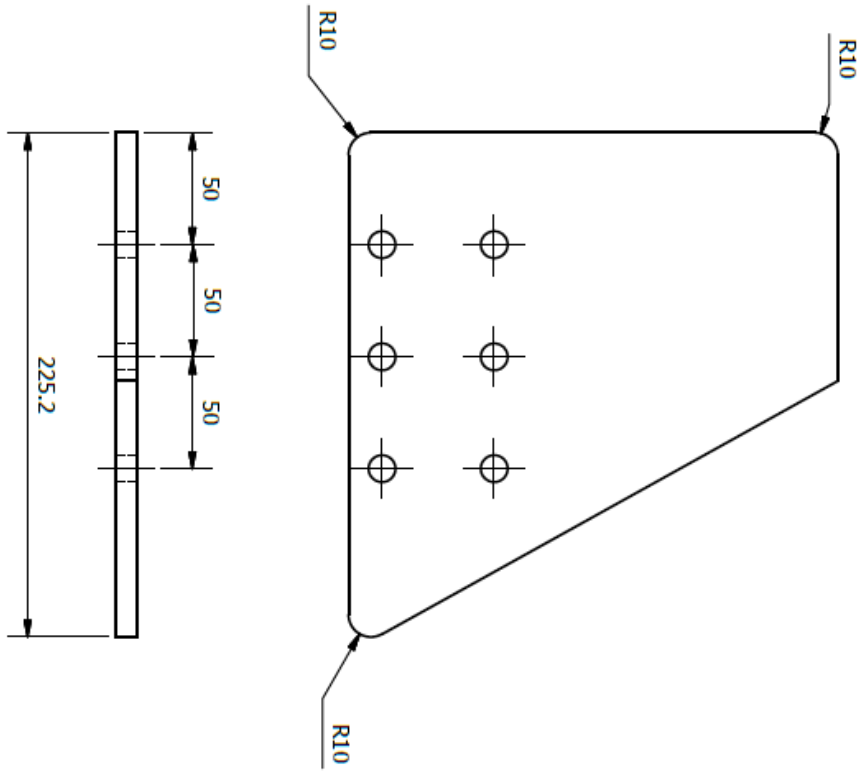


 UNIVERSITY OF KWAZULU-NATAL
 SCHOOL OF ENGINEERING
 MECHANICAL ENGINEERING

MAT.: T690 STEEL	No. REQ.: 4	SCALE: 1:3	UNITS: mm
PROJECT SUPERVISOR	CHECKED	STUDENT NAME: SHUVAY SINGH	
WORKSHOP TECHNICIAN		STUDENT No.: 211516515	
TECHNICAL OFFICER		E-MAIL: shuvaysingh@gmail.com	
		TEL. NO.: +27 (0)945882810	

PROJECT: NSW INSTALLATION TOOLING
 TITLE: SS UPPER GUSSET PLATE

NO.: 4-6




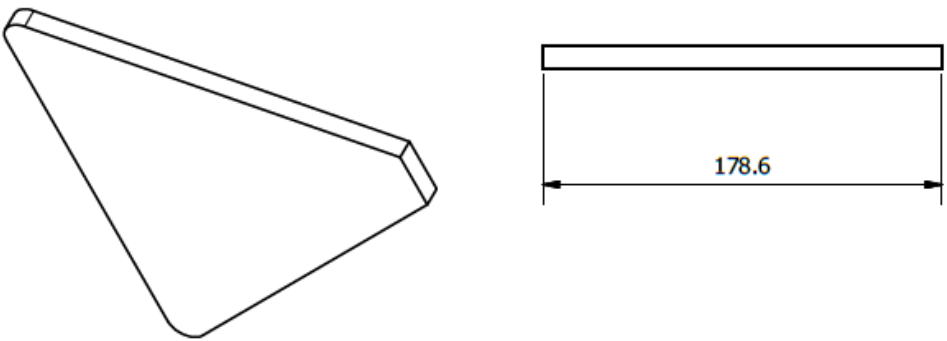
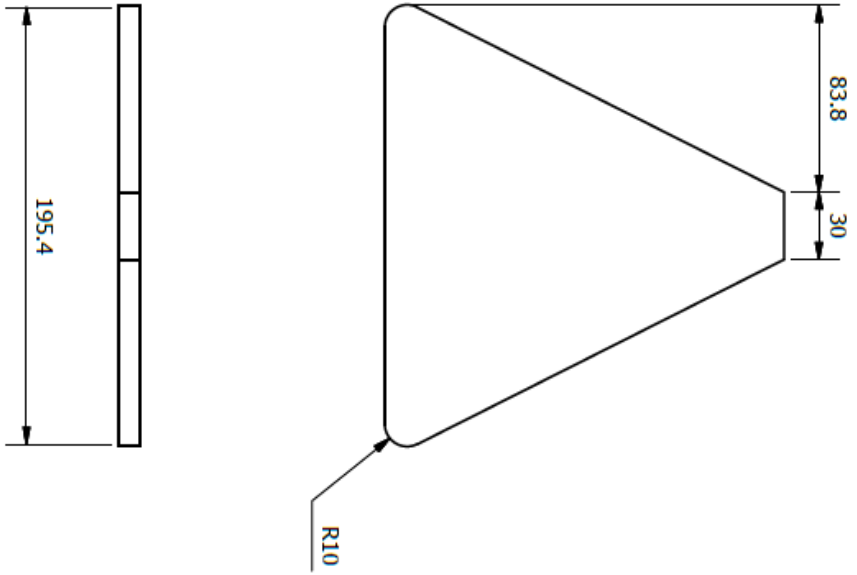
UNLESS OTHERWISE STATED GENERAL TOLERANCES: ± 0.05 mm ANGLES: $\pm 0.1^\circ$



 UNIVERSITY OF KWAZULU-NATAL
 SCHOOL OF ENGINEERING
 MECHANICAL ENGINEERING

MAT.: T690 STEEL		No. REQ.: 4	SCALE: 1:3	UNITS: mm	PROJECT: NSW INSTALLATION TOOLING	NO.: 4-7
PROJECT SUPERVISOR	DATE	CHECKED	STUDENT NAME: SHUVAY SINGH			
WORKSHOP TECHNICIAN			STUDENT No.: 211516515			
TECHNICAL OFFICER			E-MAIL: shuvaysingh@gmail.com		TITLE: SS LOWER GUSSET PLATE	
			TEL. NO.: +27 (0)845882810			





UNLESS OTHERWISE
STATED GENERAL
TOLERANCES: ± 0.05 mm
ANGLES: $\pm 0.1^\circ$




SCHOOL OF
ENGINEERING
MECHANICAL
ENGINEERING

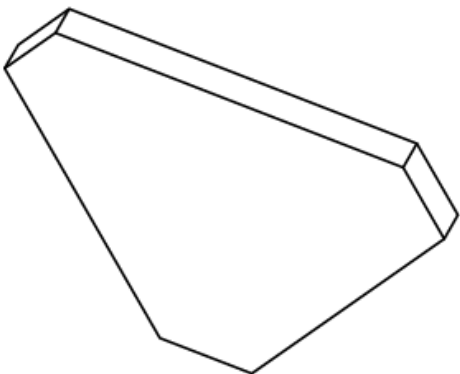
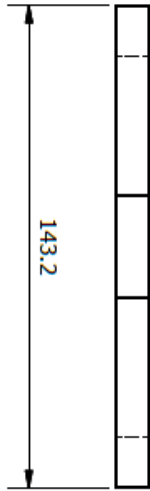
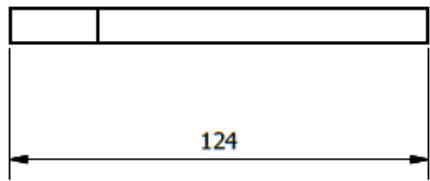
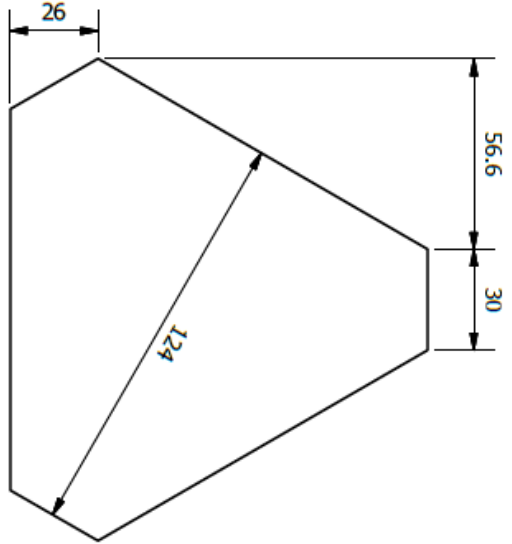
MAT.: T690 STEEL	No. REQ.: 12	SCALE: 1:3	UNITS: mm
PROJECT SUPERVISOR	CHECKED	STUDENT NAME: SHUVAY SINGH	
WORKSHOP TECHNICIAN		STUDENT No.: 211516515	
TECHNICAL OFFICER		E-MAIL: shuvay/singh@gmail.com	
		TEL. NO.: +27 (0)845882810	

PROJECT:
NSW INSTALLATION TOOLING

TITLE:
T-JOINT GUSSET PLATE

NO.:
4-8






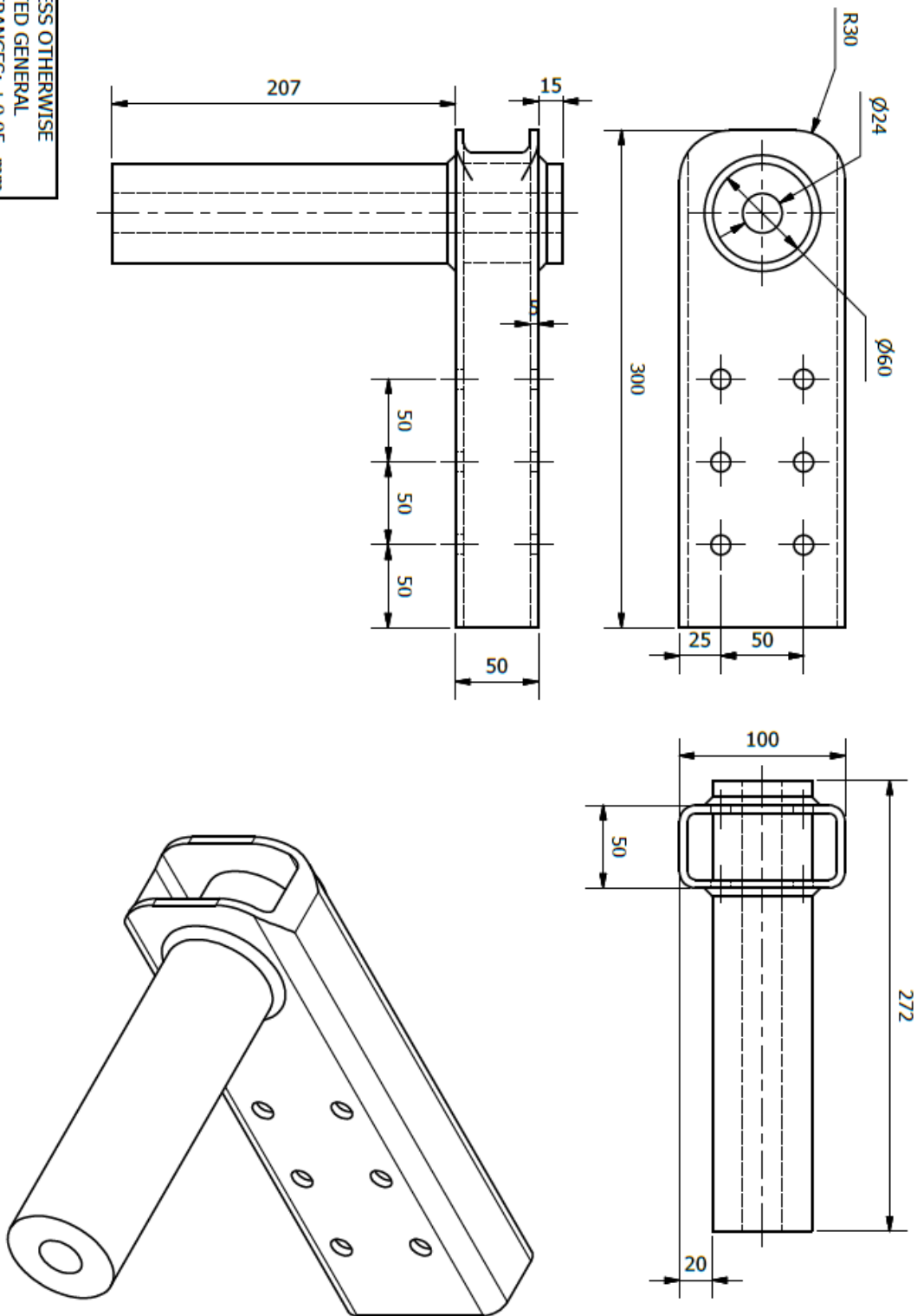
UNLESS OTHERWISE
STATED GENERAL
TOLERANCES: ±0.05 mm
ANGLES: ±0.1 °



 UNIVERSITY OF
 KWAZULU-NATAL
 SCHOOL OF
 ENGINEERING
 MECHANICAL
 ENGINEERING


MAT.: 1690 STEEL	NO. REQ.: 8	SCALE: 1:2	UNITS: mm
PROJECT SUPERVISOR	CHECKED	STUDENT NAME: SHUWAY SINGH	
WORKSHOP TECHNICIAN		STUDENT No.: 211516515	
TECHNICAL OFFICER		E-MAIL: shuwaysingh@gmail.com	
		TEL. NO.: +27 (0)945882810	

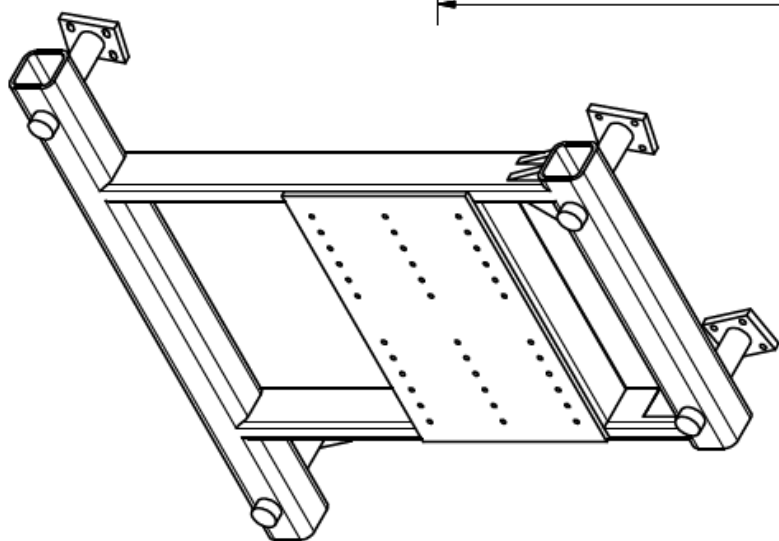
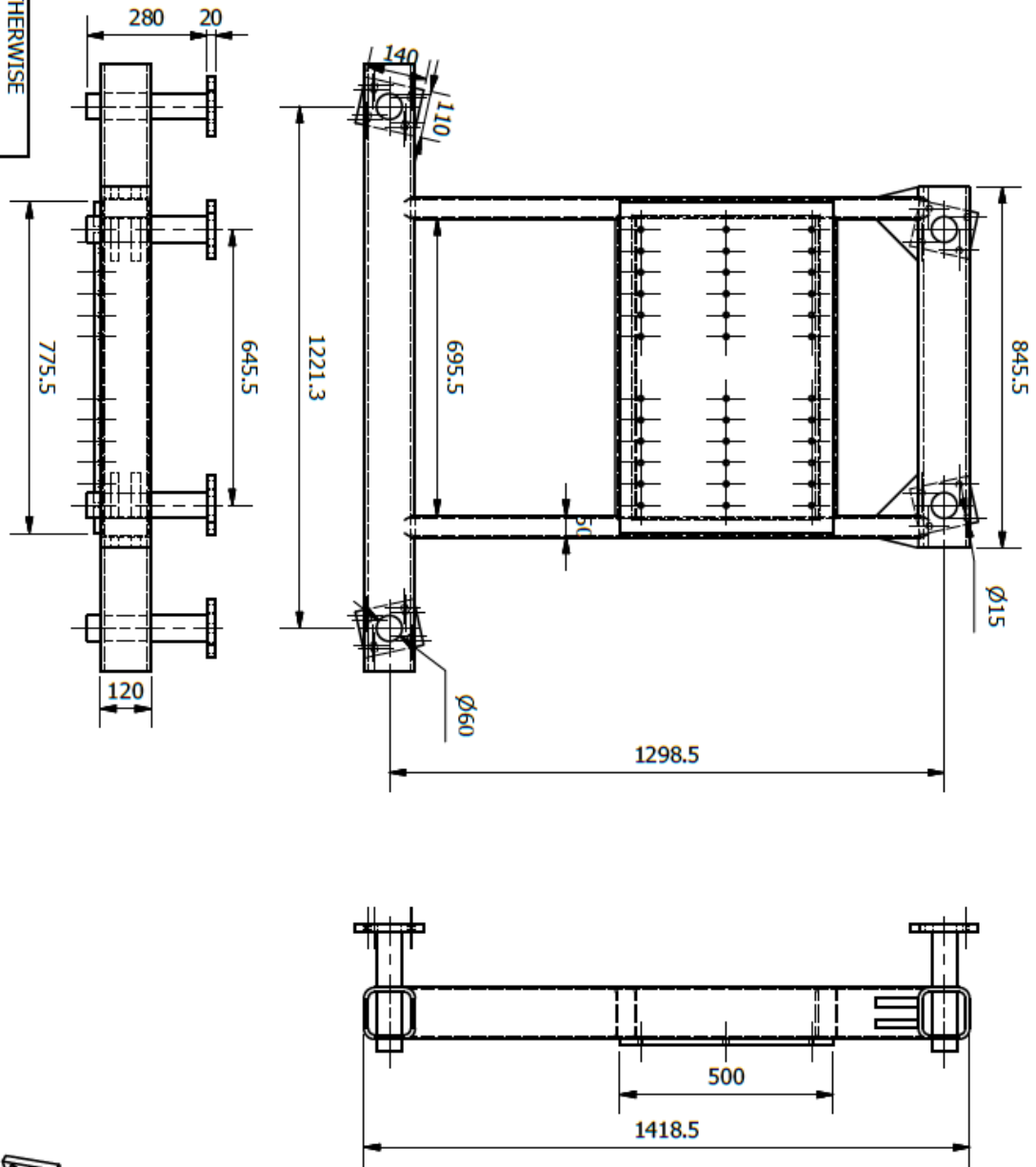
PROJECT: NSW INSTALLATION TOOLING	NO.:: 4-9
TITLE: GRABBER INTERFACE GUSSET PLATE	




UNLESS OTHERWISE STATED GENERAL TOLERANCES: ± 0.05 mm ANGLES: $\pm 0.1^\circ$


 UNIVERSITY OF KWAZULU-NATAL
 SCHOOL OF ENGINEERING
 MECHANICAL ENGINEERING

MAT.: S355 STEEL	No. REQ.: 8	SCALE: 1:3.5	UNITS: mm	PROJECT: NSW INSTALLATION TOOLING	NO.: 4-10
PROJECT SUPERVISOR	CHECKED	STUDENT NAME: SHUVAY SINGH		TITLE: GRABBER ARM	
WORKSHOP TECHNICIAN		STUDENT No.: 211516515			
TECHNICAL OFFICER		E-MAIL: shuvaysingh@gmail.com			
		TEL. NO.: +27 (0)845882810			

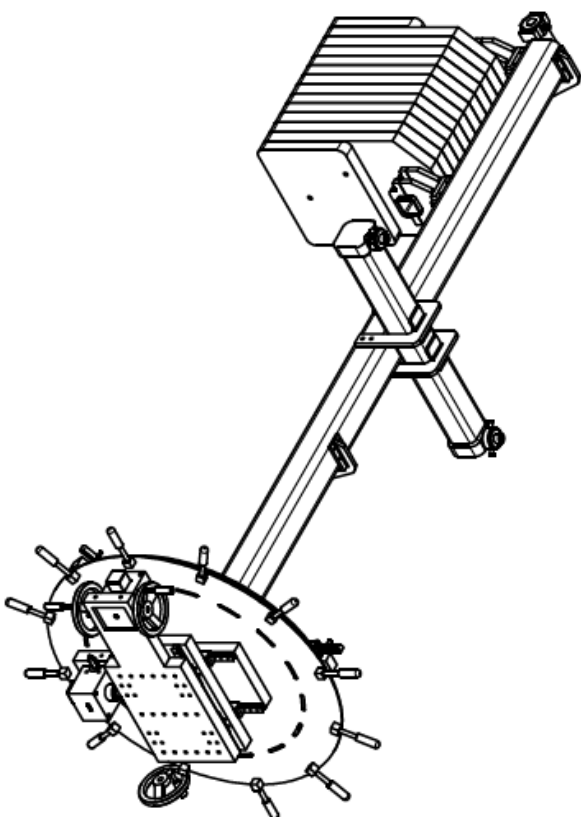
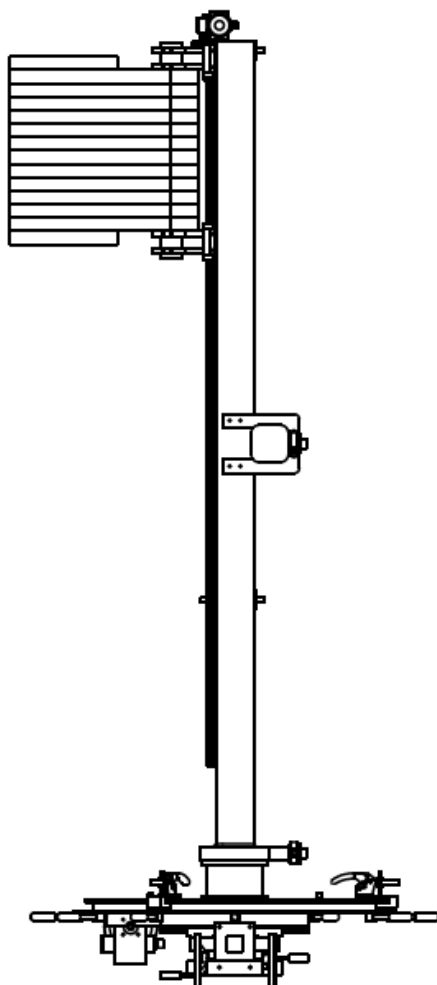
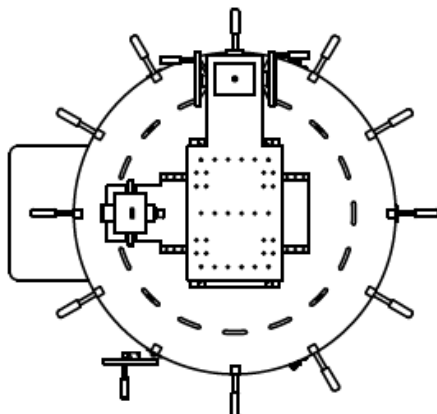


UNLESS OTHERWISE STATED GENERAL TOLERANCES: ±0.05 mm ANGLES: ±0.1°

 UNIVERSITY OF KWAZULU-NATAL SCHOOL OF ENGINEERING MECHANICAL ENGINEERING	MAT.: S355 STEEL	No. REQ.: 1	SCALE: 1:15	UNITS: mm	PROJECT: NSW INSTALLATION TOOLING	NO.:
	PROJECT SUPERVISOR	CHECKED	STUDENT NAME: SHUVAY SINGH		TITLE: FOOT SPOKE GRABBER	4-11
WORKSHOP TECHNICIAN		STUDENT No.: 211516515	E-MAIL: shuvaysingh@gmail.com			
TECHNICAL OFFICER		TEL. NO.: +27 (0)945882810				



5. Full NSW Installation Tooling




UNLESS OTHERWISE
STATED GENERAL
TOLERANCES: ± 0.05 mm
ANGLES: $\pm 0.1^\circ$



 UNIVERSITY OF
 KWAZULU-NATAL

 SCHOOL OF
 ENGINEERING

 MECHANICAL
 ENGINEERING

MAT.: N/A		No. REQ.: 1	SCALE: 1:25	UNITS: mm	PROJECT: NSW INSTALLATION TOOLING	NO.: 5
PROJECT SUPERVISOR	DATE	CHECKED	STUDENT NAME: SHUVAY SINGH		TITLE: FULL NSW INSTALLATION TOOLING ASSEMBLY	
WORKSHOP TECHNICIAN			STUDENT No.: 211516515			
TECHNICAL OFFICER			E-MAIL: shuvaysingh@gmail.com TEL. NO.: +27 (0)845882810			

Appendix D

Matlab programs

1. Main Beam Deflection and Stress Program:

```
length = 3;
F = 1700*9.81;
a = 1.194;
b = 0.306;
E = 200*10^9;
I = 1312/(100^4);

delta = ((F*a^3)*(1+(3/2)*(b/a)))/(3*E*I);
delta

y = 0.06;
M = F*a;
StressBending = 2*((M*0.07)/I)/10^6;
StressBending
```

2. Tooling Balance Program:

```
xf = 0.75;
xsector = 0.357;
xgrabber = 0.245+0.05;
xwheel = 0.153;
xbearing = 0.146;

Wsector = 1450;
Wgrabber = 240;
Wwheel = 273;

MomentLS = Wsector*9.81*(xsector+xgrabber+xwheel+xbearing+xf);
MomentGR = Wgrabber*9.81*(xgrabber+xwheel+xbearing+xf);
MomentWheel = Wwheel*9.81*(xwheel+xbearing+xf);
MomentBeam = (57+9.75)*9.81*(0.75+xf);
MomentMotor = 25*9.81*(1.5+xf);
MomentCounterbeam = 26*9.81*(xf);
Ftot = MomentLS + MomentGR + MomentWheel - MomentBeam - MomentMotor -
MomentCounterbeam;
Fcw = (1732)*9.81;
x = Ftot/Fcw;
x
```

3. Trunnion Shaft Program

```

WLS = 1450*9.81;
Wgrabber = 280*9.81;
Wadapter = 30.5*9.81;
Wworm = 65*9.81;
Wplate = 25.5*9.81;
Wwheel = 118*9.81;

XLS = 0.342;
Xgrabber = 0.09;
Xadapter = 0.09;
Xworm = 0.09;
Xplate = 0.0505;
Xwheel = 0.0255;
Xbearing = 0.15;

SpanLS = XLS + Xgrabber + Xadapter + Xworm + Xplate + Xwheel;
SpanGrabber = SpanLS - XLS;
SpanAdapter = SpanGrabber - Xgrabber;
SpanWorm = SpanAdapter - Xadapter;
SpanPlate = SpanWorm - Xworm;
SpanWheel = SpanPlate - Xplate;
Dshaft = 0.1;
Kt = 2.2;

Rb =
((WLS*(SpanLS)+Wgrabber*(SpanGrabber)+Wadapter*(SpanAdapter)+Wworm*(SpanWorm)+Wplate*(SpanPlate)+W
wheel*(SpanWheel))/(-Xbearing))*-1;
Ra = (WLS*(SpanLS+Xbearing)+
Wgrabber*(SpanGrabber+Xbearing)+Wadapter*(SpanAdapter+Xbearing)+Wworm*(SpanWorm+Xbearing)+Wplate*(
SpanPlate+Xbearing)+Wwheel*(SpanWheel+Xbearing))/Xbearing;

DRa = 2*Ra;
DRb = 2*Rb;
BendStress = Kt*((32*(DRb*Xbearing))/(pi*(Dshaft)^3))/10^6 ;
BendStress2 =
Kt*((32*2*((WLS*(SpanLS)+Wgrabber*(SpanGrabber)+Wadapter*(SpanAdapter)+Wworm*(SpanWorm)+Wplate*(Sp
anPlate)+Wwheel*(SpanWheel)))/(pi*(Dshaft)^3))/10^6 ;
I = (pi*(Dshaft)^4)/64;
Deflection = (1/3)*(Rb*(Xbearing)^3)/(206*(10^9)*I);

ReactionA = Ra/1000
ReactionB = Rb/1000
SFA = DRa/1000
SFB = DRb/1000
moment =
2*(WLS*(SpanLS)+Wgrabber*(SpanGrabber)+Wadapter*(SpanAdapter)+Wworm*(SpanWorm)+Wplate*(SpanPlate)+
Wwheel*(SpanWheel));
moment
BendStress
BendStress2
Deflection

if(Deflection < 0.001)
    disp('ok')
end

```

Appendix E

Stress Concentration Factors

Stress concentration factors for shafts under axial, torsional and moment load

